https://doi.org/10.15414/2021.9788055223384

SLOVAK UNIVERSITY OF AGRICULTURE IN NITRA
FACULTY OF HORTICULTURE AND LANDSCAPE ENGINEERING

VEDA MLADÝCH 2021 - SCIENCE OF YOUTH 2021

proceedings of scientific papers

ISBN 978-80-552-2338-4
ISSN 2585-7398

May, 21st 2021

Veda mladých 2021 - Science of Youth 2021

PROCEEDINGS OF SCIENTIFIC PAPERS

Nitra, Slovakia
21.05.2020

Reviewers

Ing. Jakub Fuska, PhD.
Ing. Elena Aydin, PhD.
doc. Ing. Simona Kunová, PhD.
MSc. Samuel Adamec
Dr. H. c. prof. Ing. Ján Supuka, DrSc.
Ing. Anna Báreková, PhD.
Ing. Tatiana Kaletová, PhD.
prof. Ing Ľuboš Jurík, PhD.
prof. Ing. Peter Halaj, CSc.
Ing. Róbert Lenárt, PhD.
doc. Ing Lenka Lackóová, PhD.
Ing. Zuzana Štefunková, PhD.
doc. Ing. Ján Čimo, PhD.
doc. Ing. Katarína Miklášová, PhD.
Ing. Ladislav Bakay, PhD.
Ing. Ján Kollár, PhD.
Doc. Ing. Ján Horák, PhD.
Ing. Martin Manina, PhD.
Doc. Ing. Lucia Tátošová, PhD.
Ing. Viktor Varga, PhD.
Ing. Marek Hus, PhD.
Ing. Beáta Novotná, PhD.
Ing. Zuzana Németová, PhD.
Ing. Peter Ivan, PhD.

Editors: Ing. Vladimír Kišš, PhD., Ing. Andrej Tárník, PhD.

Schválila rektorka Slovenskej poľnohospodárskej univerzity v Nitre
dňa 03. 06. 2021 ako online zborník vedeckých prác.

ISBN 978-80-552-2338-4

CONTENT

POSTER SECTION

ARTICLE HISTORY:
Received 30 April 2021
Received in revised form 14 May 2021
Accepted 20 May 2021

VISUAL-COMPOSITIONAL CONNECTION OF WOODY PLANTS AND ELEMENTS OF SACRAL ARCHITECTURE

Denis BECHERA[1], Gabriel KUCZMAN[1]

[1]Slovak University of Agriculture in Nitra, SLOVAKIA

Abstract

The importance of woody plants and symbolism in connection with elements of sacral architecture in Slovakia has a long history and tradition. The historical legacy of woody plants and elements of small sacral architecture (SSA) in the country and seat is reflected in the composition, species composition and location of elements of sacral architecture in rural areas. Elements of the DSA as well as sacral buildings are a significant cultural manifestation of individual regions of Slovakia. Construction activity, urban changes as well as land use affect not only the state of sacral monuments but also trees. The paper focuses on the evaluation of woody plants and their connection to small sacral architecture. The paper points out the quantitative and qualitative parameters of SSA elements in selected rural settlements of the middle Považie. The evaluation took place in the cadastres of selected rural settlements in the Piešťany district in 2021. The selected model settlements were Drahovce (1), Chtelnica (2), Moravany nad Váhom (3) and Veľké Kostoľany (4). The evaluation yielded results where the authenticity of the trees and the overall visual impact of SSA is relatively significant. The highest concentration of SSA elements and sacral structures was demonstrated in settlements (2,4). The interconnection of the evaluated elements was demonstrated in strong cultural-historical ties as well as in visual-compositional connections. The Central Považie region points to the high historical and cultural value of sacral buildings together with woody plants with a high aesthetic and functional value.

Key words: evaluation, sacral architecture, woody plants, symbolism, connection, authenticity

Introduction

The aim of the research task is to evaluate and evaluate the interconnectedness, authenticity and cultural-historical value of woody plants together with SSA elements at the level of intensity and abundance in selected cadastres of rural settlements in the Piešťany district.

History of origin, location and significance of the SSA phenomenon

The small sacral elements together with the typical sacral architecture of the rural space are manifested mainly in the form of a cross, various types of columns complemented by statues, torments, chapels and figural sculptures. They represent a manifestation of religion and belief, which are not only aesthetic but also functional and represent places for rest, meditation as well as piety and prayer. Such objects are also important in rural areas for their function of orientation in the landscape, especially in lowland areas, hills and where the terrain is mostly flat and where there is a lower concentration of trees. The elements helped to guide pilgrims, travelers and the general population (Matáková, 2012). The small sacral buildings as well as the trees, which were located nearby, together formed a harmonious whole supporting the visual impact of the cultural landscape and supported the scenery and specific regional expressions, especially in the Baroque and Gothic periods. An important period of the SSA's work was also the Renaissance and later Classicism (Katzberger, 1998).

Monuments of the sacral type and small sacral elements can be found both in the open country but also in the urban area of rural settlements and represent a part of various spatial compositions (Tóth, Verešová, 2018). Crossroads of roads, roads as well as field roads are important places for the origin and location of SSA elements (Türk, 1979). Boundaries of settlements of urban and rural type, ridges and hills in the terrain became frequent places as boundaries of vineyards and settlements, where they also indicated a change in the nature of use but also important places of ecclesiastical significance (Verešová, Supuka, 2013). The importance of crosses as well as other elements of the SSA had in the landscape of the cultural landscape was also protective. Protection was at the level of the weather, providing a temporary refuge as well as a place to rest, but also serving as protection against the evil forces and superstitions that often originate in early Christian culture as well as other sources (Katzberger, 1998; Tóth et al., 2019).

In the premises of settlements and their functional zones, SSA elements were placed in street spaces, in central spaces, in squares and frequent places were also the foregrounds of important buildings, in facades and front areas of buildings. Cemeteries and places of worship near churches also served for the prayers of visitors, and the elements were a stop for this purpose (Halajová et al., 2019). In general, these were places accessible to the public and to all visitors when elements appeared on the borders of fences as well as near road junctions and parks (Trojanowska, 2018).

Compositions, configuration and used wood species

In the open cultural landscape, the elements were often supplemented with woody plants, especially solitary or small groups in regular but also irregular compositions. Therefore, mainly long-lived, resistant and strong species were selected, such as the genus *Tilia sp., Quercus sp. and Fraxinus sp.* A significant breakthrough occurred especially in the Gothic and Baroque periods (Semanová, 2015). Later, symmetrical and arranged compositions were composed, often following the symbolism, and supported the importance and monumentality of the place. The period of classicism and later in the 19th century, new species and forms of woody plants began to appear, which naturally increased species diversity and diversity (Semanová, 2015). The Baroque period brought a significant increase in the presence of woody plants in the sacral architecture and the 19th century was characterized by a significant increase in the species diversity of woody plants (Semanová, 2015). Woody plants were often combined and we can identify in the country compositions composed of three to five woody plants close to each other (Tóth, Verešová, 2018). The most important woody plants used in the creation in the past were mainly the genus *Quercus sp., Tilia sp., Fraxinus sp., Aesculus sp.* and frequent examples are also dominant and resistant woody plants of the genus *Robinia sp.* the trees planted around the sacral buildings were a reflection of the culture of the nation as well as of Christianity and were based on the symbolism and spiritual significance of the trees. They were also used for their durability, longevity, aesthetic properties and crown structure or overall proportionality (Creutz, 2005, Semanová, 2015).

Woody plants and their symbolism

Linden - Magical power was attributed to linden wood mainly in the fight against demons and vampires. With its disintegrated and majestic crown at the time of flowering with its intoxicating scent, the linden tree has become a place for many mutual peace agreements between angry families. It was also believed where the linden tree stands, so perunian lightning rarely strikes. Lipa restored strength to the sick in the form of medicinal teas, which were prepared with certain rituals by tribal wizards (http://slovania.czweb.org/Uctievanie.htm).

Ash - The ash is also a tree of masculine nature, and it was mostly planted by our ancestors at their dwellings with faith, where the ash stands, so the lightning of Perún will not strike. Ash is a very nicely built tree and that is why they also liked it near their houses, not only because of the lightning of Perun (http://slovania.czweb.org/Uctievanie.htm)

Oak - The most revered tree of the ancient Slavs in our country was the oak. The oak has a masculine essence (which is manifested by the direction of the force outwards) and therefore it is possible to receive excess energy from it and it has a beneficial effect on man. They knew that it was possible to meditate and contemplate in the shade of an oak tree with the rustle of its leaves and the emitting positive energy. For our ancestors, the oak was a natural temple and a connection with the Gods (http://slovania.czweb.org/Uctievanie.htm).

Material and methods

The basic step for the elaboration of the paper, mapping, evaluation and objectification of the results is the determination of the criteria for the selection of model areas. The selection of model areas was made in the district of Piešťany. Due to the large number of settlements with different specifications, selected areas - cadastres and settlements with the largest cadastral area (Drahovce 2404 ha, Chtelnica 3297 ha, Moravany nad Váhom 1079 ha, Veľké Kostoľany 2708 ha) were selected (Figure 1). Selected municipalities are also the most populated in the district of Piešťany. An important criterion for the selection of model areas was also the number of significant sacral monuments in municipalities and other historical buildings that support the historical, cultural and religious significance within the Piešťany district.

The criterion was the location and existence of at least 1 Roman Catholic church and 1 chapel. Along with other criteria, the already mentioned areas were selected, where several buildings and important places are located (Drahovce - 1 church and 2 chapels, Chtelnica - 2 churches, 3 chapels, 1 pilgrimage site, 1 manor house, Moravany nad Váhom - 2 churches, 1 chapel, 1 manor house, Veľké Kostoľany - 1 church, 3 chapels, 1 manor house, 1 pilgrimage site).

The location of DSA elements as well as cultural objects and sacral buildings in individual areas is shown in maps (Figure 2 to Figure 5). List of important sacral objects and cultural objects in individual territories - Drahovce - DX1 Church of St. Martin, DX2 Chapel of St. Cyril and Methodius, DX3 Chapel of the Visitation of the Blessed Virgin Mary. Chtelnica - CX1 Church of the Holy Trinity, CX2 Church of St. John the Baptist, CX3 Chapel of the Virgin Mary of the Seven

Sorrows, CX4 Mansion, CX5 Chapel of St. Róch. Moravany nad Váhom - MX1 Church of Our Lady of the Rosary, MX2 Church of St. Martin, MX3 Chapel, MX4 Manor house. Veľké Kostoľany - VX1 Church of St. Vito, VX2 Parish Chapel, VX3 „Hájiček“ Chapel, VX4 Manor house.

The methodical work procedure consisted of identification of elements in the space with the addition of data on location, relationship to the past, connections with trees as well as identification of individual tree species, number of pieces and selected dendrological parameters (name of tree, number of pieces, age stage of trees). Pejchal, Šimek 1996, vitality - horticultural value of trees according to - Machovec, 1982, height of the tree and the circumference of the trunk at a height of 130 cm from the ground). The evaluation methodology was supplemented by the criterion of Connectivity and Authenticity, which achieved an objective assessment of woody plants in terms of originality, age, vitality and spatial arrangement in relation to SSA buildings. The allocation of percentages for the individual stages could be achieved by 400 %, which were subsequently divided by the number of evaluation subcategories of the criterion.

This achieved a percentage value of the action, which is then classified into one of four categories - the degree of interconnection. Subcategory originality: original 100 %, original-unsatisfactory 90 %, introduced 80 %, non-original 60 %, invasive 40 %. Subcategory age stage (due to the construction period of the SSA element): planting age identical to the origin of the element 100 %, planting before construction 80 %, planting after construction 60 %, planting late after planting 40 %, young planting 20 %. Vitality of woody plants: veteran - grade 5 – 100 %, adult woody plant - grade 4 - 80%, stabilized mature woody plant - grade 3 - 60%, grown planting - grade - 2 – 40 %, young planting - grade 1 – 20 %. Spatial location: regular shape next to the building – 100 %, irregular shape next to the building – 80 %, distance 2-3 m from the building – 60 %, distance 3-5 m from the building – 40 %, distance 5 and more meters from the building – 20 %. For several trees, the calculation of the assigned value was done on the basis of the arithmetic mean.

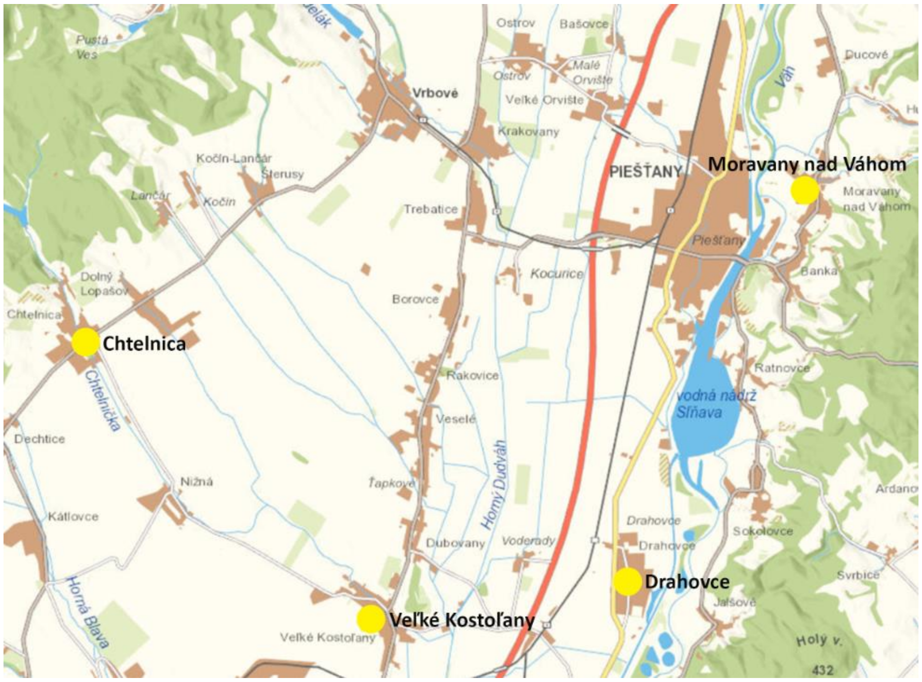

Figure 1 Localization of selected model areas (source: mapka.gku.sk)

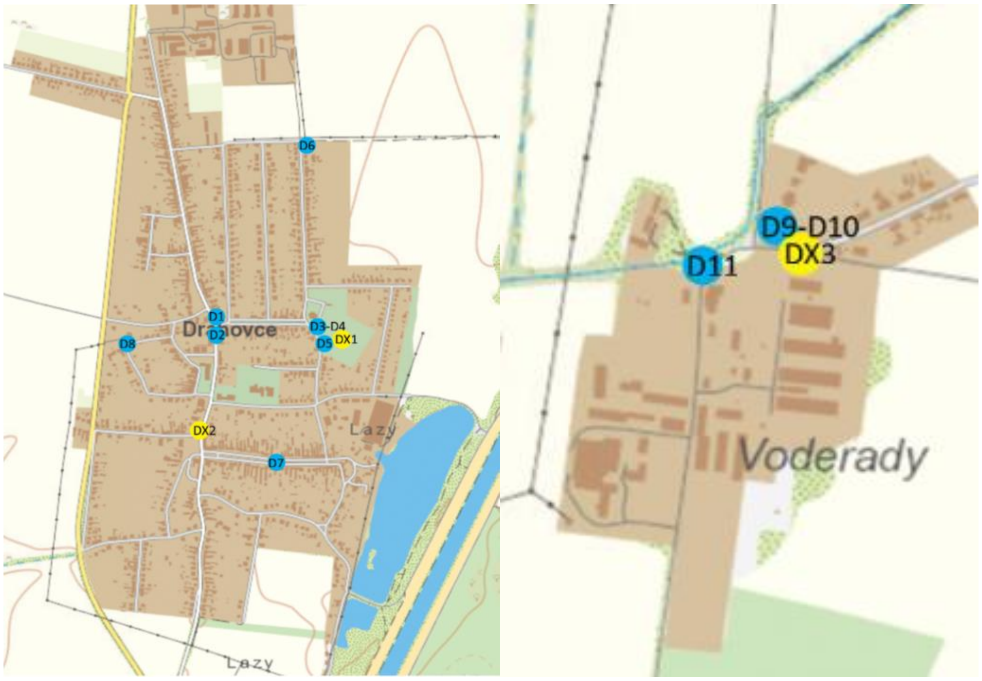

Figure 2 Localization SSA elements – Drahovce (source: mapka.gku.sk)

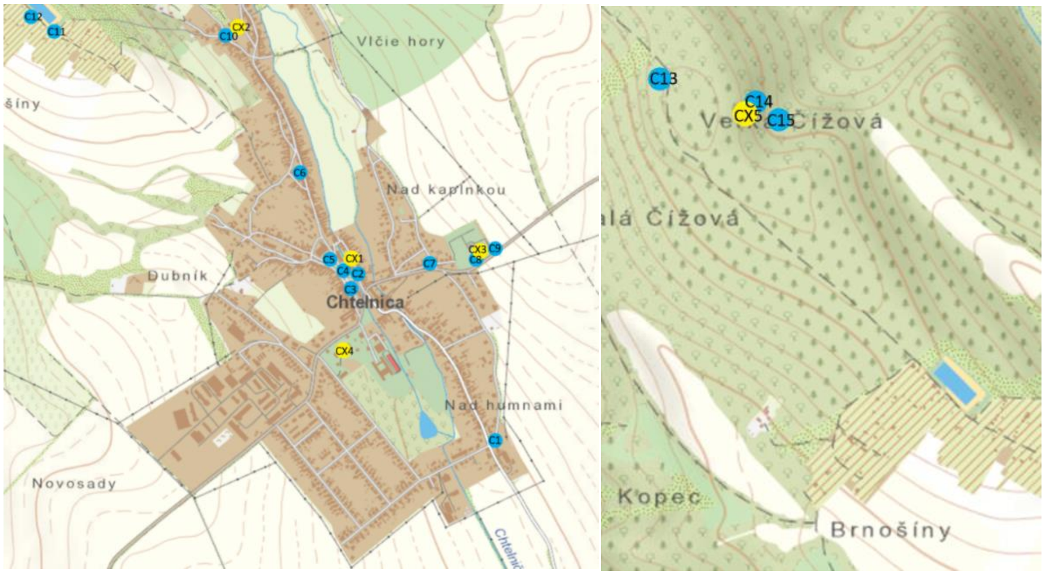

Figure 3 Localization SSA elements – Chtelnica (source: mapka.gku.sk)

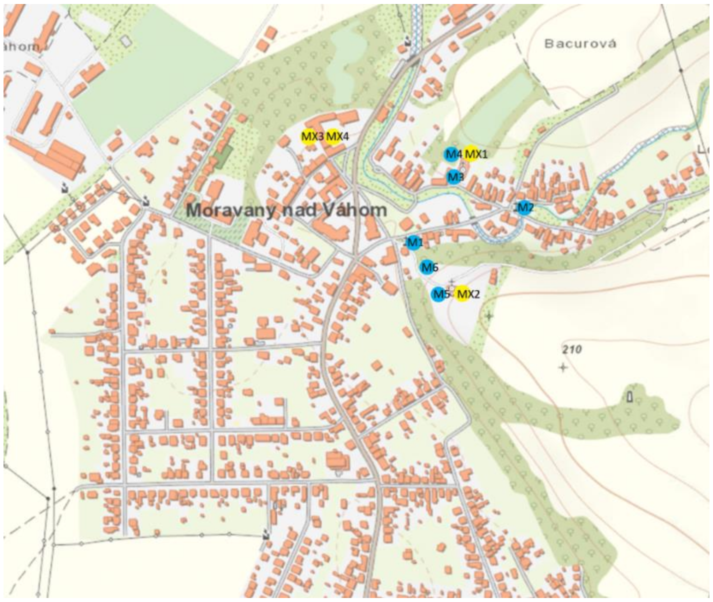

Figure 4 Localization SSA elements – Moravany nad Váhom (source: mapka.gku.sk)

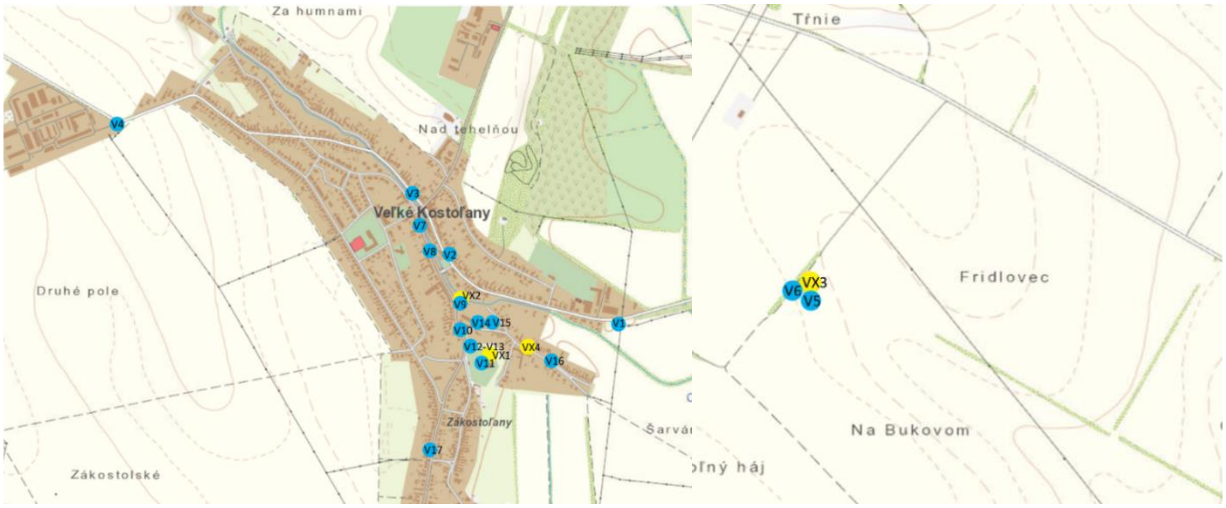

Figure 5 Localization SSA elements – Veľké Kostoľany (source: mapka.gku.sk)

Results and discussion

Selected model rural settlements and their cadastres were mapped according to the methodology for mapping small sacral architecture, which he developed (Tóth, 2017). The methodology underwent adjustments, which consisted of optimizing the table for mapping and subsequently also adjusting the evaluation criteria. The optimization contributed to the objectification of the set goal, which is the evaluation of the interconnection of woody plants and elements of sacral architecture, authenticity and the overall aesthetic and visual expression of the evaluated objects. From the mapping and the obtained data and the subsequent evaluation after the assigned point values, we came to the conclusion that the evaluation of the results should be interpreted at several levels. The first evaluated level is the concentration and abundance of elements of sacral architecture with respect to the seat and cadastre. 52 SSA facilities in four municipalities in the Piešťany district were mapped and evaluated. Tables 1 to 4 show the evaluation methodology used during mapping and evaluation.

Table 1 Evaluation table - Cadastral area Drahovce

s.n	Name of the territory	Category and name of the sacral element	Year / period of establishment	GPS coordinates	Woods number of pcs	Latin name of woody plants	Age of woody plants	Vitality	Wood parameters - height (m), trunk circumference (cm)	Connectivity and Authenticity				Summary (interconnection of DSA and tree elements)%
										Originality	Age stage	Vitality	Spatial location	
D1	Drahovce	Roadside rood - Rood stone on a pedestal	19. cent.	48.517771, 17.801223	1	*Tilia cordata Mill.*	4	3	11m, 155 cm	100	100	60	100	90
D2	Drahovce	Statue - Stone statue - St. Mary	19. cent.	48.517647, 17.801231	1	*Tilia cordata Mill.*	4	3	12m, 185 cm	100	100	60	100	90
D3	Drahovce	Statue - Stone statue - St. Vendelín	1839	48.517779, 17.804921	0									/
D4	Drahovce	Statue - Stone statue - St. Cyril and Metod	1900	48.517815, 17.804886	0									/
D5	Drahovce	Statue - Stone statue - St. Ján Nepomucký	beg. 17. cent	48.517182, 17.805562	1	*Tilia cordata Mill.*	5	3	8 m, 425 cm	100	100	60	100	90
D6	Drahovce	Roadside rood - Rood stone on a pedestal	beg. 18. cent	48.522704, 17.804650	6	*Robinia pseudoacacia L.* *Robinia pseudocacia L.* *Picea pungens L.* *3x Thuja orientalis L.*	4 4 3 3	2 2 2 3	5 m, 145 cm 5 m, 135 cm 4 m, 35 cm 2,5 m, 38 cm	40	40	50	80	52,5
D7	Drahovce	Sculptures - Stone sculpture - Holy Trinity	18. cent.	48.513878, 17.803770	1	*Prunus cerasus L.*	4	4	9 m, 122 cm	100	40	80	40	65
D8	Drahovce	Box - box with sculpture	19. cent.	48.517325, 17.797301	1	*Fraxinus excelsior L.*	4	3	11 m, 112 cm	100	60	60	100	80
D9	Drahovce	Statue - Stone statue - St. Vendelín (D. Voderady)	beg. 19. cent.	48.522282, 17.767424	1	*Robinia pseudoacacia L.*	4	2	14 m, 117 cm	40	80	60	80	65
D10	Drahovce	Box - box with sculpture	beg. 19. cent.	48.522381, 17.767413	0									/
D11	Drahovce	Statue - Stone statue - St. Ján Nepomucký (D. Voderady)	beg. 17. cent	48.521905, 17.766179	2	*2x Acer platanoides L.*	4	3	11 m, 110 cm	100	60	60	80	75

Table 3 Evaluation table - Cadastral area Moravany nad Váhom

s.n	Name of the territory	Category and name of the sacral element	Year / period of establishment	GPS coordinates	Woods number of pcs	Latin name of woody plants	Age of woody plants	Vitality	Wood parameters - height (m), trunk circumference (cm)	Connectivity and Authenticity				Summary (interconnection of DSA and tree elements) %
										Originality	Age stage	Vitality	Spatial location	
M1	Moravany n. Váhom	Statue - Stone statue - St. Ján Nepomucký	18. cent	48.602129, 17.862619	2	*Tilia cordata Mill.* *Tilia cordata Mill.*	5 4	3 2	12 m, 145 cm 4,5 m, 105 cm	100	60	50	100	77,5
M2	Moravany n. Váhom	Statue - Stone statue - St. Vendelín	1912	48.602718, 17.865626		*Tilia cordata Mill.* *Tilia cordata Mill.*	3 3	4 3	9 m, 95 cm 8 m, 80 cm	100	100	70	100	92,5
M3	Moravany n. Váhom	Main Rood - wooden rood (Church of Our Lady of the Rosary)	19. cent.	48.603151, 17.864194										/
M4	Moravany n. Váhom	Grotta - Lourdes Cave with a sculpture of the Virgin Mary	20. cent.	48.603348, 17.864181										/
M5	Moravany n. Váhom	Main Rood - wooden rood (Church of St. Martin)	19. cent.	48.601475, 17.863985										/
M6	Moravany n. Váhom	Roadside rood - Rood wooden on a pedestal (St. Martin's Church)	19. cent.	48.601759, 17.863505	1	*Tilia cordata Mill.*	4	3	12 m, 125 cm	100	100	60	100	90

Table 2 Evaluation table - Cadastral area Chtelnica

s.n	Name of the territory	Category and name of the sacral element	Year / period of establishment	GPS coordinates	Woods number of pcs	Latin name of woody plants	Age of woody plants	Vitality	Wood parameters - height (m), trunk circumference (cm)	Connectivity and Authenticity				Summary (interconnection of DSA and tree elements) %
										Originality	Age stage	Vitality	Spatial location	
C1	Chtelnica	Roadside rood - Rood stone on a pedestal	18. cent.	48.564849, 17.6297	0									/
C2	Chtelnica	Statue - Stone statue - St. Florián	18. cent.	48.570254, 17.6231	0									/
C3	Chtelnica	Statue - Stone statue - St. Ján Nepomucký	18. cent.	48.569981, 17.6231	1	*Tilia cordata Mill.*	4	4	14 m, 115 cm	100	100	80	20	75
C4	Chtelnica	Stone sculpture on a pedestal - St. Mary and Jesus	end.17. cent.	48.570439, 17.6226	2	*Tilia cordata Mill.* *Tilia cordata Mill.*	4 4	2 3	9 m, 185 cm 13 m, 210 cm	100	100	50	60	77,5
C5	Chtelnica	Main Cross - Stone Cross - Statue of Christ with sculptures	end.17. cent.	48.570741, 17.6223	2	*Thuja occidentalis 'Tedd*	2	4	0,5 m, -	60	20	80	60	55
C6	Chtelnica	Alcove box with sculpture St. Mary	18. cent.	48.575198, 17.6197	0									/
C7	Chtelnica	Chapel of St. Rood - Stone chapel with a rood	1737	48.570527, 17.6269	0									/
C8	Chtelnica	Chapel of the Virgin Mary of the Seven Sorrows - Stone Chapel	1737	48.570639, 17.6290	1	*Aesculus hippocastanum*	5	3	11 m, 195 cm	80	100	60	60	75
C9	Chtelnica	Statue - Stone statue - St. Cyril and Metod	1813	48.571058, 17.6299	2	*Tilia cordata Mill.* *Tilia cordata Mill.*	2 2	4 4	4,5 m, 30 cm 4,5 m, 34 cm	100	40	80	100	80
C10	Chtelnica	Main Cross - Steel Cross (Church of St. John the Baptist)	20. cent.	48.578102, 17.6171	0									/
C11	Chtelnica	Statue - Stone statue - St. Urban	2002	48.578119, 17.6084	3	*Tilia cordata Mill.* *2x Rosa canina L.*	1 2	3 2	2,2 m, 14 cm 1,2 m	100	20	50	100	67,5
C12	Chtelnica	Grotta - Lourdes Cave with a sculpture of the Virgin Mary	beg. 20. cent.	48.578531, 17.6076	2	*Tilia cordata Mill.* *Tilia cordata Mill.*	2 2	4 4	5,5 m, 38 cm 7,5 m, 47 cm	100	60	80	100	85
C13	Chtelnica	Roadside rood - Rood stone on a pedestal	18. cent.	48.583827, 17.5995	1	*Tilia cordata Mill.*	5	4	16 m, 225 cm	100	100	80	100	95
C14	Chtelnica	Chapel of St. Róch - stone	17. cent	48.585860, 17.6049	2	*Tilia cordata Mill.* *Tilia cordata Mill.*	5 4	2 2	17 m, 238 cm 14 m, 95 cm	100	90	40	100	82,5
C15	Chtelnica	Sculptures - Stone sculpture - Christ's baptism with John the	17. cent	48.585809, 17.6052	0									/
C16	Chtelnica	Roadside rood - Rood stone on a pedestal	1775	48.563339, 17.6151	1	*Tilia cordata Mill.*	3	4	8 m, 115 cm	100	60	80	100	85
C17	Chtelnica	Statue - Stone statue - St. Urban II.	1781	48.559817, 17.6107	3	*Tilia cordata Mill.* *Tilia cordata Mill.* *Tilia cordata Mill.*	3 3 3	3 3 3	7 m, 89 cm 7 m, 90 cm 8 m, 95cm	100	40	60	100	75
C18	Chtelnica	Chapel of the St. Mary - Stone Chapel	1704	48.555374, 17.6054	1	*Tilia cordata Mill.*	4	3	13 m, 195 cm	100	60	60	80	75

Table 4 Evaluation table - Cadastral area Veľké Kostoľany

s.n	Name of the territory	Category and name of the sacral element	Year / period of establishment	GPS coordinates	Woods number of pcs	Latin name of woody plants	Age of woody plants	Vitality	Wood parameters - height (m), trunk circumference (cm)	Connectivity and Authenticity				Summary (interconnection of DSA and tree elements) %
										Originality	Age stage	Vitality	Spatial location	
V1	Veľké Kostoľany	Statue - Stone statue - God's heart of Jesus	beg. 20. cent.	48.506205, 17.733225	2	*Acer negundo L.* *Pinus sylvestris L.*	4 3	3 2	10 m, 125 cm 6 m, 40 cm	70	60	50	60	60
V2	Veľké Kostoľany	Statue - Stone statue - Jesus	1927	48.508653, 17.724045	0									/
V3	Veľké Kostoľany	Sculpture - stone statue - St. Joseph and Jesus	end. 18. cent.	48.510906, 17.721950	1	*Tilia cordata Mill.*	4	2	10 m, 118 cm	100	60	60	100	80
V4	Veľké Kostoľany	Roadside rood - Rood stone on a pedestal	1759	48.513734, 17.704935	2	*Tilia cordata Mill.* *Tilia cordata Mill.*	4 4	4 3	12 m, 105 cm 12 m, 90 cm	100	100	70	100	92,5
V5	Veľké Kostoľany	Statue - Stone statue - God's heart of Jesus	18. cent.	48.518448, 17.672000	1	*Quercus petrea L.*	5	5	18 m, 295 cm	100	100	100	100	100
V6	Veľké Kostoľany	Hájiček Chapel - Pilgrimage place	1830	48.518615, 17.671908	1	*Tilia cordata L.*	5	2	9 m, 350 cm	100	80	40	80	75
V7	Veľké Kostoľany	Statue - stone statue - St. Ján Nepomucký	18. cent.	48.510190, 17.722390	1	*Picea abies L.*	4	2	12 m, 90 cm	90	80	40	80	72,5
V8	Veľké Kostoľany	Statue - stone statue - St. Madonna with baby	18. cent.	48.509213, 17.722832	0									/
V9	Veľké Kostoľany	Parish Chapel - stone	18. cent.	48.506988, 17.724409	0									/
V10	Veľké Kostoľany	Sculpture - Statue of the Holy Trinity	1909	48.505900, 17.724844	1	*Thuja orientalis L.*	4	3	9 m, 3x70 cm	60	40	60	60	55
V11	Veľké Kostoľany	Main Rood - wooden rood (Church of St. Vitus)	20. cent.	48.504738, 17.726105	1	*Cham. lawsoniana L.*	4	3	10 m, 90 cm	60	40	60	80	60
V12	Veľké Kostoľany	Chapel of the Missionaries (Church of	18. cent.	48.505467, 17.725172	2	*Aesc. hippocastanum L.* *Picea abies L.*	3 4	4 3	10 m, 110 cm 13 m, 115 cm	85	100	70	80	83,75
V13	Veľké Kostoľany	Grotta - Lourdes Cave with a sculpture of the Virgin Mary	20. cent.	48.505783, 17.724995	0									/
V14	Veľké Kostoľany	Statue - stone statue - Madonna with child	20 cent.	48.506057, 17.725526	0									/
V15	Veľké Kostoľany	Passion of Christ - Sculpture on a pedestal	18. cent.	48.506423, 17.726400	0									/
V16	Veľké Kostoľany	Statue - Stone statue - Jesus	20. cent.	48.504632, 17.730193	0									/
V17	Veľké Kostoľany	Roadside rood - Rood stone on a pedestal	18. cent.	48.501220, 17.722871	0									/

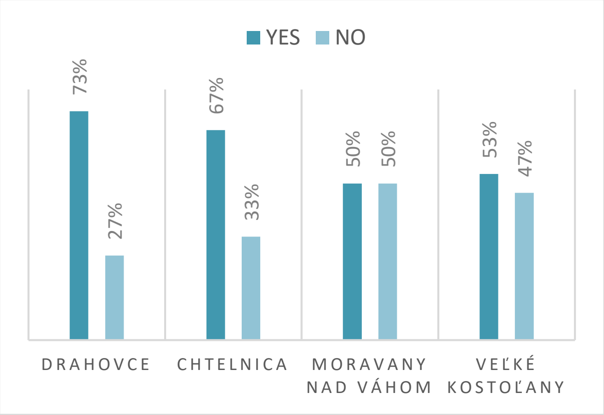

Figure 6 Number of elements SSA

Figure 7 Connection of wood to SSA elements

The total percentage distribution is shown in Figure 6. The second level evaluated is the binding of the wood to the object, where out of the total number of mapped objects 52, the binding and connection with the wood was identified in 32 SSA elements. The percentage in individual municipalities can be seen in Figure 7.

The results in individual selected rural settlements and cadastres are based on SSA elements that have interconnection and connection to woody plants according to Figure 7. 4 categories of intensity and degree of interconnection were created for evaluation. These categories also take into account the degree of aesthetic effect of SSA elements and woody plants and their authenticity and functionality in space.

Categories for evaluating connectivity and authenticity:

Category 1: 100-85 %, **Category 2:** 84-70 %, **Category 3:** 69-54 %, **Category 4:** 53 % and less. Individual distributions and percentage evaluations classified into categories are shown in Figures 8 to 11.

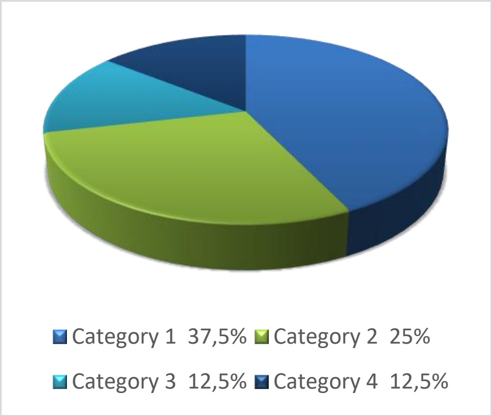

Figure 8 Interconnection of SSA elements and woody plants – categorization – Drahovce

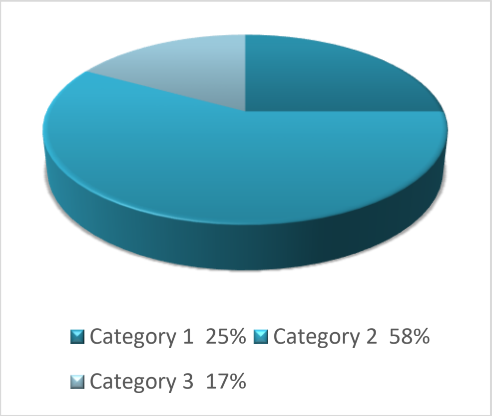

Figure 9 Interconnection of SSA elements and woody plants – categorization – Chtelnica

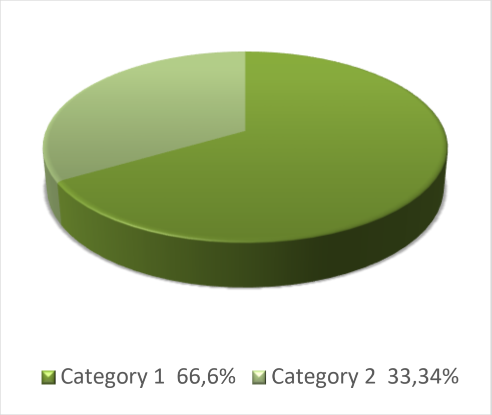

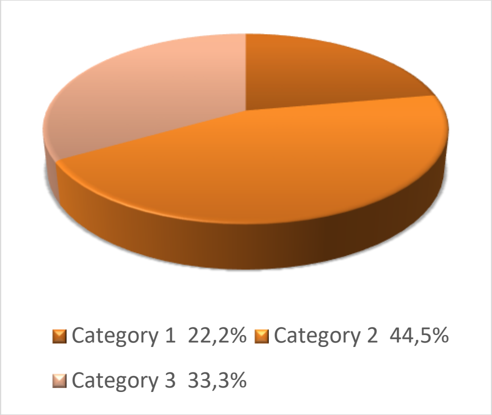

Figure 10 Interconnection of SSA elements and woody plants – categorization – Moravany nad Váhom

Figure 11 Interconnection of SSA elements and woody plants – categorization – Veľké Kostoľany

The third evaluated level is the highest degree of interconnection in category 1 in individual selected settlements and cadastres in a percentage of the total number of evaluated SSA elements within individual settlements. Figure 12 shows this percentage calculation in each seat. Due to the number of identified SSA elements and the intensity of interconnection with woody plants, the highest intensity of interconnection, authenticity and aesthetic effect of the objects was proved in the village of Drahovce with a percentage share of all mapped elements of 27.3 %. In each model area, there are objects to varying degrees that have a high connection and connection to woody plants in category 1 and category 2.

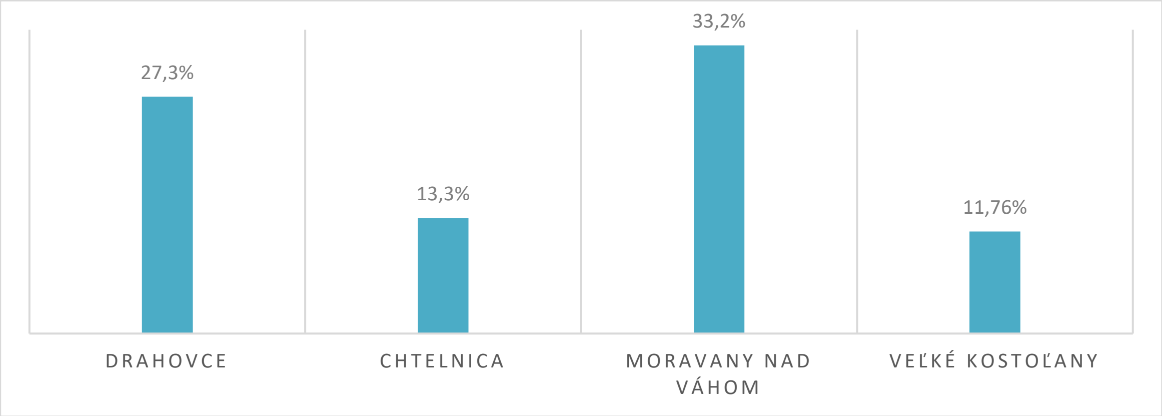

Figure 12 The highest degree of interconnection in category 1 between twins and DSA elements

Source: Bechera, 2020 - D5
Source: Bechera, 2021 - D4
Source: Bechera, 2021 - D1
Source: Bechera, 2021 - C14-C15
Source: Bechera, 2021 - C8
Source: Bechera, 2021 - C4
Source: Bechera, 2021 - M3
Source: Bechera, 2021 - M2
Source: Bechera, 2021 - M1
Source: Bechera, 2021 - V5
Source: Bechera, 2021 - V4
Source: Bechera, 2021 - V12

Figure 13 Examples of high-intensity interconnection and authenticity of model areas

Conclusions

The Central Považie region is a very rich region not only for castles, chateaux, manors and manors, but also for sacral monuments, as the contribution shows. A relatively important element are also sacral buildings and small sacral architecture with a connection to woody plants. Many of the elements of SSA are strongly linked to woody plants, which is reflected in the overall aesthetic effect. Many of the woody plants found in these sacral objects are aesthetically and visually very valuable and have a high degree of authenticity in space. Authenticity and connection is the highest manifestation of aesthetic action. They significantly influence the cultural landscape and increase its value and identity through the action of elements of sacred architecture together with woody plants.

Acknowledgment

The publication is the result of:

VEGA no. 003SPU-4/2020 ZEL:IN:KA - Integrácia ZELenej INfraštruktúry do Krajinnej Architektúry (Integration of Green Infrastructure into Landscape Architecture)

KEGA no. 015SPU-4/2020 UNI:ARCH (Slovak UNIversity of Agriculture in Nitra - ARCHitectonic values of buildings)

KEGA no. 024SPU-4/2019 Cultural and historical value of the wine-growing landscape, development and current use

References

CREUTZ, A. 2005. Gedenksteine und Wegekreuze im Grenzraum des oberen Göhltales: Spuren der Vergangenheit in Aachen-Sief--Walheim-Raeren-Eynatten-Hauset-Hergenrath. Aachen: Helios. 378 p.

HALAJOVÁ, D. et al. 2019. Small Sacral Architecture and Its Greenery in Lower Spiš Region in Slovakia. Acta Horticulturae et Regiotecturae, 22, 1, p. 29 – 36.

KATZBERGER, P. 1998. Werke der Bildhauerkunst und Kleindenkmäler in Perchtoldsdorf. Perchtoldsdorf: Verlag der Marktgemeinde Perchtoldsdorf. 1998, 615 p.

MATÁKOVÁ, B. 2012. Spiritual Values of Rural Landscape in the Czech Republic and Slovakia. Životné prostredie, 46, 4, p. 193 – 198.

SEMANOVÁ, E. 2015. Stromy v kompozičných prvkoch kultúrnej krajiny – niekoľko poznatkov a skúseností z hľadiska pamiatkovej ochrany (na príklade Prešovského kraja). Životné prostredie, 49, 4, p. 242 – 246.

TÓTH, A. – VEREŠOVÁ, M. 2018. Small Sacral Architecture and Trees as Mo-numents in Diverse Cultural Landscapes of Slovakia. Plants in Urban Areas and Landscape. Nitra: SPU, p. 7 – 13.

TÓTH, A. et al. 2019. Small Sacral Christian Architecture in the Cultural Landscapes of Europe. Acta Horticul-turae et Regiotecturae, 22, 1, p. 1 – 7.

TüRK, K. H. 1979. Christliche Kleindenkmale in Börde und Neffeltal. Köln: RheinlandVerlag. 240 p.

TROJANOWSKA, M. 2018. Sacred Places in Public Open Green Areas.Teka Komisji Urbanistyki i Architektury Pan Oddział w Krakowie, Krakow, p. 419 – 429.

VEREŠOVÁ, M. – SUPUKA, J. 2013. Changes of landscape structure and cultural values of vineyard landscape. Acta Universitatis Agriculturae et Silviculturae Mendelianae Brunensis, 61, p. 1459 – 1470.

Available on internet: (http://slovania.czweb.org/Uctievanie.htm)

Maps used as background: http://mapka.gku.sk

Contact address

doc. Ing. Gabriel Kuczman, PhD. (supervisor), Department of Landscape Architecture, Slovak University of Agriculture in Nitra, Tulipánová 7, 949 01 Nitra, Slovakia, gabriel.kuczman@uniag.sk

Ing. Denis Bechera, Department of Landscape Architecture, Slovak University of Agriculture in Nitra, Tulipánová 7, 949 01 Nitra, Slovakia, xbechera@uniag.sk

ARTICLE HISTORY:
Received 23 April 2021
Received in revised form 5 May 2021
Accepted 20 May 2021

BIOLOGICAL AND ANTIBIOFILM ACTIVITY OF *ORIGANUM VULGARE* ESSENTIAL OIL

Lucia GALOVIČOVÁ[1], Petra BOROTOVÁ[1,2], Jana ŠTEFÁNIKOVÁ[2], Veronika VALKOVÁ[1,2], Miroslava KAČÁNIOVÁ[1,3]

[1]Slovak Agriculture University in Nitra, SLOVAKIA

[2] AgroBioTech Research Centre, SLOVAKIA

[3] University of Rzeszow, POLAND

Abstract

The work was aimed to evaluate the antioxidant, antimicrobial, and antibiofilm activity of the essential oil *Origanum vulgare* against *Stenotrophomonas maltophilia* and *Bacillus subtilis*. To evaluate the molecular profiles of biofilms on glass and wood after application of *O. vulgare* essential oil using MALDI-TOF MS Biotyper. The essential oil showed strong antioxidant activity of 77.2 ± 0.8 % inhibition, corresponding to 433.56 ± 4.4 TEAC. Strong antimicrobial activity is demonstrated by low minimum inhibitory concentrations against biofilm-forming bacteria. Higher efficacy against gram-negative microorganisms was found. The lowest minimum inhibitory concentrations ranged from 0.2-58.73 µl/ml. Based on the analysis of mass spectra and created dendrograms, we found that the essential oil of *O. vulgare* affects the disruption of the polysaccharide matrix surrounding the bacteria in the form of a biofilm, thereby reducing their resistance. MALDI-TOF MS Biotyper is a suitable tool for the analysis of biofilms, which is a prerequisite for its use in food and clinical practice.

Keywords: *Origanum vulgare*, biofilm, *Stenotrophomonas maltophilia*, *Bacillus subtilis*

Introduction

Origanum vulgare L. is an aromatic herb widely used worldwide for flavouring various foods (Azizi et al., 2009). The plant has been used for centuries as a medicinal herb in ethnopharmacological preparations for the treatment of various diseases, such as cough, indigestion, menstrual problems, bronchitis, and asthma. It is often used as a carminative, diaphoretic, expectorant, stimulant, antioxidant, antihypertensive, anti-inflammatory, and antimicrobial agent among other medical applications (Sarikurkcu et al., 2015).

Along with plant compounds are essential oils, characterized as aromatic oil liquids. It has been found in the past that some essential oils have antimicrobial properties. In recent years, they have been analysed as possible alternatives to synthetic antimicrobials. Many essential oils from plants are characterized by strong antioxidant activity. Plants synthesize them by various plant organs, including leaves, stems, flowers, or fruits (Marques et al., 2015).

Many essential oils have an antioxidant properties, and the interest to use the essential oils as natural antioxidants is growing because some synthetic antioxidants such as BHA (butylated hydroxyanisole) and BHT (Butylated hydroxytoluene) are currently suspected to be potentially harmful to human health. The addition of essential oils to edible products, either by direct mixing or active packaging material and edible coatings, may therefore be a possible alternative to prevent autoxidation and prolong shelf life (Amorati et al., 2013).

Ingredients of essential oils with phenolic structures, such as carvacrol, eugenol, and thymol, are highly effective against plant pathogens. The application of essential oils is a very attractive method for controlling plant diseases due to its antimicrobial effects as well as their use after harvesting crops can extend durability of the plants (Gurjar et al., 2012).

Bacteria try to survive in inhospitable conditions and therefore began to form biofilms. The biofilm formed on the teeth was observed in 1683 by Antoni van Leeuwenhoek using a primitive microscope. However, the biofilm form of microorganisms was out of interest to medical microbiologists until the early 1970s, when they observed an association between the etiology of persistent infection and bacterial aggregates in patients with cystic fibrosis (Høiby, 2017).

Bacterial biofilms are clusters of bacteria that are attached to the surface or to each other and are incorporated into their own matrix. The biofilm matrix consists of substances such as proteins and polysaccharides. In addition to the protection provided by the matrix, bacteria in biofilms can use several survival strategies to avoid the host's defence system. This form is more resistant to antimicrobials, more resistant to antibiotics, and better resistant to environmental changes (Hall-Stoodley and Stoodley, 2009).

Stenotrophomonas maltophilia is cosmopolitan and ubiquitous bacteria found in a variety of environmental habitats, including extreme ones. *S. maltophilia* has become a global opportunistic human pathogen that does not usually infect healthy hosts but is associated with high morbidity and mortality in severely immunocompromised and debilitated individuals (An and Berg, 2018). It is also often found in the food industry, for example in raw milk, fish products, vegetables, and in drinking water reservoirs. The presence of *S. maltophilia* in food products causes degradation and also significantly endangers human health (Zhang et al., 2020).

Bacillus subtilis, a non-pathogenic, gram-positive bacterium, is one of the most studied biofilm-forming microorganisms. Its importance in the food industry lies in the formation of a colony biofilm at the water-air interface (Yahav et al., 2018). *B. subtilis* can be isolated from a variety of environments, from soil to marine habitats (Kovács, 2019).

The work was aimed to evaluate the antioxidant, antimicrobial, and antibiofilm activity of the essential oil *Origanum vulgare* against *Stenotrophomonas maltophilia* and *Bacillus subtilis*. The molecular profiles of biofilms on glass and wood were evaluated after application of *O. vulgare* essential oil using MALDI-TOF MS Biotyper.

Material and methods

Microorganisms (*Bacillus subtilis* CCM 2772, *Pseudomonas aeruginosa* CCM 1959, *Staphylococcus aureus* subsp. *aureus* CCM 2461, *Yersinia enterocolitica* CCM 5671, *Enterococcus faecalis* CCM 4224, *Salmonella enteritidis* subsp. *enteritidis* CCM 4420, *Candida krusei* CCM 8271, *Candida albicans* CCM 8186, *Candida tropicalis* CCM 8223, *Candida glabrata* CCM 8270) for analyses were obtained from the Czech collection of microorganisms. The bacteria forming the biofilm *Bacillus subtilis* and *Stenotrophomonas maltophil*ia were obtained from the dairy industry. They were identified by 16S rRNA sequencing and MALDI-TOF MS Biotyper.

Origanum vulgare essential oil was purchased from Hanus, s.r.o. (Nitra, Slovakia). It was prepared by steam distillation of fresh stalk. It was stored in the dark at 4 °C throughout the analyses.

Analysis of the antioxidant activity of *O. vulgare* essential oil was performed according to Bajčan et al. (2013) with modification to a 96-well microplate. A calibration curve was prepared with a standard solution of Trolox (Sigma Aldrich, Germania) in a concentration range of 0-100 µg/ml. The 96-well microplate was incubated for 30 minutes on a shaker (IKA Inc., Staufen im Breisgau, Germany) at 200 rpm in the dark. Absorbance was measured by spectrophotometer Glomax (Promega Inc., Madison, USA) at 515 nm against methanol. The percentage of inhibition was calculated as (A0-AA)/A0 × 100, where A0 was the absorbance of blank measurement and AA was the absorbance of sample. Antioxidant activity was expressed as antioxidant activity of Trolox related to 1 mL of sample (TEAC).

The agar microdilution method was used to determine the minimum inhibitory concentrations (MIC). All tested microorganisms were precultivated in Mueller Hinton broth (MHB) for 24 h under optimal growth conditions for each species. The bacterial inoculum was prepared to a density of 0.5 McF. 50 µl of inoculum per well was pipetted into the microplate. 100 µl MHB was added to each well. Subsequently, 100 µl of *O. vulgare* essential oil was added by serial dilution at concentrations of 400-0.1953125 µl/ml. MHB with essential oil was used as a negative control. The inoculum together with MHB was used as a control for maximal growth. The minimum inhibitory concentrations for the biofilm were determined as in work Kačániová et al. (2020a). Absorbance was measured with Glomax spectrophotometer (Promega Inc., Madison, WI, USA) at 570 nm. The analysis was performed in triplicate and the mean (n = 3) was used for further calculations.

Biofilm structure changes under the influence of *O. vulgare* essential oil were evaluated on a slide and a wooden toothpick using MALDI-TOF MS Biotyper. The experiment, including control groups, was performed in 50 ml polypropylene centrifuge tubes. A slide and a wooden toothpick were placed in the tubes, followed by the addition of 20 ml of MHB and 50 µl of bacterial inoculum prepared as in the method of minimum inhibitory concentrations. The experimental groups contained 0.1 % addition of *O. vulgare* essential oil. Samples were evaluated on days 3, 5, 7, 9, 12, and 14. Throughout the experiment, samples were placed on a shaker at inclination 45 °, 170 rpm, and 37 °C. Subsequent analysis of the developmental phases of the biofilm and evaluation of the molecular differences of the biofilms was performed in the same way as in Kačániová et al. (2020a) using MALDI-TOF MS Biotyper.

The measurements were repeated three times. Statistical variability of the data was processed using Microsoft-Excel® software. Results of the MIC value (concentration causing 50 % and 90 % reduction in bacterial growth) was determined by logit analysis. Statistical evaluation of the antioxidant activity of the obtained data was performed using GraphPad Prism 8.0.1 (GraphPad

Software Incorporated, San Diego, CA, USA). One-way analysis of variance (ANOVA) followed by Tukey's test was used for statistical analysis.

Results and discussion

Using the DPPH method, the free radical scavenging activity was determined at 77.2 ± 0.8 % inhibition, which corresponds to 433.56 ± 4.4 TEAC. There is not any standard method for measurement of antioxidant activity by DPPH and each research contains variations (solvent, incubation time, ratio of sample and DPPH solution), which makes results difficult to compare. Dutra et al. (2019) used 25 µl of essential oil and 2 ml of DPPH in the analysis and the absorbance was measured at 517 nm. They set the free radical scavenging activity at 363 TEAC. Chun et al. (2005) used DPPH diluted in ethanol, the reaction was performed in the ratio of 60 µl of essential oil and 1 ml of DPPH, the reaction was incubated for 15 minutes and the absorbance was measured at 517 nm. Using their method, they determined the antioxidant activity of *O. vulgare* to 80 %. Benedec et al. (2018) used 1 ml of DPPH diluted in ethanol and 1 ml of *O. vulgare* essential oil to determine the antioxidant activity of 70.61 ± 4.39 %. Simirgiotis et al. (2020) used 100 µl of *O. vulgare* essential oil and 2 ml of DPPH diluted in ethanol. The absorbance was measured at 517 nm and the IC_{50} of 4750 ± 91.11 µg/ml was calculated. Despite the differences in procedures as well as the expression of the results, the authors agreed on a relatively high antioxidant activity. This finding provides a premise for the use of *O. vulgare* essential oil as a source of natural antioxidants.

The minimum inhibitory concentrations for the microorganisms we tested are given in Table 1. The lowest inhibitory concentrations were recorded against the yeasts *C. glabrata* and *C. krusei* followed by gram-negative bacteria *S. enteritidis*, *S. aureus,* and *S. maltophilia*, then gram-positive *B. subtilis*. For the other tested microorganisms, the minimum inhibitory concentrations were markedly higher. The analysis shows that *O. vulgare* essential oil is suitable for the inhibition of biofilm-forming microorganisms. Another finding is that its effectiveness against gram-negative microorganisms is higher than against gram-positive microorganisms. Karaman et al. (2017) found out in their work MIC for *S. aureus* 11.4 µl/ml and *E. coli* 45.4 µl/ml. Teles et al. (2018) determined MIC for *P. aeruginosa* 483.3 ± 28.87 µl/ml. Khan et al. (2019) determined a MIC for *P. aeruginosa* 430 µl/ml and *S. aureus* 15 µl/ml. Hashemi et al. (2017) determined MIC for *S. aureus* and *B. cereus* 6.25 µl/ml. Busatta et al. (2007) found an MIC for *E. faecalis* 460 µl/ml. Özkalp et al. (2010) determined a MIC 64 µl/ml for *C. albicans*. Souza et al. (2006) determined

MIC for *C. tropicalis* 160 µl/ml and *C. albicans* 40 µl/ml. Differences in MIC values for the same species of microorganisms may be due to the different strains of the individual species as well as the origin of the plants for the preparation of the extract and also to the extraction method itself. Due to its antimicrobial properties, *O. vulgare* essential oil could be a suitable alternative to the antimicrobials used today.

Table 1 Minimal inhibition concentration

Microorganism	**MIC 50 ul/ml**	**MIC 90 ul/ml**
S. enteritidis	4.12	5.72
S. aureus	7.33	19.42
E. faecalis	270.68	513.86
P. aeruginosa	428.30	598.41
Y. enterocolitica	255.95	297.96
C. tropicalis	139.81	432.40
C. glabrata	0.57	3.01
C. krusei	0.02	2.43
C. albicans	58.73	144.04
S. maltophilia	6.25	12.5
B. subtilis	12.50	25.00

Figure 1 shows the developmental spectra of the developmental stages of *S. maltophilia* biofilm throughout the length of the experiment. *O. vulgare* essential oil was added to the experimental groups. The spectra were arranged in pairs according to their degree of growth on different surfaces except for planktonic spectra. Planktonic spectra were obtained from the culture medium of the control group as a representative spectrum for comparison between the experimental and control groups. In the control group, the similar toity of biofilm spectra on different surfaces and planktonic spectra on individual days was maintained.

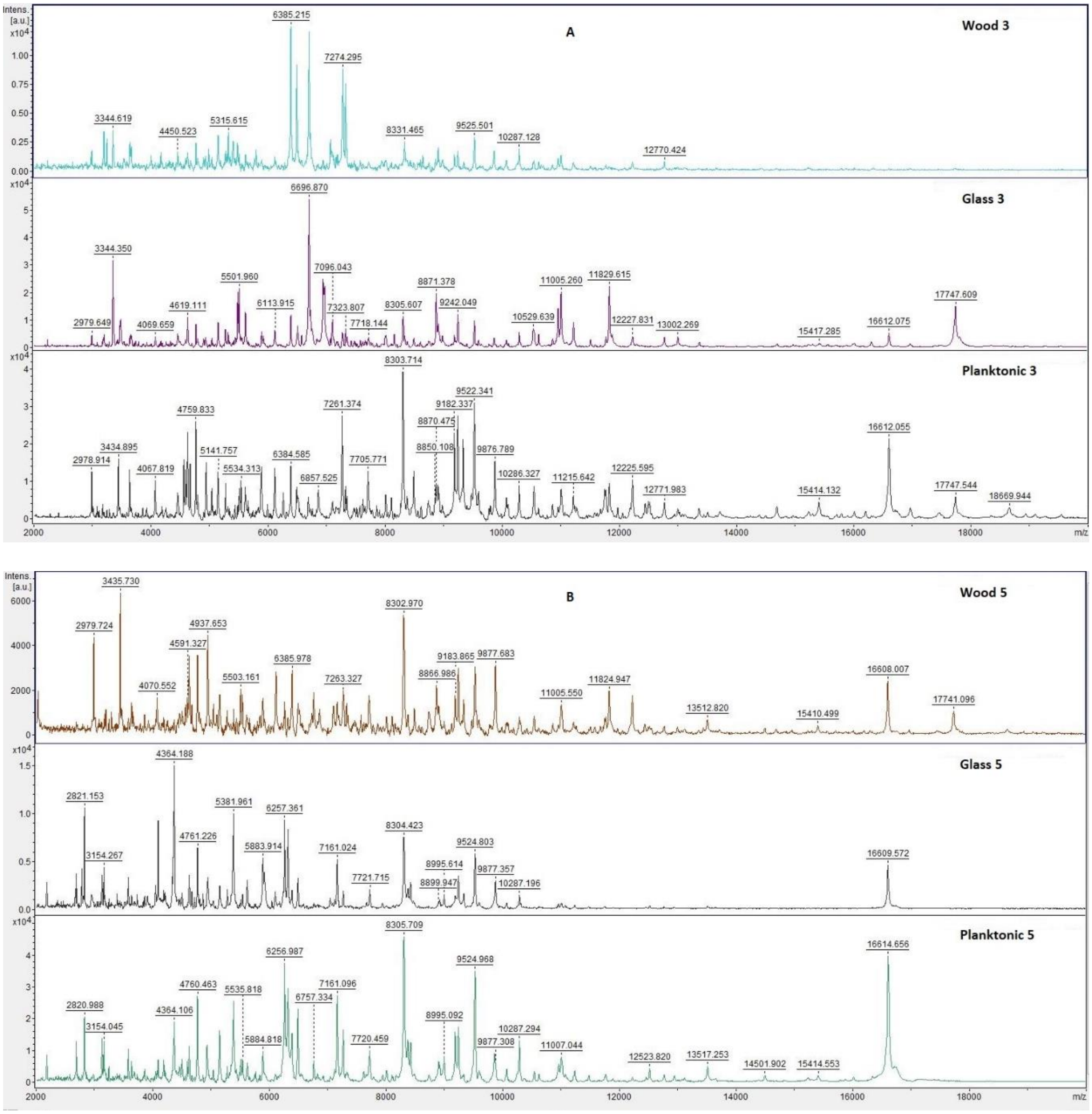
A
Wood 3
Intens. [a.u.]
x10^4
6385.215
7274.295
3344.619
4450.523
5315.615
8331.465
9525.501
10287.128
12770.424
Glass 3
6696.870
3344.350
7096.043
5501.960
8871.378
11005.260
11829.615
17747.609
2979.649
4069.659
4619.111
6113.915
7323.807
7718.144
8305.607
9242.049
10529.639
12227.831
13002.269
15417.285
16612.075
Planktonic 3
8303.714
9522.341
9182.337
7261.374
4759.833
8870.475
8850.108
3434.895
5141.757
6384.585
9876.789
2978.914
4067.819
5534.313
6857.525
7705.771
10286.327
11215.642
12225.595
12771.983
15414.132
16612.055
17747.544
18669.944
m/z
B
Wood 5
3435.730
2979.724
4937.653
4591.327
4070.552
5503.161
6385.978
7263.327
8302.970
8866.986
9183.865
9877.683
11005.550
11824.947
13512.820
15410.499
16608.007
17741.096
Glass 5
4364.188
2821.153
3154.267
4761.226
5381.961
5883.914
6257.361
7161.024
7721.715
8304.423
8995.614
8899.947
9524.803
9877.357
10287.196
16609.572
Planktonic 5
8305.709
6256.987
9524.968
16614.656
4760.463
5535.818
7161.096
6757.334
2820.988
3154.045
4364.106
5884.818
7720.459
8995.092
9877.308
10287.294
11007.044
12523.820
13517.253
14501.902
15414.553
2000
4000
6000
8000
10000
12000
14000
16000
18000
m/z

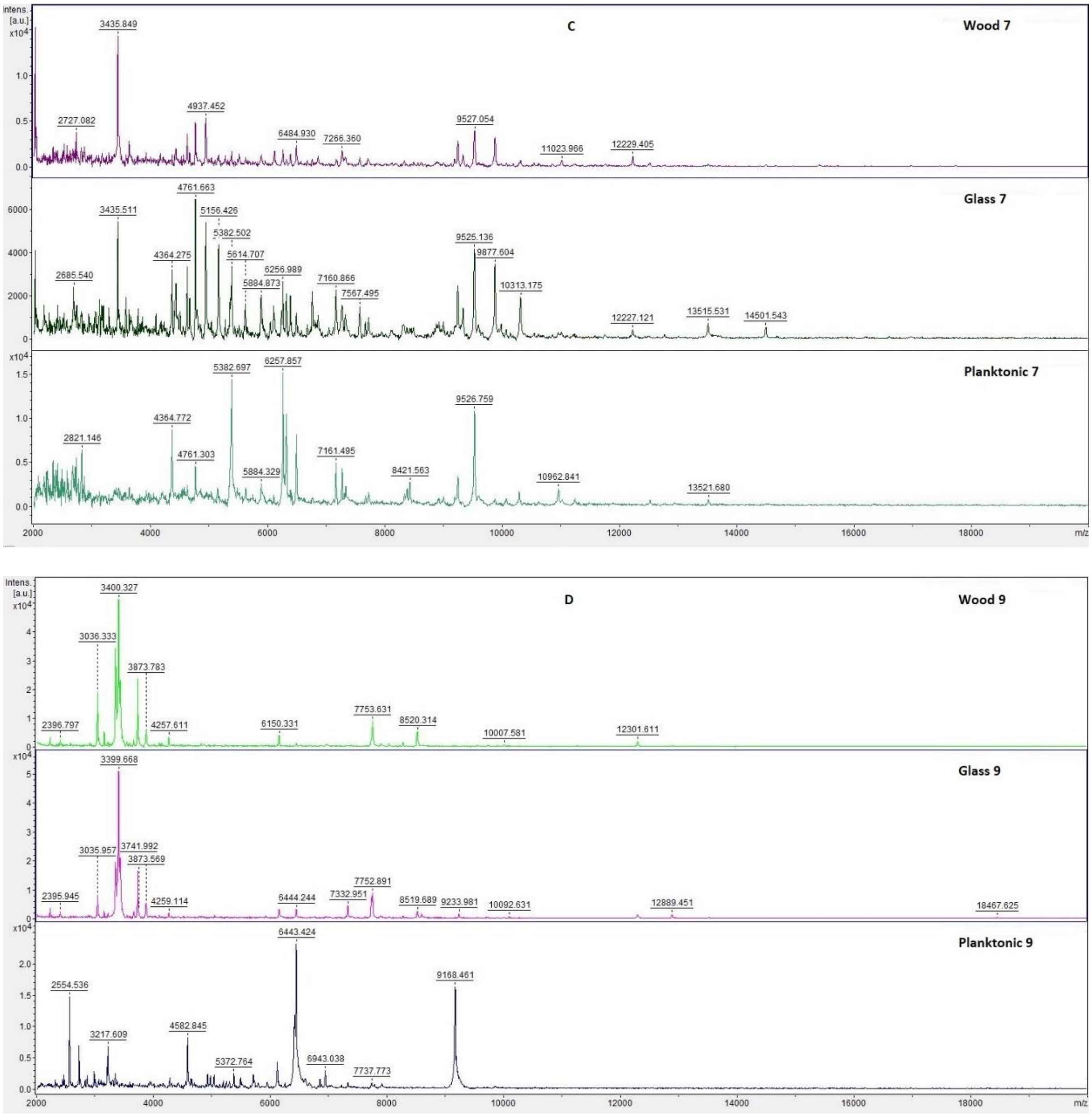
C
Wood 7
Intens. [a.u.] x10^4
3435.849
2727.082
4937.452
6484.930
7266.360
9527.054
11023.966
12229.405
Glass 7
4761.663
3435.511
5156.426
5382.502
4364.275
5614.707
2685.540
6256.989
5884.873
7160.866
7567.495
9525.136
9877.604
10313.175
12227.121
13515.531
14501.543
Planktonic 7
x10^4
5382.697
6257.857
4364.772
2821.146
4761.303
5884.329
7161.495
8421.563
9526.759
10962.841
13521.680
2000
4000
6000
8000
10000
12000
14000
16000
18000
m/z
D
Wood 9
Intens. [a.u.] x10^4
3400.327
3036.333
3873.783
2396.797
4257.611
6150.331
7753.631
8520.314
10007.581
12301.611
Glass 9
x10^4
3399.668
3035.957
3741.992
3873.569
2395.945
4259.114
6444.244
7332.951
7752.891
8519.689
9233.981
10092.631
12889.451
18467.625
Planktonic 9
x10^4
6443.424
9168.461
2554.536
3217.609
4582.845
5372.764
6943.038
7737.773
2000
4000
6000
8000
10000
12000
14000
16000
18000
m/z

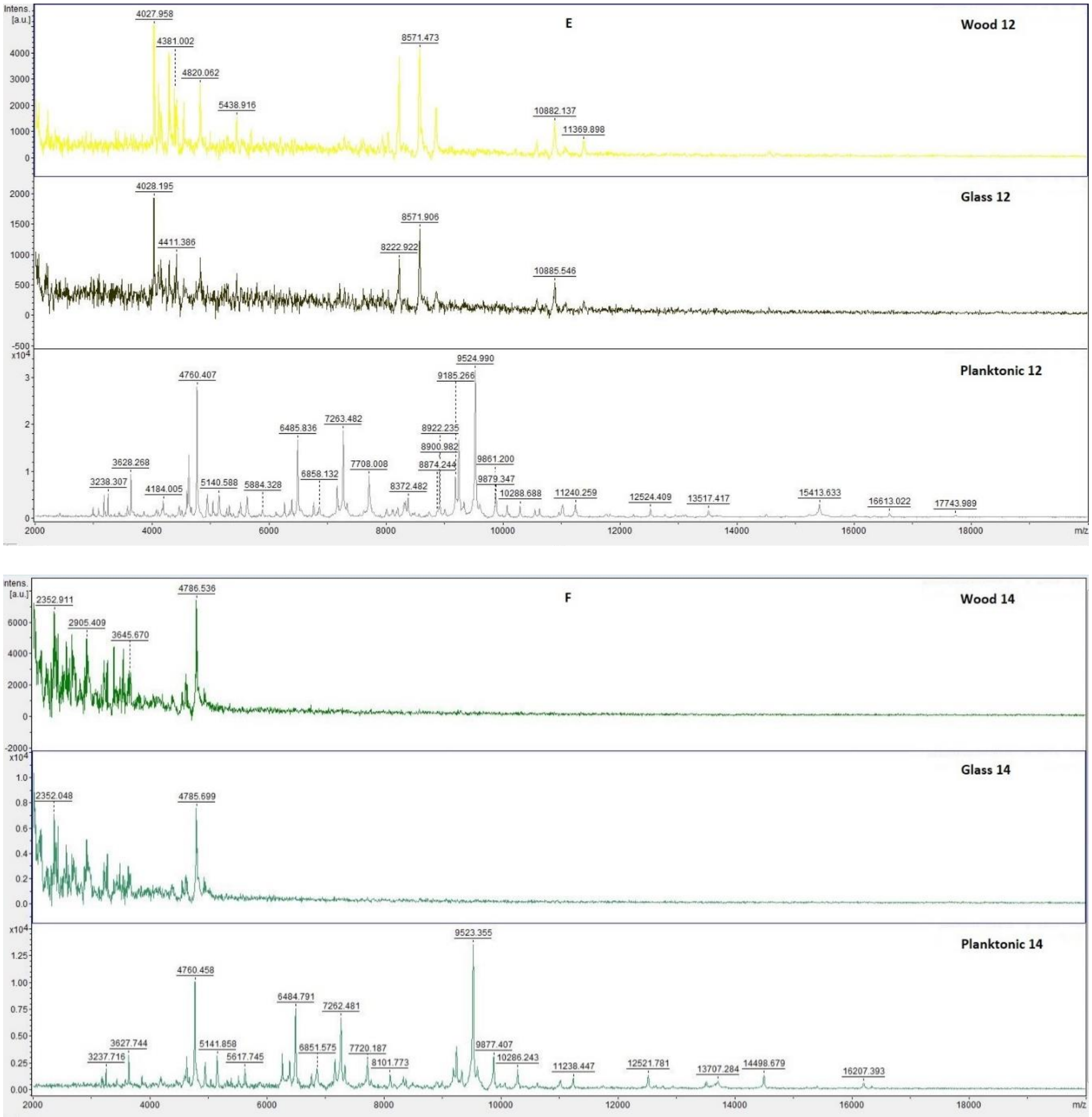

Figure 1 Representative MALDI-TOF mass spectra of *S. maltophilia*: A - 3rd day; B - 5th day; C - 7th day; D - 9th day; E - 12th day; F - 14th day

From the results of the analysis of the mass spectra of *S. maltophilia*, the comparable experimental spectra of the third and fifth day with the control planktonic spectra can be observed (Figure 1 A-B). On the seventh day of the experiment, there is a slight difference between the experimental groups and the control spectrum (Figure 1 C). From the ninth day to the end of the experiment, a significant difference between the experimental groups compared to the control planktonic spectrum was observed while maintaining the similarity of the experimental spectra (Figure 1 D-F).

From the constructed dendrogram (Figure 2) based on the distance of MSP (Main Spectra Profiles), it can be stated that the planktonic stage (P) had the shortest distance together with the control groups and with the young biofilms of the experimental group 3rd and 5th day in both groups. As the days went by, the distance of MSP experimental groups increased. The constructed dendrogram is in accordance with the findings of the mass spectral analysis of MALDI-TOF MS Biotyper. As the days progressed, the inhibitory effect of *O. vulgare* essential oil on the biofilm structure increased, which was reflected as an increase in the distance of the MSP dendrogram from the control group and planktonic cells. The greatest distance of MSP is between the experimental groups 12th and 14th days and planktonic cells.

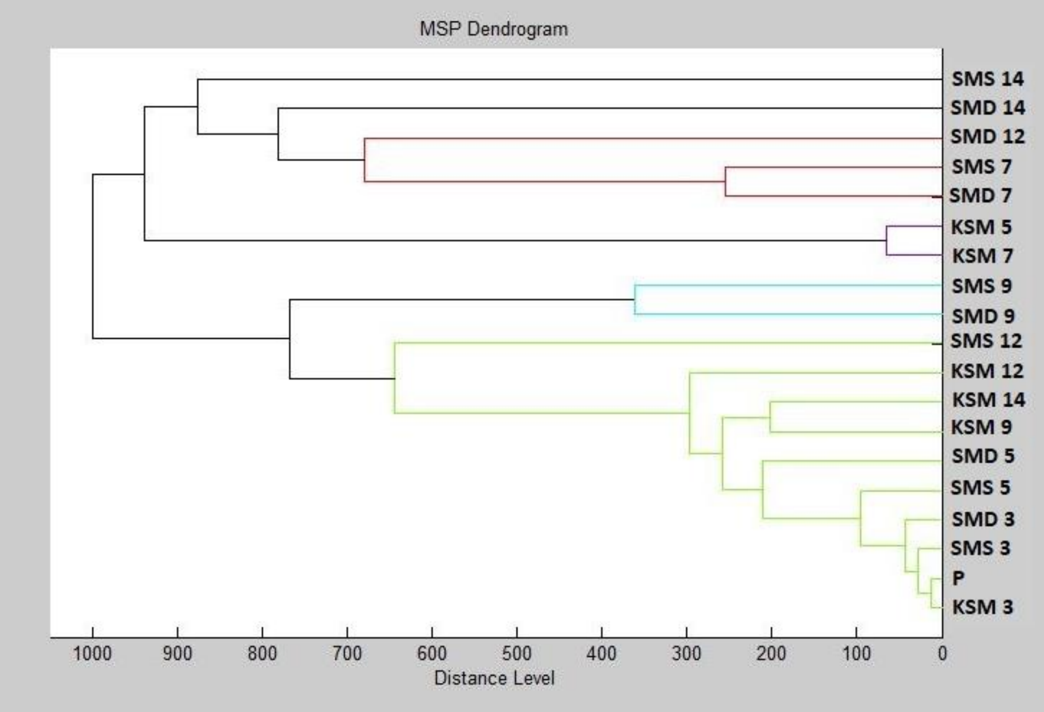

Figure 2 Dendrogram of *S. maltophilia* generated using the MSPs for planktonic cells and control. Symbols in the abbreviations are as follows: **SM** – *S. maltophilia*; **K**-control; **S**-glass; **D**-wood; **P**-planktonic cells

Figure 3 shows the developmental spectra of the developmental stages of *B. subtilis* biofilm throughout the length of the experiment. *O. vulgare* essential oil was added to the experimental groups. The spectra were arranged in pairs according to their degree of growth on different surfaces except for planktonic spectra. Planktonic spectra were obtained from the culture medium of the control group as a representative spectrum for comparison between the experimental and control groups. In the control group, the similarity of biofilm spectra on different surfaces and planktonic spectra on individual days was maintained.

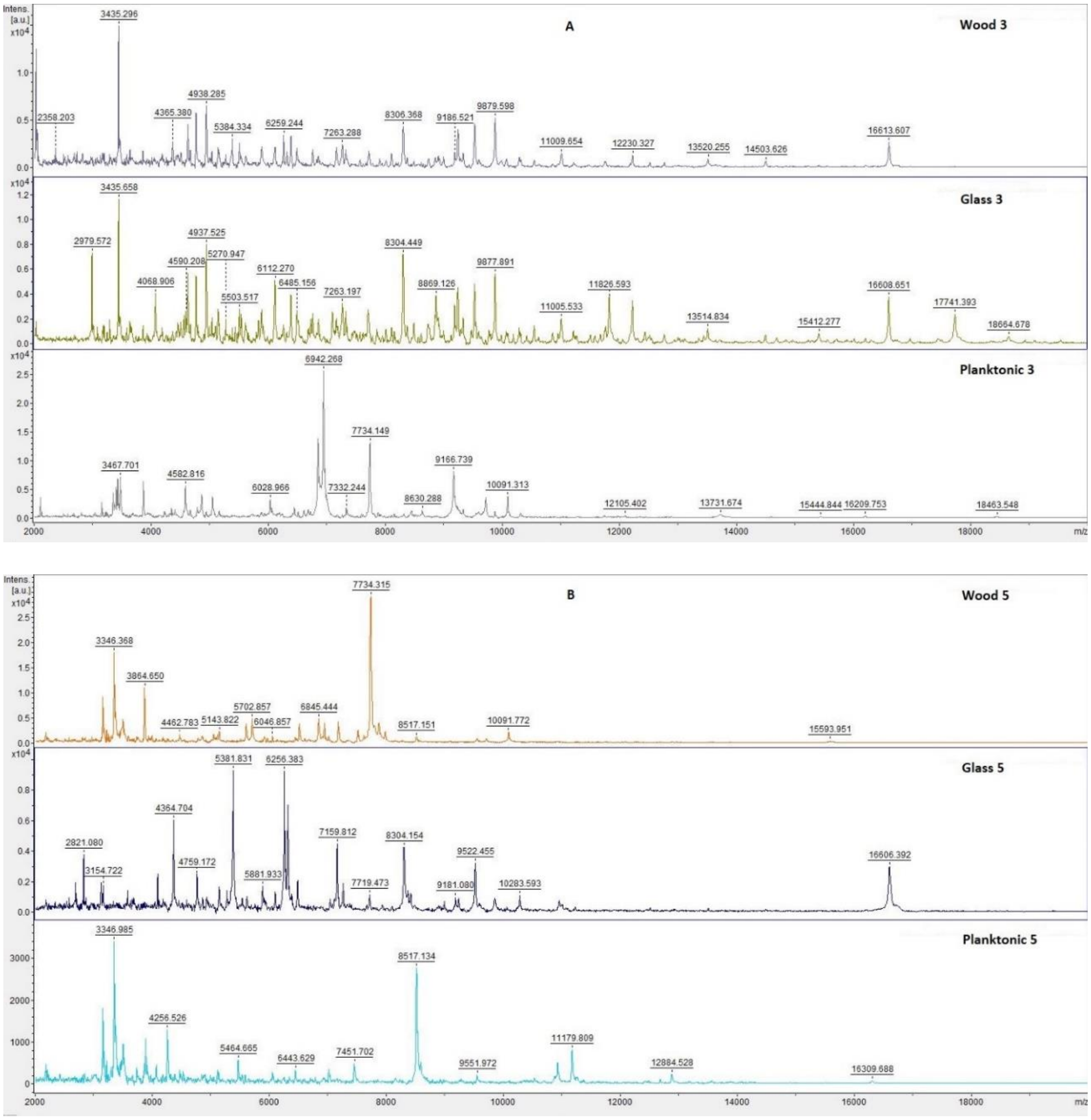

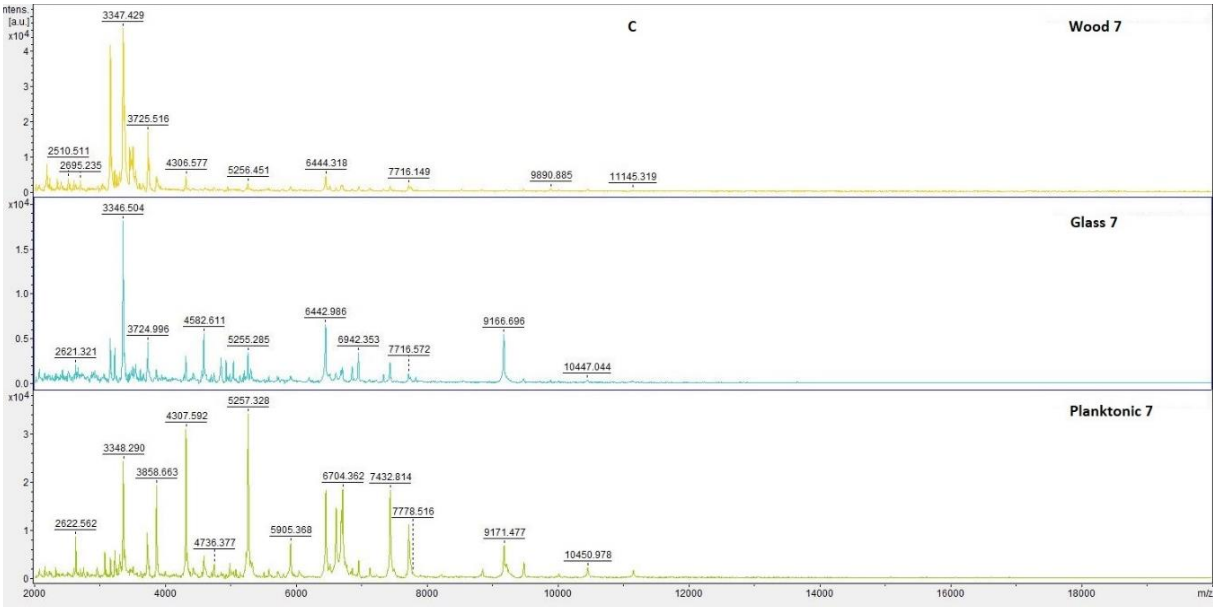
C
Intens. [a.u.]
x10⁴
Wood 7
3347.429
3725.516
2510.511
2695.235
4306.577
5256.451
6444.318
7716.149
9890.885
11145.319
Glass 7
3346.504
2621.321
3724.996
4582.611
5255.285
6442.986
6942.353
7716.572
9166.696
10447.044
Planktonic 7
5257.328
4307.592
3348.290
3858.663
2622.562
4736.377
5905.368
6704.362
7432.814
7778.516
9171.477
10450.978
2000
4000
6000
8000
10000
12000
14000
16000
18000
m/z

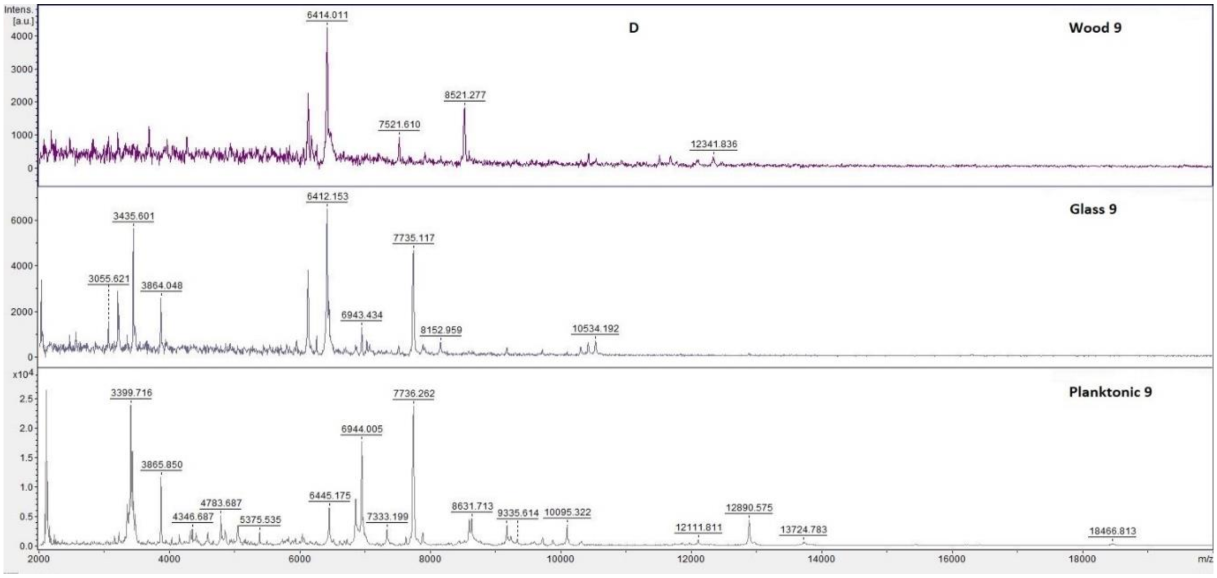
D
Intens. [a.u.]
Wood 9
6414.011
7521.610
8521.277
12341.836
Glass 9
6412.153
3435.601
3055.621
3864.048
7735.117
6943.434
8152.959
10534.192
x10⁴
Planktonic 9
3399.716
7736.262
6944.005
3865.850
4346.687
4783.687
5375.535
6445.175
7333.199
8631.713
9335.614
10095.322
12111.811
12890.575
13724.783
18466.813
2000
4000
6000
8000
10000
12000
14000
16000
18000
m/z

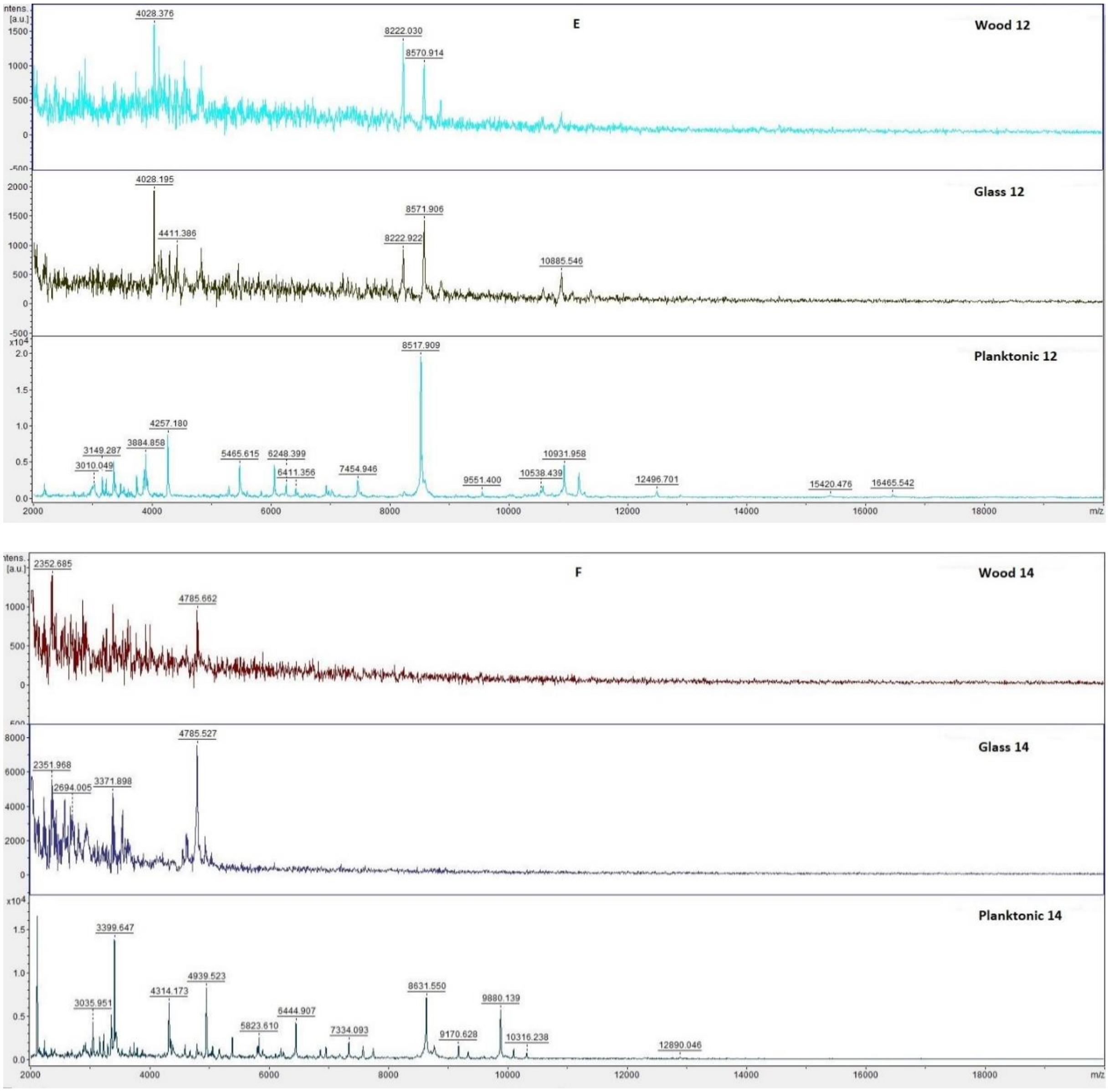

Figure 3 Representative MALDI-TOF mass spectra of *B. subtilis*: A – 3rd day; B - 5th day; C - 7th day; D - 9th day; E - 12th day; F - 14th day

From the results of the analysis of the mass spectra of *B. subtilis*, the similarity of the experimental spectra with the planktonic spectrum on the 3rd and 5th day of the experiment can be observed (Figure 3 A-B). On day 7 of the experiment, the difference of the experimental spectrum obtained from wood compared to the control planktonic spectrum can be seen, while the experimental spectrum from glass is approximate to the planktonic spectrum (Figure 3 C). From day 9, the difference of both experimental spectra compared to the planktonic spectrum can be seen until the end of the experiment, while the experimental spectra are similar to each other (Figure 3 D-F).

From the constructed dendrogram (Figure 4) based on the distance of MSP, it can be stated that the planktonic stage (P) had the shortest distance together with the control groups and with the young biofilms of the experimental group 3 and 5 days in both groups. On the seventh day of the experiment, we can see a shorter distance of the experimental group made of glass compared to the distance of the group of wood. The constructed dendrogram is in accordance with the findings of the mass spectral analysis of MALDI-TOF MS Biotyper. As the days progressed, the inhibitory effect of *O. vulgare* essential oil on the biofilm structure increased, which was reflected in an increase in the distance of the MSP dendrogram from the control group and planktonic cells. The greatest distance of MSP is between the experimental groups 9th and 14th days and planktonic cells.

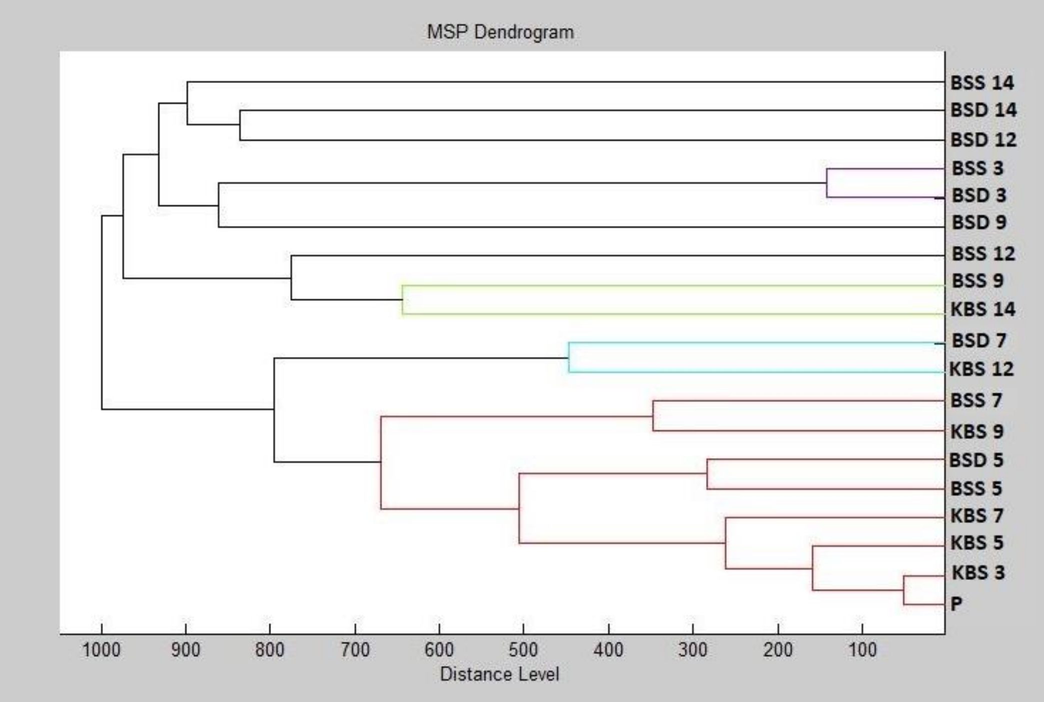

Figure 4 Dendrogram of *B. subtilis* generated using the MSPs for planktonic cells and control. Symbols in the abbreviations are as follows: **BS** – *B. subtilis*; **K**-control; **S**-glass; **D**-wood; **P**-planktonic cells

Aguiar et al. (2021) found that MALDI-TOF MS was able to detect specific biofilm proteins because the mass spectra of the isolates represented differences compared to non-producing strains. Kačániová et al. (2020a) analyzed the effect of *Coriandrum sativum* essential oil on the inhibition of *S. maltophilia* and *B. subtilis* biofilm and in another work, Káčaniová et al. (2020b) analyzed *Citrus aurantium*. They used the MALDI-TOF MS Biotyper method in their work and the result was the demonstration of the inhibitory effect of these essential oils. Our findings supported by the authors are proof of the suitability of MALDI-TOF MS Biotyper for the analysis of structural and molecular differences of biofilm.

Conclusions

The results of our analysis show that *O. vulgare* essential oil has strong antioxidant and antimicrobial activity. Its minimum inhibitory concentrations were lower for gram-negative bacteria compared to gram-positive microorganisms. Very low inhibitory concentrations against biofilm-forming bacteria *S. maltophilia* and *B. subtilis* are proof of suitability for combating bacterial biofilms. Analysis of the mass spectra by MALDI-TOF MS Biotyper and the constructed dendrograms showed that the essential oil of *O. vulgare* indicated changes in the structure of the biofilm in both tested microorganisms. These structural changes are evidence of the inhibitory effect of *O. vulgare* against biofilm-forming microorganisms. The effect of the essential oil on the structure of the biofilm may be disrupting the polysaccharide matrix surrounding the bacteria in the form of a biofilm, thereby reducing their resistance. MALDI-TOF MS Biotyper is a suitable tool for the analysis of biofilms, which is a prerequisite for its use in food and clinical practice.

Acknowledgment

This work has been supported by the grants of the VEGA no. 1/0180/20.

References

AGUIAR, A. P. et al. 2021. Rapid detection of biofilm-producing *Candida* species via MALDI-TOF mass spectrometry. Journal of Applied Microbiology [online], vol. n/a, pp. n/a [cit. 2021-04-17]. ISSN: 1365-2672. Available on internet: DOI: 10.1111/jam.15066

AN, Sh. - BERG, G. 2018. *Stenotrophomonas maltophilia*. Trends in microbiology [online], vol. 26, no. 7, pp. 637-638 [cit. 2021-04-17]. ISSN: 0966-842X. Available on internet: DOI: 10.1016/j.tim.2018.04.006

AZIZI, A. et al. 2009. Herbage yield, essential oil content and composition of three oregano (*Origanum vulgare* L.) populations as affected by soil moisture regimes and nitrogen supply. Industrial Crops and Products [online], vol. 29, no. 2-3, pp. 554-561 [cit. 2021-04-17]. ISSN: 0926-6690. Available on internet: DOI: 10.1016/j.indcrop.2008.11.001

BAJČAN, D. et al. 2013. Antioxidant Potential of Spinach, Peas, and Sweetcorn in relation to Freezing Period. Czech Journal of Food Sciences [online], vol. 31, no. 6, pp. 613-618 [cit. 2021-04-17]. ISSN: 1805-9317. Available on internet: DOI: 10.17221/529/2012-CJFS

BENEDEC, D. et al. 2018. *Origanum vulgare* mediated green synthesis of biocompatible gold nanoparticles simultaneously possessing plasmonic, antioxidant and antimicrobial properties. International Journal of Nanomedicine [online], vol. 13, pp. 1178-2013 [cit. 2021-04-17]. ISSN: 1359-5113. Available on internet: DOI: 10.2147/IJN.S149819

BUSATTA, C. et al. 2007. Evaluation of *Origanum vulgare* essential oil as antimicrobial agent in sausage. Brazilian Journal of Microbiology [online], vol. 38, no. 4, pp. 1-2 [cit. 2021-04-17]. ISSN: 1678-4405. Available on internet: DOI: 10.1590/S1517-83822007000400006

CHUN, S. S. et al. 2005. Phenolic antioxidants from clonal oregano (*Origanum vulgare*) with antimicrobial activity against *Helicobacter pylori*. Process Biochemistry [online], vol. 40, no. 2, pp. 809-816 [cit. 2021-04-17]. ISSN: 1359-5113. Available on internet: DOI: 10.1016/j.procbio.2004.02.018

DUTRA, T. et al. 2019. Bioactivity of oregano (*Origanum vulgare*) essential oil against *Alicyclobacillus* spp. Industrial Crops and Products [online], vol. 129, pp. 345-349 [cit. 2021-04-17]. ISSN: 0926-6690. Available on internet: DOI: 10.1016/j.indcrop.2018.12.025

HALL-STOODLEY, L. - STOODLEY, P. 2009. Evolving concepts in biofilm infections. Cellular Microbiology [online], vol. 11, no. 7, pp. 1034-1043 [cit. 2021-04-17]. ISSN: 1462-5822. Available on internet: DOI: 10.1111/j.1462-5822.2009.01323.x

HASHEMI, S. M. B. et al. 2017. Efficiency of Ohmic assisted hydrodistillation for the extraction of essential oil from oregano (*Origanum vulgare* subsp. *viride*) spices. Innovative Food Science &

Emerging Technologies [online], vol. 42, pp. 172-178 [cit. 2021-04-17]. ISSN: 1466-8564. Available on internet: DOI: 10.1016/j.ifset.2017.03.003

HØIBY, N. 2017. A short history of microbial biofilms and biofilm infections. Journal of pathology, microbiology and imunology [online], vol. 125, no. 4, pp. 272-275 [cit. 2021-04-17]. ISSN: 1600-0463. Available on internet: DOI: 10.1111/apm.12686

KAČÁNIOVÁ, M. et al. 2020a. Antioxidant, Antimicrobial and Antibiofilm Activity of Coriander (*Coriandrum sativum* L.) Essential Oil for Its Application in Foods. Foods [online], vol. 9, no. 3, pp. 282 [cit. 2021-04-17]. ISSN: 2304-8158. Available on internet: DOI: 10.3390/foods9030282

KAČÁNIOVÁ, M. et al. 2020b. Biological Activity and Antibiofilm Molecular Profile of *Citrus aurantium* Essential Oil and Its Application in a Food Model. Molecules [online], vol. 25, no. 17, pp. 3956 [cit. 2021-04-17]. ISSN: 1420-3049. Available on internet: DOI: 10.3390/molecules25173956

KARAMAN, M. et al. 2017. *Origanum vulgare* essential oil affects pathogens causing vaginal infections. Journal of Applied Microbilogy [online], vol. 122, no. 5, pp. 1177-1185 [cit. 2021-04-17]. ISSN: 1365-2672. Available on internet: DOI: 10.1111/jam.13413

KHAN, M. et al. 2019. Chemical diversity in leaf and stem essential oils of *Origanum vulgare* L. and their effects on microbicidal activities. AMB Express [online], vol. 9, pp. 176 [cit. 2021-04-17]. ISSN: 2191-0855. Available on internet: DOI: 10.1186/s13568-019-0893-3

KOVÁCS, Á. 2019. *Bacillus subtilis*. Trends in microbiology [online], vol. 27, no. 8, pp. 724-725 [cit. 2021-04-17]. ISSN: 0966-842X. Available on internet: DOI: 10.1016/j.tim.2019.03.008

MARQUES, J. et al. 2015. Antimicrobial activity of essential oils of *Origanum vulgare* L. and *Origanum majorana* L. against *Staphylococcus aureus* isolated from poultry meat. Industrial Crops and Products [online], vol. 77, pp. 444-450 [cit. 2021-04-17]. ISSN: 0926-6690. Available on internet: DOI: 10.1016/j.indcrop.2015.09.013

ÖZKALP, B. et al. 2010. The antibacterial activity of essential oil of oregano (*Origanum vulgare* L.). Journal of Food, Agriculture & Environment [online], vol. 8, no. 2, pp. 272-274 [cit. 2021-04-17]. ISSN: 1678-4405. Available on internet: DOI: 10.1234/4.2010.1639

SARIKURKCU, C. et al. 2015. Composition, antioxidant, antimicrobial and enzyme inhibition activities of two *Origanum vulgare* subspecies (subsp. *vulgare* and subsp. *hirtum*) essential oils.

Industrial Crops and Products [online], vol. 70, pp. 178-184 [cit. 2021-04-17]. ISSN: 0926-6690. Available on internet: DOI: 10.1016/j.indcrop.2015.03.030

SIMIRGIOTIS, M. et al. 2020. Antioxidant and Antibacterial Capacities of *Origanum vulgare* L. Essential Oil from the Arid Andean Region of Chile and its Chemical Characterization by GC-MS. Metabolites [online], vol. 10, no. 10, pp. 414 [cit. 2021-04-17]. ISSN: 2218-1989. Available on internet: DOI: 10.3390/metabo10100414

SOUZA, E. L. et al. 2006. Sensitivity of spoiling and pathogen food-related bacteria to *Origanum vulgare* L. (*Lamiaceae*) essential oil. Brazilian Journal of Microbiology [online], vol. 37, no. 4, pp. 272-274 [cit. 2021-04-17]. ISSN: 1678-4405. Available on internet: DOI: 0.1590/S1517-83822006000400023

TELES, A. M. et al. 2019. *Cinnamomum zeylanicum*, *Origanum vulgare*, and *Curcuma longa* Essential Oils: Chemical Composition, Antimicrobial and Antileishmanial Activity. Evidence-Based Complementary and Alternative Medicine [online], vol. 2019, pp. 77-85 [cit. 2021-04-17]. ISSN: 1741-427X. Available on internet: DOI: 10.1155/2019/2421695

YAHAV, S. et al. 2018. Encapsulation of beneficial probiotic bacteria in extracellular matrix from biofilm-forming Bacillus subtilis. Artificial Cells, Nanomedicine, and Biotechnology [online], vol. 46, pp. 974-982 [cit. 2021-04-17]. ISSN: 1073-119. Available on internet: DOI: 10.1080/21691401.2018.1476373

ZHANG, Y. et al. 2020. Antibacterial activity of essential oils against *Stenotrophomonas maltophilia* and the effect of citral on cell membrane. LWT - Food Science and Technology [online], vol. 117, pp. 108667 [cit. 2021-04-17]. ISSN: 1096-1127. Available on internet: DOI: 10.1016/j.lwt.2019.108667

AMORATI, R. et al. 2013. Antioxidant Activity of Essential Oils. Journal of Agricultural and Food Chemistry [online], vol. 61, no. 46, pp. 10835–10847 [cit. 2021-05-01]. ISSN: 1520-5118. Available on internet: DOI: 10.1021/jf403496k

GURJAR, M. S. et al. 2012. Efficacy of plant extracts in plant disease management. Agricultural Sciences [online], vol. 3, no. 3, pp. 9 [cit. 2021-05-01]. ISSN: 2156-8561. Available on internet: DOI: 10.4236/as.2012.33050

Contact address

Ing. Lucia Galovičová, Slovak University of Agriculture in Nitra, Horticulture and Landscape Engineering Faculty, Department of Fruit Sciences, Viticulture and Enology, Tr. A. Hlinku 2, 94976 Nitra, Slovakia, +421 907 260 116, l.galovicova95@gmail.com

ARTICLE HISTORY:
Received 28 April 2021
Received in revised form 13 May 2021
Accepted 20 May 2021

EFFECT OF LIME AND SUGAR ON LIQUID LIMIT OF BENTONITE CLAY

Sanjeet Sahoo[1], Rajesh Pradhan[1], Amod Kumar[1], Janarul Shaikh[1, 2]

[1]C.V. Raman Global University, INDIA

[2]Slovak University of Agriculture in Nitra, SLOVAKIA

Abstract

Literature shows that various geotechnical characteristics like compressibility, permeability, shearing strength and classification of clayey soil significantly depend upon its liquid limit. These properties play very crucial role for the design of geotechnical structures like landfill liner and cover system wherein bentonite clay is used as an important construction material. Explicit knowledge of controlling liquid limit of bentonite (LLB) is thus very essential in such context. The LLB might be affected due to inclusion of sugar or lime which the previous researchers rarely explored. Present study mainly aims to investigate the influence of sugar and lime on the LLB. Different mixes of bentonite clay with various percentages of sugar or lime were tested to determine their liquid limits using Casagrande method. The study indicates initial reduction in LLB with the increase in sugar quantity up to a certain limit which started to rise due to further addition of sugar. Whereas the LLB continuously kept on decreasing with increase in lime quantity considered for the study. It can also be noted that the rate of reduction in LLB with sugar was higher than that with the lime for the limit of their decreasing trend.

Keywords: landfill, bentonite clay, liquid limit, sugar, lime

Introduction

Waste disposal has always created great challenges to mankind since ages.Novel ideas of dealing with various waste have been developed throughout the years with the improvements in science and technology (Kumar et al. 2017; Swati et al. 2018). Rise in populaton and rapid industrial growth increased real estate valueand consciousness about pollution in and around the human settlement (Stein 2019). There is anecessity for a safe and engineered way of waste disposal scraping the old and traditional systemsand so came into existence the concept of engineered disposal of both domestic and industrialwastes (Tausova et al. 2020). Engineered disposal of waste involves separating the waste from natural environmentby putting in place a series of geotechnical barriers to prevent andminimize the interaction between waste and environment (Hoeks et al. 1987; Ferronato and Torretta 2019). It was observed from the available literature that thepossibility of attaining lower hydraulic conductivity ($<10^{-9}$m.s^{-1}) was considered the mostimportant criterion while selecting a geotechnical barrier material (Daniel and Benson 1990). Apart from fulfilling low hydraulic conductivity condtion, a barrieris also should have sufficient shear strength in order to prevent excessive uneven settlementscaused by the overbearing loads (Hoeks and Agelink 1982). As far as the shear strength isconcerned, compacting the barrier material to a higher density using heavy compaction techniqueswas seen to be a solution in the laboratory, which by the way isn’t always possible in site (Daniel and Wu 1993; Emmanuel et al. 2019).

Volumetric shrinkage and desiccation susceptibility is another important aspect of constructinggeotechnical barriers in the field (Tay et al. 2001). Compacted clays were seen to be capable oflow hydraulic conductivities under confinement (Dixon et al. 1999). However, high compressibility, high desiccationshrinkage, low shear strength and low achievable density etc. are some reasons of concern whileusing compacted clays, which undermine its suitability as barrier material (Moses et al. 2019; Wei et al. 2020). The soil workability depends on its plasticity characteristics which is closely related to water holding capacity of the soil. This can be quantified based on index properties such as liquid limit, plastic limit and plasticity index (Hussain and Dash 2010; Sivapullaiah and Sridharan1985). It is very problematic to handle the expansive soils in construction sites due to their large water holding capacity. This problem can be solved by converting the soil mass with help ofadding locally available non expansive soils and chemicals such as lime, cement etc. In last few decades several scientific studies have highlighted the usefulness of lime for enhancement of workability of expansive soils like bentonite clays and black cotton soil (Al-Mukhtar et al. 2010; Bell 1996; Cheshomi et.al. 2017; Kumar et al. 2014; Prakash et al. 1989; Sabat 2012; Sivapullaiah et al. 1996, 2000). This current study presents the experimental results for understanding liquidity behaviour of a highly expansive bentonite clay modified by adding lime as chemical material and sugar as an organice material.

Material and methods

Material selection

Different materials that finds its application in geo-environmental project like construction of landfill liner and cover system are considered for the present study. Commercially available high plastic bentonite clay, lime and sugar were used for the present study. The bentonite clay is collected from a bentonite mine in Barmer district of Rajasthan, India. Lime used in this experiment is calcium hydroxide. Both lime and sugar were purchased locally from Bhubaneswar market. Figure 1 pictorially presents these three materials.

Bentonite clay
(commercially procured from Barmer, Rajasthan)

Lime
(commercially available in Bhubaneswar, Odisha)

Sugar
(commercially available in Bhubaneswar, Odisha)

Figure 1 Pictorial representation of lime, sugar and bentonite clay used for the study

Basic characterization of bentonite clay

Laboratory characterization of bentonite clay chosen to be used in this proposed study was performed at Indian Institute of Technology in accordance with the procedure reported in ASTM international code or Indian standard codesummarized in Table 1. The specific gravity was determined using the small density bottle or pycnometer. The hygroscopic water content of soil was determined by standard oven drying method. The consistency limits i.e. liquid and plastic limit of the soil sample were evaluated in the laboratory by Casagrande method. The grain size distribution was obtained based on dry, wet sieve and hydrometer analyses. The classification of the soil samples was decided according to unified soil classification system (USCS). Specific surface area was determined in the laboratory following the EGME method recommended by Cerato and Lutenegger (2002). Standard Proctor tests of soil was conducted to determine its compaction characteristics. The constant head test was performed for obtaining saturated hydraulic conductivity of sand and fly ash and falling head test was used for low permeable soils (red soil, BARC soil, bentonite and their mixes). For this test the samples were compacted at OMC and MDD. Shrinkage and swelling properties were evaluated for plastic soils. Organic content, pH value and cation exchange capacity were also determined for chemical characterizations of each soil. Each tests were repeated at least thrice and the average results obtained from these tests are shown in Table2.

Table 1 Various references for basic characterization of materials

Basic characterization	Reference (IS/ASTM code/literature)
Specific gravity	IS 2720 Part 3(1980)/ASTM D854-14 (2014)
Hygroscopic water content	IS 2720 Part 2 (1973)/ASTM D4959 (2016)
Saturated hydraulic conductivity	IS 2720 Part 17 (1986)/ASTM D2434-68 (2011)
Specific surface area	Cerato and Lutenegger (2002)
Linear shrinkage	IS 2720 Part 20(1992)/ASTM D4943 (2013)
Free swell index	IS 2720 Part 40 (1977)/ASTM D4546 (2014)
Grain size distribution	IS 2720 Part 4 (19854)/ASTM D6913-17 (2009)
Liquid limit and plastic limit	IS 2720 Part 5 (1985)/ASTM D4318-17 (2010)
Shrinkage limit	IS 2720 Part 6 (1972)/ASTM D427-04 (2008)
USCS classification	ASTM D2487-06 (2006)
Compaction characteristics	IS 2720 Part 7 (1980)/ASTM D698-07 (2007)
Soil pH value	IS 2720 Part 26 (1987)/ASTM D4972-13 (2013)
Percentage of organic matter	IS 2720 Part 22 (1972)/ASTM D2974 (2014)
Cation exchange capacity	IS 2720 Part 24 (1976)/ASTM D7503 (2014)

Table 2 Various properties of bentonite clay used for the study

Properties	Bentonite clay
General	
Specific Gravity, G	2.88
Hygroscopic Water Content (%)	11
Saturated Hydraulic Conductivity ($m.s^{-1}$)	3.9E-12
Specific Surface Area ($m^2.g^{-1}$)	348
Linear Shrinkage (%)	3
Free Swell Index (%)	686
Particle size distribution	
% of Gravel (> 4.75 mm)	0
% of Coarse sand (2.00 mm – 4.75 mm)	0
% of Medium sand (0.425 mm–2.00 mm)	0
% of Fine sand (0.075 mm – 0.425 mm)	5
% of Silt (0.002 mm – 0.075 mm)	31
% of Clay (< 0.002mm)	64
Atterberg's limits	
Liquid limit (%)	320
Plastic limit (%)	42
Shrinkage limit (%)	11
Plasticity Index (%)	278
USCS classification	CH
Standard compaction	
Optimum Moisture Content, OMC (%)	33
Maximum Dry Density, MDD ($g.cm^{-3}$)	1.34
Chemical properties	
Soil pH value (at 28.5°C)	9.15
Organic Content (%)	0.22
Cation Exchange Capacity (meq per 100 g)	27

Preparation of test samples

60 g of oven dried bentonite claywas first taken and 2%, 4%, 6%, 8% and 10% lime was then added to it at an interval of 2% of dry mass of bentonite to prepare five different bentonite lime

mixes. Similarly, five various bentonite-sugar mixes were prepared. Table 3 presents ten different mixes of bentonite clay with lime and sugar. Thereafter, a suitable quantity of distilled water(in the range of 5-10% more than the lquid limit of bentonite soil for saturation of sample) was added to these mixes and left for 3 days to ensure the uniform distribution of water within the entire masses of the mixture. Figure 2 pictorially represents various stages of sample preparation for the study.

Table 3 Variation mixes of bentonite clay with sugar and lime content

Bentonite sugar mix			**Bentonitelime mix**		
% of bentonite	**% of sugar**	**Designation**	**% of bentonite**	**% of lime**	**Designation**
100	0	_	100	0	_
98	2	BS2	98	2	BL2
96	4	BS4	96	4	BL4
94	6	BS6	94	6	BL6
92	8	BS8	92	8	BL8
90	10	BS10	90	10	BL10

Adding sugar to bentonite clay **Adding lime to bentonite clay**

Adding water to bentonite sugar or lime mix **Maturation of bentonite sugar or lime mix**

Figure 2 Pictorial representation of various stages of sample preparation

Maturation of samples in progress

Sample after 72 hours maturation

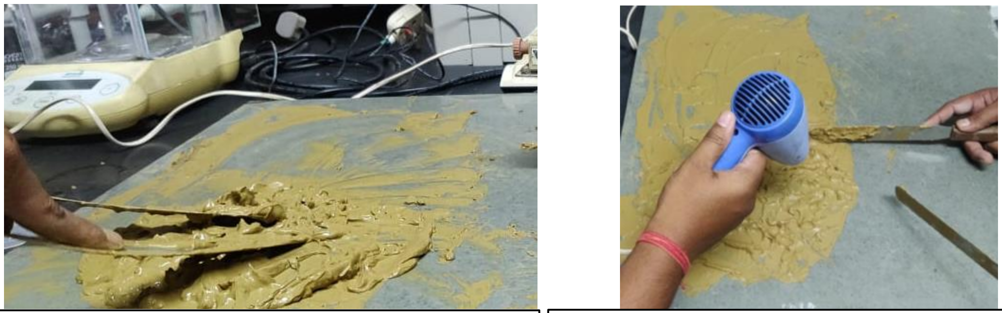

Water content adjustment by adding water

Water content Adjustment by air drying

Sample filled in cup before grooving

Sample ready for blowing after grooving

Weighing of samples before and after drying

Drying of samples in hot air oven

Figure 3 Pictorial representation of various stages of liquid limit test

Evaluation of liquid limit

The liquid limits of various bentonite-sugar and bentonite-lime mixes were determined using Casagrande liquid limit device as per the guidelines of IS 2720 Part 5 (1985). Figure 3 demonstrates the various stages of liquid limit test in geotechnical engineering laboratory.

Results and discussion

The effect of lime and sugar on the liquid limit of bentonite clay has been demonstrated in this section. The section also compares the effects of sugar and lime on liquid limit of bentonite clay.

Effect of lime

Figure 4 depicts the variation of liquid limit of bentonite-lime mix with percentage of lime. The liquid limit of bentonite-lime mix was found to be maximum (306%) at 2% of lime and minimum (185%) at 10% of lime. The result clearly indicates considerable decrease in the liquid limit of bentonite-lime mix with the increase in lime percentage. The similar observation was reported in previous literate by Sabat (2012).

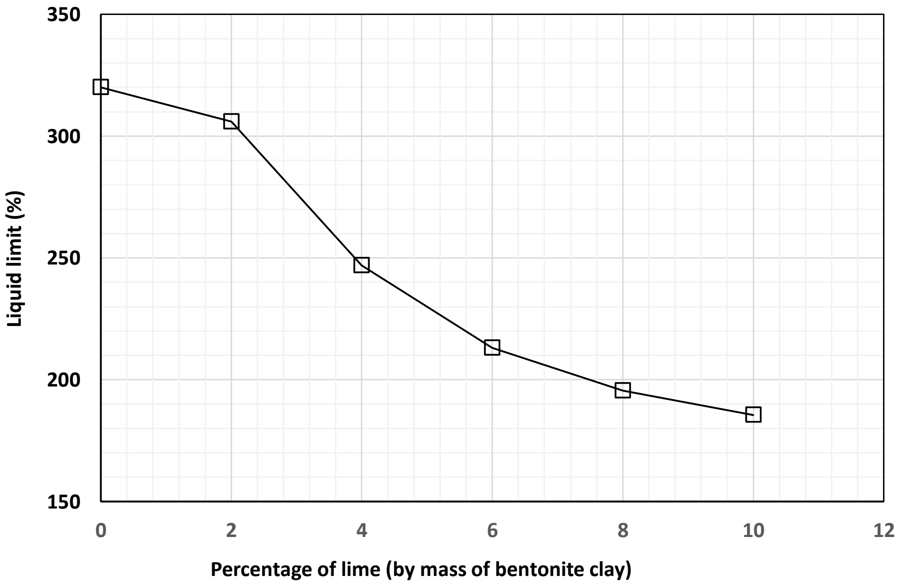

Figure 4 Variation of liquid limit of bentonite-lime mix with percentage of lime

Effect of sugar

Figure 5 illustrates the variation of liquid limit of bentonite-sugar mix with percentage of sugar. The figure shows the gradual reduction in liquid limit up to 6% of sugar. This might be due to decrease in water holding capacity of clay particles because of partial neutralization of its negative charges by the positive poles of sugar molecules.The liquid limit of bentonite-sugar mix was then found to be increased after 6% of sugar. This might be attributed to higher level of hydrophilicity of sufficiently available sugar when it was added in larger quantity beyond 6%.The least value of liquid limit was observed to be 216% at 6% of sugar.

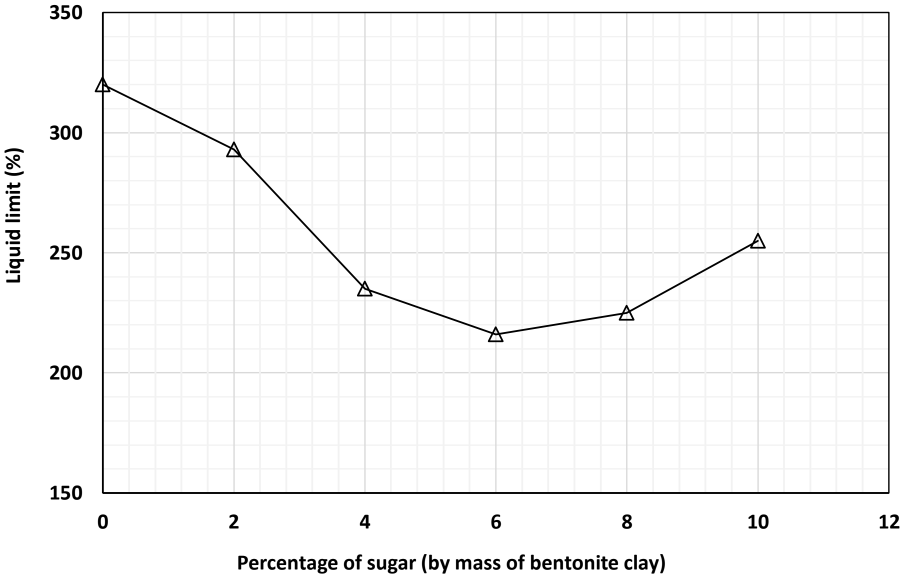

Figure 5 Variation of liquid limit of bentonite-sugar mix with percentage of sugar

Comparison between effect of sugar and lime

Figure 6 portrays the comparison of liquid limits of various bentonite-sugar and bentonite-lime mixes using bar charts. The figure shows the rate of decrement in liquid limit of bentonite-sugar mix was noticed to be higher than that of the lime bentonite mix up to 4% of their addition. However, after 6% of sugar, the liquid limit of the bentonite-sugar mix started to increase whereas the liquid limit of bentonite-lime mix keeps on decreasing.

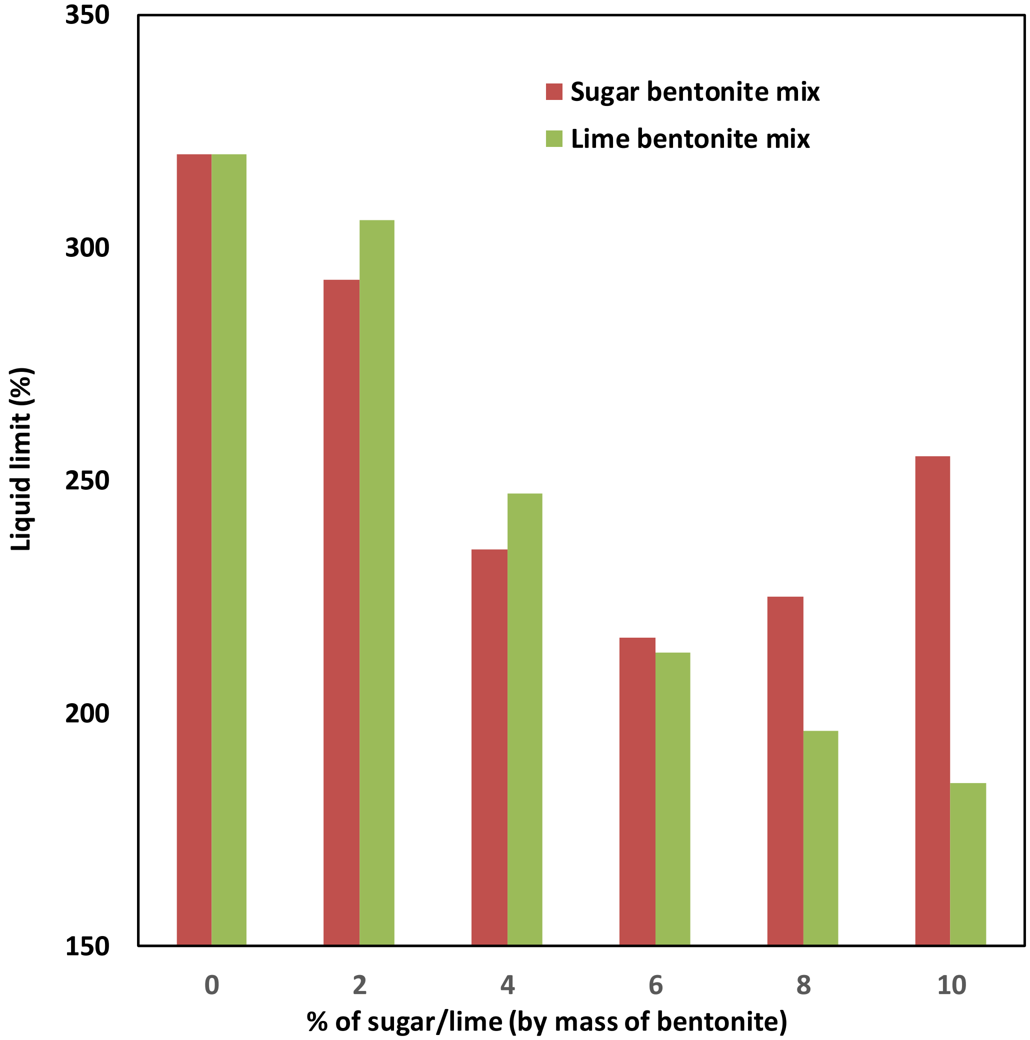

Figure 6 Comparison between the liquid limits of bentonite-sugar mix and bentonite lime mix

Conclusions

The conclusions derived from the current study are as follows.

- Liquid limits of bentonite-lime mixes continuously keep on decreasing with the increase in lime quantity.
- The rate of reduction in liquid limits of bentonite-sugar mixes is higher than that of the bentonite-lime mixes up to the limit of their decreasing trend.
- Liquid limits of bentonite-sugar mixes initially reduce with the increase in sugar quantity up to a certain limit and rise after that limit. The initial decrease in liquid limit may be due to

reduction in water holding capacity of bentonite clay for neutralization of negative charges with bipolar sugar molecules and the later increase in liquid limit might be because of higher hydrophilicity of abundantly available sugar in the mixture.

Acknowledgement

Authors would like to acknowledge C. V. Raman Global University (CGU), Bhubaneswar, Odisha, India for the laboratory facilities and financial support provided for the work reported in this study. The study was conducted in the Department of the Civil Engineering of the University.

References

AL-MUKHTAR, M. et al. 2010. Behaviour and mineralogy changes in lime-treated expansive soil at 20 ^{o}C. In Applied Clay Science, vol. 50, no. 2, pp.191-198. Available on internet: https://doi.org/10.1016/j.clay.2010.07.023

BELL, F.G. 1996. Lime stabilization of clay minerals and soils. In Engineering Geology, vol. 42, no. 4, pp.223-237.Available on internet: https://doi.org/10.1016/0013-7952(96)00028-2

CERATO, A. B. – LUTENEGGER, A. J. 2002. Determination of surface area of fine-grained soils by the ethylene glycol monoethyl ether (EGME) method. In Geotechnical Testing Journal, 25(3), pp.315-321.Available on internet: https://doi.org/10.1520/GTJ11087J

DANIEL, D. E. – BENSON, C. H. 1990. Water content-density criteria for compacted soil liners. In Journal of Geotechnical Engineering, vol. 116, no. 12, pp.1811-1830. Available on internet: https://doi.org/10.1061/(ASCE)0733-9410(1990)116:12(1811)

DANIEL, D. E. – Wu, Y.-K. 1993. Compacted clay liners and covers for arid sites. In Journal of Geotechnical Engineering, vol. 119, no. 2, pp.223-237. Available on internet: https://doi.org/10.1061/(ASCE)0733-9410(1993)119:2(223)

DIXON, D. A. et al. 1999. Hydraulic conductivity of clays in confined tests under low hydraulic gradients. In Canadian Geotechnical Journal, vol. 36, no. 5, pp.815-825.Available on internet: https://doi.org/10.1139/t99-057

EMMANUEL, E. et al. 2019. A critical reappraisal of residual soils as compacted soil liners. In SN Applied Sciences, vol. 1, no. 5, pp.1-24. Available on internet: https://link.springer.com/article/10.1007/s42452-019-0475-7

FERRONATO, N. – TORRETTA, V. 2019. Waste mismanagement in developing countries: A review of global issues. In International journal of environmental research and public health, vol. 16, no. 6, pp.1060. Available on internet: https://doi.org/10.3390/ijerph16061060

HOEKS, J. – AGELINK, G. J. 1982. Hydrological aspects of sealing waste tips with liners and soil covers. In Institute for Land and Water Management Research.Vol. 139. pp. 157-167. Available on internet: http://hydrologie.org/redbooks/a139/iahs_139_0157.pdf

HOEKS, J. 1987. Bentonite liners for isolation of waste disposal sites. In Waste Management & Research, vol. 5, no. 2, pp.93-105. Available on internet: https://doi.org/10.1016/0734-242X(87)90043-7

HUSSAIN, M. – DASH, S. K. 2010. Influence of lime on plasticity behaviour of soils. In Proc./Indian Geotechnical Conference, pp. 537-540. Available on internet: https://gndec.ac.in/~igs/ldh/conf/2010/articles/t014.pdf

CHESHOMI, A. et al. 2017. Effect of lime and fly ash on swelling percentage and Atterberg limits of sulfate-bearing clay. In Applied Clay Science, vol. 135, pp.190-198. Available on internet: https://doi.org/10.1016/j.clay.2016.09.019

KUMAR, S. et al. 2014. Engineering properties of bentonite stabilized with lime and phosphogypsum. In Slovak Journal of Civil Engineering, vol. 22, no. 4, pp.35-44. Available on internet:file:///C:/Users/J%20Shaikh/Desktop/Slovakia/Science%20of%20Youth_2021_Conference%20in%20Slovakia/sjce-2014-0021.pdf

KUMAR, S. et al. 2017. Challenges and opportunities associated with waste management in India. In Royal Society Open Science, vol. 4, no. 3, pp.1-11. Available on internet: https://doi.org/10.1098/rsos.160764

MOSES, G. et al. 2019. Desiccation-induced volumetric shrinkage characteristics of highly expansive tropical black clay treated with groundnut shell ash for barrier consideration. In Civil and Environmental Research, vol. 11, no. 8, pp. 58-74.

PRAKASH, K. et al. 1989. Lime addition and curing effects on the index and compaction characteristics of a montmorillonitic soil. In Journal of Southeast Asian Geotechnical Society, vol. 20, no. 1, pp. 39-47.

SABAT, A. K. 2012. A study on some geotechnical properties of lime stabilised expansive soil–quarry dust mixes. In International Journal of Emerging Trends in Engineering and Development, vol. 1, no. 2, pp.42-49. ISSN 2249–6149.

SIVAPULLAIAH, P. V. – SRIDHARAN, A. 1985. Liquid limit of soil mixtures. In Geotechnical Testing Journal, vol. 8, no. 3, pp.111-116. Available on internet: https://doi.org/10.1520/GTJ10521J

SIVAPULLAIAH, P. V. et al. 1996. Effect of fly ash on the index properties of black cotton soil. In Soils and foundations, vol. 36, no. 1, pp.97-103.Available on internet: https://doi.org/10.3208/sandf.36.97

SIVAPULLAIAH, P. V. et al. 2000. Role of amount and type of clay in the lime stabilization of soils. In Proceedings of the Institution of Civil Engineers-Ground Improvement, vol. 4(, no. 1, pp.37-45.Available on internet: https://doi.org/10.1680/grim.2000.4.1.37

STEIN, S. 2019. Capital city: Gentrification and the real estate state. Verso Books.Ljubljana. 177 p. ISBN 9781786636393.

SWATI W. et al. 2018. Scenario of landfilling in India: problems, challenges, and recommendations. In Handbook of Environmental Materials Management. Springer, Cham, pp.1-16.

TAUŠOVÁ, M. et al. 2020. Analysis of municipal waste development and management in self-governing regions of Slovakia. In Sustainability, vol. 12, no. 14, pp. 1-18. Available on internet: https://doi.org/10.3390/su12145818

TAY, Y.Y. et al. 2001. Shrinkage and desiccation cracking in bentonite–sand landfill liners. In Engineering Geology, vol. 60, pp. 263-274. Available on internet: https://doi.org/10.1016/S0013-7952(00)00107-1

WEI, X. et al. 2020. A review of cracking behavior and mechanism in clayey soils related to desiccation. In Advances in Civil Engineering, vol. 2020. Available on internet: https://doi.org/10.1155/2020/8880873

Contact address

Mr. Sanjeet Sahoo, PhD. Student, Department of Civil Engineering, C.V. Raman Global University, Bidyanagar, Mahura, Janla, Bhubaneswar 752054, Odisha, India, +918984621482, sanjeet476@gmail.com

ARTICLE HISTORY:
Received 31 March 2021
Accepted 10 May 2021

LAVENDER ESSENTIAL OIL: ITS CHEMICAL COMPOSITION, AND ANTIMICROBIAL AND ANTIOXIDANT PROPERTIES

Veronika VALKOVÁ[1,2], Hana ĎÚRANOVÁ[1], Lucia GALOVIČOVÁ[2], Eva IVANIŠOVÁ[2], Nenad VUKOVIC[3], Miroslava KAČÁNIOVÁ[2,4]

[1] AgroBioTech Research Centre, SLOVAKIA

[2]Slovak University of Agriculture, SLOVAKIA

[3]University of Kragujevac, SERBIA

[4]University of Rzeszow, POLAND

Abstract

The growing demand for the elimination of the use of chemicals as antimicrobials in various fields, from traditional medicine to horticulture and/or agriculture, has been leading the scientific community to find innovative natural agents to replace their application. Therefore, the aim of the present study was to characterize the chemical composition, and to assess the antimicrobial properties (*in vitro*), and antioxidant activity of lavender essential oil (LEO; *Lavandula angustifolia* x *latifolia*) as one of the potential agents. Our results proved that linalool acetate (35.0%), linalool (32.7%), and 1,8-cineole (8.1%) were detected as the main components of LEO reflecting its medium-strong value for antioxidant activity (28.78 ± 0.63%). Taking into account the screening of antimicrobial activity, LEO inhibited the growth of the most yeasts (5.00 ± 0.36 mm) and gram-negative bacteria (4.00 ± 0.47 mm) investigated, with the largest inhibition zones recorded against *Candida tropicalis*, *Pseudomonas aeruginosa* (9.50 ± 0.71 mm for both), and *Candida krusei* (6.50 ± 0.71 mm). Among the analysed species of *Penicillium* (*P.*) spp., as a frequent reason for the spoilage of vegetables and fruits, LEO showed the best antifungal actions against the growth of *P. citrinum.* Accordingly, LEO could be used as a safe and effective natural antioxidant and antimicrobial agent to improve the qualitative properties of food and horticulture products during their storage mainly in the context of their preservation against foodborne pathogens.

Keywords: *Lavandula angustifolia* x *latifolia*, volatile compounds, antifungal properties, antibacterial properties, DPPH assay

Introduction

Essential oils (EOs) are natural products containing a complex mixture of odorous and volatile compounds originated from secondary plant metabolism which are widely used in many interesting applications including traditional medicine, cosmetics (fragrance components) or the food industry (flavouring additives). In addition to their characteristic flavour, many of them exhibit also antimicrobial effect including antibacterial and antifungal activities (Mazzanti et al., 1998; D'Auria et al., 2001; Lu et al., 2002), even against multi-resistant microorganisms. In particular, as natural components, EOs respect the environment (Mayaud et al., 2008). Given the above characteristics, there is a growing demand for uses of EOs also in the food industry, especially as natural preservatives (Burt, 2004), and innovative food packages improving qualitative properties of products during storage. In effect, numerous studies have demonstrated the efficiency of EOs in the growth elimination of microbial pathogens often found in food and agricultural production (Oussalah et al., 2007; Kačániová et al., 2020).

These aromatic components are obtained from the plants using various methods such as steam distillation, expression, and so on. Among them, the distillation method has been widely used especially for commercial production (Cassel and Vargas 2006). From a total amount approximately 3000, about 300 types of EOs are used on a commercial scale (Burt and Reinders, 2003). According to Cavanagh and Wilkinson (2005), lavender essential oil (LEO) belongs to the best-known types.

Therefore, the chemical composition, antioxidant and antimicrobial activities of lavender (*Lavandula angustifolia* x *latifolia*) EO were investigated in the present study in order to assess the use of the EO as a potential antimicrobial detergent in various industry areas including horticulture.

Material and methods

Essential oil

Lavender (*Lavandula angustifolia* x *latifolia,* LEO) EO obtained from Hanus s.r.o. (Nitra, Slovakia) was applied in the present study.

Microorganisms

To determine the antimicrobial activity of the LEO, microbial strains including three gram-negative bacteria: *Pseudomonas* (*P.*) *aeruginosa* CCM 1959, *Salmonella* (*S.*) *enterica* subsp. *enterica* CCM 3807, *Yersinia* (*Y.*) *enterocolitica* CCM 5671; three gram-positive bacteria: *Enterococcus* (*E.*) *faecalis* CCM 4224, *Staphylococcus* (*S.*) *aureus* subsp. *aureus* CCM 4223, *Bacillus* (*B.*) *subtilis sub. Spizizenii* CCM 1999; and four yeast species: *Candida* (*C.*) *glabrata* CCM 8270, *C. albicans* CCM 8186, *C. krusei* CCM 8271 and *C. tropicalis* CCM 8223, and three microscopic fungi strains: *Penicillium* (*P.*) *crustosum*, *P. citrinum*, *P. expansum* were employed. The microorganisms were obtained from the Czech Collection of Microorganisms (Brno, Czech Republic), whilst the three *Penicillium* strains were isolated from grapes and consequently identified using MALDI-TOF MS Biotyper, as well as 16S rDNA sequences analysis.

Evaluation of LEO antioxidant activity

The antioxidant activity of LEO was evaluated in terms of its DPPH (2,2-diphenyl-1-picrylhydrazyl) radical scavenging activity as recently described by Kačániová et al. (2020).

Determination of LEO chemical composition

Analytical determination of volatile compounds of the essential oil was carried out in an Agilent Technologies (Santa Clara, USA) 6890 N gas chromatograph fitted with an HP-5MS fused silica column (30 m × 0.25 × 0.25 m, Agilent Technologies), interfaced with an Agilent Technologies mass-selective detector 5975B operated by HP Enhanced ChemStation software (Agilent Technologies) as reported by Kačániová et al. (2017) with minor modifications.

Evaluation of antimicrobial activity of LEO

Antimicrobial activity of LEO was evaluated using the agar disc diffusion method. For this purpose, an aliquot of 0.1 mL of bacterial, yeast and fungal suspension in Mueller Hinton Broth (MHB; Merck, Germany) was applied to Mueller Hinton Agar (MHA; Merck, Germany). Subsequently, the discs of filter paper (6 mm) were impregnated with 10 µL of analyzed EO samples and then inoculated on the MHA surface. Inoculated MHA plates were kept at 4 °C for 2 h and incubated aerobically at 37 °C for 24 h (bacteria, yeasts) and at 25 °C for 5 days (fungi). The diameters of the inhibition zones were measured in mm after incubation. The antibiotics (Cefoxitin, Gentamicin, and Fluconazole) were used as positive controls for gram-negative, gram-positive bacteria, yeasts, and fungi, respectively; and disks impregnated with ethanol served as negative controls. Each test was repeated in triplicate.

Statistical analysis

For statistical analysis of obtained data, program Prism 8.0.1 (GraphPad Software, San Diego, California USA) was used. The significance of differences between the analyzed groups of samples was assessed by One-way analysis of variance (ANOVA) followed by Tukey's test (with the level of significance $P < 0.05$).

Results and Discussion

Chemical composition of LEO

As presented in Table 1, LEO main components were linalool acetate (35.0%), linalool (32.7%), and 1,8-cineole (8.1%).

Romeo et al. (2008) have shown that linalool acetate (23.1%), linalool (23.1%), and 1,8-cineole (8.4%) were the main compounds of EO obtained from *Lavandula angustifolia*, which is in accordance with our study. On the other hand, Zuzarte et al. (2011) determined in two samples of *Lavandula viridis* as major components 1,8-cineole (34.5 % and 42.2 %), camphor (13.4 %), α-pinene (9.0 %) and linalool (7.9 and 6.7 %), contradicting our results. However, differences in the amounts of EOs individual components may be caused by various factors such as different across provinces, environmental and genetic factors, different chemotypes, or the nutritional status of the plants (Hui et al., 2010).

Antioxidant activity of LEO

In general, the antioxidant potential of diverse EOs can be largely related to their ability to scavenge radicals and quench singlet oxygen, as well as their reducing power (Loizzo et al., 2009). In our study, the potential antioxidant capacity of LEO was determined by the scavenging activity of DPPH stable free radicals. The results revealed that the value for antioxidant capacity of the EO was 28.78 ± 0.63% reflecting its medium-strong antioxidant activity. In the research conducted by Danh et al. (2013), values for antioxidant activity of the EO obtained from *Lavandula angustifolia* ranged from 12% (hydrodistillation and extraction with hexane) to 63% (supercritical CO_2 extraction) depending on the extraction method, which corresponds with our findings. Ricci et al. (2005) and Ćavar et al. (2008) reported that the presence of sesquiterpenes and oxygen terpenoids in EO compositions can weaken their antioxidant activity. In this regard, Candan et al. (2003) found that borneol and terpinen-4-ol do not show any antioxidant activity. Since these components were also present in our LEO we propose that their presence might contribute to the attenuation of the overall EO antioxidant activity.

Antimicrobial activity of LEO

Plant EOs have been known since ancient times for their antibacterial and antifungal properties, for which they have been used as antimicrobial agents in traditional medicine until now (Lopes-Lutz et al., 2008). Based on these facts, the LEO antimicrobial properties related to its inhibitory actions on the growth of selected bacteria, yeasts, and fungi species were evaluated in the current study using a disc diffusion method.

Given in Table 2, LEO showed growth inhibition of all evaluated bacteria and yeasts. As regard to the average inhibition zone, the EO exhibited the most effective inhibitory action against the growth of yeasts (5.00 ± 0.36 mm) and gram-negative bacteria (4.00 ± 0.47 mm), whereas gram-positive bacteria were found to be the most resistant (2.00 ± 0.00 mm). Specifically, the largest inhibition zone was recorded against *C. tropicalis*, *P. aeruginosa* (9.50 ± 0.71 mm for both), and *C. krusei* (6.50 ± 0.71 mm); the smallest inhibition zone have been found against *Y. enterocolitica* (1.00 ± 0.00 mm), *S. aureus* (1.00 ± 0.00 mm) and *S. enterica* (1.50 ± 0.71 mm).

Table 1 Chemical composition of LEO.

Components	LEO (%)
linalool acetate	35.0
linalool	32.7
1,8-cineole	8.1
camphor	6.4
borneol	2.4
lavandulyl acetate	2.0
(*E*)-caryophyllene	1.6
α-terpineol	1.3
4-terpineol	1.3
(*Z*)-β-farnesene	1.0
α-limonene	0.9
(*E*)-β-ocimene	0.9
hexyl butanoate	0.9
geranyl acetate	0.8
β-myrcene	0.6
germacrene D	0.4
neryl acetate	0.4
α-pinene	0.3
β-pinene	0.3
*o*cimene	0.3
α-amorphene	0.3
hexyl tiglate	0.3
α-bisabolol	0.3
trans-linalool oxide	0.3
3-octanone	0.3
camphene	0.2
n-hexanol	0.1
epi-α-cadinol; caryophyllene oxide; tricyclene; cis-3-hexenol; 3-octanol; ethyl hexanoate; cis-linalool oxide; capryl acetate; nerol; sabinene; α-thujene; α-terpinolene; γ-terpinene	tr

Source: Total components of LEO – 99.4 %; tr - compounds identified in amounts less than 0.1 %

Table 2 Inhibitory effect of LEO on bacterial and yeasts growth

	Gram-negative bacteria			Gram-positive bacteria			Yeasts			
	PA	SE	YE	BS	EF	SA	CG	CA	CK	CT
	Inhibition zone (mm)									
LEO	9.50 ± 0.71 ^{a}	1.50 ± 0.71 ^{b}	1.00 ± 0.00 ^{b}	2.00 ± 0.00 ^{bc}	3.00 ± 0.00 ^{d}	1.00 ± 0.00 ^{b}	2.00 ± 0.00 ^{bc}	2.00 ± 0.00 ^{bc}	6.50 ± 0.71 ^{d}	9.50 ± 0.71 ^{a}
Average	4.00 ± 0.47 ^{a}			2.00 ± 0.00 ^{b}			5.00 ± 0.36 ^{c}			

Source: Means ± standard deviation. Values followed by superscript within the same row are significantly different ($P < 0.05$). *Pseudomonas aeruginosa* - PA, *Salmonella enterica* - SE, *Yersinia enterocolitica* - YE, *Bacillus subtilis* - BS, *Enterococcus faecium* - EF, *Staphylococcus aureus* - SA, *Candida glabrata* – CG, *Candida albicans* - CA, *Candida krusei* - CK, *Candida tropicalis* - CT

Generally, the antimicrobial activity of EOs is influenced by the representation of active compounds and their diffusivity in the growth media (Danh et al., 2013). Several scientific studies have shown that the presence of components in EOs such as linalool (Bassole et al., 2003), linalool acetate (Peana et al., 2002), and 1,8-cineole (Lopes-Lutz et al., 2008), which were also detected in our analyzed LEO, contributes to improving the overall antimicrobial activity of the EOs. Hence we assume that the proven antimicrobial properties of our analyzed LEO are associated with the components. Interestingly, LEO showed a high inhibition effect against *P. aeruginosa* growth despite its outer membrane blocking accumulation of biologically active compounds (Gutierrez et al., 2008). This finding contradicts the results of the studies by Kunicka-Styczyńska et al. (2009) and Hanamanthagouda et al. (2010). However, this fact could be attributed to the different quantitative representation of active compounds of LEO employed in our study as compared to the two other ones. Indeed, higher content of linalool, linalool acetate, 1,8-cineole, and camphor in our LEO as compared to the LEO (34.1%, 33.3%, 2.5%, 1.2%, respectively) used in the study by Kunicka-Styczyńska et al. (2009) might be able to disrupt the blockade of this resistant microorganism. Based on the results of the analyzes, LEO appears to be a promising agent with significant antimicrobial properties conditioning its potential use in various areas of industrial production.

Many *Penicillium* spp. play a key role in the food rotting process including different types of vegetables, fruits, or seeds. For instance, *P. expansum* causes decay of oranges or rot in grapes

(Mahlo et al., 2016). However, the growth of *Penicillium* in food products is unacceptable, mainly due to the production of mycotoxins and secondary metabolites, which bring a number of health risks to consumers (Frisvad, 2014). Therefore, this part of our study was focused on the evaluation of LEO efficacy against the growth of *P. crustosum*, *P. citrinum*, and *P. expansum* (Table 3).

Table 3 Inhibitory effect of LEO on fungal growth

	P. crustosum				*P. citrinum*				*P. expansum*			
Conc.	100%	50%	25%	12.5%	100%	50%	25%	12.5%	100%	50%	25%	12.5%
Inhibition zone (mm)												
LEO	3.00 ± 0.00 ^{a}	1.00 ± 0.00 ^{b}	0.00 ± 0.00 ^{c}	0.00 ± 0.00 ^{c}	4.50 ± 0.71 ^{d}	2.50 ± 0.71 ^{ae}	1.00 ± 0.00 ^{b}	0.00 ± 0.00 ^{c}	2.00 ± 0.00 ^{e}	1.50 ± 0.71 ^{be}	1.00 ± 0.00 ^{b}	0.00 ± 0.00 ^{c}
Average	1.00 ± 0.00 ^{a}				2.00 ± 0.36 ^{b}				1.13 ± 0.18 ^{a}			

Source: Means ± standard deviation. Values followed by superscript within the same row are significantly different ($P < 0.05$). Conc. - concentration

Our results revealed that LEO at all analyzed concentrations had the highest ($P < 0.05$) inhibitory activity (on average 2.00 ± 0.36 mm) against the growth of *P. citrinum*. Against *P. crustosum* and *P. expansum*, it exhibited antifungal activity with average inhibition zones of 1.00 ± 0.00 mm and 1.13 ± 0.18 mm, respectively. From the obtained results it is clearly evident that LEO showed the highest efficiency against the growth of all *Penicillium* strains in the concentration of 100% which continuously decreased by its gradual dilution up to a complete loss of its efficacy (12.5% concentration; even 25% concentration against *P. crustosum).*

Contrary to our results, Felšöciová et al. (2020) recorded the highest efficacy of EO from *Lavandula angustifolia* Mill. against *P. expansum* (6.50 ± 1.22 mm), followed by *P. crustosum* (4.83 ± 1.17 mm) and *P. citrinum* (4.17 ± 0.98 mm). We hypothesize that these discrepancies may be linked to using different LEOs. The presented results point out to the possibility of using LEO as an antifungal substance in various areas of research including horticulture and food industry. However, further studies are needed to evaluate the antimicrobial properties of LEO on food models (*in situ*) which is our next challenge.

Conclusion

The LEO was analyzed in our study in terms of its chemical composition, antioxidant potential, and antimicrobial properties. The major constituents of LEO were linalool acetate (35.0%), linalool (32.7%) and 1,8-cineole (8.1%), and its value for antioxidant activity was medium-strong (28.78 ± 0.63%). In addition, LEO had proven antimicrobial properties with the most noted inhibitory actions against yeasts, and gram-negative bacteria (mainly *C. tropicalis* and *P. aeruginosa*, respectively). Among analyzed *Penicillium* spp., *P. citrinum* was the most sensitive to LEO and had the largest growth inhibition zone. This study provides additional data to support the application of LEO as a natural antimicrobial detergent in agriculture, as well as horticulture products against growth of foodborne pathogens.

Funding

This work was supported by the grant APVV SK-BY-RD-19-0014 “The formulation of novel compositions and properties study of the polysaccharides based edible films and coatings with antimicrobial and antioxidant plant additives.”

Acknowledgment

The research leading to these results has received funding from the grants of the VEGA no. 1/0180/20.

References

BASSOLE, I. H. N., et al. 2003. Chemical composition and antibacterial activities of the essential oils of Lippia chevalieri and Lippia multiflora from Burkina Faso. In Phytochemistry, vol. 62, no. 2, pp. 209-212. ISSN 0031-9422.

BURT, S. A. – REINDERS, R. D. 2003. Antibacterial activity of selected plant essential oils against Escherichia coli O157: H7. In Letters in applied microbiology, vol. 36, no. 3, pp. 162-167. ISSN 0266-8254.

BURT, S. 2004. Essential oils: their antibacterial properties and potential applications in foods — a review. In International journal of food microbiology, vol. 94, no. 3, pp. 223-253. ISSN 0168-1605.

CANDAN, F. et al. 2003. Antioxidant and antimicrobial activity of the essential oil and methanol extracts of Achillea millefolium subsp. millefolium Afan.(Asteraceae). In Journal of ethnopharmacology, vol. 87, no. 2-, pp. 215-220. ISSN 0378-8741.

CASSEL, E. et al. 2006. Experiments and modeling of the Cymbopogon winterianus essential oil extraction by steam distillation. In Journal of the Mexican Chemical Society, vol. 50, no. 3, pp. 126-129. 1870-249X.

CAVANAGH, H. M. A. – WILKINSON, J. M. 2005. Lavender essential oil: a review. In Australian infection control, vol. 10, no. 1, pp. 35-37. ISSN 1329-9360.

ĆAVAR, S. et al. 2008. Chemical composition and antioxidant and antimicrobial activity of two Satureja essential oils. In Food Chemistry, vol. 111, no. 3, pp. 648-653. ISSN 0308-8146.

DANH, L. T. et al. 2013. Comparison of chemical composition, antioxidant and antimicrobial activity of lavender (Lavandula angustifolia L.) essential oils extracted by supercritical CO 2, hexane and hydrodistillation. In Food and bioprocess technology, vol. 6, no. 3, pp. 3481-3489. ISSN 1935-5149.

D'AURIA, F. D. et al. 2001. In vitro activity of tea tree oil against Candida albicans mycelial conversion and other pathogenic fungi. In Journal of chemotherapy, vol. 13, no. 4, pp. 377-383. ISSN 1973-9478.

FELŠÖCIOVÁ, S. et al. 2020. Antifungal activity of selected volatile essential oils against Penicillium sp. In Open Life Sciences, vo. 15, no. 1, pp. 511-521. ISSN 2391-5412.

FRISVAD, J. C. 2014. Penicillium/Penicillia in food production. In: Encyclopedia of food microbiology. Elsevier, pp. 14-18. ISBN 9780123847331.

GUTIERREZ, J. et al. 2008. The antimicrobial efficacy of plant essential oil combinations and interactions with food ingredients. In International journal of food microbiology, vol. 124, no. 1, pp. 91-97. ISSN 0168-1605.

HANAMANTHAGOUDA, M. Sh. et al. 2010. Essential oils of Lavandula bipinnata and their antimicrobial activities. In Food Chemistry, vol. 118, no. 3, pp. 836-839. ISSN 0308-8146.

HUI, L. et al. 2010. Chemical composition of lavender essential oil and its antioxidant activity and inhibition against rhinitis-related bacteria. In African journal of microbiology research, vol. 4, no. 4, pp. 309-313. ISSN 1996-0808.

KAČÁNIOVÁ, M. et al. 2017. The antioxidant and antimicrobial activity of essential oils against Pseudomonas spp. isolated from fish. In Saudi Pharmaceutical Journal. vol. 25, no. 8, pp. 1108-1116. ISSN 1319-0164.

KAČÁNIOVÁ, M. et al. 2020. Antioxidant, antimicrobial and antibiofilm activity of coriander (Coriandrum sativum L.) essential oil for its application in foods. In Foods, vol. 9, no. 3, pp. 282. ISSN 2304-8158.

KUNICKA-STYCZYŃSKA, A. et al. 2009. Antimicrobial activity of lavender, tea tree and lemon oils in cosmetic preservative systems. In Journal of applied microbiology, vol. 107, no. 6, pp. 1903-1911. ISSN 1365-2672.

LOIZZO, M. R. et al. 2009. Chemical analysis, antioxidant, antiinflammatory and anticholinesterase activities of Origanum ehrenbergii Boiss and Origanum syriacum L. essential oils. In Food Chemistry, vol. 117, no. 1, pp. 174-180. ISSN 0308-8146.

LOPES-LUTZ, D. et al. 2008. Screening of chemical composition, antimicrobial and antioxidant activities of Artemisia essential oils. In Phytochemistry, vol. 69, no. 8, pp. 1732-1738. ISSN 0031-9422.

LU, M. et al. 2002. Muscle relaxing activity of Hyssopus officinalis essential oil on isolated intestinal preparations. In Planta medica, no. 68, vol. 3, pp. 213-216. ISSN 0032-0943.

MAHLO, S. M. et al. 2016. Antioxidant and antifungal activity of selected medicinal plant extracts against phytopathogenic fungi. In African Journal of Traditional, Complementary and Alternative Medicines, vol. 13, no. 4, pp. 216-222. ISSN 0189-6016.

MAYAUD, L., et al. 2008. Comparison of bacteriostatic and bactericidal activity of 13 essential oils against strains with varying sensitivity to antibiotics. In Letters in applied microbiology, vol. 47, no.3, pp. 167-173. ISSN 0266-8254.

MAZZANTI, G. et al. 1998. Antimicrobial properties of the linalol-rich essential oil of Hyssopus officinalis L. var decumbens (Lamiaceae). In Flavour and Fragrance Journal, vol. 13, no. 5, pp. 289-294. ISSN 1099-1026.

OUSSALAH, M. et al. 2007. Inhibitory effects of selected plant essential oils on the growth of four pathogenic bacteria: E. coli O157: H7, Salmonella typhimurium, Staphylococcus aureus and Listeria monocytogenes. In Food control, vol. 18, no. 5, pp. 414-420. ISSN 0956-7135.

PEANA, A. T. et al. 2002. Anti-inflammatory activity of linalool and linalyl acetate constituents of essential oils. In Phytomedicine, vol. 9, no. 8, pp. 721-726. ISSN 0944-7113.

RICCI, D. et al. 2005. Chemical composition, antimicrobial and antioxidant activity of the essential oil of Teucrium marum (Lamiaceae). In Journal of ethnopharmacology, vol. 98 no.1-2, pp. 195-200. ISSN 0378-8741.

ROMEO, F. V., et al. 2008. Antimicrobial effect of some essential oils. In Journal of Essential Oil Research, vol. 20, no. 4, pp. 373-379. ISSN 2163-8152.

ZUZARTE, M. et al. 2011. Chemical composition and antifungal activity of the essential oils of Lavandula viridis L'Hér. In Journal of medical microbiology, vol. 60, no. 5, pp. 612-618. ISSN 0022-2615.

Contact address

Mgr. Veronika Valková, Slovak University of Agriculture in Nitra, AgroBioTech Research Centre, Tr. A. Hlinku 2, 94976 Nitra, Slovakia; Slovak University of Agriculture in Nitra, Faculty of Horticulture and Landscape Engineering, Department of Fruit Sciences, Viticulture and Enology, Tr. A. Hlinku 2, 94976 Nitra, Slovakia, +421 37 641 4928, veronika.valkova@uniag.sk

RNDr. Hana Ďúranová, PhD., Slovak University of Agriculture in Nitra, AgroBioTech Research Centre, Tr. A. Hlinku 2, 94976 Nitra, Slovakia, +421 37 641 4975, hana.duranova@uniag.sk

Ing. Lucia Galovičová, Slovak University of Agriculture in Nitra, Faculty of Horticulture and Landscape Engineering, Department of Fruit Sciences, Viticulture and Enology, Tr. A. Hlinku 2, 94976 Nitra, Slovakia, +421 907 260 116, l.galovicova95@gmail.com

Ing. Eva Ivanišová, PhD., Slovak University of Agriculture in Nitra, Faculty of Biotechnology and Food Sciences, Department of Technology and Quality of Plant Products, Tr. A. Hlinku 2, 94976 Nitra, Slovakia, +421 37 641 4421, eva.ivanisova@uniag.sk

ASST PROF. Vukovic, Nenad L., University of Kragujevac, Department of Chemistry, Faculty of Science, P.O. Box 60, 34000 Kragujevac, Serbia. +381 343 362 23, nvukovic@kg.ac.rs

prof. Ing. Miroslava Kačániová, PhD., Slovak University of Agriculture in Nitra, Faculty of Horticulture and Landscape Engineering, Department of Fruit Sciences, Viticulture and Enology, Tr. A. Hlinku 2, 94976 Nitra, Slovakia, +421 37 641 4715, Institute of Food Technology and Nutrition, Department of Bioenergy, Food Technology and Microbiology, University of Rzeszow, Zelwerowicza St. 4, 35601 Rzeszow, Poland, miroslava.kacaniova@uniag.sk

ARTICLE HISTORY:
Received 25 April 2021
Received in revised form 11 May 2021
Accepted 20 May 2021

ELECTRICAL RESISTIVITY MEASUREMENT OF SAND, RED MUD AND CLAY USING AN INEXPENSIVE SOIL RESISTIVITY BOX

Raghava A. Bhamidipati[1], Lav Nayan[1], Rinki Mahato[1]

[1]C. V. Raman Global University, Bhubaneswar, INDIA

Abstract

Electrical resistivity measurement is an important and upcoming area of soil investigation. The information gathered from resistivity measurements can be used to assess some basic soil properties like moisture content, soil mineralogy, density etc. It can also be used to get an indication of the salinity level in the soil. In this study, red mud, sand and a clayey soil samples were prepared and their electrical resistivity was measured using an inexpensive soil resistivity box and two multimeters. First, resistivity was measured with respect to change in water content. Tap water was added to vary the moisture content of the samples. Electrical resistivity of the sand sample was then measured with respect to change in void ratio. The resistivity of the sand was also measured by adding 0.5% by weight of salt (NaCl) to the tap water used in preparing the sample. Lastly, the resistivity of the tap water and salt water were measured using the resistivity box. The test results showed that electrical resistivity of the soils reduced with increase in moisture content, soil type and salinity of water and increased with increase in void ratio. In this way, these soil parameters can be predicted from resistivity measurements and used in field studies.

Keywords: Electrical resistivity, soil, moisture, void ratio, salinity

Introduction

The exploration of soil and subsurface conditions is a very important aspect from a land use and civil engineering point of view. For a long time, conventional soil exploration methods like soil drilling and excavation were used to investigate soils at different depths. These methods are useful as they provide direct access to the subsurface conditions. However, they are time consuming and generally expensive. Geophysical testing methods like electrical resistivity testing help overcome some of these limitations. Electrical resistivity of a material is a measure of how much the flow of electric current is resisted by that material. Electrical resistivity of soils is found by passing an electric current through the soil and measuring the resulting potential difference between two electrodes, due to this current. Resistivity can also be measured directly by using a commercially available soil resistivity meter. Electrical resistivity of earth materials is dependent on a number of environmental variables like moisture content, soil mineralogy, density of soil, conductivity of pore-water, temperature etc. For most of the earth materials the electrical resistivity varies between 1 to 10,000 Ω-m (Samouelian et al., 2005). As such, measurement of soil resistivity can be used for estimating one or more of these variables.

Kalinski and Kelly (1993) used a four-probe resistivity cell to predict the volumetric moisture content of a soil sample with 20% clay. Kalinski and Vemuri (2005) used electrical conductivity measurements performed on a clayey soil from Morehead, Kentucky and developed a methodology to quickly assess the level of compaction of the soil. Bryson and Bathe (2009) used low frequency electrical conductivity measurements for predicting geotechnical properties of soils such as void ratio and volumetric water content. Syed and Siddiqui (2012) performed field electrical resistivity testing in Malaysia and correlated the values with the Standard penetration test (SPT) N values and moisture content of the soils. Pandey et al. (2015) studied the electrical resistivity of sandy soil in Western Australia, using the four electrode soil box method and determined several relationships between the soil properties and resistivity.

In this study, an inexpensive rectangular soil box made of non-conducting glass was used to study the electrical resistivity of some locally available soils and a sample of red mud. The objective was to investigate the variation in electrical resistivity of these materials with respect to change in factors like moisture content, void ratio and salinity of water. It was expected that resistivity of these materials would reduce with increase in moisture, density and salinity of water. The authors were interested in studying the resistivity trends for the different soils and tap water under the testing conditions. The study was conducted in the geotechnical engineering lab of C V

Raman Global University, Bhubaneswar, India. Bhubaneswar is located about 70 kilometers from the east coast of India along the Bay of Bengal. It experiences a tropical savanna climate.

Materials and methods

Three materials were considered for this study: A poorly graded sand, red mud (bauxite waste) obtained from a nearby Aluminum refining facility and a local sandy clay sample. Basic soil classification tests were performed on these materials which included the liquid and plastic limits (Atterberg limits) tests, wet sieve analysis and specific gravity tests. The soil properties determined from these tests are summarized in Table 1. All the soils were all passed through the 4 mm sieve before being used for resistivity tests.

Resistivity tests were performed using a rectangular four-electrode soil resistivity box made out of glass. The glass was about 1 cm in thickness. The inner dimensions of the box were 20.5 cm x 11 cm x 9 cm. Two tin plates attached to the ends of the box act as current electrodes and the two long steel nails placed in-between act as voltage electrodes. The testing methodology followed for conducting this study was that of ASTM G-57 (Standard test method for measuring soil resistivity using the Wenner four-electrode method). The mean indoor temperature while conducting the tests was 30°C.

Table 1 Basic properties of the soils used in the tests

Soil type	Fraction <0.075 mm (%)	Specific Gravity	Liquid Limit (%)	Plastic Limit (%)
Red Mud	72	3.01	27	20
Sand	3	2.61	-	-
Clay	76	2.67	38	25

Soil samples were prepared by adding tap water to dry soil and mixing them uniformly. These samples were put in the soil box and compacted lightly by tamping. Figure 1 shows a red mud sample under preparation and a sand sample ready to be tested. A 25V direct current (DC) source was used to pass an electric current through the soil specimens. The potential drop between the two inner electrodes (V) and the current passing through the circuit (i) were measured using two multimeters. The Wenner electrode configuration was used in which, the electrodes were spaced at equal distances. Resistance (Ω) is calculated as the ratio of V and i, and resistivity (Ω –m) is calculated by multiplying resistance with the box geometry constant (k). The constant 'k' is the ratio of cross-sectional area of the box to the spacing between the electrodes. A schematic of the test setup is shown in figure 2. Each resistivity measurement was calculated by averaging two resistance measurements obtained by passing current in opposite directions.

Figure 1a Red mud sample under preparation

Figure 1b Sand sample ready for testing

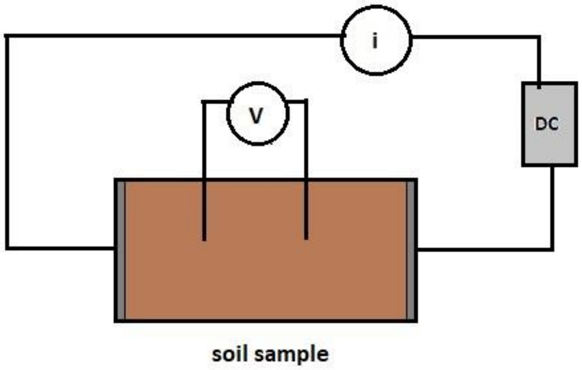

Figure 2 Circuit for soil resistivity test

Results and discussions

First the variation of resistivity was assessed with respect to gravimetric moisture content. The samples were prepared by adding the required amount of water to known weights of dry soils, so as to obtain gravimetric moisture contents ranging from 5% to 25%. The electrical resistivity values of each of these samples were measured (Figure 3). All the samples were prepared at a fairly uniform dry density of 1.2-1.3 g/cm^3. As seen from the plot, resistivity decreases rapidly with increase in moisture content of the samples. The trends showed a decreasing pattern which could be best approximated by power functions. In the tested range of moisture contents, electrical resistivity of the soil samples varied from 10 Ω-m to 200 Ω-m.

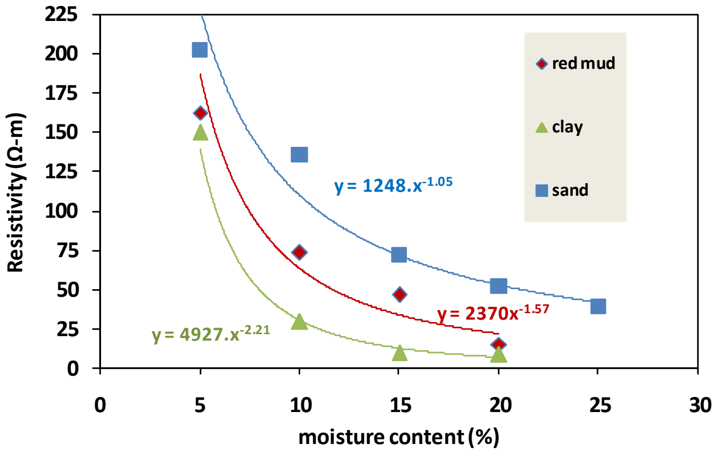

Figure 3 Resistivity versus Moisture content

Two sand samples were then taken to study the variation in resistivity with respect to void ratio. One was pure sand and the other was sand mixed with 25% by weight of clay. The moisture content of all these samples was kept constant at 10%. The samples were comoacted to different densities and void ratios (e) were calculated using mass-volume relationships. Resistivity measurements were taken for each sample and were found to increase with increase in void ratio . The value of resistivity under these condtions ranged from 100 Ω-m to 300 Ω-m. An approximately linear pattern was found in the resistivity variation, as shown in figure 4. Red mud and clay samples were not chosen for this test because of the difficulty in compacting them to higher densities in the small soil box. Clayey sand showed a lower resistivity in comparison to the sand sample.

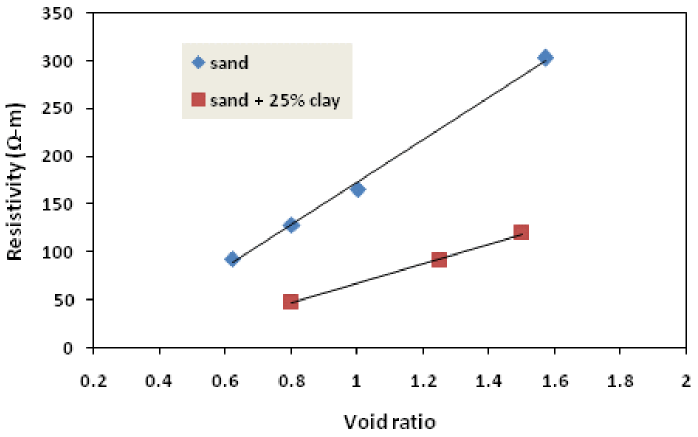

Figure 4 Resistivity versus dry density for sand sample

The next part of the study was based on the effect of water quality on the soil resistivity. To perform this test, 0.5 % by weight of table salt (NaCl) was added to the tap water. This saline water was mixed the sand samples to different moisture contents. The resistivity versus moisture test was repeated on this sample. The test showed a sharp fall in the observed resistivity values. Figure 5 shows a comparison between the resistivity values of the sand sample with tap water and saline water. Resistivity was plotted on a semi-log scale and the values were found to range from 0.7 to 8 Ω-m. This shows that the presence of any minerals or salts in the water has a marked influence on the observed soil resistivity values.

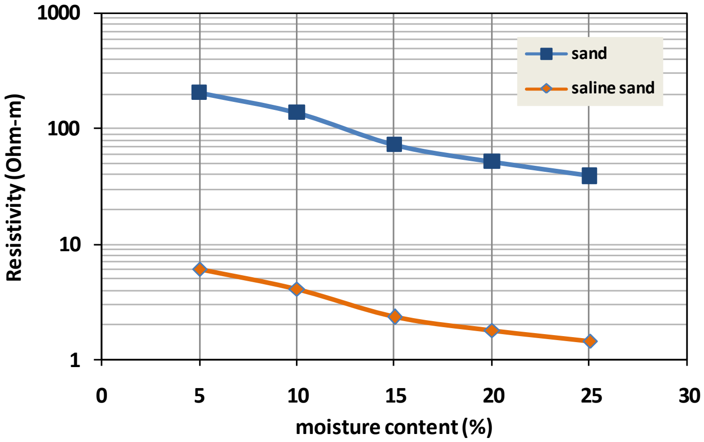

Figure 5 Resistivity versus dry density for sand sample with tap water and saline water

The last part of this study focused on measuring the electrical resistivity of the water itself. The soil box was filled with tap water mixed with different amounts of salt (by weight %) and the resistivity of the samples were measured (Figure 6). All measurements were taken at a room temperature of around 31 ° C. Tap water had a electrical resistivity of 11.7 Ω-m and its value fell substantially upon addition of salt (shown in Table 2.)

Figure 6 Measurement of tap water resistivity

Table 2 Resistivity of tap water with different amounts of salt added

Salt (% by weight)	Resistivity (Ω-m)
0	11.7
2	0.24
3	0.16
8	0.07

From all the above tests, the following inferences were made. The soil type has an influence on the resistivity values. Clay soil has a much lower resistivity than sandy soil. Red mud exhibited lower resisivity values than sand most likely because of the presence of an appreciable amount of fines and metal oxides in it. Both fines size fractions and metals are good conductors of electricity. Next it was found that resistivity increased with increase in void ratio of the samples. This could be accounted to the better water-soil partcile contact at higher densities, which leads to better conduction of electric current. The presence of salts in water has a major influence on the measured resitivity values, because saline water is known to be a much better conductor of electricty. Therefore the same soil type can display different ranges of resistivity, depending on the salinity of the water used. There is a steep reduction in resistivity of tap water, even with the addition of small amount of salt as seen from Table 2. All these factors should be considered while conducting soil resistivity measurements.

Conclusion

It can be concluded from this study that electrical resistivity of soils is dependent on factors like soil type, moisture content, density and the nature of the water. The data presented here is based on simple test setup. More accurate results can be obtained by using alternating current (AC) instead of direct current (DC), which could reduce any possible polarization effects from the latter. Field resistivity measurements of can be performed and preliminary assessment can be made about the conditions of the soil. It has also been found that most of the variations between resistivity and the soil variables are can be interpreted through simple linear or exponential type of relationships. As such, more tests can be undertaken and stronger statistical equations can be developed based on the experimental and field data. This would help engineers and practitioneers better predict the subsurface conditions from field tests.

Acknowledgement

The author expresses his gratitutde towards his undergraduate students Lav nayan, Rinki Mahato, Sourabh Singh, Sweta Padhi and Rishav Ray for taking part in this study, gathering the resources and materials and performing the tests. The author is grateful to the Head of the Department, Civil Engineering for allowing him puruse this study/ project and extending his full support. Lastly, the author thanks C V Raman Global university for facilitating the project and providing the lab and other testing facilities.

References

ASTM: G57-06,(2012),Standard Test Method for Field Measurement of Soil Resistivity Using the Wenner Four-Electrode Method

Bryson, L.S., Bathe, A., 2009, Determination of Selected Geotechnical Properties of Soil Using Electrical Conductivity Testing, Geotechnical Testing Journal, Vol 32, No. 3.

Kalinski, R.J., Kelly, W.E., 1993, Estimating the water content of soils from electrical resistivity, Geotechnical Testing Journal, pp. 323-329

Kalinski, M. E., Vemuri, S. C., 2005, A Geophysical Approach to Construction Quality Assurance Testing of Compacted Soils Using Electrical Conductivity Measurements, Geotechnical Special Publication No. 133, American Society of Civil Engineers.

Pandey, L.M.S., Shukla, S.K., Habibi, D., 2015, Electrical resistivity of sandy soil, Geotechnique Letters, 5, 178-185

Samouelian A, Cousins I, Tabbagh A, Bruand A, Richard G, 2005, Electrical resistivity survey in soil science. Soil and Tillage Research, 173-193.

Syed, A., Siddiqui, I., 2012, Use of Vertical Electrical Sounding (VES) method as an Alternative to Standard Penetration Test (SPT), Proceedings of the Twenty-second (2012) International Offshore and Polar Engineering Conference, Rhodes, Greece, ISBN 978-1-880653-94–4, pp 871-875

Contact Address

Raghava A. Bhamidipati, PhD., Civil Engineering Department, C V Raman Global University, Bhubaneswar, 752054, India, email: jones.kgp@gmail.com, Phone: +917679609321

ARTICLE HISTORY:
Received 24 April 2021
Received in revised form 6 May 2021
Accepted 20 May 2021

USE OF THE ACTIVATED SLUDGE TO REMOVE OIL POLLUTION FROM THE ENVIRONMENTALLY POLLUTED SOIL

Eszter TURČÁNIOVÁ[1], Martina LOBOTKOVÁ[1]

[1]Technical University in Zvolen. SLOVAKIA

Abstract

The petroleum substances are the most common types of the hazardous contaminants, which enter the environment mainly from the anthropogenic activities. They have a negative effect on the soil, their presence is manifested by a deterioration in the biological, chemical and physical properties. The soil contamination with the petroleum substances causes blocking the transfer of carbon dioxide from the soil to the air and also the water. The contribution presents a proposal the remediation of the contaminated soil with the petroleum substances by microorganisms. The used microorganisms are from the activated sludge from a wastewater treatment plant. Microorganisms used the contaminants in the soil as a source of the energy to create new biomass. The waste of their metabolism is harmless compounds - water and carbon dioxide. The experiment confirms the efficiency of the biodegradation process of the petroleum substances using microorganisms from the activated sludge. The efficiency of the biodegradation was determined based on the parameter - non-polar extractable substances. This parameter was determined spectrophotometrically in the infrared spectrum after solvent extraction. The soil after biodegradation was assessed from the ecotoxicological properties, using phytotoxicity tests.

Keywords: petroleum contamination, soil, active sludge, biodegradation, phytotoxicity tests

Introduction

The contamination of water and soil with petroleum substances represents a serious environmental problem which worsens the ecological and production properties of these components of the environment. The origin of the petroleum substances in the environment is very diverse, caused mainly by anthropogenic activities in which they are used widely (Jeevanantham et al. 2019; Molnárová et al. 2011).

The leaks of the petroleum substances into the aquatic environment lead to significant changes in organoleptic and physical properties, chemical and biological composition of water (Hybská and Samešová, 2009). Depending on the leaked volume, the viscosity of the petroleum substance and the flow rate of the polluted stream, they can form a homogeneous phase, or a phase dispersed in water on the surface in the form of the stable and unstable emulsions (Pinka, 2017). A layer of the petroleum substances on the surface can result in an oxygen deficiency of the aquatic environment, a reduction of the light to depth, the prevention of the process of photosynthesis and an increase of water temperature by absorption of the solar radiation. The result of these negative changes is also the eutrophication of water (Nowak et al. 2019). Some of the petroleum substances from the surface are transferred with the same harmful effects on the fauna and flora of the shore, or into the sediments to groundwater (Pinka, 2017).

The soil pollution by the petroleum substances also results of the deterioration of the physical, chemical and biological properties of the soil. The soil pollution reduces the water evaporation and increases the hydrophobicity of the soil aggregates. The formation of a greasy film on the soil surface restricts the circulation of air between the soil and the atmosphere. The soil particles are coated with petroleum substances, which prevents respiration of the soil – the leakage of CO_2 from the soil into the air (Abosede, 2013). At the same time, water is more difficult to absorb into the soil and the roots absorb water from the soil more difficult, the plants suffer from drought. The presence of the petroleum substances acts as an herbicide. The chemical properties of the soil change - the alkalization increases and the availability of the nutrients (especially phosporus and potassium) for plants reduces. The petroleum content 0.7 - 50 $ml.kg^{-1}$ of the soil (0.6 - 40 $mg.kg^{-1}$) changes the species composition of the community of the microorganisms in the soil. The proportion of *Penicillium, Aspergillus* and *Mortierella* species is increasing at the expense of *Streptomyces*, *Mucor* and others. The petroleum content higher than 300 $ml.\ kg^{-1}$ (270 $mg.kg^{-1}$) means the total death of all microscopic organisms in the soil and the soil requires radical remediation (Hybská and Samešová 2009; Frankovská 2010).

The stability of the petroleum substances in water and soil depends on their type and amount per unit area. It is true that heavier petroleum fractions are maintained for a longer time in the aquatic and rock environment than lighter fractions, which are gradually degraded by the microbial and oxidative processes (Hybská et al. 2017). The effects of the petroleum spills into the environment are unprecedented and cannot be ignored. Therefore, it is necessary to decontaminate the polluted ecosystem after the leak. The decontamination prevents the above-mentioned problems and the other serious emergencies (Okoh et al. 2019). The decontamination by the degradation processes can take place in two ways, namely the biological route, which is one of the most important processes determining the fate of the organic contaminants and in an abiotic way (Barančíková et al. 2009).

The ecotoxicological tests can be used to determine the presence or absence of the petroleum substances in the environment. The bioassays may be included in the initial screening, which identify potential sources of the pollution or are apply after chemical analyses to determine high levels of the toxicant (Fargašová, 2009). In the case of the petroleum substances, which bind to the soil matrix, bioassays are standardly used on the soil communities and higher cultivated plants, such as *Sinapis alba, Vicia sativa* and *Zea mays.* The test of the growth inhibition of the higher cultivated plants is defined in a shortened follow-up period of 3 days. In such a short-term test, the inhibition index is the best indicator to compare the results of the different tests. The inhibition index expresses the growth of the plant root inhibited by 50% - IC_{50}. Tests on seeds have a simple methodology based on STN 83 8303, so they are very well applicable. The failure caused by chemicals can manifest itself in the first days of the test by a change in the onset of the germination, respectively in later days by a change in increments (Hybská et al. 2017).

The subject of this contribution is to assess the effectiveness of the removal of the petroleum substances from soils. In this experiment, the soils are environmentally burdened by the petroleum pollution due to anthropogenic activity, and we applied process of the biodegradation using microorganisms from activated sludge from the wastewater treatment plant. These methods use the decomposition of the substances by microorganisms or the conversion of the organic pollutants into harmless products by the mineralization (Okoh et al. 2019; Mohsensadeh et al. 2010). They are currently recognized as ecological and cost-effective alternatives compared to the traditional physico-chemical method for the restoration and reclamation of the contaminated sites (Ite et al. 2019).

Material and methods

The collection of the contaminated soil with the petroleum substances was carried out in accordance with STN ISO 10381-6: Soil quality. Sampling. Part 6: Guidance on the collection, handling and storage of soil for the assessment of aerobic microbial processes in the laboratory. Subsequently, the indicators were determined in the contaminated soil samples: pH/H_2O, C, N, S and non-polar extractable substances (NES).

SenTix 21 combined glass electrode (pH 0-14/0-80 °C) and pH meter - inoLab pH Level 1 with two-point calibration were used to determine the active soil reaction – pH/H_2O (STN ISO 10390: 2005).

The determination of nitrogen, carbon and sulfur consists in burning the sample portion in excess oxygen at 900 °C, where the formed oxides (NO_x, CO_2, H_2O and SO_2) are reduced on copper and helium is carried through a chromatographic column where the individual components of the mixture are retained. After a certain time, nitrogen, carbon and sulfur exit the column in order to the detector, which registers the chromatogram and evaluates the concentration of the individual components. Chromatogram evaluation is automatic, it starts with the dosing of the sample and ends with the sending of an electrical signal, proportional to the concentration of the monitored component (ISO 13878: 1998, STN ISO 10694: 2001, ISO 15178: 2000).

The non-polar extractable substances content is determined in the samples by extraction in an organic solvent (S 316). Hydrocarbons and other non-polar and polar substances are extracted from water by the extraction. Non-hydrocarbon and polar substances are removed from the extract using a polar sorbent (e.g., silica gel). The evaluation is performed on an FTIR ATI MATSON GENESIS spectrophotometer in the infrared spectrum (Hybská et al. 2015).

The determination of the dry matter is based on STN-EN 12 880. It is based on drying the sample to constant weight at 105 °C.

Process of the biodegradation

After determining the basic parameters of the contaminated soil, we focused on the process of the biodegradation with the using microorganisms from the activated sludge from the waste water treatment plant. We evaluated the efficiency of the biodegradation based on the changes in the value of non-polar extractable substances (NES). The biodegradation was performed in the form of the vessel experiments. The contaminated soil was enriched with activated sludge at the regular intervals, for 28 days. Each sample was enriched with a different concentration of the activated sludge. Subsequently, the soil after biodegradation was also assessed from an ecotoxicological point of the view, using phytotoxicity tests, using aqueous extracts from the contaminated soil.

Test of the growth inhibition of the root of *Sinapis alba*

By the terrestrial test of the growth inhibition of the root of *Sinapis alba* was observed impact of aqueous extracts from the contaminated soil with the petroleum substances on the root’s growth of the vascular plants. The increments of white mustard roots were measured and obtained values were used for the calculation of the root growth inhibition in comparison with the control sample. The aqueous extracts from the contaminated soil were prepared from an amount corresponding to 100 ± 0.1 g of the dry matter and the volume used was a liter of the demineralized water. The samples were shaken vigorously on a ROTABIT rotary shaker at 180 rpm for 6 hours. After this time, the mixture sedimented for 18 hours. The conditions of the preliminary test with *Sinapis alba* are shown in Table 1, based on STN 83 8303: 1999: Testing of dangerous properties of wastes. Ecotoxicity. Acute toxicity tests on aquatic organisms and growth inhibition tests of algae and higher cultivated plants.

Table 1 Preliminary test with *Sinapis alba*

Testing organism	*Sinapis alba*, germination > 95 %, per 30 seeds in Petri dishes
Sample volume	10 ml
Temperature	20 °C ± 1 °C, thermostat TS 606 CZ/2-Var (WTW, Germany)
Control	reconstituted water
Measuring root length	steel calibrated measuring instrument
Exposure time	72 hours
The response monitored	the inhibition of root´s growth of *S. alba* compared with the control

Results and discussion

The values of the determined non-polar extractable substances (NES) from the individual experimental samples during the biodegradation process are recorded in Figure 1 and the statistical characteristics are in Table 2.

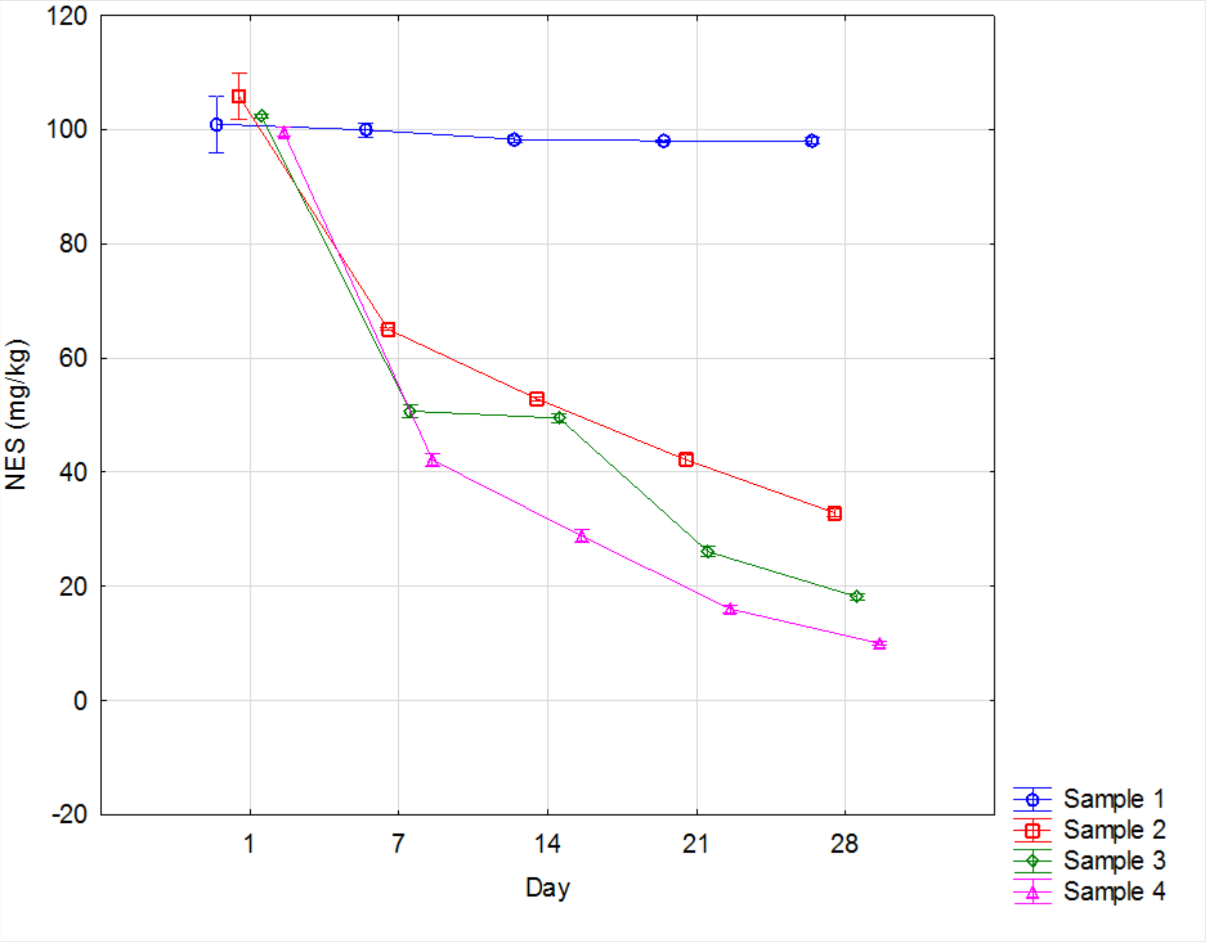

Figure 1 The process of the biodegradation according to removal NES

Notes (uniform for all tables and figures in the contribution):

1 – sample without addition of the activated sludge

2 - sample with the addition of 0.5 g of the dry matter of the activated sludge

3 - sample with the addition of 1.0 g of the dry matter of the activated sludge

4 - sample with the addition of 2.0 g of the dry matter of the activated sludge

Table 2 Basic statistical characteristics

The sample	Day	NES [mg/kg]			Average [mg/kg]
		SD (standard deviation)	-95.00 %	95.00 %	
1	1	1.55	96.03	105.90	100.97
1	7	0.39	98.70	101.21	100.97
1	14	0.15	97.84	98.82	98.33
1	21	0.06	97.85	98.25	98.05
1	28	0.18	97.44	98.61	98.02
2	1	1.26	101.81	109.85	105.83
2	7	0.08	64.81	65.31	65.06
2	14	0.10	52.55	53.21	52.88
2	21	0.28	41.31	43.11	42.21
2	28	0.21	32.25	33.59	32.92
3	1	0.12	101.94	102.70	102.32
3	7	0.36	49.58	51.84	50.71
3	14	0.26	48.65	50.31	49.48
3	21	0.28	25.20	26.98	26.09
3	28	0.17	17.65	18.75	18.20
4	1	0.24	98.80	100.36	99.58
4	7	0.37	40.98	43.31	42.14
4	14	0.34	27.76	29.93	28.85
4	21	0.19	15.44	16.66	16.05

Table 3 The evaluation (%) of the biodegradation process

The sample	Day	NES [mg/kg] average	Decrease NES [%]
1	1	100.97	2.92
	28	98.02	
2	1	105.83	68.89
	28	32.92	
3	1	102.32	82.21
	28	18.20	
4	1	99.58	83.88
	28	16.05	

According to the results, we can state that the regular addition of the activated sludge, which the volume corresponded to the reported sludge dry matter, showed a significant biodegradation effect of the oil pollution determined by NES compared to a soil sample without the addition of the activated sludge. There is no significant difference in the amount of the oil pollution degraded between the addition of 1 g and 2 g of the activated sludge dry matter. This follows from Table 3.

For comparison, the authors (Hybská and Villárová 2012) found in their study that the most significant decrease in the concentration of NES was found in a soil sample where BIOROP FAT was applied. Among the samples where sewage sludge and BIOROP preparation were used, the steepness of the decrease in NES concentration was almost the same. At the beginning of the experiment, the average concentration of NES in the samples was 1.972 mg / kg. Natural biodegradation without the addition of microorganisms degraded 29.9% of petroleum substances. The efficiency of the sludge in the samples was 43.6%. 76.7% of petroleum substances were removed from the samples with the addition of the commercial reagent BIOROP FAT, while in the case of using BIOROP up to 83.6%.

For example, Hazim and Al-Ani (2019) found in their study that at the end of twelve weeks the result indicates the higher percentage of biodegradation 49.6% was recorded in soil contaminated with 5% kerosene while the lower percentage of biodegradation 10.8% was recorded with soil contaminated 10% non-used lubricate. The percentage of hydrocarbons biodegradation in the soil contaminated with 5% diesel, 5% non-used lubricate oil and 5% used lubricate oil were 32%, 28% and 24% respectively. However, the biodegradation of Kerosene 10%, diesel 10%, and used lubricate oil were 30%, 25.6% and 12.4% respectively. Positive correlation was found between hydrocarbon utilizing bacteria (HUB) count and percentage of hydrocarbons biodegradation. This result show there was reversal relationship between hydrocarbons biodegradation percentage and the contaminant concentration and this consistence with. High concentration of contaminant causing decreasing in biodegradation percentage due to high concentration can be inhibitory of microorganisms by toxic effects for this reason reported that bioremediation is a useful method of soil remediation if contaminant concentrations are moderate. The biodegradation percentage in hydrocarbons contaminated soil was in the order of kerosene > diesel> lubricate oil > used lubricate oil. The kerosene, diesel, and lubricate oil consisted mainly of n-alkanes with chain length of C10–C16, C10–C22 and C15 - C50 respectively. The results show there was no huge differences in biodegradation percentage between non-used and used lubricate oil.

By reducing the NES in the experimental samples by the biodegradation process, there was a slight increase in pH (Figure 2). The soil reaction of the weakly acidic soil changes to alkaline due to the presence of the petroleum substances, which was also reflected in our experiment (Frankovská et al. 2010).

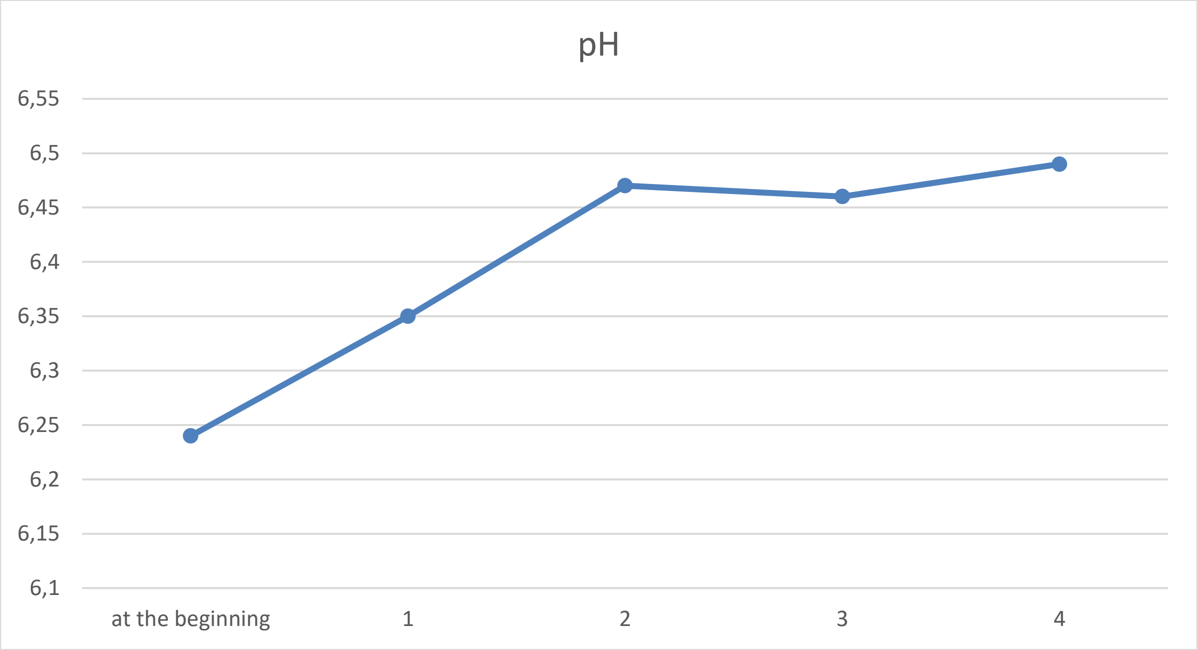

Figure 2 pH changes in experimental samples

Table 4 The results of C, N, S analysis in soils

The sample	N %	C %	S %
Harvested soil			
1	0.685	23.5	0.165
2	0.596	20.1	0.158
3	0.538	18.4	0.147
4	0.534	17.3	0.143

The values of the elements C, N and S determined in the samples are recorded in Table 4. They show that during the biodegradation process there was a decrease in carbon in particular due to increased soil respiration, in which the production of the petroleum substances by microorganisms added to the soil in activated sludge has increased CO_2 production.

The last part of the experiment was focused on the assessment of the ecotoxicological properties of the investigated soil using phytotoxicity tests by the aqueous extracts. We applied a preliminary test with the use seeds of *Sinapis alba* at the first and the last day of the biodegradation process. The test results are shown in the following table (Table 5).

Table 5 A preliminary test with *Sinapis alba*

The sample	Day	Inhibition (%) average
1	1 (the first day)	87.49
	28 (the last day)	85.17
2	1 (the first day)	85.69
	28 (the last day)	29.21
3	1 (the first day)	83.14
	28 (the last day)	22.23
4	1 (the first day)	86.26
	28 (the last day)	21.78

The Table 5 shows that the percentage inhibition at the first day, in each sample, indicates a high growth inhibition compared to the control. In this case, in accordance with STN 83 83 03, it is necessary to determine the IC_{50} value of the aqueous extract and perform a basic test. This soil is toxic for agriculture plants.

At the same time, the table shows that after 28 days, in each case (in samples 2-4), the percentage inhibition of *Sinapis alba* growth fell below 30 %, which means that the test is negative. The result is reported, and testing is no longer performed. A reduction in the percentage inhibition in the biodegradation process indicates a reduction in soil toxicity and the fact, that the soil is suitable for agricultural plants. In the case of the sample 1, without activated sludge, the percentage of the inhibition not added decreases not significantly.

Regeneration of waste oils is an environmentally friendly solution to the renewal of their basic properties, which also helps reduce the volume of the hazardous waste they produce. From an overall assessment of the impact of wear and tear on the properties of the tested mineral oil Turbinol X-EP 46, it appears that the regeneration process of electrostatic precipitation has a positive impact on the ecotoxicological and biodegradation properties of oils. By eliminating the many products resulting from the use of the oil, the composition of the regenerated oil is similar to the composition of new oil, and we also assume that the process causes no significant changes to the required properties (viscosity, pour point, and other) in terms of the use of the oil in practice. From comparison of the inhibition of said products in the ecotoxicological tests of the model samples, in ecotoxicological terms, the used mineral oil possesses the worst characteristics, and the regenerated oil has the best, although they are always toxic, given their petroleum origin. Providing that the ecotoxicological effects of the recovered oil are comparable to or more favorable than those of the new oil, oil regeneration is found to be an effective method (Hybská et al. 2017).

Conclusions

The limit value for non-polar extractable substances in agricultural land is set in Act no. 220/2004 Coll. on protection and use agricultural land - 0.1 mg/kg. This value could not be reached with this method. Nevertheless, we can state that the application of the activated sludge to remove the petroleum pollution is a suitable method and its significance of the application is described as follows.

The obtained and presented results of the petroleum pollution removal by biological method ex situ - by removing the petroleum substances from contaminated soil by adding the activated sludge show that this method is suitable and applicable in practice for the polluted soils with NES content of about 100 mg/kg of the soil.

In addition to the reduction of NES content in contaminated soil samples, it can be stated that there was also a decrease in the percentage inhibition of *Sinapis alba* growth. After the biodegradation process, the soil was tested as non-toxic, and the percentage of the inhibition is below 30 %, which means that the soil does not need to be tested further.

Acknowledgment

This work was supported by the Technical University in Zvolen under the project IPA TUZVO 11/2020 “Využitie aktivovaného kalu pri odstraňovaní environmentálnej záťaže spôsobenej ropným znečistením.“

References

ABOSEDE, E. 2013. Effect of crude oil pollution on some soil physical properties. In Journal of Agriculture and Veterinary Science, vol. 6, no. 3, pp. 14-17. ISSN: 2319-2380

BARANČÍKOVÁ, G. et al. 2009. Chémia životného prostredia. Prešovská univerzita. Prešov. 255 p. ISBN 978-80-555-0082-9

FARGAŠOVÁ, A. 2009. Ekotoxikologické biotesty. Perfekt. Bratislava. 317 p. ISBN 978-80-8046-422-6

FRANKOVSKÁ, J et al. 2010. Atlas sanačných metód environmentálnych záťaží. Štátny geologický ústav Dionýza Štúra. Bratislava. ISBN 978-80-89343-39-3

HAZIM, R. N. and AL-ANI, M. A. 2019. Effect of petroleum hydrocarbons contamination on soil microorganisms and biodegradation. In Rafidain Journal of Science, vol. 28, no. 1. p. 13-22

HYBSKÁ, H. – SAMEŠOVÁ, D. 2009. Ropné látky - kontaminanty lesného prostredia. In Monitorovanie a hodnotenie stavu životného prostredia VIII: zborník referátov z odborného seminára. Technická univerzita vo Zvolene. p 71-78. ISBN 978-80-228-2072-1

HYBSKÁ, H. – VILLÁROVÁ, M., 2012. Účinnosť vybraných produktov pri odbúraní ropného znečistenia. In Acta Facultatis Ecologiae, vol. 27

HYBSKÁ, H. et al. 2015. Impact of organic pollutants on the environment. Technical University in Zvolen. Zvolen. 186 p. ISBN 978-80-228-2766-9

HYBSKÁ, H. et al. 2017. Study of the regeneration cleaning of used mineral oils - ecotoxicological properties and biodegradation. In Chemical and biochemical engineering quarterly, vol. 31, no. 4, pp. 487-496. ISSN 0352-9568

ISO 13878. 1998. Soil quality — Determination of total nitrogen content by dry combustion

ISO 15178. 2000. Soil quality — Determination of total sulfur by dry combustion

ITE, A. et al. 2019. Role of plants and microbes in bioremediation of petroleum hydrocarbons contaminated soils

JEEVANANTHAM, S. et al. 2019. Removal of toxic pollutants from water environment by phytoremediation: a survey on application and future prospects. Environmental technology & innovation, vol. 13. p. 264-276

MOHSENZADEH, F. et al. 2010. Phytoremediation of petroleum-polluted soils: Application of Polygonum aviculare and its root-associated (penetrated) fungal strains for bioremediation of petroleum-polluted soils. Ecotoxicology and environmental safety, vol. 73, no. 4. p. 613-619

MOLNÁROVÁ, M. et al. 2011. Anthropogenic influences on the atmosphere, hydrosphere and pedosphere. Comenius University in Bratislava. Bratislava

NOWAK, P. et al. 2019. Ecological and health effects of lubricant oils emitted into the environment. In International journal of environmental research and public health, vol. 16, no. 16

PINKA, J. 2017. Znečisťovanie vody a pôdy pri vyhľadávaní, ťažbe a pri preprave ropy a ropných produktov. In Situácia v ekologicky zaťažených regiónoch Slovenska a Strednej Európy: z XXVI. vedecké sympózia s medzinárodnou účasťou, ktoré sa konalo 19. – 20. október 2017 v Hrádku

STN 83 8303. 1999. Testing of dangerous properties of wastes. Ecotoxicity. Acute toxicity tests on aquatic organisms and growth inhibition tests of algae and higher cultivated plants

STN ISO 10381-6. 2002. Soil quality. Sampling. Part 6: Guidance on the collection, handling and storage of soil for the assessment of aerobic microbial processes in the laboratory

STN ISO 10390. 2005. Soil quality — Determination of pH

STN ISO 10694. 2001. Soil quality. Determination of organic and total carbon after dry combustion (elementary analysis)

STN-EN 12 880. Characterization of sludge. Determination of dry matter and water content

Contact address

Ing. Eszter Turčániová, Technical University in Zvolen, Faculty of ecology and environmental sciences, Department of Environmental Engineering, T. G. Masaryka 24, 960 01 Zvolen, +421 45 520 6448, xturcaniovae@is.tuzvo.sk

Ing. Martina Lobotková, Technical University in Zvolen, Faculty of ecology and environmental sciences, Department of Environmental Engineering, T. G. Masaryka 24, 960 01 Zvolen, +421 45 520 6448, xlobotkova@is.tuzvo.sk

ARTICLE HISTORY:
Received 30 April 2021
Received in revised form 12 May 2021
Accepted 20 May 2021

DRAFT ANTI-FLOOD AND ANTI-EROSION MEASURES IN THE CADASTRAL AREA VEĽKÉ ZÁLUŽIE

Jakub PAGÁČ[1], Alexandra PAGÁČ MOKRÁ[1], Jozefína POKRYVKOVÁ[1], Vladimír KIŠŠ[1]

[1]Slovak University of Agriculture in Nitra, SLOVAKIA

Abstract

This paper on the topic of the proposal of anti-flood and anti-erosion measures deals with a part of the cadastral area of Veľké Zálužie on Lúčna and Vodná streets, where approximately 50 family houses are endangered, which flood during heavy rains. In the article, we dealt with the causes of frequent floods in a given locality, which are periodically repeated at higher rainfall intensity. Based on the current land use and terrain survey, we have identified that the cause of floods arises on agricultural land, which makes up 80 ha (70%) of the total model area of 114 ha. Based on the identified causes of floods, the calculated intensity of water erosion using a modified USLE equation by Wischmeier, Smith (Wischmeier and Smith, 1978) we have prepared a draft for anti-flood and anti-erosion measures, such as grassed waterway in the thalweg, anti-erosion agrotechnics, anti-erosion flow diversion banks, vegetated waterway (bioswale), infiltration and detention basin. Based on the recalculation of soil loss after the incorporation of the draft of anti-flood and anti-erosion measures, we can conclude that by applying the draft measures it would be possible to reduce the intensity of water erosion in the model area by 123 t. ha^{-1}.$year^{-1}$ which represents a decrease of 38% from the original calculated soil loss of 329 t. ha^{-1}.$year^{-1}$.

Keywords: water erosion, floods, USLE, soil loss

Introduction

The flood is defined as the transient flooding of the water flow surroundings caused by the rise of water level above the shores. It is usually a natural disaster that occurs due to sudden or unexpected changes in the meteorological situation (Veľký, 1980). A violent flood cause extensive deaths and large economic losses every year (Zhang et al., 2021). Floods occur for several reasons, such as insufficient capacity of a watercourse trough to carry out a flood wave. The water subsequently pours out of the trough and floods the adjacent areas. Another reason may be the internal waters that arise in certain areas from precipitation or snowmelt, so that it cannot flow freely from this area and creates floods. The cause of floods can also be an increase in the groundwater level and the rise of groundwater above the ground surface (SVP, 2017). In Slovakia, we characterize the degree of flood activity according to Act no. 7/2010 coll. on flood protection is defined as a natural phenomenon in which water temporarily floods an area that is not normally flooded. During extreme meteorological-hydrological events, mud floods occur, which result in intense water erosion (especially potholes). Mud floods are streams of water flowing from fields on slopes, carrying large amounts of soil. According to Stankoviansky (2010) assumes a link between soil erosion and muddy floods on agricultural land. One of the most significant problems during floods is the land that is carried from the property of one owner at second owner on foreign land (Pagáč Mokrá et al., 2021). Water erosion is considered to be the most critical form of soil degradation. Loss of soil by water erosion can be a major threat to agronomic productivity and soil quality (Panagos et al., 2018). The extent of soil loss due to erosion and consequent environmental damage arises from a combination of farming, land use factors and heterogeneous natural factors. Agricultural land is particularly prone to soil erosion: intensive soil machining, selve, cultivation of row and special crops, as well as the use of herbicides lead to temporarily soil-free vegetation that is not protected from the erosive forces of wind and water (Borrelli et al., 2020). The authors Borrelli et al. (2018) claim that more erosion as well as land loss in rivers is caused by agriculture. Soil erosion is classified according to the factor (water, wind, glacial, snow, earth, anthropogenic erosion), form (surface, pothole, jet, sliding, dust erosion), and intensity (harmful, balanced, harmless erosion) (Antal, 2005). The Wischmeier-Smith universal soil loss equation is one of the most widely used methods for calculating soil erosion by water erosion (Wischmeier and Smith, 1978). In the conditions of Slovakia, the soil is most endangered by degradation processes by water erosion. The extent of erosion (soil loss) is divided into four categories (none to weak, medium, high and extreme erosion) (Kročková, 2016). Erosion has a detrimental effect on the fertility of the soil that we desperately need for our lives. People gradually studied and found out how to partially or completely eliminate the effect of erosion on the soil. The impact of erosion can be eliminated by various land management, designing anti-erosion measures such as ditches, terraces or a suitable combination of growing different crops. The basic principles of soil protection against water erosion include organizational anti-erosion measures, agrotechnical anti-erosion measures and technical anti-erosion measures (Muchová and Vanek, 2009). The aim of the paper is to solve the outflow regime in the rural zone cadastral area Veľké Zálužie. Protect the village from storm water from the valley below the motorway feeder for Lúčna and Vodná streets. Retain water in the landscape and prevent its negative effect on the landscape.

Material and methods

The boundary of the model area was determined on the basis of a digital model relief (DMR) created from the basic map of the Slovak Republic scale 1:10 000. In the creation of DMR, an interpolation method with a grid resolution of 5x5m was used. An orthophotomap was used to create a map of the current land use. ArcGIS software was used to analyze the erosion risk of soils by water erosion. Was used a modified USLE equation from Wischmeier, Smith (Wischmeier and Smith, 1978). The length and slope factor was replaced by the LS factor.

$$SP = R. K. L. S. C. P \qquad (1)$$

where:

SP - loss of soil caused by water erosion [$t.ha^{-1}.year^{-1}$],
R - rainfall-runoff erosivity factor [$MJ.ha^{-1}.year^{-1}$],
K - soil erodibility factor [$t. MJ^{-1}$],
L - slope length factor, non-dimensional,
S - slope steepness factor, non-dimensional,
C - cover management factor, non-dimensional,
P - support practice factor, non-dimensional.

The R-factor is calculated as the product of the total kinetic energy of rain and its maximum 30-minute intensity (Malíšek, 1990) Values from ombrographic records were used to determine the R factor (Ilavská et al., 2005). Factor K is defined as the soil loss per unit of rain factor R from a unit plot. Determination the K factor in the conditions of Slovakia is tentatively determined according to the type of soil (Ilavská et al., 2005). A significant difference was the combination of

S factor and L factor into one common called topographic factor. The LS factor expresses the ratio of soil loss from the investigated slope to soil loss from unit land. To calculate the LS factor, we also took into account barriers such as watercourses, roads, built-up areas, strips of non-forest woody vegetation and forests. Factor C is defined as the ratio between the intensity of erosion on soil with vegetation cover and the intensity of erosion on cultivated eel. Factor C of the protective effect of vegetation is also expressed by the agrotechnics used and the sowing procedure (Alena 1986) according to the type of land use in the given river basin. The P factor defines the ratio between the erosion intensity in the investigated area and the applied anti-erosion measures and the erosion intensity on the same plot cultivated in the direction of the slope.

Description of the area

Figure 1 Model area

The village of Veľké Zálužie lies in the Nitra Uplands, which is part of a larger bulk, the Podunajska pahorkatina. The development of the village was influenced not only by good natural conditions for growing agricultural crops and grapevines, but also by its location in relation to the town of Nitra, which until the end of the 19th century developed as a town with a toll station (Keresteš, 2011). The village of Veľké Zálužie (Figure 1) is located 10 kilometres west of the regional and district town of Nitra. In terms of hydrological conditions, the village of Veľké Zálužie belongs to the Nitra river basin. The most important stream is the river Dlhý kanál, which is a right-hand tributary of the Nitra with a length of 51 km. It springs in the Podunajskej pahorkatine of the geomorphological part of the Zálužianska pahorkatina, in the cadastral territory of the village of Lehota (200 m). The Veľké Zálužie reservoir also stretches along this stream. From a climatic point of view, we classify the village into a warm climatic area, specifically into a warm, dry district with a mild winter. The average annual rainfall is 550 to 750 mm (Čeman, 2010).

The most affected area occurs in the northwestern part of cadastral area Veľké Zálužie. In the micro-basin (11,394 ha), which threatens approximately 50 family houses in the problem area, there is a bridge over the R1 expressway, arable land, local roads, field roads and non-forest woody vegetation. The terrain is slightly sloping. The slopes are converged to the valley in which two streets are located during distinctive rains. The flood wave subsequently follows under road III. class moves to Podvinohrady Street. The houses on one side of this street have sloping gardens, in the lower part of which passes the Čerešňový potok, which cannot absorb the torrential wave until the water out and the gardens are flooded. This street is affected by water coming from Lúčna and Vodná streets, and from the lower part by water from a stream. The cause of the floods was due to inappropriate sowing procedures with a preference for crops such as corn, non-compliance with the delimitation principles of the division of the type of land use on the slope, unpaved slopes, improper outlet of the outlets from the road body and neglected maintenance of the culvert under the road body. In the urban area, the cause of floods is due to the construction of IBVs on arable land, irregular maintenance of drainage channels, absence of infiltration elements for retaining rainwater from roofs and yards and drainage of roof gutters to the local road. The current of the land use in the model locality is mostly represented by arable land in the area of 80 ha, which represents 70% of the total area of the model area. A map of land cover and land use has been created (Figure 2).

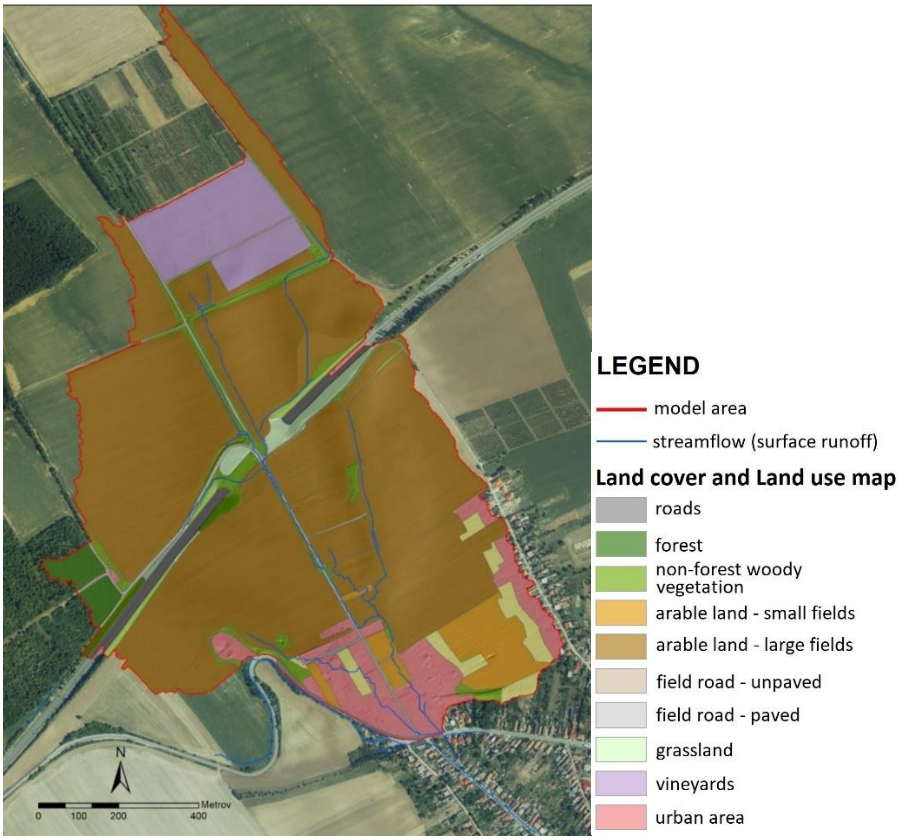

Figure 2 Land cover and Land use

Results and discussion

To perform the calculated water erosion intensity by the modified USLE equation in the model area, we used the factor values: R factor 24.62; K factor 0.25 - 0.72; LS factor 0 - 142; C factor 0.005 for permanent grassland, 0.36 for arable land, 0.80 for vineyards, 0.90 for field roads, 0.55 for non-forest woody vegetation. Due to the lack of data on land management, we determined the value of the P factor = 1. A map of the calculated water erosion intensity was created based on the current land use (figure 3).

Table 1 presents statistics on the values of soil loss that is withdrawn to land types. Based on the results, it follows that from the arable land area of the model area on an area of 80 ha, we can assume a soil loss of 306 t. ha $^{-1}$. year $^{-1}$. If we assume that the soil loss of 0.13 mm per 1 ha of area is equivalent to a soil loss of 1.5 t. ha $^{-1}$. year^{-1} (Antal, 2005) on arable land, the soil loss could average up to 0.33 mm per 1 ha.

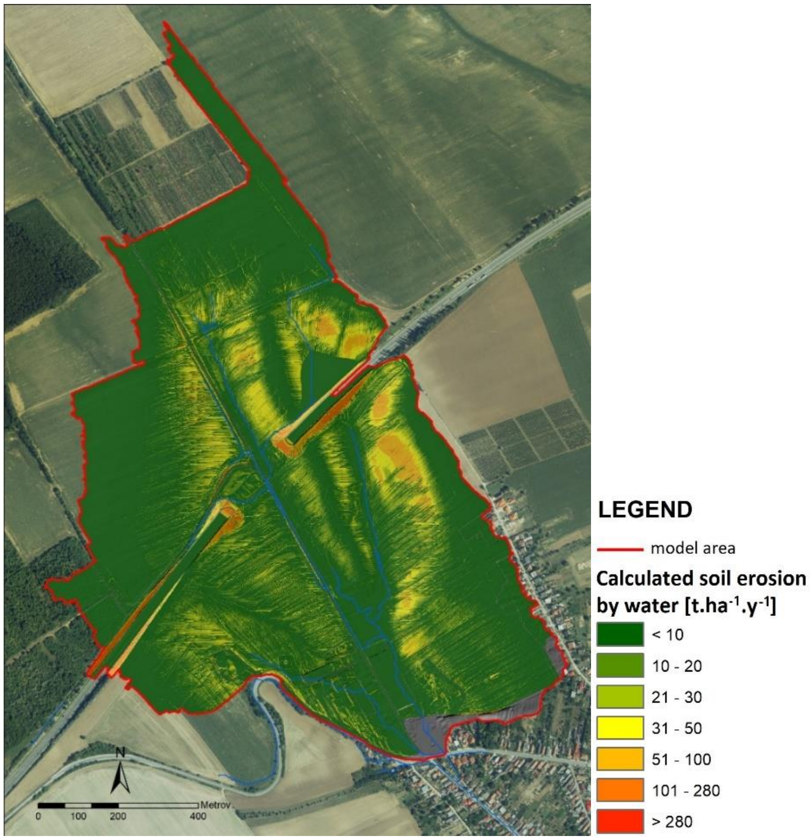

Figure 3 Calculated intensity of water erosion in the model area

Table 1 Calculated intensity of water erosion in the model catchment area related to the land use

Soil loss (t. ha $^{-1}$. year $^{-1}$)	Area (ha)	Median (t. ha $^{-1}$. year $^{-1}$)	Calculated soil loss (t. ha $^{-1}$. year $^{-1}$)	Calculated soil loss (%)
arable land	80.35	3.808	305.99	92.98
vineyards	8.20	2.752	22.55	6.85
grassland	1.72	0.323	0.55	0.17
together	90.27		329.10	100.00

From the results shown in Table 1, we can state that the expected soil loss is largely represented on arable land and represents up to 93% of the total soil loss from the model area.

In identifying the causes of floods accompanied by water erosion and subsequent clogging of watercourses in the lower parts of the village, we mainly focused on land that is used as arable land. Terrain survey, we found problems in poor agrotechnics on arable land, large arable land with the cultivation of one crop, non-compliance with sowing procedures in larger slopes of the area, plowing to the border of the forest path and drainage channel and, last but not least, non-compliance with the delimitation principles of the division of land use on the slope (figure 4).

Figure 4 Problems in the model area – arable land / large fields (left picture); erosion grooves (right picture)

Based on the identified causes of floods, calculated intensity of water erosion, slope slope, uninterrupted slope length and accumulation we prepared a draft for anti-flood and anti-erosion measures (figure 5). In the model area, we draft the following elements to mitigate water erosion and support surface water infiltration: grassed waterway in the thalweg (ZÚ1 – ZÚ6); anti-erosion agrotechnics; anti-erosion flow diversion banks (PPP1 – PPP6); grass drainage swale (VP1 – VP2); vegetated waterway (bioswale) (OR1); infiltration basin (RN1 – RN3); detention basin (VN1).

We have re-incorporated the draft anti-flood and anti-erosion measures into the map of the current land use due to the occupation of arable land on these elements. We also reclassified the values of the factors of the modified USLE equation and added support practice factor based on anti-erosion measures (Ilavská et al., 2005). For re-execution of the calculated intensity of water erosion in the model area with incorporated measures, we used the values of factors: R factor 24.62; K factor 0.25 - 0.72; LS factor 0 - 142; C factor 0.005 for permanent grassland, 0.36 for arable land, 0.80 for vineyards, 0.90 for field roads, 0.55 for non-forest woody vegetation; P factor 0.60 - 1 (figure 6).

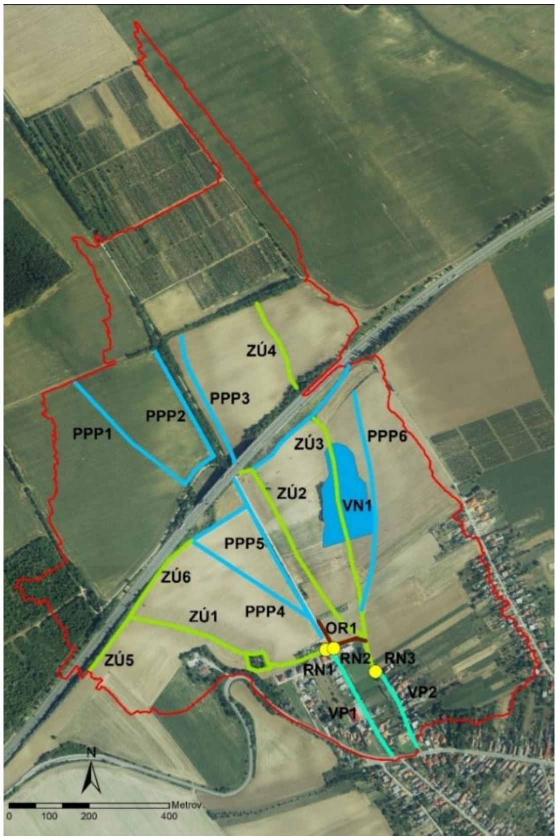

Figure 5 Draft anti-flood and anti-erosion measures

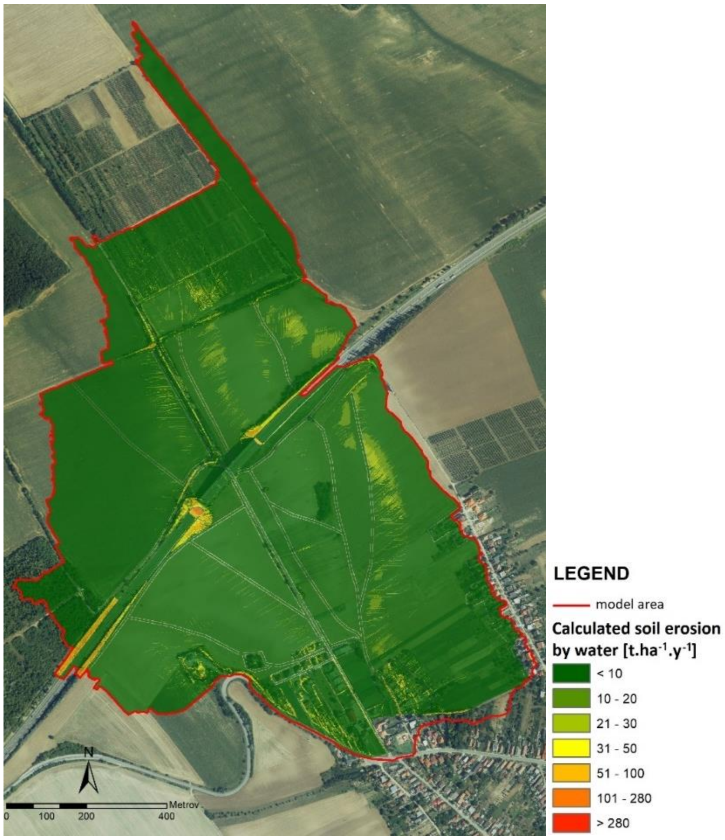

Figure 6 Calculated intensity of water erosion in the model area after incorporation of the draft of anti-flood and anti-erosion protection

Table 2 summarizes the results after recalculating the soil loss. After the incorporation of the draft of anti-flood and anti-erosion protection in the model area, the value of soil loss decreased by approximately 123 t. ha $^{-1}$. year $^{-1}$ of total agricultural land to 206,20 t.ha^{-1}.year^{-1}. The largest decline occurred on arable land from the original 306 t. ha $^{-1}$. year $^{-1}$ on the 182 t. ha $^{-1}$. year $^{-1}$, which represents a reduction in soil loss of more than 40%. With these drafts, we would be able to reduce the average soil loss from 0.33 mm to 0.21 mm from 1 ha.

Table 2 Calculated intensity of water erosion in the model catchment area related to the types of land use after the incorporation of the draft of anti-flood and anti-erosion measures

Soil loss (t. ha $^{-1}$. year $^{-1}$)	Area (ha)	Median (t.ha^{-1}.year^{-1})	Calculated soil loss (t. ha $^{-1}$. year $^{-1}$)	Calculated soil loss (%)
arable land	75.19	2.421	182.06	88.29
vineyards	8.20	2.748	22.53	10.93
grassland	6.88	0.235	1.62	0.78
together	90.27		206.20	100.00

We can state that by building the draft anti-flood and anti-erosion measures in the model area on an area of 5.16 ha (mostly on arable land) it is possible to reduce the value of soil loss by 123 t. ha $^{-1}$. year $^{-1}$ which represents 0.12 mm of soil from 1 ha.

Conclusions

The aim of the paper was to create a model draft of the runoff in the rural area of cadastral area Veľké Zálužie. In the draft, we addressed the retention of water in the country and prevented its negative impact on the country. The result of the draft was to retain water in the country as much as possible by means of elements supporting the infiltration of surface water into the subsurface. Also, these proposed elements are able to reduce soil degradation and thus prevent the deposition of sediments in the streams of the village. We draft these elements in the model area: six grassed waterways in the thalweg; six anti-erosion flow diversion banks, two grass drainage swales; one vegetated waterway (bioswale); three infiltration basin and detention basin. The intensity of water erosion was calculated for the model area on the basis of the current land use, and subsequently, after incorporating the draft of anti-flood and anti-erosion measures, we recalculated the loss of soil. Based on the performed modeling, the following conclusions can be presented:

- after incorporating draft for anti-flood and anti-erosion measures in the model area, it would be possible to reduce the intensity of water erosion by 123 t. ha^{-1}. year^{-1},

- reduction of arable land on the soil loss from the original 306 t. ha $^{-1}$. year $^{-1}$ on the 182 t. ha^{-1}. year^{-1}, which represents a reduction of soil loss by more than 40%, which represents 0.12 mm of soil from 1 ha.

Acknowledgment

"This publication is the result of the project implementation: „ Scientific support of climate change adaptation in agriculture and mitigation of soil degradation" (ITMS2014+ 313011W580) supported by the Integrated Infrastructure Operational Programme funded by the ERDF."

References

ALENA, F. 1986. Stanovenie straty pôdy erozívnym splachom pre navrhovanie protieróznych opatrení: Metodická pomôcka. Bratislava: ŠMS. 58 s.

ANTAL, J. 2005. Protierózna ochrana pôdy. Nitra: SPU v Nitra, 79 s. ISBN 80-8069-572-5.

BORRELLI, P. et al. 2020. Land use and climate change impacts on global soil erosion by water (2015-2070). Proceedings of the National Academy of Sciences Sep 2020, 117 (36), ISSN 21994-22001.

BORRELLI, P. et al. 2018. A step towards a holistic assessment of soil degradation in Europe: Coupling on-site erosion with sediment transfer and carbon fluxes, Environmental Research, Volume 161, 2018, Pages 291-298, ISSN 0013-935.

ČEMAN, R. et al. 2010. Zemepisný atlas Slovenská republika. Bratislava: MAPA Slovakia, 2010. 96 s. ISBN 80-8067-138-9.

ILAVSKÁ, B. et al. 2005. Identifikácia ohrozenia kvality pôdy vodnou a veternou eróziou a návrh opatrení. Bratislava: VÚPOP 2005. 60 s.

KERESTEŠ, P. 2011.Veľké Zálužie obec s históriou, ENARS, s. r. o., Nitra, 328 s. ISBN 978-80-970612-2-7.

KROČKOVÁ, B. 2016. Erózia poľnohospodárskych pôd. Slovenská agentúra životného prostredia. [online]. 2016 [cit. 2021-01-04]. Dostupné na internete: <https://www.enviroportal.sk/indicator/detail?id=221&print=yes>

MALIŠEK A., Zhodnotenie faktora eróznej účinnosti prívalové zrážky, Geographic journal, vol. 42, pp. 410 – 422, 1990.

MUCHOVÁ, Z. – VANEK, J. et al. 2009. Metodické štandardy projektovania pozemkových úprav. Nitra, Slovenská poľnohospodárska univerzita v Nitre v spolupráci s Ministerstvom pôdohospodárstva 2009, ISBN 978-8-552-0267-9.

PAGÁČ MOKRÁ, A. et al. 2021. Analysis of Ownership Data from Consolidated Land Threatened by Water Erosion in the Vlára Basin, Slovakia. Sustainability 2021, 13, 51.

PANAGOS, P. et al. 2018. Cost of agricultural productivity loss due to soil erosion in the European union: from direct cost evaluation approaches to the use of macroeconomic models. Land Degr Dev 29(3):471–484.

STANKOVIANSKY, M. 2010. Erózia pôdy a problémy, ktoré s tým súvisia, Univerzita Komenského, Bratislava, Realizácia projektu LPP-0130-09.

SVP 2017. Charakteristika povodní. Slovenský vodohospodársky podnik – štátny podnik. [online]. 2017 [cit. 2021-15-04]. Dostupné na internete:< https://www.svp.sk/sk/uvodna-stranka/povodne/charakteristika-povodni/>

WISCHMEIER, W. H. – SMITH, D. D. 1978. Predicting Rainfall Erosion Losses – a Guide to Conservation Planning. U. S. Department of Agriculture, Agricultural Handbook 1978 No. 537, Hyatsville, p. 58.

YUE, Z. et al. 2021. Projection of changes in flash flood occurrence under climate change at tourist attractions. Journal of Hydrology. Volume 595, 2021,126039, ISSN 0022-1694.

Contact address

Ing. Jakub Pagáč, PhD., Slovak University of Agriculture in Nitra, AgroBioTech Research Centre, Tr. A. Hlinku 2, 949 76, Nitra, Slovakia, +421 37 641 4947, jakub.pagac@uniag.sk

Ing. Alexandra Pagáč Mokrá, Slovak University of Agriculture in Nitra, Horticulture and Landscape Engineering Faculty, Department of Landscape Planning and Land Consolidation, Hospodárska 7, 949 76 Nitra, Slovakia, alexandra.mokra@gmail.com

Ing. Vladimír Kišš, PhD., Slovak University of Agriculture in Nitra, Horticulture and Landscape Engineering Faculty, Department of Biometeorology and Hydrology, Hospodárska 7, 949 76 Nitra, Slovakia, vladimir.kiss@uniag.sk

Ing. Jozefína Pokrývková, PhD., Slovak University of Agriculture in Nitra, Horticulture and Landscape Engineering Faculty, Department of Water Resources and Environmental Engineering, Hospodárska 7, 949 76, Nitra, Slovakia, jozefina.pokryvkova@uniag.sk

ARTICLE HISTORY:
Received 05 May 2021
Accepted 20 May 2021

BENEFITS OF LAND CONSOLIDATION WITH AN EMPHASIS ON LANDSCAPE ACTIVITIES IN THE AREA OF ADAPTATION IN AGRICULTURAL LAND TO CLIMATE CHANGE AND MITIGATION OF SOIL DEGRADATION IN THE CATHEDRAL AREA PRESEĽANY

Alexandra PAGÁČ MOKRÁ[1], Jakub PAGÁČ[1], Jozefína POKRÝVKOVÁ[1], Martina KOVÁČOVÁ[1]

[1]Slovak Agriculture University in Nitra, SLOVAKIA

Abstract

The publication deals with the benefits of land consolidation with an emphasis on landscape activities in the adaptation of agricultural land to climate change and mitigation of soil degradation in the cadastral area of Preseľany. The implementation of land consolidation has an undeniable benefit after registration in the real estate cadastre. The project of the LC took place in the village of Preseľany, which started to be implemented in June 2006, when a decision on the order of the LC was issued and lasted until May 2013. After land consolidation, proprietary relation in the municipality decreased by up to 88.5 % and the number of plots by 56 %. In addition to a significant benefit for the population in terms of proprietary relation have land consolidation a positive contribution to the landscape-ecological part of the country. The aim of our paper is to identify suitable localities and describe the benefits of LC in the cadastral area of Preseľany. Selected measures include water management measures to mitigate climate impacts in the agricultural landscape, the construction of windbreak and accompanying vegetation and revitalization of the network of hydromelioration canals.

Keywords: land consolidation, common facilities and measures, benefits of land consolidation, climate change

Introduction

Land consolidation (LC) are defined as planned reorganization, settlement of ownership and land readjustment. Through landscaping, it is possible to improve agricultural infrastructure and soil quality, such as construction of anti-erosion and water management facilities, field, and forest roads. Furthermore, it is possible to reduce soil fragmentation with the help of land use and at the same time significantly improve the efficiency of land use (Pašakarnis, Maliene, 2010). Land consolidation combines fragmented land into one plot or into larger parts, in a way that reduces fragmentation. Land fragmentation is eliminated in favor of better soil productivity, improves rural production and thus living conditions (Du et al., 2018). In Slovakia, Act no. 330/1991 coll. on land consolidation, land ownership arrangements, land offices, land fund and land associations. According to this law, LC can be performed in two forms. The first way is simple land consolidation, which has one or more objectives and does not address wider territorial relations and public interests (Muchová and Tárniková, 2018). They are paid for by investors or municipalities and are used mainly for the consolidation of land intended for investment construction. The second way is complex land consolidation. Their goal is a new arrangement of ownership relations to land in the district of land consolidation, spatial and functional arrangement, ensuring the accessibility of land and levelling the boundaries of land to create the best possible conditions for management. The district of land readjustment includes land usually of one cadastral area, except for land of the urban area part of the municipality (Muchová et al., 2015). The new arrangement of land ownership is also an opportunity to organize ownership of land that serves as common facilities and measures (field roads, anti-erosion, water retention and environmental measures) (Urban, 2015). Studies are increasingly focusing on ecology and the effects of agroecosystems in an agricultural landscape, which can be understood as a landscape with a mosaic of agroecosystems, human infrastructure, and possibly natural vegetation. (Silveria dos Santos et al., 2021). Modern agroforestry systems on arable land are also compatible with current agrotechnical practices using existing mechanization, reduce environmental risks and are promising in terms of production and economics (Kacálek et al., 2016). The environmental integration of woody plants into production systems offers many benefits, both for soil and for biodiversity. Planting trees between or near crops and meadows creates an environment for associated flora and fauna, increasing aboveground and underground biodiversity. Not only can trees significantly reduce water and wind erosion by improving the infiltration of precipitation into the soil and providing vegetation cover, but they also improve the soil structure by their fall and roots and the return of organic matter to the soil (Lojka et al., 2020). Among the beneficial effects of land consolidation are the support of other sectors of the economy through the creation of new infrastructure and the stimulation of investment in rural areas (Denac et al., 2021). The aim of the paper is to point out the benefits of land consolidation and to describe landscaping procedures with emphasis on landscaping activities.

Material and methods

The decisive fact in the selection of the model area Preseľany were already completed LC. Implementation began on 5 June 2006, when the decision on the LC Regulation was issued. They lasted until 29 May 2013, when the LC project was registered in the real estate cadastre. The materials and documents of the project with which we work were provided to us from the District Office in Topoľčany of the Land and Forestry Department (Table 1).

Table 1 Basic information about the project, the LC in the model area

	Start project	Completed project	Running time [years]	Area [ha]	The number of ownership relation
Preseľany	05.06.2006	29.05.2013	7	1019	17 665

The village of Preseľany is in located the district of Topoľčany in the Nitra Region and belongs to the Podunajská nížina and the Podunajská rovina. Preseľany covers an area of 1,189.80 ha and is divided from a geomorphological point of view into two different parts, namely the upland, which is divided into the Bojniansku pahorkatinu and the Tribečské podhorie. The area has a relative elevation of 112 m and undulating terrain with a predominance of arable land, with slopes from 0 to 12 °. From a climatic point of view, the area is in a warm climate area. The average annual temperature is 9.3ºC, the number of summer days in the year is over 50 and the average annual precipitation is 610 mm. Hydrologically, the cadastral area of Preseľany belongs to the Nitra basin. Most of the area is drained by the river Nitra, which flows through the area from north to south and has no tributary in the cadastral area. The water level of the Nitra River fluctuates significantly during the year depending on surface precipitation (Atlas krajiny SR, 2002).

Stages of the land consolidation project in Slovakia

The stages of the land consolidation project in the cadastral area of Preseľany are elaborated in the time schedule for the LC project (Table 2). LC is governed by Act no. 330/1991 coll. on Land Consolidation, Land Ownership Arrangements, Land Offices, Land Fund and Land Communities, as amended.

Table 2 Time schedule of the project, the LC in cadastral area Preseľany

Name project LC	**Completed project LC**
The decision on the regulation LC	05.06.2006
The point field	30.06.2006
Labelling on the area LC	30.11.2006
Planimetric mapping	31.08.2007
Elevation mapping	30.11.2007
The valuation of land	31.03.2008
Initial state registry	31.03.2008
Territorial system of ecologic stability	31.05.2008
General principles of functional organization of the territory	31.05.2008
The principles of the placement of new plots	31.01.2009
Plan shared facilities and measures and plan public facilities and measures	31.10.2010
Partitioning plan in the form of placement and marking plan	31.01.2011
Implementation of LC project	31.01.2012
Partitioning plan in the form of reconstruction of the cadastral operate by new mapping	31.01.2013
Registration in the cadastre of evidence of real estates	**29.05.2013**

Results and discussion

The project of land consolidation in the village of Preseľany lasted 7 years, with the last stage, which is the implementation and construction of joint facilities and measures to date, has not begun. Only the stages related to the engineering-design process were completed, which can be divided into two basic activities, namely: geodetic-cadastral and landscape.

Geodetic-cadastral activities in the given locality concerned the reconnaissance of the terrain, stabilization, signalling of minor horizontal geodetic control. Demarcation, focus and permanent marking of the boundary of the district project. Measurement work was carried out for the purposeful mapping of the planimetric and elevation, in which the topography of the topography was re-focused as a basis for a new cadastral map. Elevation mapping measured a network of detailed points of sufficient density on arable land 20 to 40 m apart, terrain edges with a height difference of more than 1 m, longitudinal and transverse profiles of small watercourses, existing roads. In the cadastral stages of the LC project activities, a register of the original state with the valuation of land is prepared, which was also used by the updated BPEJ map. The task of the register of the original state was to create an overview of land and ownership relations in the district of the LC project, as well as to inform individual participants of the LC project about the state of their ownership in the territory. At the stage of drawing up the partitioning plan, the proposal for the location of new land was discussed individually with each owner, and the owner's requirements for the location of new land were also incorporated. Table 3 presents an analysis of the basic ownership characteristics before and after the registration of the land consolidation project.

Table 3 Basic information about ownership before and after the LC project

	Before the start of the LC project	After the completion of the LC project
Number proprietary relation	17 665	2 007
Number of plots	2 995	1 307
Average number of co-owners per plot	5.90	1.20
Average number of plots per one owner	10.95	1.54
Average plot area [ha]	0.34	0.61

In landscape activities, the local territorial system of ecological stability was developed, which was part of the LC project. Interactive elements, biocorridors and biocentres are proposed in the district of the PU, which affect the ecologically unstable or even unstable intensively used agricultural landscape. (Pagáč et al., 2019). The model area of is extremely poor in ecological elements. The basis of the framework of ecological stability in the cadastral area of Preseľany is the regional biocorridor of the Nitra River. However, it is a regulated, artificially straightened stream, its importance for ecological stability is also reduced by heavy water pollution, unsuitable structure, and species composition of riparian vegetation. In an area such as Preseľany, the design of a local territorial system of ecological stability was really considered primarily with existing ecological elements and only to a limited extent with the implementation of new elements. For this reason, it was necessary to apply the proposed measures in the area, which can significantly contribute to improving the environment. Within the area of interest, existing elements such as 1 regional biocorridor, 4 local biocentres, 4 local biocorridors, 7 interaction elements and 2 line of trees were defined within the creation of a territorial system of ecological stability. Within the general principles of the functional organization of the territory, the establishment of new exits to regional roads from the network of field roads was not proposed in the cadastral area of Preseľany, because all existing and proposed field roads are connected to the local road network. In terms of anti-erosion measures, it was proposed to build vegetated waterway (bioswale) and flow diversion banks. In the area of interest, the establishment of a dry polder is being considered, which is to be built in the Liahne locality to capture torrential rainwater from the slopes in the central part of the area.

Implementation of common facilities and measures

For the cadastral area of Preseľany, 102 plots were allocated in the project of the land consolidation for the construction or earmarking of common facilities and measures (Figure 1). The area of these lands is 57.5 ha, and the lands are intended for the purposeful protection of agricultural land and ecological greenery, field and forest roads and water areas.

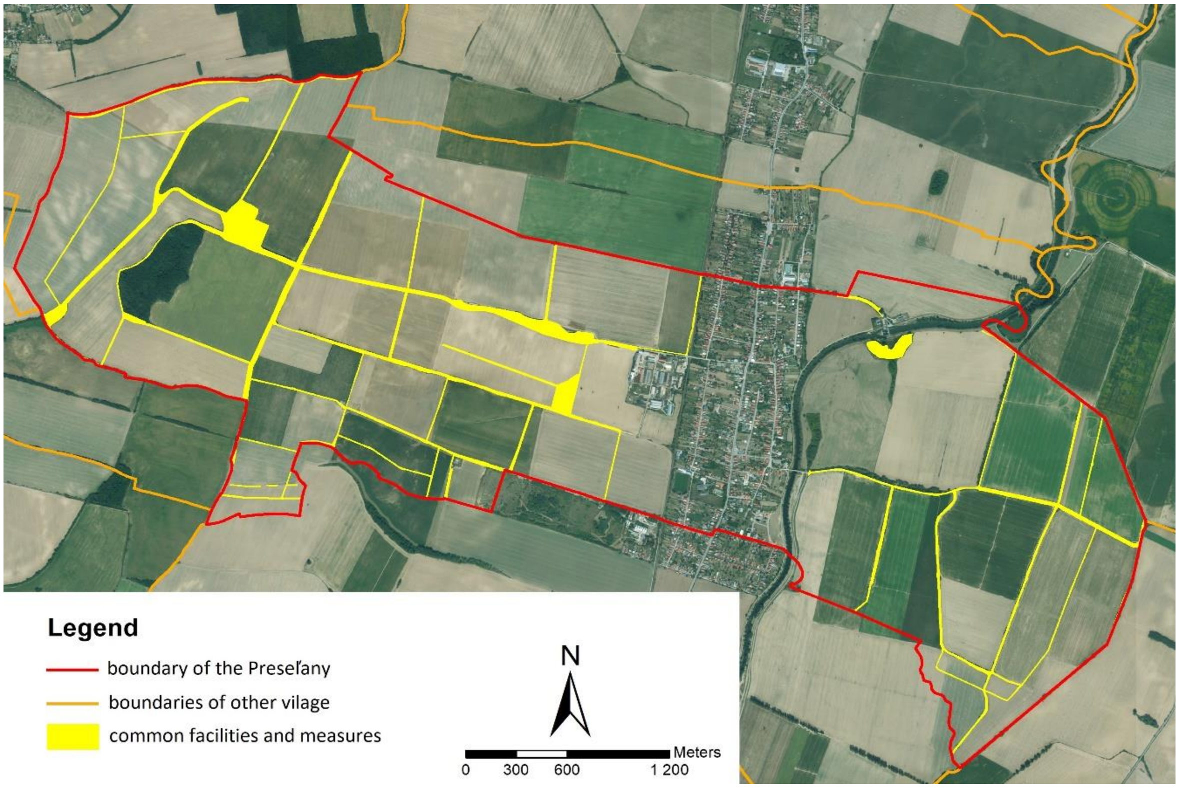

Figure 1 Design of common facilities and measures in the village of Preseľany

The result of our work was an analysis of the current state of the area after the completion of land consolidation and the selection of sites where it is necessary to build common facilities and measures. Figure 2 graphically shows the localities on which we propose the construction of water retention facilities, grassy valleys, non-forest woody vegetation along field roads, field and forest roads, windbreaks, and revitalization of hydromelioration canals.

During the field survey of the area, we took a series of photographs of the entire area and assigned the numbering points on the figure 2.

Figure 2 Design of common facilities and measures in the village of Preseľany with the numbering points

Figure 3 Locality intended for revitalization of hydromelioration canal (inspiration Vrbovce, Czech Republic)

Figure 3 shows site number 1, where there is currently arable land - large fields. We propose the construction of a water retention facility in the place of concentrated runoff, which will improve the water and microclimatic conditions in the country.

Figure 4 Locality intended for the construction of a grassy valley (inspiration USA)

Locality number 2 (Figure 4) is currently prone to water erosion and erosion furrows appear on arable land, on which we propose the construction of grassy valleys, which will increase the infiltration of surface water and prevent the formation of soil loss.

Figure 5 Locality intended for the construction of a paved field road with accompanying vegetation (Inspiration of Blížejov, Czech Republic)

Lokality number 3 (Figure 5) is in the north-western part of the area, which is characterized by a high slope and intensive agricultural activity without paved access roadways. We propose the construction of a paved field road in this part of the territory, so that the road is not devastated by agricultural machinery with the construction of accompanying vegetation.

Figure 6 Localities intended for the construction of accompanying greenery along field roads (inspiration Melek, SR)

At site number 4 (Figure 6) there are currently field roads without accompanying greenery. We propose to supplement the missing accompanying greenery along the field roads and thus create a landscape element that will form a more purposeful function in the country.

Figure 7 Location intended for the construction of a windbreak (inspiration Vrbovce, Czech Republic)

In the area, which we have marked as site number 5 (Figure 7), we propose the division of arable land with a large field windbreak, which will eliminate the manifestations of wind erosion in the area and increase biodiversity in the country.

Figure 8 Locality intended for revitalization of hydromelioration canal (inspiration Vrbovce, Czech Republic)

The southeast of the area (number 6, figure 8) is characterized by a flat area on which there is a network of hydromelioration canals, which are currently in a fully functional state. We propose the revitalization and cleaning of these canals in order to better drain the area and improve the water status during the drought.

Conclusions

The implementation of land consolidation has an undeniable benefit and advantages after registration in the real estate cadastre. It is mainly about reducing the fragmentation of land ownership, creating better user units of agricultural land, creating a new vector cadastral map in the district of the LC project and, finally, creating settled land for the construction of common facilities and measures (Dumbrovský et al., 2000). In this publication, we dealt with and analyzed the benefit in terms proprietary relation with the number of plots 2,995 before the start of LC. After the implementation of the LC, this number decreased to 1,307 from a decrease of 56%. The number of proprietary relations before the start of the LC was 17,665, which decreased by up to 88.5% to 2,007 proprietary relation after the LC. The average plot area increased from 0.34 ha to 0.61 ha and the average number of co-owners per plot decreased from 10.95 to 1.54. In addition to a significant benefit for the population in terms of ownership, LC also has a positive contribution to the landscape-ecological part of the country. Unfortunately, the vast majority of completed LC end when they are registered in the real estate cadastre, and the implementation of common facilities and measures is postponed due to a lack of financial resources. Recently, we have been noticing the demand, either from the company but also from farmers, for the completion of the proposed joint facilities and measures. It is common facilities and measures that play an irreplaceable role in the country in the fight against climate change and reducing soil degradation. The aim of the paper was to identify suitable localities and describe the benefits of LC in the cadastral area of Preseľany. Among the selected measures, we included water management measures to mitigate climate impacts in the agricultural landscape, the construction of windbreak and accompanying vegetation and the revitalization of the network of hydromelioration canals. These measures will form the backbone of the country's ecological stability in the future.

Acknowledgment

"This publication is the result of the project implementation: „ Scientific support of climate change adaptation in agriculture and mitigation of soil degradation" (ITMS2014+ 313011W580) supported by the Integrated Infrastructure Operational Programme funded by the ERDF."

References

ATLAS KRAJINY SLOVENSKEJ REPUBLIKY, 2002. Bratislava: Ministerstvo životného prostredia Slovenskej republiky; Banská Bystrica: Slovenská agentúra životného prostredia, 2002. 342 s. ISBN 80-88833-27-2.

CENTRÁLNY REGISTER ZMLÚV SR [online]. [cit. 2021-04-20]. Dostupné na internete: <https://www.crz.gov.sk/>

DENAC, K. – KMECL, P. 2021. Land consolidation negatively affects farmland bird diversity and conservation value, Journal for Nature Conservation, Volume 59, 2021, 125934, ISSN 1617-1381.

DU, X. et al. 2018. Assessing the effectiveness of land consolidation for improving agricultural productivity in China. In Land Use Policy. vol. 70, pp. 360-367.

Dumbrovský, M. – Mezera, J. 2000. Metodický návod pro pozemkové úpravy a související informace. 1.vyd. Praha: Výzkumný ústav meliorací a ochrany půdy Praha, 189s., 2000, ISSN: 1211-3972.

KACÁLEK, D. et al. 2016. Agrolesnictví v současnosti. Česká Akademie Zemědělských Věd.

LOJKA, B. et al.. 2020. Zavádění agrolesnických systémů na zemědělské půdě. Česká zemědělská univerzita v Praze. ISBN 978-80-213-3061-0.

MUCHOVÁ, Z. – TÁRNIKOVÁ, M. 2018. Land cover change and its influence on the assessment of the ecological stability. In Applied Ecology and Environmental Research. ISSN 1589-1623, 2018, vol. 16, no. 3, s. 2169-2182.

MUCHOVÁ, Z. et al. 2015. A more detailed approach to the assessment of the water erosion threat for a territory. In SGEM 2015. 1st ed. 738 s. ISBN 978-619-7105-37-7. SGEM. Sofia: STEP92 Technology, 2015, s. 3-10.

PAGÁČ, J. et al. 2019. The description of benefits and procedures of land consolidation with emphasis on landscaping activities on the example of the cadastral territory of Melek, Slovakia. In 19th International Multidisciplinary Scientific Geoconference SGEM 2019, Albena, Bulgaria, vol. 19, pp. 709-716.

PAŠAKARNIS, G. – MALIENE, V. 2010. Towards sustainable rural development in Central and Eastern Europe: Applying land consolidation. In Land Use Policy. vol. 27, pp. 545-549.

SILVEIRA DOS SANTOS, J. et al. 2021. Landscape ecology in the Anthropocene: an overview for integrating agroecosystems and biodiversity conservation, Perspectives in Ecology and Conservation, Volume 19, Issue 1, 2021, Pages 21-32, ISSN 2530-0644.

URBAN, J. 2015. Spoločné zariadenia a opatrenia. Komora pozemkových úprav SR. [online]. 2015 [cit. 2021-04-27]. Dostupné na internete: <http://www.kpu.sk/obsah-clenenie-projektu-pu/5-spolocne-zariadenia-opatrenia>

Contact address

Ing. Alexandra Pagáč Mokrá, Slovak University of Agriculture in Nitra, Horticulture and Landscape Engineering Faculty, Department of Landscape Planning and Land Consolidation, Hospodárska 7, 949 76 Nitra, Slovakia, alexandra.mokra@gmail.com

Ing. Jakub Pagáč, PhD., Slovak University of Agriculture in Nitra, AgroBioTech Research Centre, Tr. A. Hlinku 2, 949 76, Nitra, Slovakia, +421 37 641 4947, jakub.pagac@uniag.sk

Ing. Jozefína Pokrývková, PhD., Slovak University of Agriculture in Nitra, Horticulture and Landscape Engineering Faculty, Department of Water Resources and Environmental Engineering, Hospodárska 7, 949 76, Nitra, Slovakia, jozefina.pokryvkova@uniag.sk

Ing. Martina Kováčová, Slovak University of Agriculture in Nitra, Horticulture and Landscape Engineering Faculty, Department of Water Resources and Environmental Engineering, Hospodárska 7, 949 76, Nitra, Slovakia, m.tinkakovacova@gmail.com

ARTICLE HISTORY:
Received 23 april 2021
Received in revised form 5 May 2021
Accepted 20 May 2021

ANALYSIS OF ENVIRONMENTAL IMPACTS OF MINE WATER IN THE AREA OF CENTRAL SLOVAK NEOVOLCANITES

Veronika PREPILKOVÁ[1], Juraj PONIŠT[1]

[1]Technical University in Zvolen, SLOVAKA

Abstract

The research is focused on assessing the environmental impacts of mine water. Water quality assessment was performed by analysis of physico-chemical indicators. Samples were taken at the discharge of the selected mine object and from the recipient where the discharge flows in. The measured values were compared with the limit values of government regulation 269/2010. The highest value of conductivity was found in a sample taken from the locality Voznická dedičná štôlňa adit (exceeding of 61.513 mS/cm). The highest exceeding of calcium was found in the discharge sample from sludge reservoir in Hodruša-Hámre (exceeding of 126.452 mg/l). The highest exceedance of ammonia nitrogen was found in a sample taken from the locality Hodrušský potok creek under adit Zlatý stôl (exceeding of 3.75 mg/l). The highest concentration of sulfates was found in the discharge from sludge reservoir in Hodruša-Hámre – 7 906.768 mg/l (exceeded limit about 7 656.768 mg/l). The lowest pH value under acceptable range was found in a sample taken from the locality adit Horná Ves (4.74). Despite exceeding the values in mine discharges, in recipients we did not observe worse quality of surface water. The analysis confirmed low negative impact of mine water on the environment in the area of Central Slovak neovolcanites.

Keywords: mine water, water quality, environmental impacts, Central Slovak neovolcanites

Introduction

The favourable geological composition of the Slovakia territory enabled mineral resources mining in several regions. An associated problem of ore and mineral mining is the formation of water affected by mining – any type of mine and rock discharges, process solutions and degradation products of process solutions (Society for Mining, Metallurgy, and Exploration, 2008). Mining water may be similar in composition to natural water but are often acidic with a high content of risk elements.

The most common type of mining water is acid mine drainage from the oxidation of sulfide-containing rock, especially pyrite (Kefeni et al., 2017). However, there is a great variety in mine water chemistry. Mine water can be acidic, circumneutral, basic, dilute, mineralized, and saline (Nordstrom et al., 2015). The speed of the formation reaction is influenced not only by physicochemical factors such as reaction surface, pH, humidity, oxygen concentration, but also by the activity of bacteria. The effect of bacteria can increase the reaction rate of sulfides oxidation 6-8 times (Society for Mining, Metallurgy, and Exploration, 2008).

For example, acid mine drainage (AMD) continues to be a concern in coal mining because it reduces surface water and groundwater quality and may perhaps persist for several years. In the U.S. only, AMD pollutes over 20,000 km of streams. Blasting and dewatering exposes sulfide minerals, posing threats to environment. Treatment of AMD is often complex, costly, and challenging, but any discharge from mine sites ought to comply with local, regional, national, and international laws and regulations (Acharya and Kharel, 2020).

Also, in many European countries mine water are still a big issue. In Norway, the mining of massive sulfide deposits has been especially harsh to the local environment by discharging tailings into nearby lakes. Before reclamation drainage pH ranged from 2.4–3.2. Groundwater from wells in the area were also acidic (pH 2.8–5) (Walder and Nilssen, 2005). In the Hitura mine area in western Finland groundwater contamination (elevated sulphate, nickel, and chloride) around the tailings area were detected in the early 1980’s (Räisänen et al., 2005).

Due to their composition, mine water pose an environmental risk of pollution of soil, groundwater and surface water sources. The mine water differs from site to site, which is related to the geological, hydrological, climatic and pedological conditions in the locality. In Slovakia, the most common is the contamination of surface water with arsenic, antimony, copper, zinc and manganese (Bajtoš, 2016). In order to choose an effective method of remediation or preventive measures, it is necessary to know the genesis and volume of mine water in risk areas.

The first comprehensive research was carried out in the 70s of the last century and its results were published in the third volume of Hydrology of the Czechoslovak Socialist Republic - Hydrogeology of mineral deposits (Homola and Klír, 1975). Further extensive research under the leadership of the State Geological Institute of Dionýz Štúr took place in the years 2008 - 2011 (State Geological Institute of Dionýz Štúr, 2016). The body of knowledge is complemented by other less extensive works on the quality, quantity, possibilities of use and environmental problems of mining discharges (Cicmanová et al., 1999; Bajtoš, 2005; Bajtoš et al., 2011; Bajtoš, 2016).

In Slovakia, we can identify 14 mining regions with more than 70 mining districts. Spatially, the sources of mine water are unevenly distributed, but they are concentrated in historical mining regions, which correspond to the geological division of Slovakia (Vass et al., 1988).

The aim of the study was to assess the environmental impacts of mine water in region Central Slovak neovolcanites on surface water through physico-chemical analysis. In the area there are several sources of mine water that could be possibly risky for surface water (as their recipients) and could worsen their quality.

Material and methods

For our study we have chosen mining region Central Slovak neovolcanites divided into 2 mining districts – the Kremnica mining district and the Štiavnica-Hodruša mining district with several sources of mine water. In the region of Central Slovak neovolcanites, 190 sources of mine water were documented with a yield of 460.94 $l.s^{-1}$, which represents 26 % of the total amount of mine water in Slovakia. The largest amount originates in the Štiavnica-Hodruša mining district (341.45 $l.s^{-1}$), followed by the Kremnica mining district (83.75 $l.s^{-1}$). Other resources are less abundant (Bajtoš, 2016).

Banská Štiavnica and Hodruša-Hámre are historically important sites of precious metal mining. At present, the last mining company focused on the mining and processing of precious and non-ferrous metals is the plant in Hodruša-Hámre, which mines ore containing gold, silver, lead and zinc. Almost the entire Štiavnica-Hodruša area is drained by two hereditary adits - the Voznická dedičná štôlňa adit and the Nová odvodňovacia štôlňa adit.

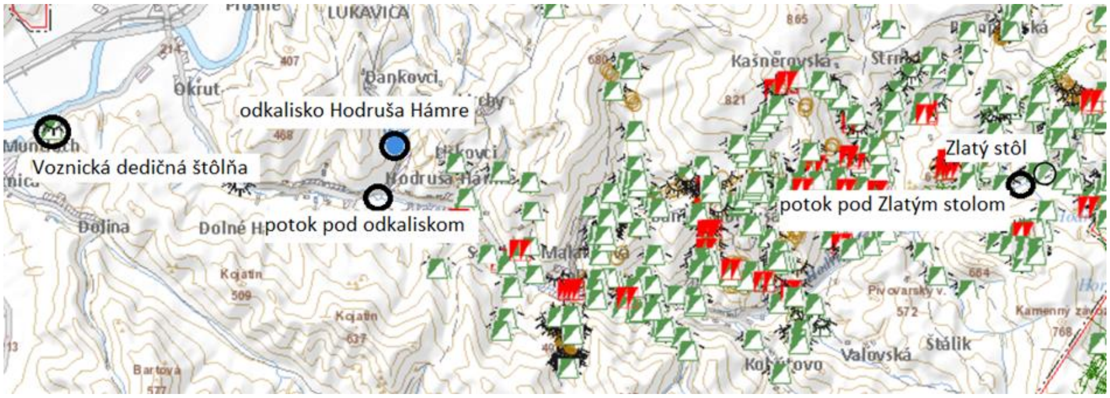

Figure 1 Sampling sites in Štiavnica-Hodruša mining district (1 : 50 000) (GÚDŠ, 2021)

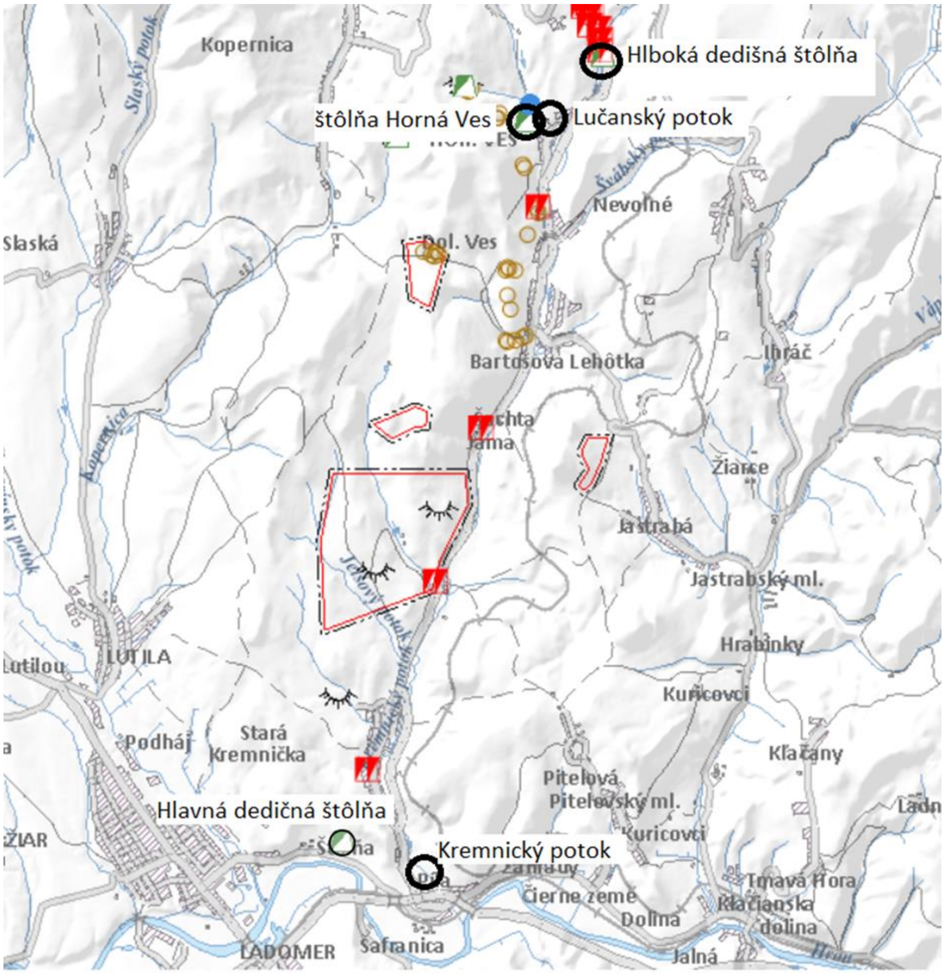

Figure 2 Sampling sites in Kremnica mining district (1 : 75 000) (GÚDŠ, 2021)

Mine water from the Zlatý stôl adit flows into the Hodrušský potok creek. The mining of precious metals culminated in the Kremnica area in the 14th and 15th centuries. The main part of the mining works in the Kremnica mining district is drained by the Hlavná dedičná štôlňa adit into the Hron river. Mine water is mixed with a part of surface water fed underground for the operation of a hydroelectric power plant. Mine water from other hereditary adits flow into the Kremnický potok creek or its tributaries (State Geological Institute of Dionýz Štúr, 2016).

The samples of mine water at 6 mining sites and the samples of their recipients – 4 sites were collected (Picture 1, Picture 2). Collecting and storage of samples were according to STN EN ISO 5667-1: 2007 Water quality. Sampling. Part 1: Guidelines for the design of sampling programs and sampling techniques. The samples were collected one time per month on May, June, July, August, September and November.

In samples were monitored basic parameters – pH, dissolved oxygen, conductivity, concentration of ammonia nitrogen, chlorides, calcium, magnesium and sulfates and total hardness.

To determine pH, the device inoLab pH Level 1 of the company WTW Weilheim was used. To measured conductivity, the device WTW LF318 Conductivity meter of the company WTW Weilheim was used. The dissolved oxygen was measured by Oxi 340i with electrode StirrOx G.

Chlorides

The concentration of chlorides was determined by Mohr method. The pH of the sample was measured. If the value was not in the range 5 – 9.5, HNO_3 or NaOH were adjusted the pH of the sample. 100 ml of each water sample was measured into the titration flask, and 1 ml of chromate indicator (K_2CrO_4) was added. The solution was titrated, stirring constantly, with a standard volumetric solution of silver nitrate until a reddish-brown colour was obtained. A blank test was determined in the same way with 100 ml of demineralized water instead of the sample for the determination (Shukla and Arya, 2018; Hybská and Samešová, 2014).

Sulfates

The concentration of sulphates was determined by gravimetric method with barium chloride. The volume 200 ml of samples was measured into a 500 ml beaker, 2 drops of methyl orange were added. Depending on the pH range the sample was neutralized with HCl or NaOH solution. Then 2 ml of HCl were added to the sample. The solution in the beaker was brought to the boil for at least 5 minutes and 10 ml of hot (80 °C) $BaCl_2$ solution was added. The mixture was heated for 1 hour to allow better coagulation and to crystallize the $BaCl_2$ precipitate. After heating, the beaker was covered with a watch glass and let stand overnight. The formed precipitate was quantitatively transferred and filtered through a dried and weighed frit S4. The precipitate was washed on a frit with demineralized water. The frits with trapped precipitate were dried at 105 °C to constant weight. After cooling in a desiccator, frits were weighed to the nearest 0,0002 g. As in the sample, a blank test was determined where the volume of 200 ml of demineralized water is measured instead of the sample (Hybská and Samešová, 2014; Harvey, 2000).

Total hardness, calcium, magnesium

Total hardness and the amount of Ca ions were determined and then the amount of Mg ions was counted. 100 ml of the sample was dispensed into a titration flask. 5 ml of buffer solution with pH = 10 was add and to the tip of a teaspoon of indicator mixture - eichrome black. The sample with the resulting burgundy colour was titrated to a blue colour with a standard solution of Chelaton 3. 100 ml of the sample was dispensed into a titration flask. 2 ml of KOH and murexide indicator were added to the sample. The sample with the resulting pink colour was titrated to a violet-pink colour with a standard solution of Chelaton 3. The magnesium content of the sample was calculated from the difference between the Chelaton 3 volumetric solution consumed for the determination of the total hardness in ml and the volume consumed for the determination of calcium in ml (Betz and Noll, 1950; Hybská and Samešová, 2014).

Ammonia nitrogen

The concentration of ammonia was determined spectrophotometric. To 50 ml of the sample 1 – 2 drops of potassium sodium tartrate were added and mixed. 1 ml of Nessler's reagent was added and mixed again. After 10 minutes, the absorbance against water at 400 – 412 nm was measured in a manner appropriate to the type of instrument used – Cintra 20 UV-visible spectrometer. The absorbance of the blank was read to which 1 ml of sodium hydroxide solution was added instead of Nessler's reagent (Hybská and Samešová, 2014; Zadorojny et al., 1973).

Results and discussion

The results were compared with requirements of Government Regulation no. 269/2010 Coll. Regulation of the Government of the Slovak Republic laying down requirements for achieving good water status (see Table 1).

Table 1 Requirements of Government Regulation no. 269/2010 that were monitored

parameter	unit	limit
dissolved oxygen	mg/l	more than 5
pH		6 – 8.5
conductivity	mS/m	110
calcium	mg/l	100
magnesium	mg/l	200
chlorides	mg/l	200
sulfates	mg/l	250
ammonia nitrogen	mg/l	1

In the Kremnica mining district the samples of 3 adits were taken (Table 2). All samples of mine water met the criteria for conductivity, total hardness, chlorides and magnesium. Parameters that did not meet limit are tinted red. Problematic was pH value in samples from the adit Horná Ves adit. In 4 samples the measured pH value was under 6. The lowest pH value was measured in June – 4.74. The recipient of this water is Lučanský creek. Acidic pH value may cause acidification of water body. The concentration of Ca ions exceeded limit 2 times – in May and September in sample of Hlboká dedičná štôlňa adit. The discharge of this adit is relatively small. Discharge out of Hlavná dedičná štôlňa adit in one sample exceeded conductivity, ammonia nitrogen, calcium and also sulfates. However, there is a big variability between samples, mostly in conductivity. This is probably caused by mixing mine water with surface water fed underground for the operation of a hydroelectric power plant. The amount of surface water is affected by hydrological condition.

Table 2 Results of mine water analysis – Kremnica mining district

	Date of sampling	pH	conductivity	ammonia nitrogen	Ca	sulfates
			mS/cm	mg/l	mg/l	mg/l
adit Horná Ves	24.05.2020	5.13	11.968	0.127	12.024	42.8
	29.06.2020	4.74	12.078	0.328	14.028	47.53816
	22.07.2020	5.63	12.243	0.090	12.024	44.03968
	19.08.2020	5.59	12.111	0.000	12.024	47.12657
	29.09.2020	7.62	13.356	0.000	42.084	53.09456
	24.11.2020	6.76	11.407	0.172	16.032	53.71194
Hlavná dedičná štôlňa adit	24.05.2020	6.6	50.186	0.808	56.112	185.21
	29.06.2020	5.94	100.533	0.870	136.272	478.88
	22.07.2020	7.35	53.9	0.958	68.136	195.0916
	19.08.2020	6.83	42.484	0.674	54.108	138.9102
	29.09.2020	7.64	39.41	0.618	46.092	120.3888
	24.11.2020	7.22	116.394	1.420	172.344	618.8192
Hlboká dedičná štôlňa adit	24.05.2020	6.98	99.64	0.447	104.208	126.56
	29.06.2020	6.44	95.03	0.667	48.096	109.8934
	22.07.2020	6.92	105.092	0.478	94.188	128.6205
	19.08.2020	6.76	103.87	0.169	84.168	129.6495
	29.09.2020	6.3	108.878	0.775	166.332	138.7044
	24.11.2020	6.55	93.912	0.504	36.072	131.0901

In Štiavnica-Hodruša mining district the samples from 2 adits and 1 sample of settling pit discharge were taken (Table 3). In all samples the concentration of dissolved oxygen, chlorides, magnesium and total hardness met limits of Government Regulation no. 269/2010. Mine water of Voznická dedičná štôlňa adit exceeded in all samples conductivity, Ca and sulfates concentration. On the other hand, pH values were always in range 6 – 8.5. The recipient of the discharge is Hron river with relatively high flow volume during whole year. Problematic may be discharge from sludge reservoir in Hodruša-Hámre that drains into Hodrušský potok creek. Limits did not meet conductivity, ammonia nitrogen, calcium and sulfates. The highest concentration of sulfates was measured in July sample and it was several times higher than in other samples. The limits for ammonia nitrogen were exceeded 3 times – in June, July and November. The discharges from adit Zlatý stôl are the less risky.

Table 3 Results of mine water analysis – Štiavnica-Hodruša mining district

	Date of sampling	pH	conductivity	ammonia nitrogen	Ca	sulfates
			mS/cm	mg/l	mg/l	mg/l
Voznická dedičná štôlňa adit	24.05.2020	7.23	146.556	0.169	204.408	658.13
	29.06.2020	6.89	147.246	1.832	156.312	642.2796
	22.07.2020	7.18	146.744	3.516	124.248	633.6363
	19.08.2020	7.3	153.136	1.840	198.396	622.1119
	29.09.2020	6.95	153.577	2.272	208.416	630.7552
	24.11.2020	7.04	138.24	2.093	166.332	628.903
adit Zlatý stôl	24.05.2020	6.74	87.494	0.208	102.204	123.48
	29.06.2020	6.67	89.052	0.522	36.072	126.5626
	22.07.2020	7.25	90.968	0.502	60.120	121.212
	19.08.2020	7.11	95.546	0.261	54.108	124.7105
	29.09.2020	6.83	95.455	0.545	122.244	134.7943
	24.11.2020	7.37	83.835	0.552	14.028	126.151
discharge from sludge reservoir Hodruša-Hámre	24.05.2020	7.34	127.44	0.808	154.308	537.12
	29.06.2020	7.3	145.038	2.035	98.196	593.0951
	22.07.2020	7.74	143.507	1.179	150.300	7906.768
	19.08.2020	7.63	124.653	0.470	142.284	482.5843
	29.09.2020	6.88	171.513	1.595	226.452	667.3863
	24.11.2020	6.73	135.585	1.673	128.256	455.8312

For sampling recipients Lučanský potok creek (adit Horná Ves recipient), Kremnický potok creek (Hlboká dedičná štôlňa adit and Lučanský potok creek recipient) and Hodrušský potok creek (adit Zlatý stôl a sludge reservoir Hodruša-Hámre recipient) were chosen (Table 4). Dissolved oxygen, chlorides, total hardness and magnesium met criteria in all recipients' samples. The most frequently the amount of ammonia nitrogen did not meet limit for surface water, especially in samples from Kremnický potok creek. However, this is probably not caused by mine drainage but by faecal contamination because many households along Kremnický potok creek are not connected to public sewer. In upstream of Hodrušský potok creed the ammonia nitrogen limit was exceeded 2 times after mixing with discharge of adit Zlatý stôl. At the downstream, where it mixes with discharge from sludge reservoir, the concentration of ammonia nitrogen was below the limit. Although several parameters exceeded limits in samples of discharge from sludge reservoir, usually all parameters met criteria after its mixing with Hodrušský potok creek.

Table 4 Results of recipients water analysis

	Date of sampling	**pH**	**conductivity**	**ammonia nitrogen**	**Ca**	**sulfates**
			mS/cm	**mg/l**	**mg/l**	**mg/l**
Lučanský potok creek	24.05.2020	6.61	40.888	0.523	46.092	66.68
	29.06.2020	6.68	38.36	0.786	60.120	57.8278
	22.07.2020	7.51	43.329	0.661	48.096	66.88269
	19.08.2020	7.38	48.532	0.669	44.088	76.76074
	29.09.2020	7.52	48.074	0.682	58.116	72.2333
	24.11.2020	7.07	38.798	0.566	54.108	81.28819
Kremnický potok creek	24.05.2020	6.29	26.184	2.011	26.052	42.6
	29.06.2020	6.45	14.84	1.753	22.044	26.54728
	22.07.2020	7.72	32.132	0.520	32.064	40.3354
	19.08.2020	7.65	30.267	2.725	46.092	218.9636
	29.09.2020	7.63	32.509	1.038	34.068	42.39333
	24.11.2020	7.2	17.476	0.594	30.060	34.5732
Hodrušský potok creek under adit Zlatý stôl	24.05.2020	6.81	66.246	0.365	36.072	115.04
	29.06.2020	6.77	53.214	0.318	64.128	119.5657
	22.07.2020	7.58	58.353	0.326	32.064	118.1251
	19.08.2020	7.47	68.381	4.751	106.212	116.6846
	29.09.2020	6.88	65.667	1.595	50.100	124.9163
	03.01.1900	7.41	42.517	0.173	46.092	101.8675
Hodrušský potok creek under sludge reservoir	24.05.2020	7.49	71.676	0.686	80.160	215.47
	29.06.2020	7.39	66.898	0.964	48.096	178.834
	22.07.2020	8.66	81.45	0.528	58.116	259.9164
	19.08.2020	7.84	60.372	0.413	76.152	155.3736
	29.09.2020	6.9	58.396	0.315	74.148	138.2928
	24.11.2020	7.51	66.368	0.313	50.100	208.2624

For all parameters average values were made from analysis samples taken May-November (in Table 5 presented as 2020). Obtained average values were similar to results of monitoring by State Geological Institute of Dionýz Štúr 2013-2018. However, monitoring by State Geological Institute of Dionýz Štúr did not follow all parameters as in our research. The difference between results was in ammonia nitrogen concentration in Voznická dedičná štôlňa adit, adit Zlatý stôl and sludge reservoir Hodruša-Hámre although the same method of determination (UV-VIS spectrometry) was used.

Table 5 Comparison of the reseach results with results of monitoring by State Geological Institute of Dionýz Štúr

	Period	**conductivity**	**pH**	**sulfates**	**ammonia nitrogen**
		mS/cm		**mg/l**	**mg/l**
Voznická dedičná štôlňa adit	2007-2013	136	7.49	643	0.22
	2014	135	6.90	630	0.06
	2015	132	7.80	690	0.11
	2016	128	7.45	622	0.12
	2017	132	7.49	621	0.04
	2018	134	7.37	618	0.05
	2020	147.583	7.10	635.97	1.95
settling pit drainage Hodruša-Hámre	2007-2013	75	8.00	195	0.21
	2014	83	7.46	296	0.21
	2015	111	7.51	577	0.15
	2016	101	7.87	446	0.27
	2017	126	7.70	590	0.11
	2018	135	7.37	699	0.27
	2020	141.29	7.27	1773.8	1.29
adit Zlatý stôl	2007-2013	80	7.39	152	0.04
	2014	84	6.99	132	0.03
	2015	93	7.31	142	0.03
	2016	73	7.39	97	0.06
	2017	87	7.44	139	0.03
	2018	89	7.36	141	0.03
	2020	90.392	7.05	126.15	0.43
Hlavná dedičná štôlňa adit	2007-2013	54.9	7.41	202	
	2014	100.3	7.35	574	
	2015	58.2	7.03	258	
	2016	55.2	7.18	224	
	2017	44.7	7.19	163	
	2018	71.2	7.36	308	
	2020	70.5	6.93	289.55	0.891
adit Horná Ves	2007-2013	13.3	6.10	47	
	2014	13.0	5.90	45	
	2015	13.6	7.35	48	
	2016	13.5	5.38	46	
	2017	12.9	5.45	43	
	2018	13.4	5.47	49	
	2020	12.2	5.91	48.05	0.12
Hlboká dedičná štôlňa adit	2007-2013	94.1	7.00	216	
	2014	75.9	6.98	101	
	2015	58.2	7.03	258	
	2016	55.2	7.18	224	
	2017	89.4	7.09	111	
	2018	93.3	7.08	127	
	2020	101.1	6.66	127.42	0.507

The specific conductivity at the mine outlets was found to be 3 mS/cm (Viadero et al., 2006). Our study confirmed higher values of specific conductivity (maximum value 170 mS/cm). Acid mine effluents are specified by low pH. The research showed a pH level of 4.8. (Mahiroglu et al., 2009). Another study found an even lower pH – 2.5 (Wolkersdorfer and Bowell, 2005). According to our study, the lowest pH level was 4.74. In the case of extremely polluted discharges, the value of sulphates can reach the value of 6,700 mg/l (Mahiroglu et al., 2009). In some studies, an even higher concentration in mining discharges was confirmed – 20,000 mg/l (Wolkersdorfer and Bowell, 2005). The highest concentration of sulfates according to our study was 7,906.768 mg/l. Mining effluents can reach high concentrations of ammonium nitrogen – 430 mg/l (Viadero et al., 2006). Our study observed much lower values of ammonium nitrogen (about 1 mg/l). The concentration of ammonium nitrogen depends on the specific locality in which the mining activity was carried out. In this fact, we see the difference between the stated values.

Conclusions

The results show that the composition of mine water in Central Slovak neo-volcanoes region is relatively stable although there are small differences between months. The mine water was characterized by higher conductivity and the concentration of sulfates and calcium. However, in recipients worse quality of surface water was not observed.

For next research is recommended to determine concentrations of heavy metals both in mine water and recipients because heavy metals from ore soak into mine water and even small concentrations could be risky for aquatic life.

References

ACHARYA, B. – KHAREL, G. 2020. Acid Mine Drainage from Coal Mining in the United States – An Overview. Journal of Hydrology, vol. 588. ISSN: 0022-1694.

BAJTOŠ, P. 2005. Mine Water Issues in Slovakia. In Mine Water and the Environment, vol. 23, no. 4, pp. 162-182. ISSN: 1025-9112.

BAJTOŠ, P. 2016. Mine waters in the Slovak part of the Western Carpathians - distribution, classification and related environmental issues. In Slovak Geol. Mag., vol. 16, no. 1, pp. 139-158. ISSN: 1335-096X.

BAJTOŠ, P. et al. 2011. Mine water of Slovakia in relation to the rock environment and mineral deposits. ŠGÚDŠ. Bratislava. 231 p. ISBN 978-80-89343-70-6.

BETZ, J. D. – NOLL, C. A. 1950. Total-Hardness Determination by Direct Colorimetric Titration. In Journal AWWA, vol. 42, no. 1, pp. 49-56. ISSN: 0003-150X.

CICMANOVÁ, S. et al. 1999. The Slovak Mine Waters - Possibility of Utilization. In Slovak Geol. Mag., vol. 5, no. 1-2, pp. 85-91. ISSN: 1335-096X.

HARVEY, D. 2000. Modern Analytical Chemistry by David Harvey. Mc-Graw-Hill Companies. New York, USA. 798 p. ISBN 0–07–237547–7.

HOMOLA, V. – KLÍR, S. 1975. Hydrogeology of ČSSR. III, Hydrogeology of mineral deposits. Academia. Praha. 426 p.

HYBSKÁ, H. – SAMEŠOVÁ, D. 2014. Water treatment and purification processes. TUZVO. Zvolen. 124 p. ISBN 978-80-228-2629-7.

KEFENI, K. K. et al. 2017. Acid mine drainage: Prevention, treatment options, and resource recovery: A review. In Journal of Cleaner Production, vol. 151, pp. 475-493. ISSN: 0959-6526.

MAHIROGLU, A., et al. 2009. Treatment of combined acid mine drainage (AMD)—Flotation circuit effluents from copper mine via Fenton's process. Journal of Hazardous Materials, vol. 166, pp. 782-787. ISSN: 0304-3894.

No. 269/2010. 2010. Regulation of the Government of the Slovak Republic laying down requirements for achieving good water status

NORDSTROM, D. K. et al. 2015. Hydrogeochemistry and microbiology of mine drainage: An update. In Applied Geochemistry, vol. 57, pp. 3-16. ISSN: 0883-2927.

Old mining works and mining works: 1 : 50 000. 2021. GÚDŠ : Bratislava.

Old mining works and mining works: 1 : 75 000. 2021. GÚDŠ : Bratislava.

RÄISÄNEN, M. L. et al. 2005. Finland – Mine Water Quality in some Abandoned and Active Finnish Metal Sulphide Mines. Mine Water and the Environment, vol. 24, pp. 7-10. ISSN: 1025-9112.

Regional geological division of the Western Carpathians and the northern outcrops of the Pannonian Basin in the Czechoslovak Socialist Republic: 1 : 500 000. 1988. GÚDŠ : Bratislava.

SHUKLA, M. – ARYA, S. 2018. Determination of chloride ion (Cl-) concentration in Ganga river water by Mohr method at Kanpur, India. In Green Chemistry and Technology Letters, vol. 4, no. 1, pp. 06-08. ISSN: 2455-3611.

Society for Minig, Metallurgy, and Exploration, 2008. Management Technologies for Metal Mining Influenced Water: Basics of Metal Mining Influenced Water. Society for Mining, Metallurgy, and Exploration. Littleton, Colorado, USA. 103 p. ISBN-13: 978-0873352598.

State Geological Institute of Dionýz Štúr, 2014. Impact of mineral extraction on the environment - Report for 2013 [online]. [cit. 2021-03-30]. Available on the Internet: https://dionysos.geology.sk/cmsgf/files/Hodn_monitor_2013/04_Vplyv_tazby_2013.pdf

State Geological Institute of Dionýz Štúr, 2015. Impact of mineral extraction on the environment - Report for 2014 [online]. [cit. 2021-03-30]. Available on the Internet: https://dionysos.geology.sk/cmsgf/files/Hodn_monitor_2014/04_Vplyv_tazby_2014.pdf

State Geological Institute of Dionýz Štúr, 2016. Impact of mineral extraction on the environment - Report for 2015 [online]. [cit. 2021-03-30]. Available on the Internet: http://dionysos.gssr.sk/cmsgf/files/Hodn_monitor_2015/04_Vplyv_tazby_2015.pdf

State Geological Institute of Dionýz Štúr, 2017. Impact of mineral extraction on the environment - Report for 2016 [online]. [cit. 2021-03-30]. Available on the Internet: https://dionysos.geology.sk/cmsgf/files/Hodn_monitor_2016/04_Vplyv_tazby_2016.pdf

State Geological Institute of Dionýz Štúr, 2018. Impact of mineral extraction on the environment - Report for 2017 [online]. [cit. 2021-03-30]. Available on the Internet: https://dionysos.geology.sk/cmsgf/files/Hodn_monitor_2017/04_Vplyv_tazby_2017.pdf

State Geological Institute of Dionýz Štúr, 2019. Impact of mineral extraction on the environment - Report for 2018 [online]. [cit. 2021-03-30]. Available on the Internet: https://dionysos.geology.sk/cmsgf/files/Hodn_monitor_2018/04_Vplyv_tazby_2018.pdf

STN EN ISO 5667-1: 2007 Water quality. Sampling. Part 1: Guidelines for the design of sampling programs and sampling techniques

VIADERO, R. et al. 2006. Characterization and Dewatering Evaluation of Acid Mine Drainage Sludge from Ammonia Neutralization. Environmental Engineering Science, vol. 23, no. 4, 734-743. ISSN: 1557-9018.

WALDER, I. F. – NILSSEN, S. 2005. Acid Rock Drainage from Norwegian Mines. Mine Water and the Environment, vol. 24, pp. 4-7. ISSN: 1025-9112.

WOLKERSDORFER, C. – BOWELL, R. 2005. Contemporary Reviews of Mine Water Studies in Europe. Mine Water and the Environment, vol. 24. ISSN: 1025-9112.

ZADOROJNY, C. et al. 1973. Spectrophotometric Determination of Ammonia. In Journal Water (Pollution Control Federation), vol. 45, no. 5, pp. 905-912. ISSN: 0043-1303.

Contact address

Ing. Veronika Prepilková, Technical University in Zvolen, Faculty of Ecology and Environmental Sciences, Department of Environmental Engineering, T. G. Masaryka 24, 960 01 Zvolen, Slovakia, +421 948 508 069, v.prepilkova@gmail.com

Ing. Juraj Poništ, Technical University in Zvolen, Faculty of Ecology and Environmental Sciences, Department of Environmental Engineering, T. G. Masaryka 24, 960 01 Zvolen, Slovakia, +421 944 933 407, jurajponist1111@gmail.com

ARTICLE HISTORY:
Received 25 April 2021
Received in revised form 18 May 2021
Accepted 20 May 2021

OVERLOAD OF COMBINED SEWER SYSTEM IN TRNAVA DURING EXTREME RAINFALL EVENT

Marek CSÓKA[1], Štefan STANKO[1]

[1]Slovak University of Technology in Bratislava, SLOVAKIA

Abstract

Extreme, intense rainfalls are occurring more, and more often, what is consequence of climate change. In cities, and towns these events are usually causing urban flooding. The goal of this work is to point out impact of a rainfall that can occur at least once per five years (periodicity 0,2) on a combined sewer system model of Trnava city. Results shows that yield of such rainfall can cause malfunctioning – overload more than 50 % of sewer system. Exactly via this model the deficiency of dated combined sewer system can be pointed out. The importance of finding and implementing new, different methods of rainwater harvesting in contrast with convectional discharge in drainage, or combined sewer systems.

Keywords: combined sewer system, extreme rainfall, rain, SeWaCAD.

Introduction

The main goal of this work is to visualize impact of a heavy rainfall to selected combined sewer system in Trnava. The occurrence of an intense heavy rainfall events is increasing because the climate change. Experiment should point out the significance of problem with conventional, combined sewer systems and decrease of permeable areas in urban environment during extreme climatic conditions.

Problem with sewer flooding can negatively affect human being, urban assets, and environment. Urban sewer flooding occurs when the combined sewer system (in case of this article), or drainage system is overloaded during intense extreme rainfall event. This cause that combination of stormwater and untreated sewage to overflow onto the surface from manholes (Garofalo et al. 2017).

Rainfall intensity and quantity grow is consequence of climate change, it has direct influence onto urban stormwater collection system. The climate change impact can be processed by the mathematical modelling thus it can lead to better climate change adaptation. Better implementation of technical solutions or knowledge from previous project can help to mitigate flood risk and damage (Stancu et al. 2017).

Material and methods

Case study area

The city of Trnava is a main city in Trnava region, which is located in Wester Slovakia. Climatic conditions are minor in differences because of the small cadastral area. Average rainfall depth is 560 mm. Heigh differences are in interval 134 – 188 meters above the sea level and the city centre varies from 140 to 156 meters above sea level. City of Trnava is divided into six city districts – Trnava centre, Trnava north, Trnava west, Trnava south, Trnava east, and Modranka (PHSR Trnava, 2014).

Combined sewer system

Within the city the combined sewer system is built. According to Trnavas technical infrastructure (2014) the sewer network was finished in 1997 and it is 111,236 km long. Sewer network consist of main collectors A, B, C, D, G, I, II, III, and V and 20 combined sewer overflows. Combined sewer system in the city centre and connected areas is hydraulicly undersized and often overloaded.

The model focus on the collector G located in Trnava west and continuing into Trnava south where it is connected into combined sewer overflow. Selected sewer network contains 160 sections, together 3297,53 meters long. In Table 1 bellow are listed pipe diameters with individual lengths for each dimension. Model of selected section of sewer system G is displayed in the Figure 1. The average inclination of the sewer system is around 4 %.

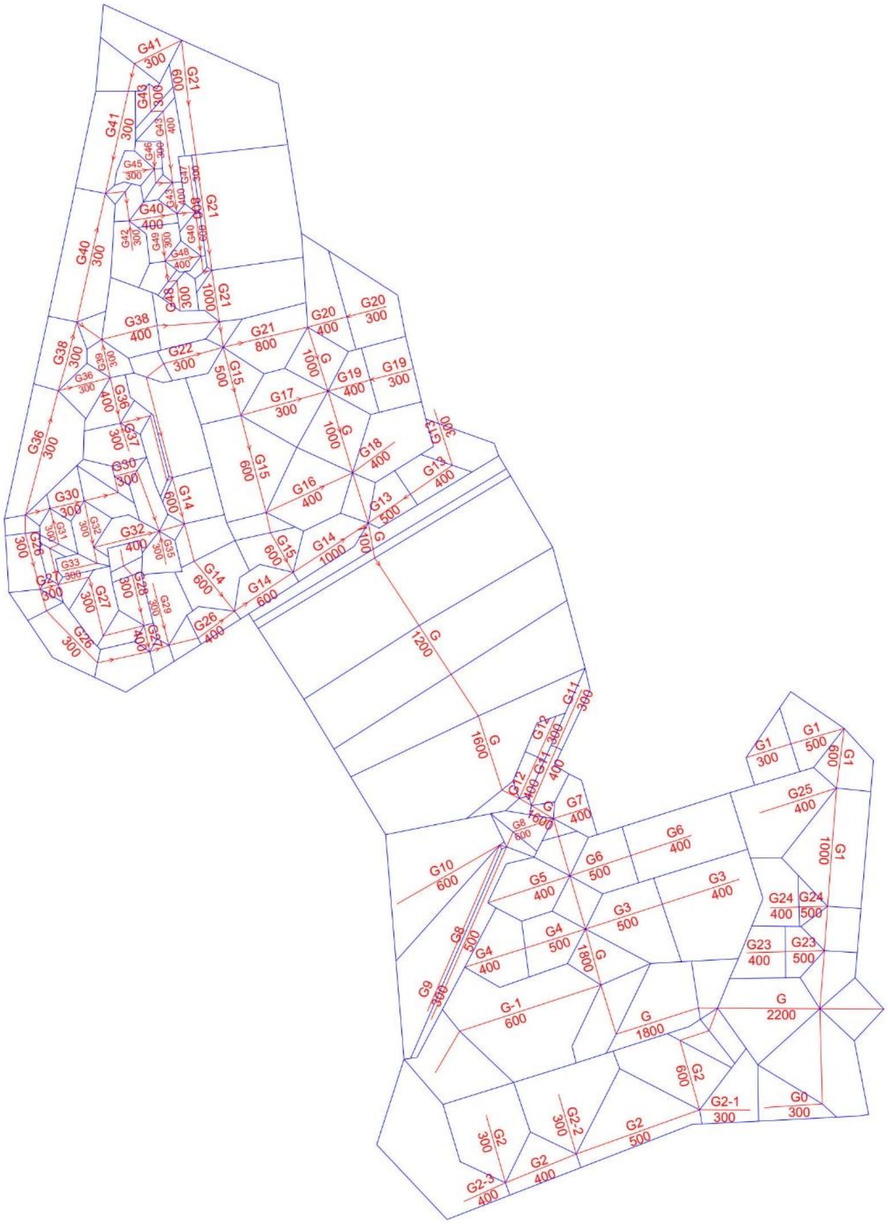

Figure 5 Combined sewer system G

Table 2 Pipe dimensions of sewer system G

Dimension (mm)	**Length (m)**
2200	66,3
1800	124,3
1600	81,6
1200	59,0
1100	10,6
1000	271,5
800	46,4
600	461,8
500	317,5
400	694,6
300	1164,0

Model of a sewer system

Block design rainfall

Design rainfalls are used for calculation process during designing rain sewer systems, or combined sewer systems, since they represent calculated, or historically measured rainfall events for area of interest. Simplest type of a model rain is a block rain. Block design rainfalls are defined by simple rectangular shape, because the intensity of rainfall is constant during its duration. They are created as a yield curve with set periodicity of occurrence. Intensity represents depth of a rainfall (mm) during time period (min) (Rusnák 2018). Yield of the rain is decreasing with increasing rainfall duration, and the periodicity represents chance of rainfall appearance with same yield for one year. There have been several formulas to calculate block rainfall, but for Slovakia is used formula published by Urcikán and Horváth, 1979 which is based on collected and processed data by Šamaj and Valovič from 1973 (Urcikán and Rusnák, 2011)

$$q = \frac{K}{(t^{a}+B)}$$ (Equation 1 Urcikán and Rusnák, 2011)

q – yield of block rain (l.s^{-1}.ha^{-1})

t – duration of a block rain (min)

K, a, B – parameters calculated for specific periodicity and location (-)

SeWaCAD software

The calculations were made in SeWaCAD software. Software was developed for the effective problem solving and calculations for separated, or combined sewer systems (Stanko 2006).

SewaCAD is using Bartošek method (Equation 2) to calculate flow in the pipe sections. It is modified version of rational method, which is dated to the half of the 19th century for rainwater discharge design. This method is recommended by the technological standard STN 75 6101 for calculation of stormwater flow in urban areas. District areas S belongs to the certain section of sewer system. Each of it have its own runoff coefficient based on the type of surface in its area.

$$Q = q \,.\, \sum_{i=1}^{n} \Psi_i \; x \; S_i$$ (Equation 2 Urcikán and Rusnák, 2011)

Q – flow in the pipe ($m^3.s^1$)

q – yield of rain ($l.s^{-1}.ha^{-1}$)

Ψ – runoff coefficient (-)

S – area of the district (m^2)

Bartošek method is using reduced time t_z for duration of compensated rainfall event t = 15 min.

$$t_{z(15)} = t - (t_{ri} - t_p)$$ (Equation 3 Urcikán and Rusnák, 2011)

$t_{z(15)}$ – reduced duration of 15 min rainfall (min)

t – duration of rainfall (min)

t_{ri} – time until the surface runoff can occur (min)

t_p – time needed for water particle to flow from surface into drain = 3,33 min

$$t_{ri} = \frac{166{,}67 \,.r}{\varphi.q}$$ (Equation 4 Urcikán and Rusnák, 2011)

r – retention of area 1 – 3 (mm)

φ – runoff coefficient (-)

The reduced rain duration t_z is then appointed to the equation 1, which is calculated by interpolation.

The design block rain with reduced 15 min duration was calculated based on parameters from precipitation-gage station – 61 Trnava. By choosing precipitation-gage station from SeWaCAD database, the rainfall with periodicity p = 0,2 was selected. For this periodicity the yield of a block rain is q_{15} = 209,47 $l.s^{-1}.ha^{-1}$ and parameters are K = 3637,40, B = 4,37, and a = 0,95 (Figure 2).

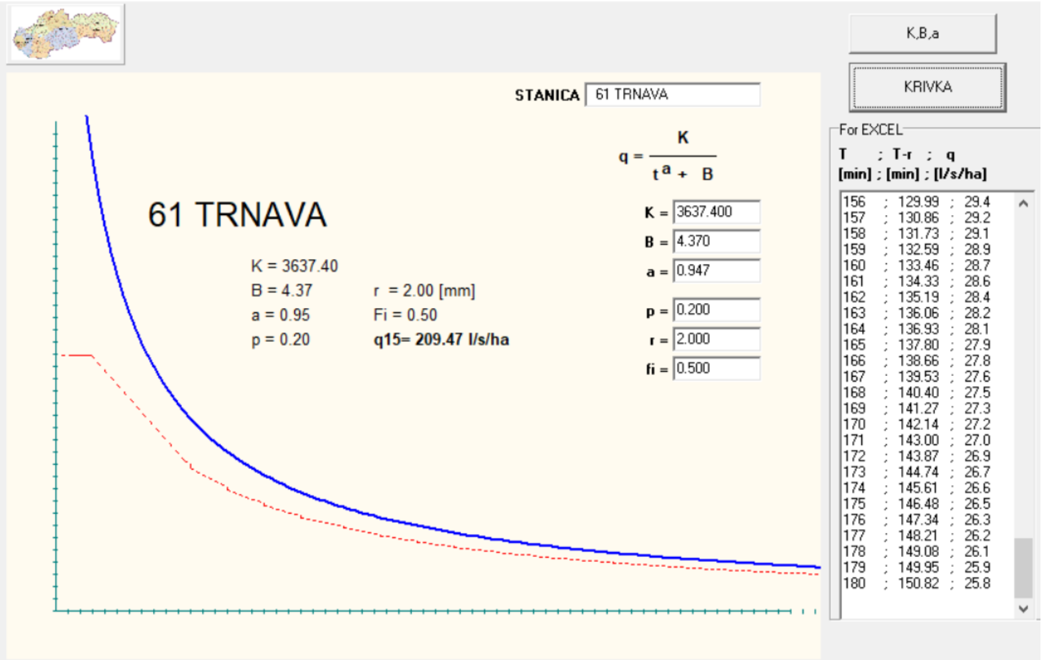

STANICA 61 TRNAVA

$$q = \frac{K}{t^a + B}$$

K = 3637.400
B = 4.370
a = 0.947
p = 0.200
r = 2.000
fi = 0.500

K = 3637.40
B = 4.37
a = 0.95
p = 0.20
r = 2.00 [mm]
Fi = 0.50
q15= 209.47 l/s/ha

For EXCEL

```
T     ; T-r    ; q
[min] ; [min]  ; [l/s/ha]
156   ; 129.99 ; 29.4
157   ; 130.86 ; 29.2
158   ; 131.73 ; 29.1
159   ; 132.59 ; 28.9
160   ; 133.46 ; 28.7
161   ; 134.33 ; 28.6
162   ; 135.19 ; 28.4
163   ; 136.06 ; 28.2
164   ; 136.93 ; 28.1
165   ; 137.80 ; 27.9
166   ; 138.66 ; 27.8
167   ; 139.53 ; 27.6
168   ; 140.40 ; 27.5
169   ; 141.27 ; 27.3
170   ; 142.14 ; 27.2
171   ; 143.00 ; 27.0
172   ; 143.87 ; 26.9
173   ; 144.74 ; 26.7
174   ; 145.61 ; 26.6
175   ; 146.48 ; 26.5
176   ; 147.34 ; 26.3
177   ; 148.21 ; 26.2
178   ; 149.08 ; 26.1
179   ; 149.95 ; 25.9
180   ; 150.82 ; 25.8
```

Figure 6 Block rain yield curve p = 0,2 for precipitation-gage station 61 Trnava

<u>Overload of combined sewer system</u>

For the experiment model of a combined sewer system G was exposed to the design block rain with periodicity p = 0,2, this represents rainfall event that can occur at least once per five years.

Results shows that 89 sections from 160 are overloaded. Overload of the sewer system was divided into four categories: Overload 100 – 150 %, 150 – 250 %, 250 – 500 %, and 500 % and more of the hydraulic capacity. The suitable sections were based on load less than 100 % of their capacity. Number of suitable sections is 71, with total length around 1,4 km, which represent 42,36 % of the sewer system G. First category of overload is present in 22 sections, which is 15 % (495 meters) of total length of sewer system. Overload 150 – 250 % is on 523,95 meters (around

16 %) with 23 overloaded sections. 414 meters of 21 sections are in category 250 – 500 %, and 466 meters, 14,16 % are overloaded more than five times of their capacity. This happens in 23 sections. Overload is visualized in the figure 3 where are all categories located on the model of the combined sewer system G. The results are in Table 2.

Figure 7 Overload of sewer system p = 0,2

Table 3 Overload results for p = 0,2

	Overloaded sections				**Suitable sections**	**Σ**
	100 - 150 %	**150 - 250 %**	**250 - 500 %**	**> 500%**		
(meters)	495,17	523,95	414,69	466,87	1396,85	3297,53
(%)	15,02	15,89	12,58	14,16	42,36	100,00
(n)	22	23	21	23	71	160

Results and discussion

Experiment shows that during intense rainfall event with periodicity p = 0,2 more than 50 % of assessed sewer system is overloaded. In all overloaded areas and their surroundings, it can be expected sewer flooding. This phenomenon can create to severe property damage, environmental pollution, and negatively affect human life in area as was mentioned in introduction.

As was mentioned in part 1.1.1 according to Trnavas technical infrastructure description the sewer network is outdated, and hydraulicly undersized. It can be expected that occurrence of extreme rainfall events can increase.

Urban environment should adapt to worsening of the climatic condition. Solutions to problem with stormwater in urban area can be renovation of the existing sewer system or rainwater harvesting. The rainwater harvesting can help to mitigate precipitation flow into the combined sewer system or to slow down the surface runoff.

Conclusions

The western and southern part of the combined sewer system in Trnava was modelled and assessed with extreme design rainfall event, that can occur one per 5 years. Sewer system G was overloaded in 89 sections from 160 with total length around 1,9 km from 3,3 km. Experiment shows that the importance of the stormwater in urban area have significant role and should not be underestimated.

Acknowledgment

This work was supported by the Scientific Grant Agency of the Ministry of Education, Youth and Sports of the Slovak Republic and the Slovak Academy of Sciences within the project VEGA 1/0574/19 and 1/0727/20, co-funded by the Slovak Research and Development Agency under contract No. APVV-18-0203.

References

GAROFALO, G. et al. 2017. A distributed real-time approach for mitigating CSO and flooding in urban drainage systems. In Journal of Network and Computer Applications, no. 78, pp. 30-42. ISSN 1084-8045.

RUSNÁK, D. 2018. Importance of boundary conditions in hydraulic assessment of sewer systems. Slovak University of Technology in Bratislava, Faculty of Civil Engineering. Bratislava. ISBN 978-80-227-4861-2

STANCU, M. et al. 2017. Climate change adaptation in urban areas. Case study for the Tineretului area in Bucharest. In Procedia Engineering, no. 209, pp 188-194. ISSN 1877-7058.

STANKO, Š. 2006. SeWaCAD user's Guide. Department of Sanitary and Environmental Engineering, Faculty of Civil Engineering, Slovak University of Technology in Bratislava. Bratislava.

Technical infrastructure. www.trnava.sk [online]. Mesto Trnava ©2003 – 2014 [cit. 2021-04-24] Available on internet (Slovak): https://www.trnava.sk/sk/clanok/technicka-infrastruktura

Trnava city profile, economic and social development plan. [online] [cit. 2021-04-24] Available on internet (Slovak): https://www.trnava.sk/sk/clanok/strategickedokumenty.

URCIKÁN, P. – RUSNÁK, D. 2011. Wastewater collection and treatment, Sewer networks 1, Design of sewer systems (Slovak). Slovak University of Technology in Bratislava, Bratislava. ISBN 978-80-227-3435-6.

Contact address

Ing. Marek Csóka, Slovak University of Technology in Bratislava, Faculty of Civil Engineering, Department of Sanitary and Environmental Engineering, Radlinského 11, 810 05, Bratislava, Slovakia, +421 (2) 32 888 584, marek.csoka@stuba.sk

ARTICLE HISTORY:
Received 1 May 2021
Received in revised form 17 May 2021
Accepted 20 May 2021

ASSESMENT OF COMBINED SEWER OVERFLOWS IN THE CITY OF TRNAVA

Marek ŠUTÚŠ[1], Štefan STANKO[1]

[1]Slovak Technical University in Bratislava, SLOVAKIA

Abstract

Due to the climate change, which results in a change in the time distribution of precipitation, and also due to the high degree of urbanization in cities, we are seeing increasing amounts of pluvial floods. In the cities in Slovakia we have a combined sewerage system and therefore there are combined sewer overflow (CSO) on these networks for the separation of stormwater and wastewater. CSO actually permit these overflows deliberately, in order to protect the treating facility. These waters contain contaminants, coarse solids, fine suspended solids and solutes. The correct function of the CSOs depends on proper design and regular maintenance. The article summarizes the current state and the proposed adjustment of some CSOs in order to achieve the set environmental limits.

Keywords: combined sewer overflow, sewerage, water pollution

Introduction

One of the most significant impact of climate change is the change of time variability of precipitation events. In recent decades, we can see the alternation of dry and rainy periods (Gdina et al. 2017). According to Ministry of Enviroment of the Slovak Republic (2018), change in the temporal and spatial distribution of precipitation, in some areas even a 10% reduction in total is predicted by climate models. We can observe that longer and longer periods of drought occur, which are then alternated by extreme rainfall, often heavy torrential rains. Due to these impacts of climate change, the function of the sewerage system is affected and we can see increasing numbers of urban floods. Increase in extreme meteorological phenomena are confirmed by IPCC (2014). Increasing rainfall intensity and frequency of torrential rains from Central and Northern Europe is expected (Prokić et al. 2019).

Pluvial floods

The surface runoff wave is deformed due to high proportion of impermeable materials. In an urbanized area, the concentration-time is shorter, but the total runoff volume is more significant. Surface runoff is discharged by a combined sewerage network to the wastewater treatment plant or by a stormwater sewer network to the recipient. The capacity of these networks may not be sufficient in case of torrential rains (Van Ootegem el al. 2015). During these rains, the capacity flow can be reached. The cross-section of pipe is filled with water and that results in creation of pressre flow, backflow and subsequently pluvial flooding.

Trnava sewer system

The city of Trnava has built a public sewerage system within the existing urban area. Near the village of Zeleneč, which is located south of the city, is located a mechanical-biological wastewater treatment plant. Sewerage has the character of a combined network for the drainage of sewage, industrial and stormwater.

In 2015, sewerage network had total length of 111,236 km. To the Trnava City sewerage network is connected 36 municipalities. Sewerage in the city centre and in older parts of city is obsolete and overloaded. Operational difficulties are also caused due to insufficient, respectively undersized pipe diameter (trnava.sk, 2021).

Assesment of CSO

Acorrding to Law 269/2010 expert assessment of precipitation and runoff conditions and determination of the number of cases of overflow is needed. In addition, each CSO must meet a basic criterion, i.e. mixing ratio.

In the §6, section 3 of Law 269/2010, the mixing ratio is defined by as „the ratio of the average daily flow of municipal wastewater in the non-rainy period to the flow of water from the surface runoff that is discharged to the wastewater treating plant during the rain“.

In the §6, section 4 of Law 269/2010, minimum ratio is set to 1:4. In the event of the need for increased protection of the recipient, the state water administration body may prescribe a value of the mixing ratio of up to 1:8. When discharging wastewater from CSO, the limit values of pollution indicators are not determined.

According to §6, section 5 of Law 269/2010, „the basis for proving the number of cases of overflow during the year in the case of large sewerage networks with the number of CSOs greater than 10 is an expert assessment of precipitation conditions and runoff conditions.

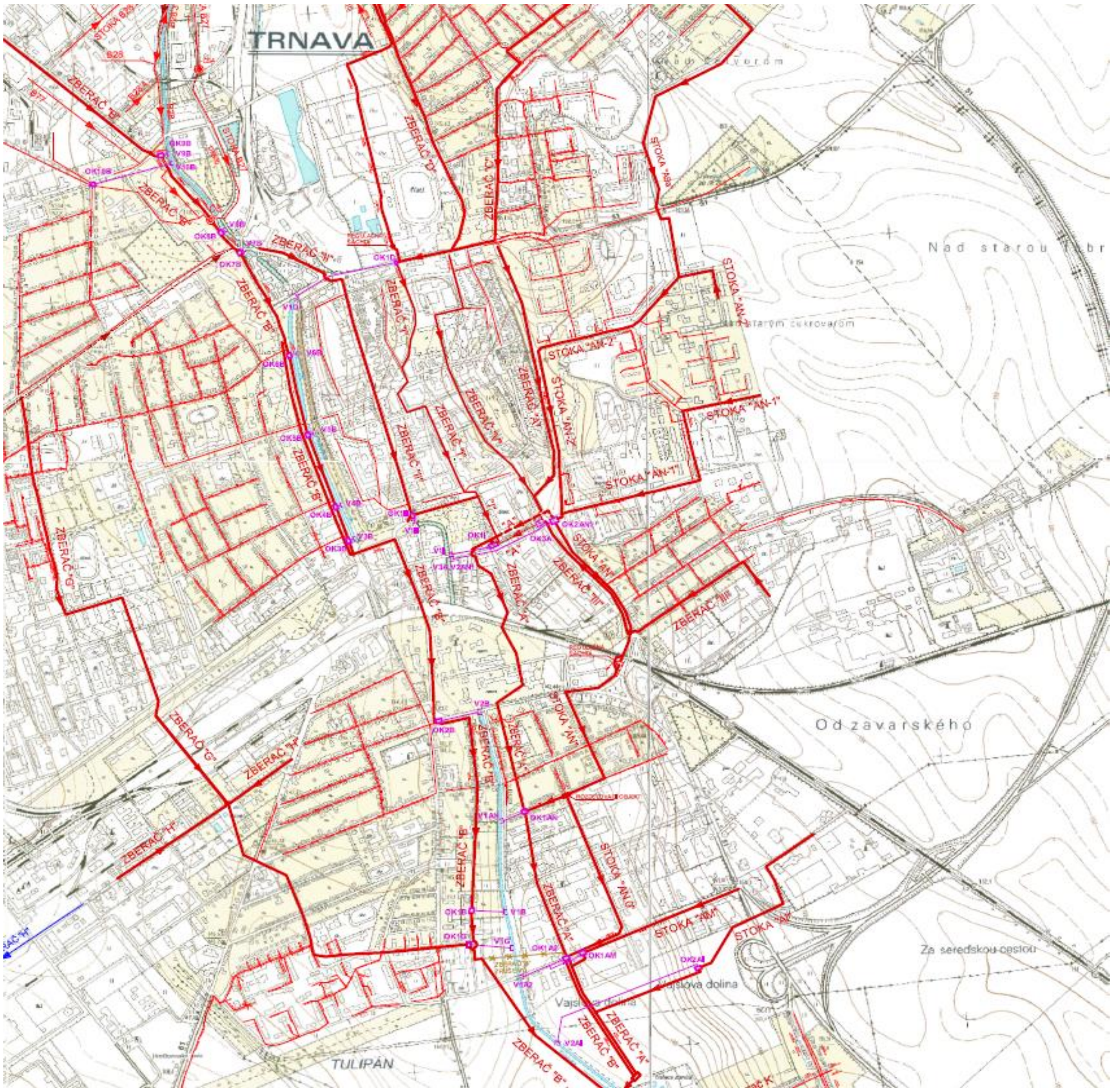

Figure 8 Sewerage system with highlighted CSOs

With a flow time through the sewer network to the CSOs equal to or longer than 15 minutes, the number of overflow cases may not exceed 15 per year on a long-term average. With a flow time through the sewer network to the CSO of less than 15 minutes, the number of overflow cases may not exceed 20 per year on a long-term average“.

Due to the number of 22 CSO in Trnava, sewerage network is assessed by the number of overflows.

Flow measurement

In several cases, sediments at the bottom of the pipeline, clogged and contaminated CSOs, were an obstacle to the hydraulic measurement of flows. The condition for measurements were not optimal. Measurements were taken during the morning or before midday, when the average or above-average flow in the sewerage networks was assumed.

Table 4 Measured values

	CSO1	CSO2	CSO3	CSO4	CSO5	CSO6	CSO7	CSO8	CSO9	CSO10	CSO11
Depth [mm]	30	200	50	200	150	400	150	100	30	50	200
Velocity [m.s^{-1}]	0,4	0,3	1,35	0,2	0,2	0,05	0,5	0,1	0,4	0,7	1
	CSO12	CSO13	CSO14	CSO15	CSO16	CSO17	CSO18	CSO19	CSO20	CSO21	CSO22
Depth [mm]	500	50	300	300	100	400	550	100	20	50	-
Velocity [m.s^{-1}]	0,3	0,5	0,4	0,3	0,5	0,35	0,2	0,2	0,1	0,2	-

Hydraulic calculations

As a basis for calculating the mixing ratio, which is a criterion for hydraulic evaluation, the inflow of wastewater into the CSO during the inspection was measured. To determine the average daily inflow, we need to know the values of water depth and flow rate in the sewer. We then determine the flow by multiplying the flow area and the flow velocity. To determine the velocity in the throttle drain, we then calculate using equation (1):

$$v_{zv} = \sqrt{\frac{2g*(p+h_p+i_0*l-m*D)}{\alpha+\xi_{vt}+\lambda*\frac{l}{D}}}$$ (Equation 1, [5])

g (m/s^2) - gravitational acceleration
p (m) - water pressure height above the throttle drain
h_p (m) - overflow height
i_0 (-) - inclination of the throttle drain
l (m) - length of the throttle drain
m (-) - coefficient for determining the pressure line
D (m) - diameter of the throttle drain
α (-) - Coriolis number
ξ_{vt} (-) - coefficient of local losses at the inlet to the throttle drain
λ (-) - coefficient of friction

Using the equation (2), flow to the throttle drain is calculated.

$$Q = v_{zv}\frac{\pi*D^2}{4}$$ (Equation 2 Butler, Davies, 2011)

v_{zv} – flow velocity in the throttle drain
π – Ludolf number
D (m) – diameter of pipe

The flow area had to be estimated for some drains as not all drains had a circular diameter.

Mixing ratio

The operating state, in which the level is at the level of the overflow edge, i.e. when the water starts to flow over the overflow edge, is used to assess the mixing ratio. According to equation (3), mixing ratio is calculated.

$$n = \frac{Q_{odt}}{Q_{24}} - 1$$ (Equation 3 Butler, Davies, 2011)

Q_{odt} ($m^3.s^{-1}$) – outflow from CSO
Q_{24} ($m^3.s^{-1}$) – averrage daily inflow

Number of overflows

Number of overflow was calculated using equation (4). To determine orographic characteristic an ombrographic station Trnava – Vrútky was choosed. The outflow time for each CSO was assumed 15 minutes in calculations.

$$m_0 = \left[(1-\tau) * \left(Q_m * \frac{n_0}{Q_d}\right)^{0,83} * \left(1 + c_1 * \frac{log}{p}\right) + \tau\right]^{-3} \qquad \text{(Equation 4 Butler, Davies, 2011)}$$

τ (-) – climatic coefficient,
c_1 (-) – local coefficient,
Q_m ($l.s^{-1}$) – average urban waste water flow,
Q_d ($l.s^{-1}$) - design flow of stormwater flowing from the river basin above the CSO,
n_0 (-) - is the mixing ratio in a particular CSO,
p ($year^{-1}$) – periodicity.

Results

The results of the calculations for the number of overflows and the mixing ratio are shown in the Table 2.

Table 5 Comparison

	Before		After	
	Mixing ration	Number of overflows	Mixing ration	Number of overflows
	[-]	[-]	[-]	[-]
CSO2	2,7	35,6	6,5	14
CSO7	6,9	18,3	8,4	14,3
CSO8	20	2,4	14	5,9
CSO11	1,2	51	4,6	13,9
CSO12	2,8	63,6	10,6	14,2
CSO13	11,8	39,3	30,8	14,6
CSO14	4,1	39,9	8	14,7
CSO17	4,2	20,5	5,2	12,2
CSO20	11,5	35	20,8	14,8
CSO21	18,6	20,8	37,4	13,4

Table 6 Condition of CSO

	Mixing ration [-]	Number of overflows [-]	Condition
CSO1	4,10	4,1	Satisfactory
CSO2	2,7	35,6	Unsatisfactory
CSO3	14,3	2,1	Satisfactory
CSO4	10,3	10,3	Satisfactory
CSO5	16,9	3,6	Satisfactory
CSO6	14,8	8,5	Satisfactory
CSO7	6,9	18,3	Unsatisfactory
CSO8	20	2,4	Satisfactory
CSO9	8,3	12,8	Satisfactory
CSO10	10,1	14,1	Satisfactory
CSO11	1,2	51	Unsatisfactory
CSO12	2,8	63,6	Unsatisfactory
CSO13	11,8	39,3	Unsatisfactory
CSO14	4,1	39,9	Unsatisfactory
CSO16	33,2	1,3	Satisfactory
CSO17	4,2	20,5	Unsatisfactory
CSO18	6,6	5,4	Satisfactory
CSO19	31,4	14,3	Satisfactory
CSO20	11,5	35	Unsatisfactory
CSO21	18,6	20,8	Unsatisfactory
CSO22	6,1	0,8	Satisfactory

As we can see, in 9 CSOs the conditions are not suitable according to Law 269/2010. In order to achieve suitable conditions, a building modification, an increase of the overflow edge, was proposed in these CSOs. Height change values ranged from 90 to 400 mm. Table 3 compares the results before and after the proposed building modification.

Conclusion

Construction modifications must be made so that the limits on the mixing ratio and the number of reliefs per year, given by Law 269/2010, are met. According to §6, section 5 of Law 269/2010, the CSO must include a device for catching floating substances in form of rakes. As can be seen in

Figure 2, none of these CSOs contains such a device. It follows that even if the CSO complied with the limits, a building modification is required.

Figure 9 Missing capturing device on overflow edge

Acknowledgment

This work is supported by „Excelentných tímov mladých výskumníkov STU “, funded by the Rectors office of the STU in Bratislava (from September 2020 to September 2021), the Scientific Gant Agency of the Ministry of Education, Youth and Sports of the Slovak Republic, and the Slovak Academy of Sciences within the project VEGA 1/0727/20 and VEGA 1/0574/19.

References

BUTLER, D. – DAVIES, J. W. 2011. Urban Drainage. Spon Press is an imprint of the Taylor & Francis Group. 2 Park Square. Milton Park. Abingdon. Oxon. ISBN 0-203-84905-1.

GDINA, M. et al. 2017. The Seventh National Communication of the Slovak Republic on Climate Change. Under the United Nations Framework Convention on Climate Change and the Kyoto Protocol . Bratislava : s.n., 2017.

Government Regulation n. 269/2010, Regulation of the Government of the Slovak Republic laying down requirements for achieving good water status, in Slovak.

https://www.trnava.sk/sk/clanok/technicka-infrastruktura, 19.04.2021, 10:00.

Ministry of the Environment of the Slovak Republic. Strategy for the Adaptation of the Slovak Republic to Climate Change, in Slovak, 2018.

PROKIĆ, M. et al. 2019. Pluvial flooding in Urban Areas Across the European Continent. Geographica Pannonica. Vol. 23, 4, pp. 216-232.

Trnavská vodárenská spoločnosť, a.s., 2015, Reconstruction of combined sewer overflows - Technical report, in Slovak.

VAN OOTEGEM, L. et al. 2015.Multivariate pluvial flood damage models. Environ. Impact Assess. Rev. Vol. 54.

Contact address

Ing. Marek Šutúš, Slovak University of Technology in Bratislava, Faculty of Civil Engineering, Department of Sanitary and Environmental Engineering, Radlinského 11, 810 05 Bratislava, Slovakia, e-mail: marek.sutus@stuba.sk

ARTICLE HISTORY:
Received 30 April 2021
Accepted 10 May 2021

POSSIBILITIES OF RAINWATER MANAGEMENT IN THE CURRENT CLIMATE CONDITIONS

Jozefína POKRÝVKOVÁ[1], Jakub PAGÁČ[1] Richard HANZLÍK[1], Alexandra PAGÁČ MOKRÁ[1]

[1]Slovak University of Agriculture in Nitra, SLOVAKIA

Abstract

The possibilities of sustainable rainwater management in many ways face various barriers, but the change of traditional practices is not just a purely technical issue. Most cities face major and growing problems with rainwater. The reason is the increasing urbanization of the territory and the expansion of impermeable areas in the form of roofs of residential houses, parking lots and the like. The result is a change in the local natural water cycle, a change in climatic conditions and an increasing surface runoff. Equally significant is the reduction in groundwater supply, which has a major role in the dry seasons. There are several proposals that can be applied in urban areas.

Keywords: Rainwater management, blue-green infrastructure, urban landscape, retention

Introduction

In 2013, a document entitled „Research of Rainwater Retention and Use in an Urban Landscape“ (Hudeková, 2013) was created in Slovakia, which had to be the basis for rainwater management in an urbanized country. However, a spatial planning methodology or similar implementing regulation has not been updated yet to help local governments manage rainwater properly in an effort to collect precipitation at the point of impact and to create area for gradual infiltration into groundwater.

An operative small water cycle (Figure 1a) portrays a healthy balanced area (Figure 1b). In a country, it is defined that the area is saturated with water vapor and the water circulates over short distances (Durand, 2019). A damaged or unstable area with a disturbed small hydrological cycle (Figure 1c) is described by an irregular total precipitation, which leads to a reduction and formation of groundwater reserves and an increase in surface runoff. This interference also has a negative effect on the local microclimate, when heat islands are formed in the area and other undesirable phenomena.

a) b) c)

Figure 1 a) Impermeable surface disrupts small water cycle, b) Healthy area, c) Damaged area (Durand, 2019)

Berggren et al. (2007) assessed the overall effects of climate change on urban areas. Willems et al. (2012) provided a critical review of current modern methods for assessing the effects of climate change on urban river basin precipitation. Arnbjerg-Nielsen et al. (2013) have shown that there are still many limitations in understanding how to describe precipitation in a changing climate when proposing and operating urban drainage infrastructure. Zhou (2014) proposed an integrated and transdisciplinary approach to the proposal of sustainable drainage (Kang et al., 2016).

Gradual improvement and evaluation of the rainwater management effect created a system called blue-green infrastructure (BGI). BGI represents an environmental urban infrastructure, which includes urban greenery with ingenious hydrological elements of the urban drainage system. BGI (Liao et al., 2017) is based on rainwater management, only emphasizing the role of greenery as a key tool for protecting cities from the effects of warm weather without precipitation. In this consideration, greenery no longer plays an aesthetic role in the city, but plays the role of air conditioning (Vítek, 2018). This benefit needs to be named, measured, evaluated, given a scale and a concrete form through different types of greenery. Blue-green infrastructure (Drosou et al., 2019) is a response to the challenges of climate change and urbanization [95]. Blue-green infrastructure requires the cooperation of several sectors, therefore it is necessary to create a suitable team and cover each domain by experts in the field (Table 1).

Table 1 Fields and areas of experts involved in the creation of a water-sensitive city (Deister et al., 2016)

<table>
<tr><th></th><th colspan="4">Sustainable water management</th><th colspan="4">Spatial planning</th><th colspan="2">Urban landscape creation</th></tr>
<tr><td rowspan="2">Fields</td><td>Securing water supply</td><td colspan="2">Rainwater management</td><td>Wastewater treatment / recycling</td><td colspan="2">Ecological requirements</td><td colspan="2">Economic requirements</td><td rowspan="2">Aesthetic quality</td><td rowspan="2">Urban infrastructure</td></tr>
<tr><td colspan="2">Ensuring and improving water quality</td><td colspan="2">Protection of surface and groundwater</td><td colspan="2">Social requirements</td><td colspan="2">Cultural requirements</td></tr>
<tr><td>Areas</td><td>Environmental protection technicians and engineers</td><td colspan="2">Environmental experts, landscape engineers</td><td>Environmental planners</td><td>Urban planners and landscape architects</td><td colspan="2">Government</td><td>Architects / engineers</td><td>Landscape architects</td><td>Urban planners / architects</td></tr>
</table>

Materials and methods

The use of rainwater is one of the oldest ways of managing water resources in the country. Examples are often data on the use of rainwater in households or buildings for flushing toilets, washing cars or floors and, last but not least, washing (Szomorová et al., 2013). With this system, the rainwater is again converted into wastewater and needs sewage systems to drain into the wastewater treatment plant. In many buildings, rinsing or watering green water with retained water has prevailed. However, its use is precisely affected by its quality, water from rain or snow belongs to special types of wastewater, its pollution is either organic or inorganic. Depending on the origin, its quantity or pollution is also managed. Water is most often polluted mechanically from impurities on solid surfaces, but also chemically due to emissions in the air (so-called acid rain). Runoff follows almost immediately after its occurrence.

Water retention in cities and urban areas has to be subject of what happens to water. There are several possibilities that are used today:

- short retention of groundwater or surface reservoirs and subsequent discharge into the sewer network at a selected distance after the end of the rain;

- longer water retention in surface or groundwater storage and consequent slower consumption, e.g. for flushing, etc .;

- longer water retention in surface or groundwater storage and consequent slower infiltration into the soil environment;

- longer retention of water in surface or groundwater storage and subsequent slower infiltration into roots overgrown environment of trees or other vegetation and subsequent evapotranspiration with an effect on the temperature and humidity of the environment;

- longer water retention in surface or groundwater storage and consequent slower consumption for the needs of vegetation by means of irrigation or technical supply to plants, which are e.g. in green roofs or walls;

- longer retention of water in the soil environment and subsequent use for artificial wetland habitats;

- longer water retention in surface water tanks or reservoirs creating evaporation and humidification of the surrounding environment;

- other options and combinations for delay (Jurík, Pokrývková, 2018).

Results and discussion

Measures related to the rainwater management in cities should be increasingly supported by multiple functions, so as to increase aesthetics of the city for life in addition to the classic drainage function. The so-called „Three-point approach“ describes the three levels at which rainwater management is decided and that needs to be taken into account when looking for sustainable solutions (Pokrývková et al., 2020).

Domain A deals with daily rain (80% of total precipitation) and is aimed at improving the annual water balance (retention, evaporation) and using rainwater as a source to increase the sustainability or aesthetics of cities.

Domain B deals with the design rainfall (with a repetition period of 10 years) (19% of the total precipitation) and the reduction of the sewer network overload and flooding of the terrain using traditional technical solutions.

Domain C is the domain of extreme torrential rains (with a repetition period of about 100 years) (1% of total precipitation), when traditional sewer networks fail and it is necessary to propose measures to reduce the impact of floods in cooperation with urban planners (safe drainage of water from the city using selected streets, or tunnels) (Kabelková, 2018).

The solutions must work for all three areas. This approach also makes it possible to respond to climate change and is a good basis for communication with various stakeholders, including non-experts (Kabelková, 2018).

Distribution of facilities and objects according to their function of rainwater management:

1. Measures to improve the microclimate or to prevent precipitation
    - lawns
    - trees
    - semi-permeable surfaces
    - vegetation roofs
    - vegetation facades
    - shallow infiltration swales and its variants
2. Infiltration equipment without regulated drain
    - surface infiltration (without retention)
    - infiltration swales and its variants
    - infiltration retention tank
    - infiltration retention furrow and its various forms
    - infiltration swale with retention furrow and its variants
    - infiltration shaft
3. Infiltration devices with regulated outflow
    - infiltration swale with retention furrow and regulated drain (and its variants)
    - infiltration retention tank with regulated drain
    - infiltration retention furrow with regulated outflow
4. Retention objects with regulated outflow
    - dry retention rainwater tank and its variants (eg water square, water playground, park)
    - retention rainwater tank with storage
    - underground retention rainwater reservoir
    - artificial wetland
5. Accumulation and rainwater use (Pokrývková et al., 2020, Krejčí et al., 2002).

Table 2 divides the measures applicable to efficient rainwater management according to the type of measure. Types of measures are selected as green measures of BGI and gray technical measures.

Table 2 Types of rainwater management measures in urban areas (Vítek, 2015)

Type of rainwater management measures (green - BGI measure; gray – technical measure)	
Vegetation roofs	
Gravel roofs	
Vertical greenery (green fascades)	
Area vegetation elements	
Trees / tree lines	
Artifical wetlands	
Water areas	
Permeable and semi-permeable surfaces	grassed
without grass	
Infiltration facilities	surface
subterranean	
Pre-cleaning equipment	grassy humus layer
others	
Natural / revitalised watercourse	
Retention objects with regulated outflow	surface
subterranean	
Retention spaces for sewer networks and improvement of their utilization by means of controlled outflow in real time	
Additional retention areas in public space	park, green areas
parking lot, playground, ..	
Emergency paths for safe drainage	undeveloped corridors
streets	
Accumulation tanks (reservoirs) and water distribution and their use	
Aesthetic and recreational elements	associated with water and greenery
associated only with water	

Surface infiltration objects

In the case of surface infiltration, it has to be ensured that the soil infiltration capacity is greater than the expected runoff from rainfall, which leads to relatively high infiltration area requirements. This type of infiltration is used when there is enough space to spill rainwater. This type of infiltration can be used in large areas where short-term retention of rainwater is not expected. Area infiltration objects (Figure 2) are proposed as areas with grass or at parking lots with vegetation blocks.

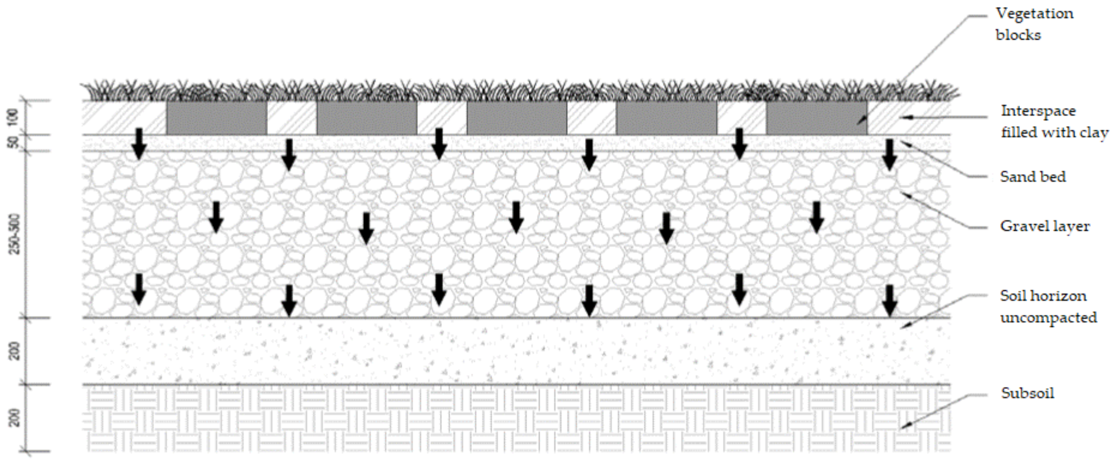

Figure 2 Example of surface infiltration

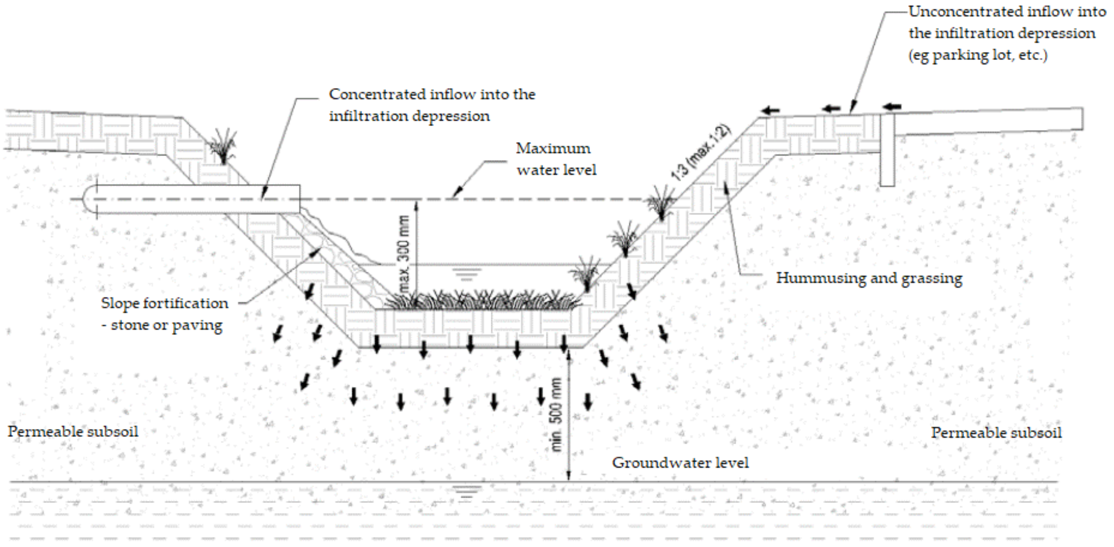

Figure 3 Example of infiltration depression solution

<u>Infiltration ditches, depressions, furrows</u>

The ditch or furrow infiltration device is usually linear (Figure 3). It can combine the function of accumulation and infiltration. The surface material should be naturally permeable (eg grass, gravel, sand) or truly permeable material. Furrows are built along roads, sidewalks, railways for drainage and infiltration. The ditch can have the shape of a trapezoidal, cup-shaped or triangular cross-section with a water depth of about 0.4 m and slopes of 1: 2 – 1: 2.5, depending on the material used and the space available.

Infiltration tanks

The infiltration takes place through a revitalized layer of soil in a ground tank. For infiltration tanks, the ratio between the connected impermeable surface and the infiltration area is generally greater than 1:15.

Rain gardens

There are several ways to drain rainwater from the roof and paved areas into the rain garden. You can easily disconnect the rain gutters from the rain sewer and redirect the water to the rain garden through a surface-sloping ditch. Alternatively, you can install an underground PVC pipe under the surface with rainwater coming from the roof to the rain garden. To protect against strong water jets and erosion from the pipeline to the rain garden, it is advisable to install the pipeline outlet with geotextiles and stones. The rain garden can be combined before entering by installing a barrel into which rainwater flows from the roof.

Infiltration blocks

These products are an alternative to classic infiltration drains, built of aggregate and gravel, or of plastic drainage pipes. Infiltration cages and tunnels can be interconnected to create an infiltration field with a large capacity.

In contrast to conventional gravel drainages with an absorption capacity of 30 - 35%, the infiltration cages achieve an absorption capacity of about 3 times higher (up to 95%). Thanks to its construction, the infiltration block guarantees a high load capacity. With a backfill height of 800 mm, it is also passable by trucks. The distance of the excavation from neighboring buildings should be equal to minimum of 2 meters for buildings that are waterproof and 5 meters for buildings that are not waterproof.

Green roofs

The most common type of green roofs are just compositions with undemanding low vegetation. Green roofs are easy to maintain and are also the most affordable. In addition to its aesthetic function, greenery helps reduce air pollution in the urban environment.

Conclusions

Rainwater management is a fundamental task within urban infrastructure in an urbanized area. Since ancient times, the solution of water management infrastructure of urban settlements (Lewis, 2000) has been a fundamental role in planning the structure of the city. In addition to street and road solutions, the most important task was to propose a system of drinking water distribution and drainage of wastewater (Evans, 1994), (Koutsoyiannis et al., 2007), where rainwater was considered as waste.

Nowadays, cities and their decision-making authorities are facing many complex challenges related to balancing urban development and its impact on the environment. The urbanization trend continues at a global peak pace - as the majority of the world's population now lives in cities and is expected increase to 66 % by 2050. As a result, there is a growing demand for the construction of new infrastructure (Wouters, 2020).

Further, water management of cities and villages fights with much more obstacles than before . Aging infrastructure systems operated for many years after their theoretical lifetime (operation) with a very high need for reconstruction and repair (Mark et al., 2008, Grum et al., 2006). At the same time, the effects of climate change, pressures due to demographic change or growing fears of new pollutant threats are facing increasingly tense socio-economic contradictions. If an urbanized area faces such problems, it also offers the possibility to adapt the new drainage concept to a sustainable, flexible aspect and to propose it according to the currently available technical possibilities and environmental protection requirements (Mark et al., 2008).

In accorandce with the current climatic situation, cities should be more inclined to increase local retention and infiltration of rainwater and to apply new knowledge, technologies to the construction and renewal of sewerage networks (Kleidorfer et al., 2009). It is necessary to address the generation of groundwater resources and the evaporation of retained rainwater with positive effects on the urban microclimate (Berggren et al., 2012, Shahrestani et al., 2015, Yao et al., 2011).

Acknowledgment

"This publication is the result of the project implementation: „ Scientific support of climate change adaptation in agriculture and mitigation of soil degradation" (ITMS2014+ 313011W580) supported by the Integrated Infrastructure Operational Programme funded by the ERDF."

"This research was funded by the Slovak Research and Development Agency (APVV), grant number 16-0278".

References

ARNBJERG-NIELSEN, K. et al. 2013. Impacts of climate change on rainfall extremes and urban drainage systems: A review. Water Sci. Technol. 2013, 68, 16–28..

BERGGREN, K. et al. 2012. Hydraulic Impacts on Urban Drainage Systems due to Changes in Rainfall Caused by Climatic Change. Journal of Hydrologic Engineering, 17(1).92-98. 10.1061/%28ASCE%29HE.1.

BERGGREN, K. et al. 2007. Tools for measuring climate change impacts on urban drainage systems. In Proceedings of the NOVATECH 2007: Sixth International Conference on Sustainable Techniques and Strategies in Urban Water Manag.

DEISTER, L. et al. 2016. Wassersensible Stadt- und Freiraumplanung - Handlungsstrategien und Maßnahmenkonzepte zur Anpassung an Klimatrends und Extremwetter. SAMUWA – Publikation. Univers, Publikation. Universität Stuttgart.

DROSOU, N. et al. 2019. Key Factors Influencing Wider Adoption of Blue–Green Infrastructure in Developing Cities. Water 2019, 11, 1234. https://doi.org/10.3390/w11061234.

DURAND, R. et al. 2019. Obnovenie vody na zachovanie našej klímy, http://peopleandwater.international/wp-content/uploads/2020/02/Manual-obnova-klimy.pdf, 2019.

EVANS, H. B. 1994. Water Distribution in Ancient Rome: The Evidence of Frontius. University of Michigan Press, Ann Arbor, USA.

GRUM, M. et al. 2006. The effect of climate change on urban drainage: An evaluation based on regional climate model simulation. Water Science & Technology 54(6-7), 9-15..

HUDEKOVÁ, Z. 2013 Výskum zadržiavania a využívania dažďových vôd v urbárnej krajine, PODKLAD PRE METODIKU SPRACOVANIA ÚPD,, Bratislava : UrbEco, https://docplayer.cz/45077916-Vyskum-zadrziavania-a-vyuzivania-dazdovych-vod-v-urbannej-krajine.html, 2013.

JURÍK, L. – Pokrývková, J. 2018. Urban Water retention – Theoretical Aspects and Practical Measures Zadržiavanie vody v mestách – teória a praktické riešenia. Životné Prostr. 2018, 52, 42–48.

KABELKOVÁ, I. „voda.tzb-info.cz,“ 2018. [Online]. Available: https://voda.tzb-info.cz/destova-voda/18198-hospodareni-s-destovou-vodou-poznatky-z-realnych-projektu-v-cr-nemecka-a-danska. [Cit. 31 01 2021].

KANG, N. et al. 2016. Urban Drainage System Improvement for Climate Change Adaptation. Water 2016, 8, 268. https://doi.org/10.3390/w8070268.

KLEIDORFER, M. et al. 2009. A case independent approach on the impact of climate change effects on combined sewer system performance. Water Science and Technology 60(6), 1555-64.

KOUTSOYIANNIS, D. et al. 2007. Urban water management in Ancient Greece: Legacies and lessons. ASCE, Journal of Water Resources Planning & Management.

KREJČÍ, V. et al. 2002. Odvodnění urbanizovaných území - koncepční přístup, Brno: NOEL 2000, 2002.

LEWIS, M. D. 2000. “The Hellenistic Period”. In Handbook of Ancient Water Technology. Ed. by Ö. Wikander. Leiden and Boston: Brill, 2000, 631–648., 2000.

LIAO, K.-H. et al. 2017. Blue-Green Infrastructure: New Frontier for Sustainable Urban Stormwater Management. In Tan P., Jim C. (eds) Greening Cities. Advances in 21st Century Human Settlements. Springer, Singapore. https://doi.org/10.1007/978-.

MARK, O. et al. 2008. Analyses and Adaptation of Climate Change Impacts on Urban Drainage Systems. In 11th International Conference on Urban Drainage, Edinburgh, Scotland, UK.

POKRÝVKOVÁ, J. et al. 2020. Water retention in urban areas in the Danube Region: Study on facts, activities, measures and their financial assessment. 1st ed. Nitra: Slovenská poľnohospodárska univerzita, 2020. 69 s. Dostupné na internete: <https://doi.org/10.15414/2021.9788055222998>. ISBN 978-80-552-2299-8.

SHAHRESTANI, M. et al. 2015. A field study of urban microclimates in London. Renewable Energy, 73, 3-9. https://doi.org/10.1016/j.renene.2014.05.061.

VÍTEK, J. 2018. Hospodaření se srážkovými vodami – cesta k modrozelené infrastruktuře, Brno, 2018.

VÍTEK, J. et al. 2015. Hospodaření s dešťovou vodou v ČR. Praha: 01/71 ZO ČSOP Koniklec, 2015. ISBN 978-80-260-7815-9.

WILLEMS, P. et al. 2012. Climate change impact assessment on urban rainfall extremes and urban drainage: Methods and shortcomings. Atmos. Res. 2012, 103, 106–118..

WOUTERS, P. et al. 2020. Blue-Green infrastructures as tools for the management of urban development and the effects of climate change, 2020.

YAO, R. et al. 2011. A simplified mathematical model for urban microclimate simulation. Building and Environment, 46(1), 253-265. https://doi.org/10.1016/j.buildenv.2010.07.019.

ZHOU, Q. 2014. A review of sustainable urban drainage systems considering the climate change and urbanization impacts. Water 2014, 6, 976–992.

Contact address

Ing. Jozefína Pokrývková, PhD., Slovak University of Agriculture in Nitra, Research Centre Agrobiotech, Horticulture and Landscape Engineering Faculty, Tr. A. Hlinku 2, 949 76 Nitra, Slovakia, +421 37 641 5228, jozefina.pokryvkova@uniag.sk

ARTICLE HISTORY:
Received 28 April 2021
Received in revised form 6 May 2021
Accepted 10 May 2021

EFFECT OF BIOCHAR APPLICATION ON CO_2 EMISSIONS DURING THE SUMMER PERIOD

Tatjana KOTUŠ[1], Ján HORÁK[1]

[1]Slovak University of Agriculture in Nitra, SLOVAKIA

Abstract

Although many research's suggested that biochar has the potential to mitigate the soil carbon dioxide (CO_2) emission, investigating how biochar effects on CO_2 emission emissions from different soil types under field conditions are limited. Furthermore, there is limited knowledge on how interactions between biochar and nitrogen fertilizer (N-fertilizer) effect on CO_2 emissions from different soils. This field study, conducted in Malanta (Nitra), Slovakia in 2019 measured the soil CO_2 emissions from silt loam Haplic Luvisol. In our study, we evaluated the impact of biochar application (10 and 20 t.ha^{-1}) applied in 2014 combined with N-fertilizer in three fertilization levels (N0, N1, N2) on CO_2 in field conditions during growing season (June to September) in 2019. Biochar at dose of 10 t.ha^{-1} with or without N-fertilizer decreased daily and cumulative soil CO_2 emissions, compared to control without biochar. We found statistically significant ($P<0.05$) increasing effect of biochar treatment B20N1 compared to control treatment B0N1. We observed the significant correlation between CO_2 emission and soil temperature. According to ours results we can say that the biochar applied to soil in 2014 is able to reduce CO_2 emission after five years of its application with or without N-fertilizer.

Keywords: soil CO_2 emissions, soil temperature, biochar, N-fertilizer

Introduction

Greenhouse gases such as carbon dioxide (CO_2), methane (CH_4) and nitrous oxide (N_2O) are the basis of human air pollution. The main contributions to the global greenhouse effect are people, whose CO_2 emissions are produced in unimaginably high amounts and released into the atmosphere. 80% of the total CO_2 emissions are caused by exhaust gases from fossil fuels and about 20% is released by agriculture such as deforestation, conversion of grassland into arable land (Glaser, 2012). Agriculture is a main source of GHGs emission, and reducing GHGs from agriculture and increasing carbon sequestration to terrestrial ecosystem play an important role in dealing with climate changes (Smith et al., 2007). CO_2 emission from soil organic matter (SOM) is result from the mineralization of resident soil C and are strongly affected also by soil temperature (Cook and Orchard, 2008). Biochar is product of pyrolysis of biomass under hypoxic conditions (Chen et al., 2013). It is resistant to biochemical degradation thanks to its molecular stability (Glaser, 2012). Fresh biochar addition may add a large amount of labile C to the soil, therefore increasing soil CO_2 emissions. However, this is only a short-term effect (Zimmerman et al., 2011). In the longer term, biochar is hypothesized to increase recalcitrant soil C and can even increase soil microbial biomass by agglomeration of SOM and nutrients onto the biochar surface (Lehmann et al., 2011). Biochar application may also reduce the activity of multiple C mineralizing enzymes, therefore reducing soil CO_2 emissions (Jin, 2010). So, it gradually starts to be a form of new way to increase carbon storage and reduce CO_2 emissions (Lehmann et al., 2006). The objectives of this study were to evaluate the impact of biochar application on CO_2 emission and also to determine if air temperature and soil temperature have an effect on soil CO_2 emissions. We hypothesized that under field conditions, biochar amendment would suppress soil CO_2 emissions during summer period. Also, we hypothesized that soil temperature will correlate with soil CO_2 emissions during summer months.

Material and methods

Experimental site and climatic conditions

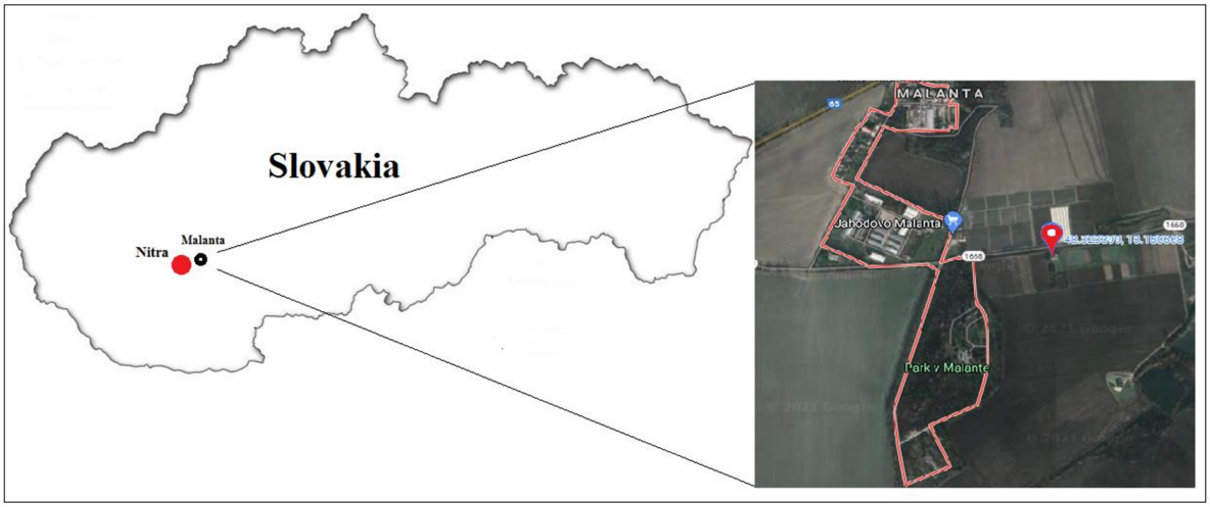

Figure 1 Location of the study site

The field experiment was conducted starting in 2014 and continuing until now at the experimental site Dolna Malanta in region Nitra (Fig. 1) (48˚19’00’’; 18˚09’ 00‘‘) (Slovakia). The average annual temperature is 9.8°C with average annual rainfall 539 mm (according to the 30-year climate normal, 1960 – 1991) (Šiška et al., 2005). The annual average air temperature during experiment in 2019 was 8.5°C and annual average rainfall was 625 mm. The data were taken from the weather station in Nitra.

The soil used in this study is silt loam Haplic Luvisol according to the soil taxonomy (IUSS, 2015) with a silty loam soil texture (content of sand 15.2%, silt 59.9% and clay 24.9%). The basic properties of the topsoil before the experimental field were pH 5.71 and soil organic carbon 9.13 $g.kg^{-1}$. Cropping system in this experimental field in 2019 included corn (Zea mays L) growing season.

Experiment material - Biochar

The biochar used for the experiment was produced by the pyrolysis of paper fibber sludge and grain husk at the temperature of 550°C for 30 minutes in Pyreg reactor at the Pyreg GmbH in Dörth, Germany. The biochar had the following physical and chemical characteristics which are shown in Table 1.

Table 1 The physical and chemical characteristics of used biochar

pH	**Organic C**	**Total N**	**C : N**	**Bulk density**	**Specific surface area**	**Ash**
(-)	(%)	(%)	(-)	($g.cm^{-3}$)	($m^2.g^{-1}$)	(%)
8.8	53.1	1.4	37.9	0.21	21.7	38.3

Experiment design

The experimental design consisted of a completely randomized block design with 9 variants in three replicates. It was arranged in 27 experimental plots with 4 m x 6 m for each plot with a buffer zone of 0.5 m between every two plots (Fig. 2). Biochar was applied by hand in 2014 at doses of 0, 10 and 20 $t.ha^{-1}$ and reapplied in 2018 (plots were divided into two plots – 4 m x 3 m) with the same doses and were labelled B0, B10 and B20, respectively. Nitrogen fertilizer in 2019 was applied at rates of 0, 108 and 162 kg $N.ha^{-1}$ (labelled N0, N1 and N2) after seeding of corn. The plots were harvested as the maize ripened in late October. In our study we used results measured during the growing season from June to the first part of September (during summer period) in 2019, only plots “A” where the biochar was applied in 2014 (five years after its application). Treatments are shown at following Figure 2 below the text.

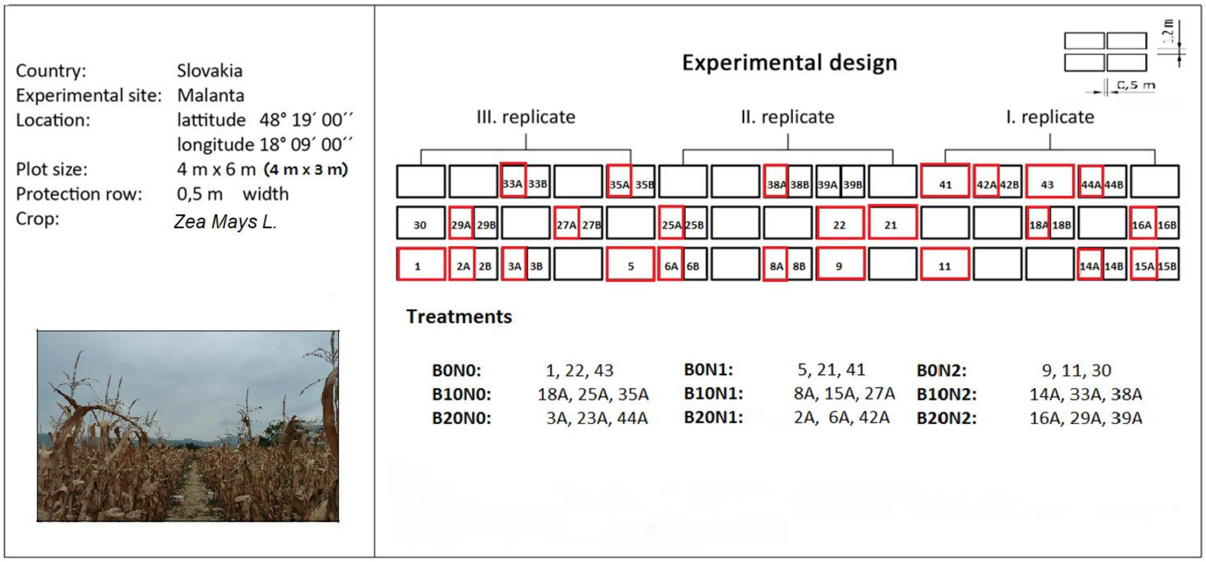

Figure 2 Schematic placement of the biochar application in the research site

<u>Gas sampling and Measurements</u>

Daily CO_2 emissions were measured using the closed static chamber method in every plot from June 2019 to September 2019. In each experimental plot, one chamber consisted of a base frame and a removable top chamber. The frame had a water-filled groove to form an airtight seal in the upper chamber during sampling. Each measurement, CO_2 emissions were measured between 8.30 a.m. and 11.30 a.m. in the morning. From each plot the emissions were taken consecutively, using plastic gas-tight syringes at 0.30 and 60 minutes after the chambers were closed. 12 ml pre-evacuated glass vials (Labco Exetainer) were used in advance to transport a 20 ml gas sample. The CO_2 emissions were analysed by gas chromatograph using thermal conductivity detector (TCD) (GC-2010 Plus Shimadzu). Cumulative CO_2 emissions over the monitoring period were calculated by interpolation. The soil temperature was measured at a depth of 0.05 m (Volcraft DET3R thermometer) every two weeks.

<u>Statistical Analyses</u>

A one-way analysis of variance (ANOVA) was used to evaluate the effect of different biochar application rates on the measured parameter, and differences between the treatment averages were compared using the least significant difference testing (LSD). Further, regression analyses to determine the relationship between the CO_2 emission and soil temperature were used.

Results and discussion

The influence of biochar on soil CO_2 emissions

Figure 3 shows the effect of biochar treatments on CO_2 emission from the soil in the course the studied period during the summer months in 2019 from June to September. Also, in graph is shown air temperature and how it impacts on soil CO_2 emission peaks. With increasing air temperature the soil CO_2 emissions increased and with decreasing air temperature the soil CO_2 emission decreased. In general, CO_2 emission trend, during the considered period, were similar in all treatments, however the CO_2 emissions differed between the treatments, especially at peak events (Fig. 3).

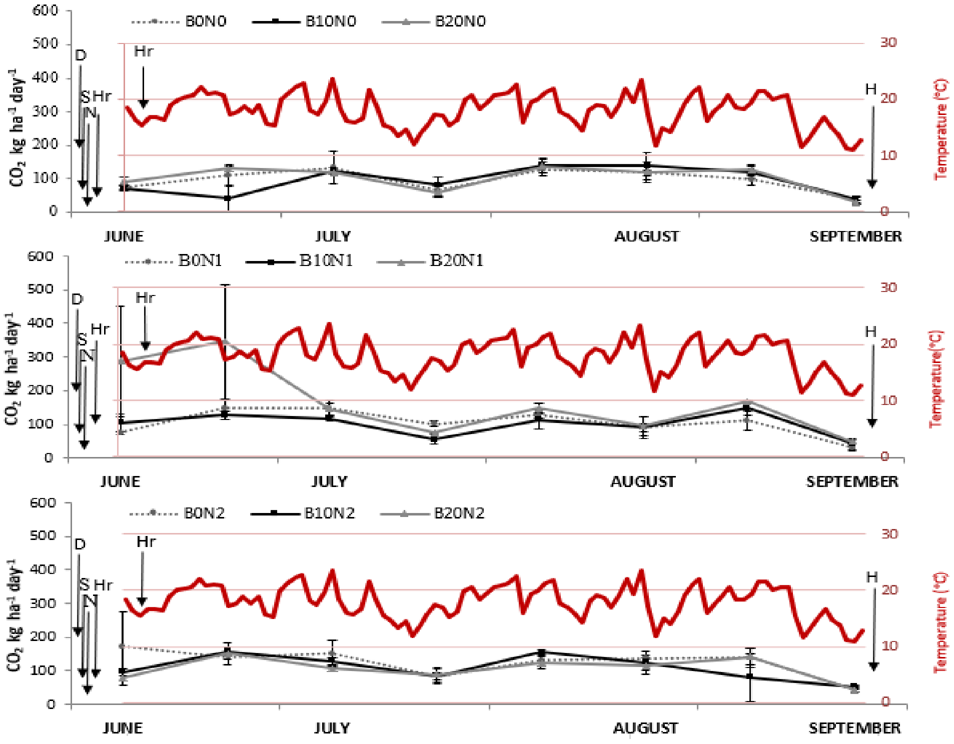

S - sowing (03.04.2019)
N - nitrogen application (05.04.2019)
Hr - herbicide application (18.04; 05.06.2019)
H - harvesting (28.10.2019)

Figure 3 Carbon dioxide fluxes emission (kg.ha^{-1}.day^{-1}) from the soil amendment with or without biochar addition and N-fertilizer in 2019. Error bars indicate standard errors of the means (n=3)

Table 2 Effect of biochar treatments on average soil CO_2 emission (means ± standard error; n=3) over the studied period (≥15 °C) in 2019 (June–September).

Treatments	**Average daily CO_2 emissions**	**Cumulative CO_2 emissions**	**Increasing / decreasing of cumulative CO_2 emission**
	($kg.ha^{-1}.day^{-1}$)		**(%)**
Not fertilized group (0 $kg.N.ha^{-1}$)			
B0N0	95.65 ± 20.0 ^{a}	9959.4 ± 2382.3	-
B10N0	94.01 ± 34.8 ^{a}	9904.7 ± 2595.8	-0.6 %
B20N0	101.86 ± 23.7 ^{a}	10583.6 ± 1733.7	+6 %
Fertilized group (108 $kg.N.ha^{-1}$)			
B0N1	104.04 ± 24.6 ^{a}	10965.8 ± 1843.6	-
B10N1	99.95 ± 34.3 ^{a}	10234.7 ± 3242.9	-7 %
B20N1	168.99 ± 88.9 ^{b}	16113.1 ± 6767.1	+47 %
Fertilized group (162 $kg.N.ha^{-1}$)			
B0N2	125.43 ± 50.6 ^{a}	12013.7 ± 4001.5	-
B10N2	109.70 ± 35.4 ^{a}	11256.6 ± 2522.6	- 6 %
B20N2	105.25 ± 33.6 ^{a}	11036.1 ± 2454.0	-8 %

Table 2 shows, that average soil CO_2 emissions and cumulative CO_2 emissions over the studied period during summer months. Fertilization is an important factor affecting CO_2 emission from soils (Reicovsky et al. 1995; Pascual et al., 1998), which was also confirmed by our study. The average daily CO_2 emissions over the whole studied period from treatments combined with N-fertilizer were generally higher compared to treatments without N-fertilizer. Almost all biochar treatment with or without N-fertilizer decreased the average daily soil CO_2 emissions compared to the control treatments. There were two biochar treatments (B20N0 and B20N1) which showed increase of average daily CO_2 emissions compared to their individual controls (B0N0 and B0N1). In case of B20N1 treatments it was statistically significant increase ($P<0.05$) compared to the control treatment (B0N1). The cumulative CO_2 emissions differed in all variants (Fig. 4). Additions of biochar application at dose of 10 $t.ha^{-1}$ without N-fertilizer (B10N0) decreased cumulative CO_2 emissions by 0.6% compared to control treatment B0N0. However the treatment B20N2 showed the reverse (6% increase). The treatments with biochar application at dose of 10 and 20 $t.ha^{-1}$ in combination with highest N-fertilization lever (B10N2 and B20N2) decreased the cumulative CO_2 emissions by 6% and 8% respectively in comparison with the control treatment (B0N2). Biochar treatment with lover level of N-fertilization (B10N1) also decreased the cumulative CO_2 emission by 7% in comparison with the control (B0N1). However, the biochar treatment (B20N1) increased cumulative CO_2 emissions by 47% when compared with control (B0N1). Our study is in line with the study of Hawthorne et al. (2017) which found that the biochar application increased CO_2 emissions when applied without N-fertilizer. The increase of average daily CO_2 emissions was probably due to the increased air temperature and it also decreased as the air temperature decreased during the observed period (Fig. 3). According to Zimmerman et al. (2011) increases of soil CO_2 emissions were induced by the biochar and it might be due to the labile C input as well as increased belowground net primary productivity. The suppression of soil CO_2 emissions may be due to reduced enzymatic activity and the capturing of CO_2 onto the biochar surface (Case et al., 2014). Our results are also in line with study Fidel et al. (2019) which reported that cumulative CO_2 emissions were reflected with average daily CO_2 emissions. The study of Horák et al. (2020) from the same experiment in Malanta also reported that the cumulative CO_2 emissions were lower in comparison with the control treatments without biochar, however not in all biochar treatments.

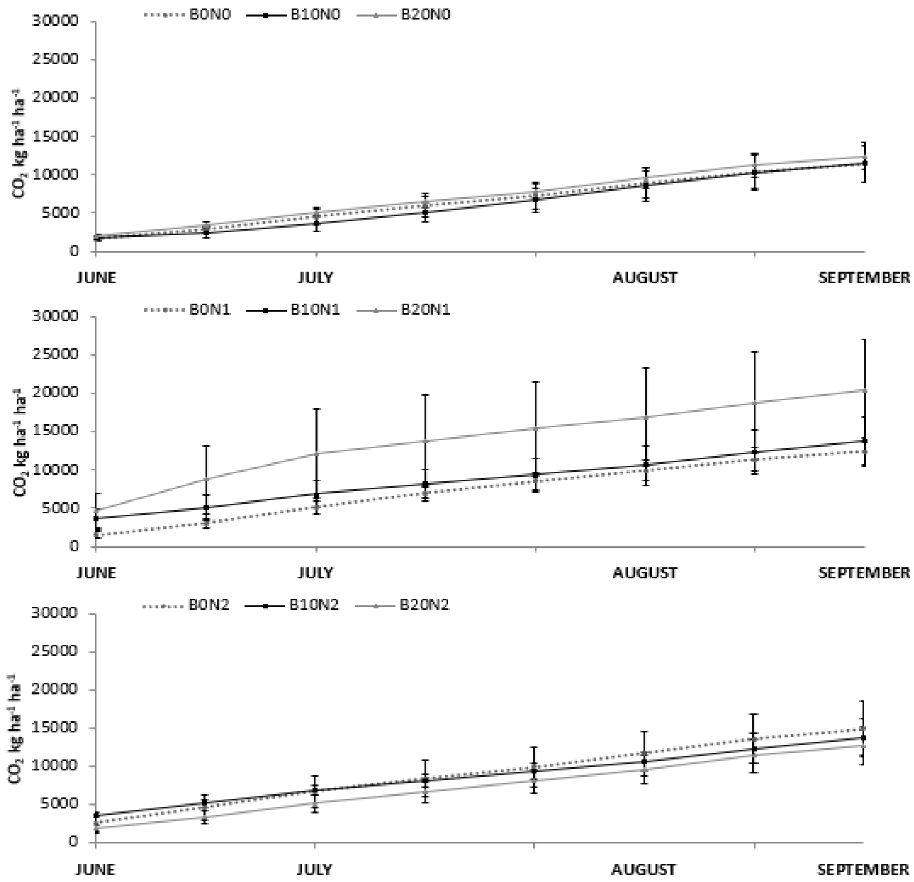

Figure 4 Cumulative CO_2 emission during the study period from control, biochar application at dose of 10 and 20 t.ha^{-1} and treatments combined with N-fertilizer at dose of 0.108 and 162 kg.N.ha^{-1} Error bars indicate standard errors of the means (n=3).

Relations between soil CO_2 emissions and soil temperature

Table 3 shows relations between daily soil CO_2 emissions and soil temperature. Our study showed that CO_2 emissions were influenced by changes in soil temperature. The results showed a significant correlation between CO_2 emission and soil temperature in treatments B0N0, B0N1, B0N2 and B10N2. The most pronounced effect between soil temperature and soil CO_2 emission was found in treatment B0N1 (r=0.92; P<0.001). Our results are in agreement with the findings of the study Shen et al. (2017) which reported that CO_2 emissions were in good correlation with the soil temperature.

Table 3 Pearson correlation coefficient between soil CO_2 emission and soil temperature (t_p) for different treatments (* P<0.05; ** P<0.01; *** P<0.001).

Treatments	**Soil temperature (t_p)**
	(°C)
Not fertilized group (0 kg.N.ha^{-1})	
B0N0	**0.87 ****
B10N0	0.44
B20N0	**0.84 ****
Fertilized group (108 kg.N.ha^{-1})	
B0N1	**0.92 *****
B10N1	0.67
B20N1	0.56
Fertilized group (162 kg.N.ha^{-1})	
B0N2	**0.87 ****
B10N2	**0.83 ****
B20N2	0.65

Conclusions

The objective of this study was to determine the effects of different doses of biochar application in combination with N-fertilizer or without N-fertilizer on the reduction CO_2 emission from the soil. Generally the effects of biochar amendment on soil CO_2 fluxes varied with dose of biochar application. Our results showed that application of lower dose of biochar (10 t.ha^{-1}) combined with or without N-fertilization is able to decreased cumulative CO_2 emissions compared to control treatments without biochar. Higher dose (20 t.ha^{-1}) of biochar application combined with lower level of N-fertilization and without N-fertilization increased soil CO_2 emissions compared to control treatments without biochar. Our findings showed a significant correlation between the soil temperature and average daily CO_2 emissions in most of the treatments. Biochar applied in 2014 is still able to reduce soil CO_2 emissions during summer period after five years of its application. However further studies are needed in the different agroecosystems before the final recommendation of the biochar for standard agronomic practice application could be made.

Acknowledgment

This study was supported the Cultural and Educational Grant Agency, KEGA (No. 019SPU-4/2020).

References

CASE, S. et al. 2014. Can biochar reduce soil greenhouse gas emissions from a Miscanthus bioenergy crop? In GCB Bioenergy, 6, pp. 76–89.

CHEN, W. et al. 2013. Researches on biochar application technology. In Engineering Science, 46, pp. 3324–3333.

COOK, F. – ORCHARD, V.. 2008. Relationships between soil respiration and soil moisture. In Soil Biology and Biochemistry, 40, pp. 1013–1018.

FIDEL, R. et al. 2019. Effect of Biochar on Soil Greenhouse Gas Emissions at the Laboratory nad Field Scale. In Soil System, 3, pp. 8.

GLASER, B. 2012. Biochar use: a productive alternative to carbon storage. Climate Action Report, London, 2011–2012, pp. 137–139.

HAWTHORNE, I. et al. 2017. Application of biochar and nitrogen influences fluxes of CO_2, CH_4 and N_2O in a forest soil. In Journal of Environmental Management, vol. 192, pp. 203-214.

HORÁK, J. et al. 2020. Effects of Biochar Combined with N-fertilization on Soil CO_2 Emissions, Crop Yields and Relationships with Soil Properties. In Polish Journal of Environment Studies, 5, pp. 1-3.

IUSS. 2015. World reference base for soil resources 2014. *International soil classification system for naming soils and creating legends for soil maps* - Update 2015. FAO: Rome, Italy. 203.

JIN, H. 2010. Characterization of Microbial Life Colonizing Biochar and Biochar-Amended Soils. Unpublished PhD thesis, Cornell University, New York, USA, pp. 199.

LEHMANN, J. et al. 2006. Biochar sequestration in terrestrial ecosystems-a review. Mitig. Adapt. In Strat Glob Change, 11, pp. 403–427.

PASCUAL, J. et al. 1998. Carbon mineralization in an arid soil amended with organic wastes of varying degrees of stability. In Communication in Soil Science and Plant Analysis, 29, pp. 835.

REICOSKY, D. et al. 1995. Impact of fall tillage on short-term carbon dioxide flux. In Soil and Global Change. Lal R., Kimble J., Levine E., Stewart B.A. Eds., CRC Press, Inc.: Boca Raton, USA, Chapter, 14, pp. 177.

SHEN, Y. et al. 2017. Effect of Biochar Application on CO_2 Emissions from a Cultivated Soil under Semiarid Climate Conditions in Northwest China. In Sustainability, 9, pp. 1482.

ŠIŠKA, B. et al. 2005. Practická biometeorológia. Nitra: SPU. 102 p. ISBN 80-8069-486-9.

SMITH, P. et al. 2007. Agriculture. In: Climate Change: Mitigation. Contribution of Working Group III to the Fourth Assessment Report of the Intergovernmental Panel on Climate Change, Cambridge University Press, Cambridge, United Kingdom and New York, NY, USA. pp. 497–540.

ZIMMERMAN, A. et al. 2011. Positive and negative carbon mineralization priming effects among a variety of biochar-amended soils. In Soil Biology and Biochemistry, 43, pp. 1169–1179.

Contact address

Ing. Tatijana Kotuš, Slovak University of Agriculture in Nitra, Faculty of Horticulture and Landscape Engineering, Department of Biometeorology and Hydrology, Hospodárska 7, 949 76 Nitra, Slovakia, tatijanakotus@gmail.com

ARTICLE HISTORY:
Received 25 April 2021
Received in revised form 11 May 2021
Accepted 20 May 2021

ANALYSIS OF THE SHORTCOMINGS OF THE WASTE COLLECTION POINT FOR COLLECTING SEPARATED MUNICIPAL WASTE IN THE VILLAGE MIEROVO

Gergely RÓZSA[1], Ivona ŠKULTÉTYOVÁ[1]

[1]Slovak Technical University in Bratislava, SLOVAKIA

Abstract

Waste causes problems all around the world. One of the options how to reduce the quantity of municipal waste is selective collection. By improving the container stands, the quality of the environment of residents can be increased. This improvement can lead to a higher interest of inhabitants in using the new technologies in waste management.

The paper focuses on analysing the current state of the waste collection point in the village of Mierovo. It also points out the shortcomings of the waste collection point and the advantages of semi-underground containers. The paper's conclusion is a proposal for a semi-underground container stand in the village of Mierovo based on an analysis of the condition of the waste collection point.

Keywords: separation, smart city, waste, waste collection point, waste management

Introduction

Waste is a product of human society and is generated in virtually every human activity in the manufacturing and consumer spheres. Unlike nature, people create types of waste that nature cannot deal with on its own. That is why environmental protection is essential to ensure the quality of life of present and future generations. One of the activities aimed at protecting the environment is waste management, which seeks to prevent and reduce the generation of waste and reduce its hazard (Trošanová, 2018).

Within Slovakia, the area of waste and waste management is experiencing a period of change. Every one of us can contribute to solving waste problems. It is not enough what the law obliges us to do. Waste is not only a source of environmental pollution but also a valuable source of secondary raw materials. Therefore, it is essential to have a plan on managing waste not only from an ecological but also from an economic point of view.

Until recently, smart ideas and urban management based on state-of-the-art waste management technologies could only be heard abroad (Office on the net, 2021). Following the sample of successful examples, smart ideas are also beginning to reach Slovakia to increase the quality of life of citizens and the benefit of cities. These places can be called Smart City (Smart city point, 2021).

This work aims to analyse a specific waste collection point, referring out the shortcomings and the proposal of a better form of a collection of sorted types of municipal waste. The results of the analysis could also be applied to other waste collection points to improve their usability.

Material and methods

Separate waste collection system

We can collect separated waste in households or a designated place. The aim of separate waste collection is the material recovery of waste as much and as possible. Other goals are to reduce the amount of municipal waste and increase the use of secondary raw materials. The types of separated components from municipal waste are paper, plastic, glass, metals, multilayer composite materials based on cardboard, textiles, biodegradable waste, and electrical waste (Agovino, 2020).

According to the method of waste collection, we can divide the system into a container and a non-container system (Čermák, 2007). Globally container system is the most widespread, where sorted waste is collected in dedicated containers. There are so-called waste collection points in the zones with apartment buildings, where containers for separate waste collection are placed. In the zone with family houses, some waste is collected for each household separately in containers or bags, and somewhere near the residential zone, there is a container stand for the remaining types of separated waste (Rousta, 2015). Waste not collected either in households or on container stands can be stored at the nearest collection point or civic amenity site.

Lack of space for the habitat, due to increased demands on the location of collection containers for separate collection, constant pollution of the containers' surroundings, and lack of space in cities caused a solution to be gradually developed. The collection container is located under the terrain (Rodrigues, 2016). Only a throw-in superstructure with an insertion hole is located over the terrain. It is advantageous to build the mentioned system in new housing estates, where the habitats belong to the objects that form the city's infrastructure. The method is also advantageous for separate waste collection (Čermák, 2007).

Waste collection system without container less known. It is also called an automated vacuum waste collection system (AVAC) (Čermák, 2007). It is used most in developed countries. In AVAC, the waste is piped to a collection point, taken for recycling, or to a final disposal site (Envac, 2021).

Results and discussion

Analysis of the waste collection point

The waste collection point is located in the village centre in front of the department store, near the cultural centre, and the municipal office. The containers are located on a paved area but not on land owned by the municipality. The container's position in terms of the frequency of waste removal is located correctly; the locals can easily reach them. The types of waste that can be recycled or recovered are collected here.

Figure 1 The waste collection point in Mierovo (Authors, 2019)

The current 1100 l containers were no longer sufficient incapacity, due to which the number of containers for some types of waste was increased. After increasing the amount of sorted waste again, it would be necessary to change the periodicity of waste exports due to the lack of paved areas where the stand could be expanded.

The export of waste from the container stand is determined according to the schedule. The processor does not consider the fullness of the containers, which may have been filled for a long time or half-empty.

From an aesthetic point of view, the container stand does not fit into the environment. It is located next to the park and the main square of the village. It can cause negative sentiment that can affect the population when deciding on waste separation. Handling 1100 l containers is problematic. They slide easily when opened as they are mobile. They are not accessible to people with disabilities. Other shortcomings of the container stand are:

- odour at higher temperatures or with incorrect sorting of waste,
- unclosed containers attract rodents,
- short service life of containers and frequent need for disinfection,
- is unrepresentative.

Design of a semi-underground container stand

Instead of the original container stand, we design a stand with semi-underground containers. The new container stand would be located on the plot of the village Mierovo.

Semi-underground containers will be located next to the park; currently, it is a grassy area. Semi-underground containers will be located 300 mm from the local road. The first semi-underground container will be located 300 mm from the sidewalk; the distance between individual semi-underground containers will be 300 mm.

A paved area was designed around the semi-underground containers, which will consist of paving stones, which will also serve as an access road to the semi-underground containers. Ornamental trees have been designed to incorporate the stand into the surrounding environment, namely *Thuja occidentalis 'Smaragd,' Syringa Vulgaris, Forsythia x intermedia.* Existing plant species in the area were considered when selecting plants.

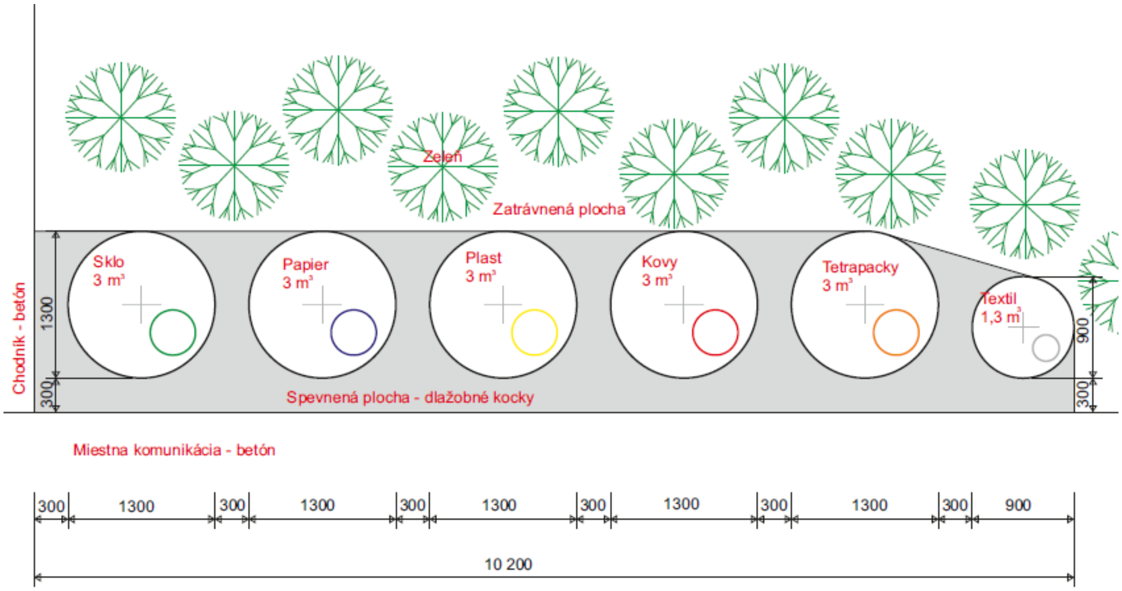

Figure 2 Design of the location of the container stand (Authors, 2019)

Semi-underground containers will replace the original 1100 l containers for glass, paper, plastic, metals, tetra packs with a volume of 3 m^3. A semi-underground container will replace the textile container with a volume of 1.3 m^3. All factors influencing functionality and aesthetics were contemplated in the design. The design envisaged the transfer of the oil collection drum to the civic amenity site.

When installing 3 m^3 of semi-underground containers, it is necessary to dig a construction pit to a depth of 1600 mm, with crushed gravel with a fraction of 0–16 mm and a thickness of 100 mm to be added to the bottom of the excavation pit. The minimum thickness of crushed gravel with a fraction of 0-16 mm is 50 mm. The shaft body, which has a height of 1500 mm with a diameter of 1300 mm and is made of HDPE material, is placed on the levelled gravel layer. The thickness of the shaft body is 10 mm. The body of the shaft is waterproof, so groundwater cannot enter the shaft body. The groundwater level in the village is approximately 4-5 m below the ground. The excavation pit around the shaft body is first backfilled with gravel with a fraction of 16–32 mm in a thickness of 600 mm. The minimum thickness of the gravel with the fraction around the bottom of the shaft body is 500 mm. A sealing foil 1.5 mm thick is placed on the gravel, on which the excavated soil is poured to a height below the surface of 100 mm. The excavated soil layer is compacted, and the last layer is aggregate with a fraction of 0–4 mm, on which paving stones are then placed, which will serve as an access road to semi-underground containers. The same installation procedure is for semi-underground containers with a volume of 1.3 m^3.

Above the ground, the shaft body has a height of 1200 mm, which can have various fencing, in this case, recycled plastic. For the resolution of semi-underground containers, a board shall be placed stating which types of waste are collected in the container and which are not. The lid at the discharge opening will be of the appropriate colour according to the type of waste, such as green for the glass container, blue for the paper container, yellow for the plastic container, red for the metal container, and orange Tetra Pack container. The textile is not assigned with a colour; the lid will be grey.

Figure 3 Designed semi-underground waste collection point (Authors, 2019)

Advantages of a semi-underground waste collection point

Several advantages of these collection containers have influenced the choice of semi-underground containers. The installation of semi-underground containers increases the aesthetic value of public space. The renewed waste disposal site will bring several pragmatic enhancements besides improved visual. The added value of the new site psychologically influences the inhabitants' behaviour and support a responsible approach to waste sorting. Semi-underground containers are not mobile, they have a lower opening for spreading waste, so they are easily accessible even to the disabled population (Rodrigues, 2016).

By installing containers in a vertical plane, space is created for other uses of public space, such as rest areas. Most of the semi-underground container is located below the surface, so it occupies only half the area on the surface. The cold of the earth slows down the decomposition of bacteria and reduces the associated odour. The containers are emptied from the bottom of the collection bag so that the insertion opening remains clean. Handling the container during export is clean and straightforward. The depth of the containers makes it impossible to re-select their contents, which also prevents pollution of their surroundings. The construction of semi-underground containers prevents the access of animals and insects.

The bodies of semi-underground containers are made of impermeable material, so it is also suitable for environments where the groundwater level is higher. The cold environment caused by placing the container underground reduces the risk of fire and odour.

Sensors

Sensors for semi-underground containers are based on ultrasonic technology, are robust, water-resistant and impact-resistant, while their endurance reaches up to 10 years. They are adapted for operation in a wide temperature range and set to measure to a depth of 1500 - 4000 mm, depending on the type of sensor. In addition to the height of the waste, they also measure the temperature and its GPS position. The sensors can be equipped with an alarm in case of fire. The endurance of the sensors is ensured by high-performance replaceable batteries, while they regularly inform the customer about the charge level. All data recorded by the sensors are transferred to the system, where they are processed and evaluated for application purposes. In addition to an updated overview of the amount of filling the containers, the application allows optimal transport routes. It also provides visualizations, graphs, enables complete container management and obtaining notifications from citizens (Sensoneo, 2021).

Conclusions

This work was focused on the analysis of the current state of the waste collection point. According to the analysis, a semi-underground waste collection point achieved a greater capacity for the collection of selected types of waste. The design also considered the aesthetic aspect of the semi-underground container stand. This contributes to the improvement of waste separation and sustainability of the environment. With the design of semi-underground containers with sensors, the export of waste can also be made more efficient, protecting the environment and reducing costs.

This type of container stand will improve the functioning of waste management in a given locality, whether from an economic or ecological point of view.

Acknowledgment

This work was supported by the Scientific Grant Agency of the Ministry of Education, Youth and Sports of the Slovak Republic and the Slovak Academy of Sciences within the project VEGA 1/0727/20 and 1/0574/19.

References

AGOVINO, M. et al. 2020. Separate waste collection in mountain municipalities. A case study in Campania, In Land Use Policy, vol. 91, ISSN 0264-8377

ČERMÁK, O. 2007. Waste management, STU Publishing House, Bratislava, 106p. ISBN 978-80-227-2662-7

ENVAC. 2021 [ONLINE] © Envac, [cit. 18. 04. 2021], Available on internet: https://www.envacgroup.com/

OFFICE ON THE NET. 2021 [ONLINE] © 2013 NETEN A HIVATAL, [cit. 19. 04. 2021], Available on internet: http://allampolgar.netenahivatal.gov.hu/allampolgari-kisokos/intelligens-varosok

RODRIGUES, S. et al. 2016. Waste collection systems. Part A: a taxonomy. In Journal of Cleaner Production, vol. 113, pp. 374-387. ISSN 0959-6526

ROUSTA, K. et al. 2015. Quantitative assessment of distance to collection point and improved sorting information on source separation of household waste. In Waste Management. Vol. 40, pp. 22-30. ISSN 0956-053X

SENSONEO. 2021 [ONLINE], © 2021 SENSONEO, [cit. 23. 04. 2021], Available on internet: https://sensoneo.com/sk/

SMART CITY POINT. 2021 [ONLINE] © 2017 SMART CITY POINT z. ú., [cit. 19. 04. 2021], Available on internet: http://scpoint.eu/chytre-zivotni-prostredi/

TROŠANOVÁ, M. et al. 2018. State of the management of municipal waste in the context of reverse logistics, Pollack Periodica, Vol. 13, No. 2, pp. 117–128.

Contact address

Ing. Gergely Rózsa, PhD., Faculty of Civil Engineering STU in Bratislava, Department of Sanitary and Enviromental Engineering, Radlinského 2766/11, 810 05 Bratislava, Slovakia, +421 917 430 587, gergely.rozsa@stuba.sk

ARTICLE HISTORY:
Received 30 April 2021
Received in revised form 17 May 2012
Accepted 20 May 2021

USE OF DENDROMETRIC AND SAP FLOW MEASUREMENTS ON ROYAL WALNUT (*JUGLANS REGIA* L.*)* TO SELECT PLANT DAILY CYCLE

Martina KOVÁČOVÁ[1], Alexandra PAGÁČ MOKRÁ[1]

[1]Slovak Agriculture University in Nitra

Abstract

Climate change is reflected in processes in the atmospheric systems, especially in the distribution and volume of precipitation and changes in atmospheric temperatures. Plant ecosystems are dependent on liquid water. Plant water stress develops if water loss by transpiration exceeds the rate of water absorption, is accompanied by wilting, reduction in photosynthesis, loss of turgor, cessation of cell enlargement, closure of stomata, cessation of plant growth even death of plant and many others (Kumar et al., 2014). The driving force of transpiration flow is gradient in total water potential between soil and the atmosphere (Manzoni et al., 2013). Part of our research is focused on plant water regime monitoring in conditions of drought by using sap flow and dendrometric measurements. This study was compared proceedings of sap flow and dendrometric measurements in the daily cycle of 108 day of the year (DOY) in two different irrigation variants. In both irrigation variants was measured time lag between maximum of sap flow velocity, which was measured between 6 am and and 16 pm. And maximum of radial stem fluctuation during night hours, that caused internal water storage replenishment.

Keywords: water stress, xylem, dendrometer, sap flow, walnut, irrigation

Introduction

The World Meteorological Organization has been collecting and evaluating data from all meteorological stations in the world since 1866. According to reports, a global air temperature increase of + 0.74°C in the last 100 years (WMO, 2020). Climate change is reflected in processes in the atmospheric systems, especially in the distribution and volume of atmospheric precipitation and changes in atmospheric temperatures. Since 1981 the average annual total precipitation decreases by 5.6% in Slovakia (MŽP SR, 2019). In the last three decades, the result of climate change has been monitored as more frequent and longer periods of drought. Plant ecosystems are dependent on liquid water. It is the most important production factor. The purpose of all biological processes as is absorption, transporting, unloading, and maintaining water in the plant cells are related to plant water balance (Rehák et al., 2015).

Kramer and Boyer (1995) describe plant water balance as the dependence of the relative rate of water loss in the transpiration process and water absorption from the soil by root hairs. Plant water stress develops if water loss by transpiration exceeds the rate of water absorption, is accompanied by wilting, reduction in photosynthesis, loss of turgor, cessation of cell enlargement, closure of stomata, cessation of plant growth even death of the plant and many others (Kumar et al., 2014). The movement of water, transpiration flow, in plants from roots to the leaves is conducted in xylem vessels. The driving force of transpiration flow is a gradient in total water potential between soil and the atmosphere (Manzoni et al., 2013). The main plant biological regulation mechanism of transpiration flow is stomatal closure to restricting transpiration rate during exposure to water stress (Agurla et al., 2018). The elasticity of sapwood in trees is a tool to regulate daily time lags between water absorption and transpiration in the morning. The transpiration process in the morning causes the water withdrawn from internal water storage.

Part of our research is focused on plant water regime monitoring in conditions of drought by using sap flow and dendrometric measurements. Dendrometric measurements are focused on plant vessel elasticity, e. g. stem or branch, and plant radial growth in the vegetation season. One of the aims of plant water status monitoring is to design an irrigation system based on the plant water status measurements, not soil moisture. The purpose of this paper was to set the methodology of plant sap flow measurements and dendrological measurements on Royal walnut (*Juglans regia* L.) trees in a field experiment.

Material and methods

Field measurements were performed in 2019 in a walnut orchard in the cadastral area of the city of Nové Zámky, situated in the west part of Slovak republic (47°59´49´´ north latitude and

18°11´26´´ east longitude, 119 m a.s.l.) (Figure 1). This part of Slovakia geologically belongs to the Danubian Hill unit. This territory is characterized by very dry, warm climate with mild winter. This territory is classified as the driest and warmest areas in Slovakia, with an average annual temperature 9 – 10 °C and a total annual precipitation 500 – 550 mm (Atlas krajiny SR, 2021). The orchard is equipped with an irrigation system.

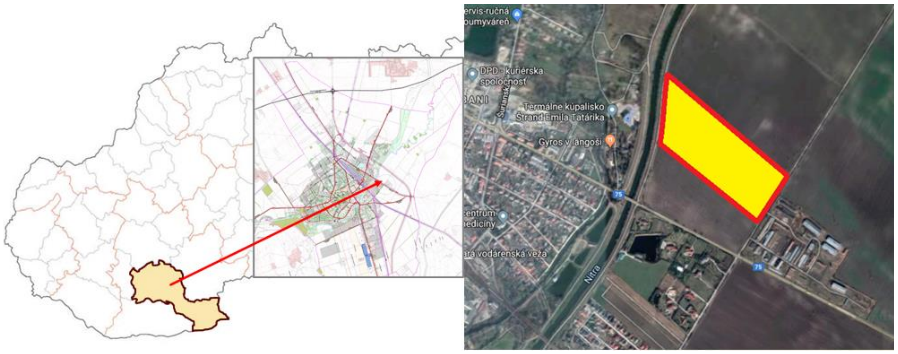

Figure 1 Study area of walnut orchard in Nové Zámky (source: Kováčová, 2021)

For cultivation of Royal walnut (*Juglans regia* L.) trees requires an average annual temperature from 10 to 20 °C, the temperature during vegetation period from 18 to 22 °C and 900 mm of rainfall per year. The root system grows to a depth of 2.5 meters; therefore it is not appropriate to cultivate these trees in areas with high groundwater level (Navara, 2010). For this study were used two different variant of irrigation variants A and B, with 3 tree samples per variant. Irrigation variant A irrigation those of 30 mm and variant B irrigated only with atmospheric precipitation.

To measure sap flow values were used Dynagage Trunk Gage sensors (Figure 2). These sensors are installed on the stem or branch with radius of 32 – 125 mm. They use the heat balance principles to measure the sap flow velocity. The sensor consists of a thermocouple, is placed around the stem. During the measurement thermocouple heats up part of the plant and sensor measures the heat balance between sap below and above the sensor. Sensors need to be connected to the datalogger system Dynagage Flow31-1K (Dynamax Inc., 2021).

Dendrometric changes were measured by Diameter Dendrometer small (DD-S) (Figure 3). The advantage of this sensor is its low weight which does not cause any damages to the plant. To measure changes in diameter of plant part sensor user electrical resistance with a range of 0 – 11000 ohms. This type of dendrometers is suitable for plant parts with a diameter of up to 50 mm. Sensors were connected to datalogger DL-18. This system is working with measurement accuracy ± 1.5 µm (Ecomatic, 2021).

Figure 2 Sap flow measurement equipment (source: Kováčová, 2019)

Figure 3 Diameter dendrometer small and datalogger DL-18 (source: Kováčová, 2020)

Results and discussion

This study was compared proceedings of sap flow and dendrometric measurements in the daily cycle of 108 day of the year (DOY). Daily radial changes are divided according to sunlight conditions. Figure 4 represents DOY 108, in variant A diurnal cycle begins at 6 am when transpiration begins, and stomata began to open. At this point, plant used the water stored in internal water storage (IWS) and stem radius started to decrease. After dawn water is water supplied from IWS flows to the crown. In the case of our experimental objects, this process caused the considerable lag between the shrinkage of the branch and sap flow velocity. According to our measurements in irrigated variant (Figure 4. a) the sap flow started at the same time when diameter started to decrease. At this point the sap flow has negative value what predicts water deficit. Sap flow velocity started increasing and this process continued until the 11 am when the sap flow velocity reached 106.7 g·h^{-1}. After this point sap flow velocity continuously decreased to 0 g·h^{-1} at 6 pm. Radial shrinkage was measured from 6 am to 4 pm with difference of 0.005 mm. At this hour sap flow velocity was less than 20 g·h^{-1} and in the later afternoon the tree began water refill to the (IWS).

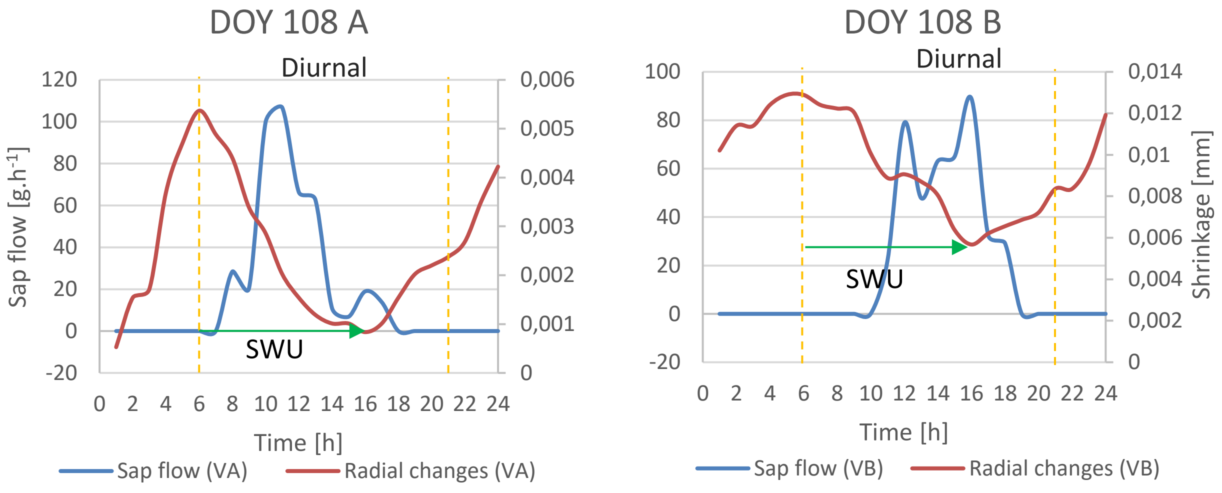

a) b)

Figure 4 Storage water usage (SWU) represents the lag between measured stem fluctuation and sap flow in selected trees.

The fluctuation of diameter of irrigation variant B (Figure 4. b) began at 6 am as stem shrinkage from 0.0129 mm by using IWS. The radial stem shrinkage stopped at 4 pm when reduction of stem was -0.0072 mm. In early morning after sunrise sap flow velocity was 0 g·h^{-1} and the flow began at 10 am. The highest sap flow value 89 g·h^{-1} was reached at 4 pm. After this moment sap flow velocity decreased to 0 g·h^{-1} at 18 pm and tree started with water refilled to IWS.

Daily cycle or circadian rhythms is subset of biological rhythms and it is defined as endogenously generated and self-sustaining mechanisms, what means that they persist under constant environmental conditions (light and temperature) in period of ~ 24h (Pittendrigh, 1954). Most of the biochemical reactions in plant metabolism are light sensitive. It is caused by the temperature changes during daily light conditions changes (Inoue *et al.*, 2017). The diurnal sap flow and stem fluctuation revealed the dynamic time lags between internal water storage usage and water replenishment to plant reservoirs (Köcher et al., 2013). According to Daudet et al. 2005, stem reaches diurnal maximum of radius in the morning between 6 and 9 am and the minimum in the late afternoon between 3 and 8 pm. Subsequently, stem begin to refill the water in internal water storage and stem radius starts to expand again. The amount of sap flow also depends on the age of tree, condition, and canopy coverage (Scholz et al., 2011). Photosynthesis and stomatal opening are one the daily cycle regulation processes, which were observed during Hennessey´s study on bean in 1993. Hennessey *et al.* (1993) measured higher stomatal conductance during day compares to the night.

Conclusions

This paper is focused to monitoring of plant daily cycle of radial fluctuation of stem and sap flow movement in xylem vessels. As study area was chosen walnut orchard in agricultural part of the city of Nové Zámky. This orchard was chosen for possibly of managing of irrigation system. The experimental equipment for dendrometric measurements DD-S and sap flow measurements Dynagage Trunk Gage sensors was installed on Royal walnut (*Juglans regia* L.) trees. Our results support the daily cycle mechanism with detected time lag between rise of transpiration flow and radial stem elasticity caused by changes in between water potential of soil and atmosphere. In the early morning when stomata start to open and water evaporate from leaves, plants use the internal water storage as source of water to this process. Sap flows to the canopy and leaves and diameter of stem decrease. In the late afternoon transpiration flow slows and water is refilling to the plant vessels and diameter increases until next daily cycle.

Acknowledgements

This research was funded by APVV project under the contract No. APVV- 15–0562.

References

AGURLA, S. et al. 2018. Mechanism of stomatal closure in plants exposed to drought and cold stress. In Survival strategies in extreme cold and desiccation. Singapore : Springer, pp. 215-232. ISBN 978-981-13-1244-1.

DAUDET, F.-A. et al. 2005. Experimental analysis of the role of water and carbon in tree stem diameter variations. In Journal of experimental botany, vol. 56, no. 409, pp. 135-144. DOI: 10.1093/jxb/eri026

Dynagage sap flow sensor user manual. Available online: https://dynamax.com/images/uploads/papers/Dynagage_Manual.pdf (accessed on 26th April 2021).

Ecomatic: Diameter Dendrometer small (DD-S). Available online: https://ecomatik.de/en/products/dendrometer/diameter-dd-s/ (accessed on 26th April 2021).

ENVIROPORTAL Atlas krajiny Slovenskej republiky. Available online: http://geo.enviroportal.sk/atlassr/ (accessed on 21st April 2021).

HENNESSEY, T. L. et al. 1993. Environmental effects on circadian rhythms in photosynthesis and stomatal opening. In *Planta*, vol. 189, pp. 369-376. https://doi.org/10.1007/BF00194433.

INOUE, K. et al. 2017. Integration of input signals into gene network in the plant circadian clock. In *Plant and cell physiology*, vol. 58, no. 6, pp. 977-982. https://doi.org/10.1093/pcp/pcx066.

LIESKOVÁ, Z. et al. 2019. Správa o stave životného prostredia Slovenskej republiky v roku 2018 (Rozšírené hodnotenie kvality a starostlivosti). MŽP SR. Bratislava. SAŽP. Banská Bystrica. 222 p. ISBN 978-80-821-007-5.

KRAMER, P. J. – BOYER, J. S. 1995. Water relations of plants and soils. Academic press. San Diego. 512 p. ISBN-13 978-0124250602.

KÖCHER, P. et al. 2013. Stem water storage in five coexisting temperate broad-leaved tree species: significance, temporal dynamics and dependence on tree functional traits. In Tree physiology, vol. 33, no. 8, pp. 817-832. DOI: 10.1093/treephys/tpt055

MANZONI, S. et al. 2013. Biological constraints on water transport in the soil–plant–atmosphere system. In Advances in Water Resources, vol. 51, pp. 292-304. ISSN 0309-1708.

NAVARA, J. 2010. Orech kráľovský (Juglans regia L.) a jeho pestovanie. Bratislava : Veda. 76 s. ISBN 978-80-224-1123-3.

REHÁK, Š. et al. 2015. Zavlažovanie poľných plodín, zeleniny a ovocných sadov. Bratislava : VEDA. 640 p. ISBN 978-80-224-1429-6.

PITTENDRIGH, C. S. 1954. On the temperature independence in the clock system controlling emergence time New Jersey : Drosophila. PNAS USA, vol. 40, pp. 1018–1029. https://doi.org/10.1073/pnas.40.10.1018

SCHOLZ, F. G. et al. 2014. Hydraulic capacitance: Biophysics and functional significance of internal water sources in relation to tree size. In Size- and age-related changes in tree structure and function. Dordrecht : Springer, pp. 341-361. ISBN 978-94-007-1242-3.

SURESH KUMAR, P. et al. 2014. Influence of moisture stress on growth, development, physiological process and quality of fruits and vegetables and its management strategies. In Approaches to plant stress and their management. New Delhi : Springer India, pp. 125 – 148. ISBN 978-81-322-1619-3.

WORLD METEOROLOGICAL ORGANIZATION, 2020. WMO statement on the state of the global climate in 2019. WMO. Geneva. 44 p. ISBN 978-92-62-11248-5.

Contact address

Ing. Martina Kováčová, Slovak University of Agriculture in Nitra, Horticulture and Landscape Engineering Faculty, Department of Water Resources and Environmental Engineering, Hospodárska 7, 949 76 Nitra, Slovakia, +421 37 641 5215, xkovacovam@uniag.sk

Ing. Alexandra Pagáč Mokrá, Slovak University of Agriculture in Nitra, Horticulture and Landscape Engineering Faculty, Department of Landscape Planning and Land Consolidation, Hospodárska 7, 949 76 Nitra, Slovakia, xmokraa@uniag.sk

ARTICLE HISTORY:
Received 28 April 2021
Received in revised form 6 May 2021
Accepted 20 May 2021

ANALYSIS OF AIR TEMPERATURE AND PRECIPITATION IN THE 30 YEAR PERIOD IN NITRA, SLOVAKIA

Vladimír KIŠŠ[1], Andrej Tárník[1], Slavomír Hološ[1,2], Jakub Pagáč[1]

[1]Slovak Agriculture University in Nitra, SLOVAKIA

[2]Institute of Hydrology, Slovak Academy of Science, SLOVAKIA

Abstract

The climate change is here and is all around us. It influences every part of landscape ecosystems. Air temperature and precipitation are the most essential indicator of the climate change. This paper brings the analysis of air temperature and precipitation trend in period of the last three decades for locality Nitra, Slovakia. Yearly averages were compared with long term climatic normal 1991-2020. We can observe increasing trend of air temperature in the last period clearly. This trend is significant in the last decade mainly. Even every year was warmer than long term climatic normal. Changes in temperature also caused increase of extreme situation incidence (summer, tropical and super tropical days and tropical nights). Decline of precipitation is not significant as we expected. On the other hand data shows changes in time variability of rainfall events. Main part of precipitation was moved to winter season. Summer season brings lack of rainfall events. Some changes may look favourable but we have to be really careful when we evaluate them.

Keywords: air temperature, precipitation, climate change, climate indices

Introduction

Recent findings of changing climate, water scarcity, soil degradation, and greenhouse gas emissions have brought major challenges to sustainable agriculture worldwide (Horák et al., 2021). Regarding the general climate change effect in Europe, the temperature of the European continent has risen on average by 1.2 °C over the last century and 0.45 °C over the last three decades. The trend in the rise of average temperature has been around 0.1 °C per 10 years across Europe over the last century; however, it has more than doubled in the last thirty years. The Central European region also shows general signs of climate change (Čimo et al., 2020). There is a growing consensus that high temperature extremes have increased more rapidly than the regional mean in central Europe (Jézéquel et al., 2020). Lack of precipitation influencing drought propagation in the basin, including the availability of data on hydro-meteorological factors, groundwater, and major human activities that might influence the water cycle in the region (Karamuz et al., 2021). Managing water-human systems in times of water shortage and droughts is key to avoid overexploitation of water resources, particularly for groundwater, which is a crucial water resource during droughts sustaining both environmental and anthropogenic water demand (Wendt et al., 2021).

Climate is more than just temperature and precipitation. It is a spectrum of climate indicators that describe the climate, such as hot days and frost days, and serve to illustrate how the climate is changing. Climate indicators are parameters that are derived from meteorological measurement data, such as temperature and precipitation (MeteoSwiss, 2021).

Material and methods

Locality

Meteorological data were used from the Nitra station (48°18´09” 18°05´58”) owned by the Department of Biometeorology and Hydrology of the Slovak University of Agriculture. The area is classified as warm to very warm. Average annual temperatures range from 7.5 to 10.0 ° C. The average annual rainfall ranges from 500 to 800 mm. The Nitra area generally belongs to the precipitation deficit area (Hreško et al., 2006; Korec, Popjaková, 2019).

Data analysis

Climatic normal serve as a benchmark against which recent or current observations can be compared, including providing a basis for many anomaly-based climate datasets. They are also widely used, implicitly or explicitly, as a prediction of the conditions most likely to be experienced in a given location (WMO, 2017). Averages of climatological data for Nitra locality

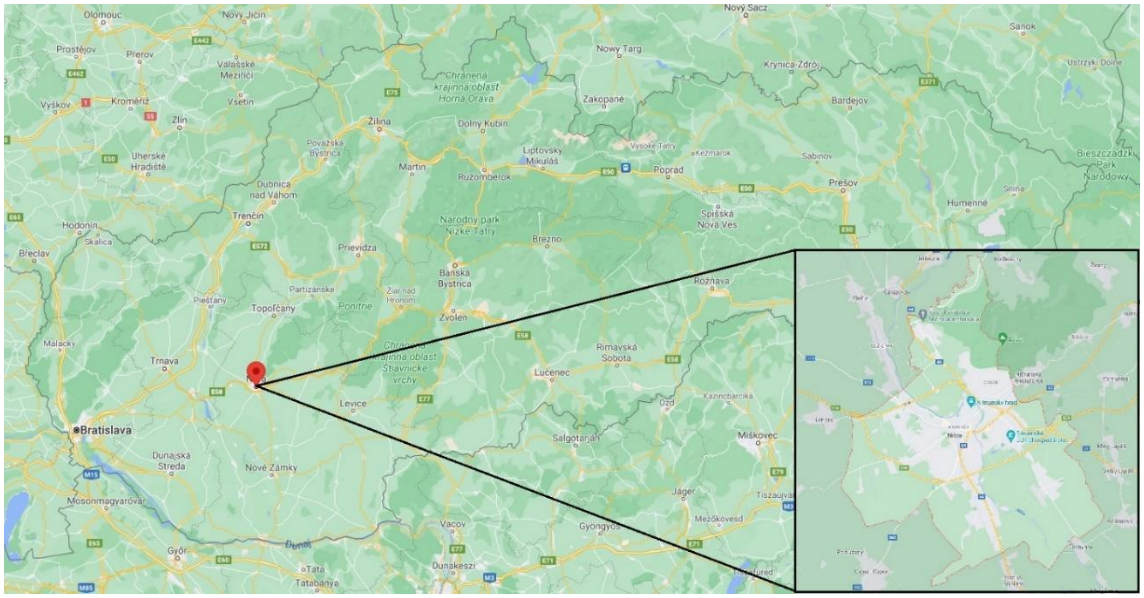

Figure 1 Nitra locality (Google Maps, 2021)

was computed for the following consecutive periods of 30 years: 1 January 1991 – 31 December.

The analysis of temperature conditions is based on the number of days with characteristic air temperatures - frost days (T_{min} ≤ 0.0 °C), ice days (T_{max} ≤ 0.0 °C), summer days (T_{max} ≥ 25.0 °C), tropical days (T_{max} ≥ 30.0 °C), tropical nights (T_{min} ≥ 20.0 °C) and super-tropical days (T_{max} ≥ 35.0 °C). The distribution of precipitation was divided according to the number of days with precipitation above 0.1 mm, the number of days with precipitation above 1.0 mm and the number of days with precipitation above 10.0 mm (WMO et al., 2009).

The determination of the period with the onset of great vegetation period and main vegetation period (mean daily temperatures ≥ 5 °C and ≥ 10 °C) was calculated according to formulas (Čimo et al., 2012):

- onset of temperatures: $r_v = R\frac{T_n - T_2}{T_1 - T_2}$ (days) (1)

- termination of temperatures: $r_p = R\frac{T_1 - T_u}{T_1 - T_2}$ (days) (2)

Where:

T_n – onset temperature (°C),

T_u – termination temperature (°C),

T_1 – the nearest average monthly temperature above the onset or termination of temperature (°C),

T_2 – the nearest average monthly temperature below the onset or termination of temperature (°C),

R – the difference in days between the middle of the months with the average temperature T_2 and the average temperature T_1, can be expressed as an average number R = 30,

r_v – difference in days between the middle of the month with temperature T_2 and the date of onset of temperature T_n,

r_p – difference in days between the middle of the month with temperature T_2 and the date of termination of temperature T_u.

Results and discussion

When we want to evaluate climate and its changes we have to analyse 30 years at least. Data from 1991 to 2020 was analysed in this paper. Many discussions are about air temperature changing mainly. However climate change has impact also on precipitation in the central Europe region.

Figure 2 shows running of annual precipitation and average air temperature in comparison with climatic normal. Our data confirm well known trend of climate change also for western Slovak region. Count of years with precipitation below the climatic normal increase in last decade. Another problem with precipitation is their time layout changes. Number of rainfall events increase in winter season in contrast with summer season (Figure 4).

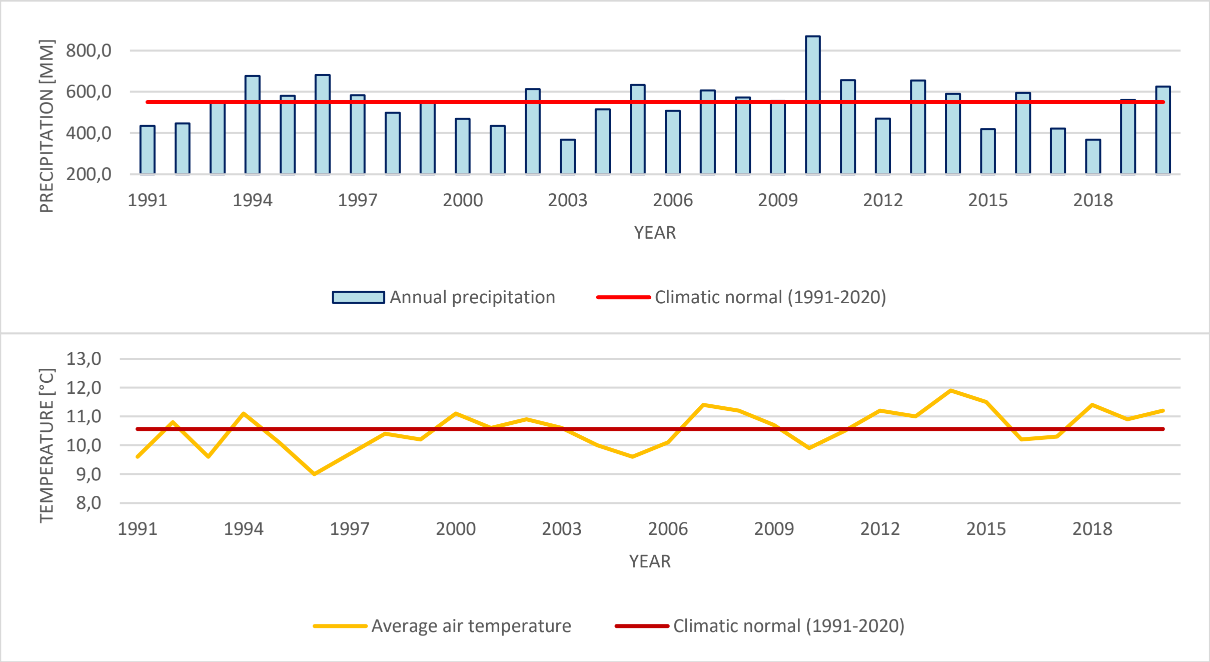

Figure 2 Annual precipitation in comparison with climatic normal (up), average annual air temperature in comparison with climatic normal (down)

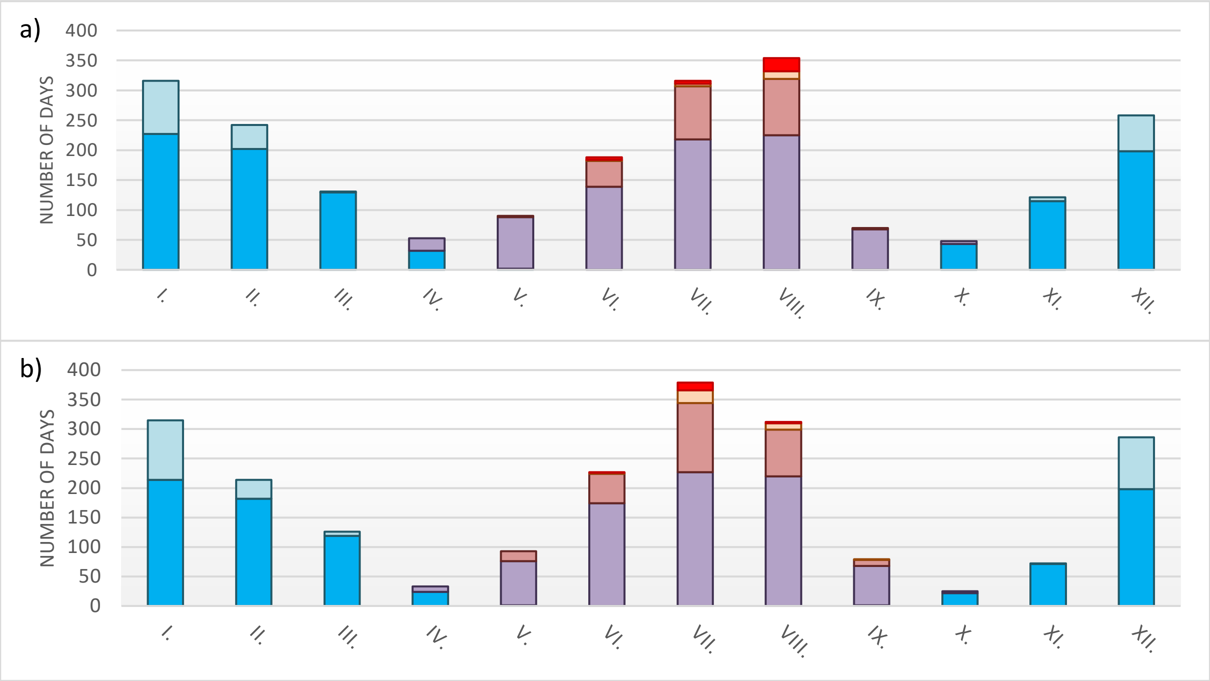

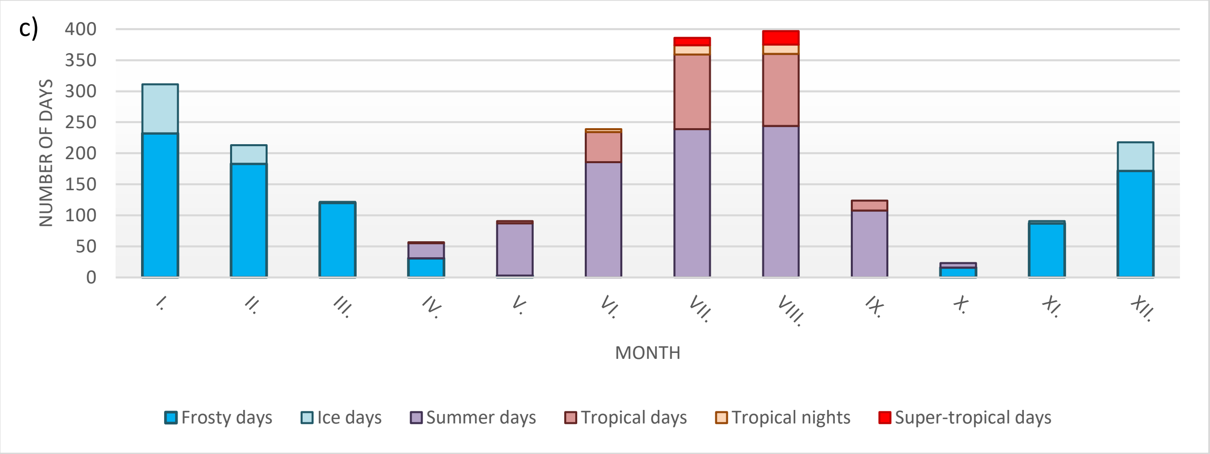

Figure 3 Number of days with characteristic air temperature per decades: a) 1991-2000, b) 2001-2010, c) 2011-2020

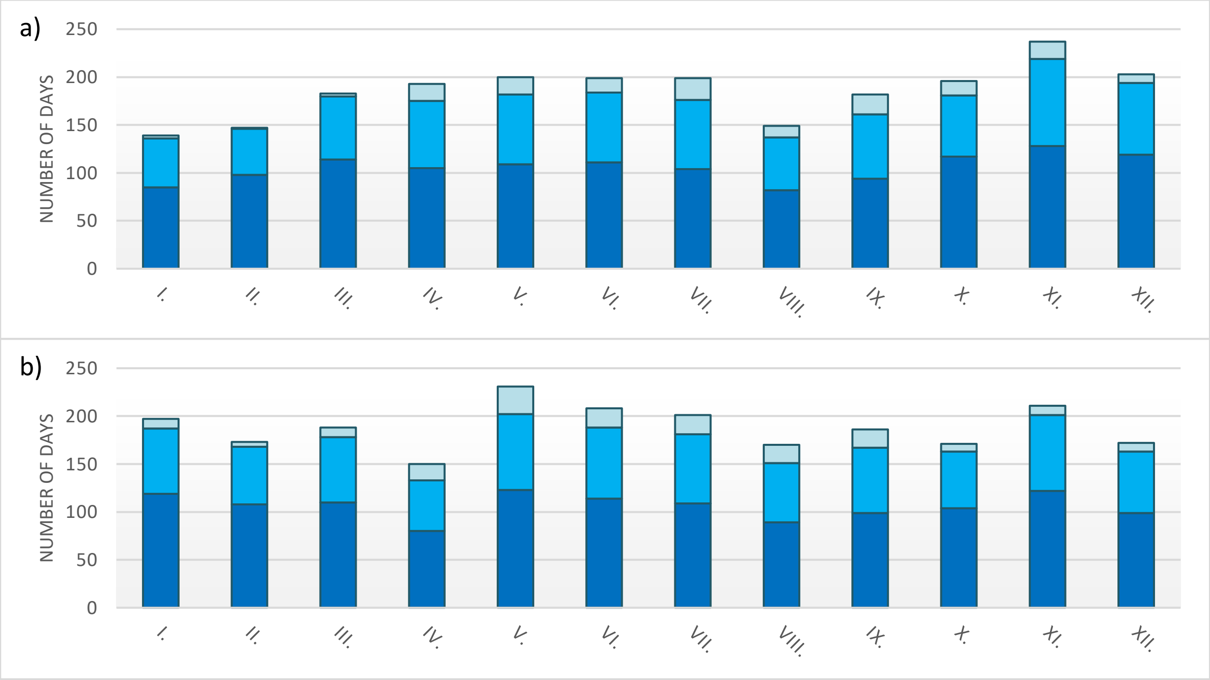

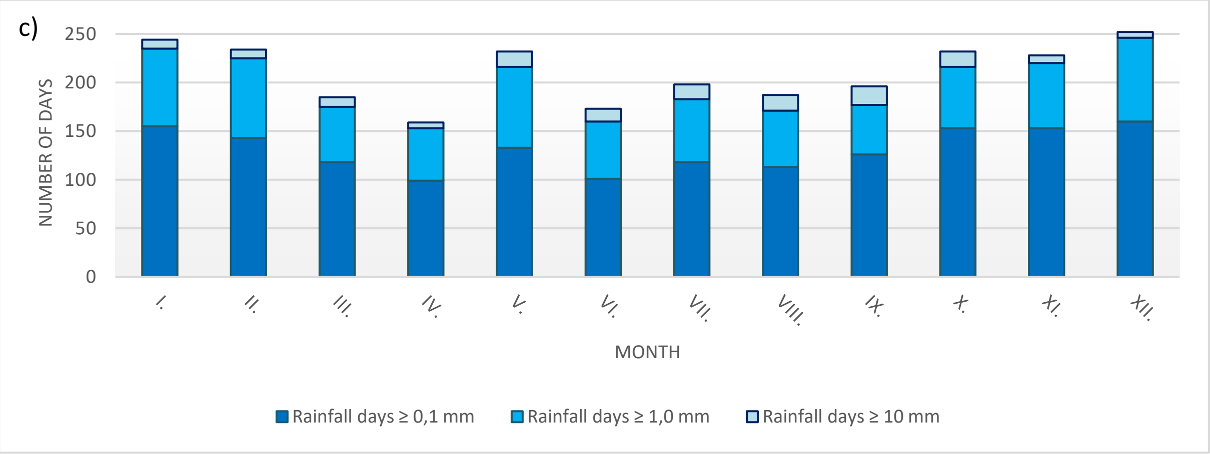

Figure 4 Number of days with characteristic amount of precipitation per decades: a) 1991-2000, b) 2001-2010, c) 2011-2020

Another demonstration of climate change is growth of extreme temperature situation. Figure 3 shows trend of incidence of frost, ice, summer, tropical and super tropical days and tropical nights during three analysed decades. Hot days (summer, tropical and super tropical) occur more often in last decade. Also period of their occurrence is longer (increase in April and October). We can observe also tropical nights more often, mainly in June, July and August.

As we mentioned above, we can observe changes in time variation of precipitation. Figure 4 shows number of days with characteristic amount of precipitation per decades. We can see trend of more numerous rainfall events in winter season clearly (December, January and February). There were more than 250 days with precipitation in December of 2011-2020 decade compared with 200 days in decade 1991-2000. Even more pronounced increase of rainfall days can be observed in January and February. There were less than 150 days in January, approximately 150 days in February respectively in decade 1991-2000 compared to decade 2011-2020 where were almost 250 days in both months.

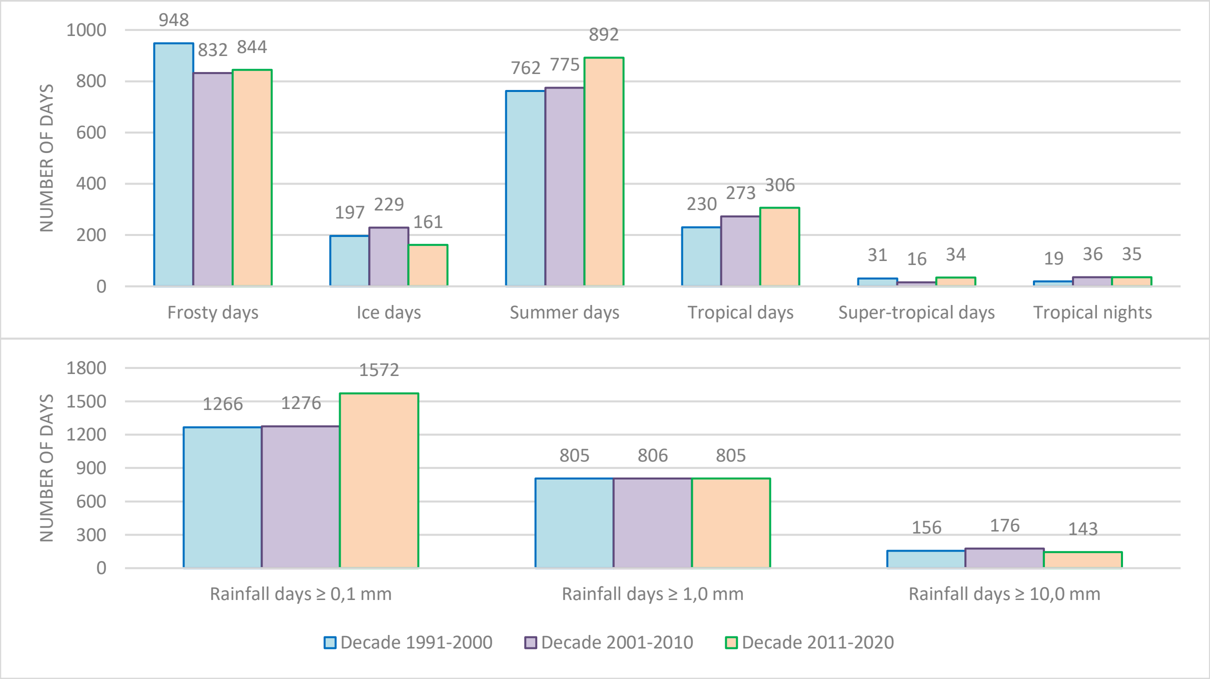

Figure 5 Comparison of summary of days with characteristic air temperature per decades (up), comparison of summary of days with characteristic amount of precipitation per decades (down)

The air temperature is rising definitely. We are able to observe decreasing trend of frosty and ice days occurrence and on the other there is increasing trend of summer, tropical and super tropical days and tropical nights occurrence recognizably. Number of days with characteristic rainfall is not changing in last three decades significantly. Summaries of days with characteristic air temperature and days with characteristic amount of precipitation per decades show Figure 5.

Changes of temperature also caused changes of vegetation period. Table 1 shows average duration of the great vegetation period and the main vegetation period per decades in comparison with climate normal 1951 - 2000. We can observe extension of great and also main vegetation period during last three decades, mainly in two last one.

Climate changes consequences are undesirable and really very quick. On the other hand, extension of vegetation period brings new possibilities for agricultural practice. But we have to be still very careful, because these changes can constitute risk and unknown consequences.

Table 1 Average duration of the great vegetation period and the main vegetation period per decades in comparison with climate normal 1951 - 2000

Period	Onset GVP (date)	Termination GVP (date)	Duration (days)	Onset MVP (date)	Termination MVP (date)	Duration (days)
1951-2000	16.3.	13.11.	243	13.4.	16.10.	187
1991-2000	16.3.	14.11.	244	11.4.	16.10.	189
2001-2010	11.3.	20.11.	255	11.4.	20.10.	193
2011-2020	7.3.	20.11.	259	13.4.	22.10.	193

Many authors deal with climate change, which includes temperature changes and changes in the distribution of precipitation during the year. Burić et al. (2013) found out that the number of hot days in Montenegro has been increasing since the 1980s. Unkašević et al. (2013) analysed the extreme temperature indices and suggested that the Serbian climate generally tended to become warmer in the last 61 years. The most significant temperature trends were revealed for the summer season. Popov et al. (2017) analysed the annual number of frost days in Bosnia and Herzegovina and suggests that a decreasing trend has become more pronounced since 1990s and particularly since the beginning of the 21st century.

Repel et al. (2021) show that there have been no significant changes in the total annual precipitation in Slovakia. There has also been no significant increase in extreme precipitation events, which have been observed in the past as well as now. In our study for Nitra station, we observed the same results for total annual precipitation, but throughout the year is the distribution of precipitation is uneven. Decrease of days with precipitation at the beginning of the vegetation period is considerable. Ionita et al. (2020) in their study show that the period 2007–2020 was characterized by a reduction of ~50% of the usual April rainfall amount over large areas in central Europe. The precipitation deficit and the record high temperatures were triggered by a multiyear recurrent high-pressure system centred over the North Sea and northern Germany and a decline in the temperature gradient between the Arctic region and the mid-latitudes, which diverted the Atlantic storm tracks northward.

Conclusions

Climate change is the most important environmental task of nowadays. It has impact on every sphere of our life. We have to try to mitigate changes as much as possible. Climate change affects mainly air temperature and precipitation in central Europe region. These meteorological elements have significant effect for agriculture and landscape. We can observe increase of hot days and changes in time variation of precipitation clearly in last three decades. These changes have impact on environmental processes as well as on landscape. We have to study these changes and trying to give solutions for sustainable future.

Acknowledgment

This publication was supported by the Operational Programme Integrated Infrastructure within the project: Sustainable smart farming systems taking into account the future challenges 313011W112, co-financed by the European Regional Development Fund.

References

BURIĆ, D. et al., 2013. Recent trends in daily temperature extremes over southern Montenegro (1951-2010). In Natural Hazards and Earth System Sciences, vol. 1, no. 5, pp. 5181 – 5198. DOI: 10.5194/nhessd-1-5181-2013.

ČIMO, J. et al. 2012. Praktická biometeorológia. SPU: Nitra. 201 p. ISBN 978-80-552-0771-1 (in Slovak).

ČIMO, J. et al., 2020. Change in the Length of the Vegetation Period of Tomato (Solanum lycopersicum L.), White Cabbage (Brassica oleracea L. var. capitata) and Carrot (Daucus carota L.) Due to Climate Change in Slovakia. In Agronomy, vol. 10, no. 8. DOI: 10.3390/agronomy10081110.

HORÁK, J. et al., 2021. A Sustainable Approach for ImprovingSoil Properties and Reducing N_2O Emissions Is Possible through Initialand Repeated Biochar Application. In Agronomy, vol. 11. DOI: 10.3390/agronomy11030582.

HREŠKO, J. et al. 2006. Krajina Nitry a jej okolia: Úvodná etapa výskumu. UKF. Nitra. 182 p. ISBN 80-8094-066-5 (in Slovak).

IONITA, M. et al., 2020. On the curious case of the recent decade, mid-spring precipitation deficit in central Europe. In npj Climate and Atmospheric Science, vol. 3, no. 49, pp. 1-10. DOI: 10.1038/s41612-020-00153-8.

JÉZÉQUEL, A. et al., 2020. Conditional and residual trends of singular hot days in Europe. In Environmental Research Letters, vol. 15, no 6, pp. 1-11. DOI: 10.1088/1748-9326/ab76dd.

KARAMUZ, E. et al., 2021. Is It a Drought or Only a Fluctuation in Precipitation Patterns?—Drought Reconnaissance in Poland. In Water, vol. 13, no. 6. DOI: 10.3390/ w13060807.

KOREC, P. – POPJAKOVÁ, D. 2019. Priemysel v Nitre: globálny, národný a regionálny kontext. UK: Bratislava. 2018 p. ISBN 978-80-223-4829-4 (in Slovak).

METEOSWISS, 2021. Hot days, frost days and other climate indicators [online][cit. 2021-05-08]. Available on internet: <https://www.meteoswiss.admin.ch/home/climate/climate-change-in-switzerland/hot-days-frost%20days-and-other-climate-indicators.html>.

POPOV, T. et al., 2017. Trends in frost days in Bosnia and Herzegovina. In Glasnik Srpskog Geografskog Drustvam, vol. 97, no. 1, pp. 35-55. DOI: 10.2298/GSGD1701035P.

REPEL, A. et al., 2021. Long-Term Analysis of Precipitation in Slovakia. In Water, vol. 13, no. 7, pp. 1-13. DOI: 10.3390/w13070952.

UNKAŠEVIĆ, M. – TOŠIĆ, I. 2013. Trends in temperature indices over Serbia: Relationships to large-scale circulation patterns. In International Journal of Climatology, vol. 33, no. 15. DOI: 10.1002/joc.3652.

WENDT, D. E. et al., 2021. Demonstrating the impact of integrated drought policies on hydrological droughts. In Natural Hazards Earth System Science [preprint]. DOI: 10.5194/nhess-2021-129.

WORLD METEOROLOGICAL ORGANIZATION (WMO) et al. 2009. Guidelines on Analysis of extremes in a changing climate in support of informed decisions for adaptation. WMO. Geneva. 52 p. WMO/TD- No. 1500; WCDMP- No. 72.

WORLD METEOROLOGICAL ORGANIZATION (WMO) et al. 2017. Guidelines on the Calculation of Climate Normals. WMO. Geneva. 29 p. WMO-No. 1203. ISBN 978-92-63-11203-3.

Contact address

Ing. Vladimír Kišš, PhD., Slovak University of Agriculture in Nitra, Faculty of Horticulture and Landscape Engineering, Department of Biometeorology and Hydrology, Hospodárska 7, 949 76 Nitra, Slovakia, +421 37 641 5247, vladimir.kiss@uniag.sk

POSTER SECTION

Electrification of the small-scale forwarder – a case study

Ondřej Nuhlíček, Václav Štícha

Faculty of Forestry and Wood Sciences, Czech University of Life Sciences Prague, Kamýcká 129, 165 00 Praha 6, Czech Republic.

Introduction

The general trend in reducing fossil fuel use is generating an increasing demand for alternative energy sources (DOE, 2007; Nitsch, 2008; Noll and Jirjis, 2012). Biomass as an energy source is considered one way of achieving carbon neutrality (Schlamadinger and Spitzer, 1995; Schlamadinger et al., 1995, 1997; Schlamadinger and Marland, 1996; Ferrero et al., 2011). Biomass from logging residues in forests may help carbon neutrality compared with the use of fossil fuels. Still, the use of fast-growing short-rotation coppice (SRC) on otherwise difficult to use land seems much more beneficial (Zanchi et al., 2011). Short-rotation coppice plantations of the Czech Republic's private owners are commonly about 1-2 hectares large (Štícha, 2019). For such area, the use of specialized harvester is not rentable and therefore prevailing machinery is agriculture tractor with trailer combined with moto manual felling. Tractors are usually overpowered for such task, as the plain terrain does not require their off-road abilities, nor does the operator need such a carry capacity. They are too large for work in the typical spacing of the SRC. These factors lead to underperformance in terms of productivity, fuel consumption and, therefore, too large carbon footprint, which mitigates the effect of growing the SRC in the first place.

Aim of the research

With the rapid development of electromobility, commercial parts are becoming available for building custom machines.

The aim of this research is the design, manufacture and testing of the small electric machine, which would allow:

- Easy use in conditions of the SRC plantations, namely, to be able to go between the tree lines, which are usually set 1.5 meters apart
- Modularity for repurposing the machine for other tasks needed on small agriculture properties
- It could be used in small scale forestry and sanitary fellings
- It would be ergonomic and efficient for the operator walking with it – no need to embark and disembark as with a typical tractor.

From these goals, technical requirements were set:

- Maximum width of 150 cm, preferably 90 cm
- Maximum wheel track width 130 cm, preferably 75 cm
- Total width of the wheels 30 cm, preferably 15 cm
- Machine carry capacity of 1000 kg
- Control of the machine by the handle in front for turning and speed control

Powertrain design

Given the required low speed and large mass, the rolling friction is the main resistance to the movement. Therefore, power requirement can be estimated using a simplified equation:

$$Ft = \xi * Fn/R$$

Where: Ft – rolling friction
ξ – rolling friction coefficient (Tire at asphalt- 0.0045, with use on the offroad surface, this coefficient rises to 20 times)
Fn – vertical force (20 kN – cargo and machine weight)
R – wheel radius (0.3m)

Given the required speed of the walking person, 1kW of power is required for rolling resistance. With reserve for the acceleration and uphill ride, the 6 kW power requirement was set.

For basic testing, 100Ah 13S 48V Li-Pol batteries were used, with the potential for expanding the batteries up to 200Ah. Power capacity is therefore 4,8 kWh. For braking during descent, recuperation is possible.

With such a setup, expected operational time is highly dependent on the terrain conditions.

Movement of the machine is – based on the forwarder operation time studies - around 40-50 % of the shift time. In proper conditions, eight hours shift could be achieved.

Preliminary testing

As testing SRC plantations are not ready for harvest, testing was so far done only in alternative configurations with electric winch for forwarding wood from bark beetle sanitary fellings. In four stands, with different log lengths ranging from 2 to 4 meters. As a prototype testing, the only viability of such use was being evaluated. With recuperation and manual loading, the machine was able to work throughout the whole work shift, forwarding the logs on the average distance of 110 m, carrying about 13,7 m3 under bark during shift. Compared to dedicated forest tractors and forwarders, this low productivity is balanced out by less soil compaction and, due to manoeuvrability, minimal damage to the standing trees.

Potential savings

During a standard eight hour shift, with a tractor idling or moving with a maximum of 60% power output, a 50 kW tractor of the older generation consumes about 41.5 liters of diesel. (Kulovaná, 2001). For the same shift, 4.8 kWh of electric energy is available and sufficient, based on calculations and trials. The difference in the price of running such a machine for a shift, considering only the energy, is shown in Table 1.

Average shift fuel consumption (l)	41.5	4.8	Battery capacity for the shift (kWh)
		5.3	Power required for charging (+10% for charging loss) (kWh)
Diesel price (average) (€/l)	1.16	0.16	Price per kWh (average) (€/kWh)
Fuel price per shift (€)	48.14	0.85	Price per battery charge (€)

Table 1 : Difference in energy price of a diesel fueled tractor and electric forwarder machine.

Alternative configurations

Given the small scale and simplicity, this machine is highly modifiable to serve different purposes such as:

- Forwarder with delimber – with electrical winch, cut down trees of small diameter can be delimbed while being loaded on the forwarder

- IBC container carrier – with removing the side barriers from their mounting points, an IBC container or other tank can be mounted and used for spraying, watering, etc.
- Crate transporter – crate racks can be mounted on the machine for fruit harvest in smaller orchards, seedlings in nurseries, animal feedstock and others.

Conclusion, further research

The developed machine prototype suggests the possibility of small agroforestry operations electrification. It proved that terrain crossing capability, load carry capacity and battery time are sufficient for the intended purpose. As the industry of electric motors and batteries evolves, new possibilities arise. Modular design allows these new technologies to be incorporated into the machine to take advantage of the latest development. Even though complete productivity testing on SRC plantation is ahead, the crude comparison based on tractor diesel consumption and electricity price suggests possible savings – both monetary and environmental.

Long term use research is necessary to fully understand the pros and cons of the electrical forwarders, as their electrification is a novel concept.

Acknowledgement

Machine was made under the grant of the TAČR Gama TG03010020 „Aktivity Proof-of-Concept na ČZU v Praze“

Literature cited

- DOE, 2007. Roadmap for bioenergy and biobased products in the United States. Department of Energy, Washington DC.
- Ferrero, F., Malow, M., Noll, M., 2011. Temperature and gas evolution during large scale outsid
- Kulovaná, Eliška, 2001. Chcete snížit spotřebu nafty? Mechanizace zemědělství [online] [vid. 2021-04-20]. Available online: https://www.mechanizaceweb.cz/chcete-snizit-spotrebu-nafty/
- Nitsch, J., 2008. Strategy to increase the use of renewable energies. German Federal Ministry for the Environment, Nature Conservation and Nuclear Safety (BMU), Stuttgart.
- Noll, M., Jirjis, R., 2012. Microbial communities in large-scale wood piles and their effects on wood quality and the environment. Appl Microbiol Biotechnol. 95, 551–563. doi:10.1007/s00253-012-4164-3.
- Schlamadinger, B., Spitzer, J., 1995. CO2 mitigation through bioenergy from forestry substituting fossil energy. In: Biomass for Energy, Environment, Agriculture and Industry. Proceedings of the 8th European Biomass Conference, Vienna, Austria, 3–5 October 1994, 1 (eds Chartier, P., Beenackers, A.A.C.M., Grassi, G.), 310– 321. Oxford, Pergamon.
- Schlamadinger, B., Canella, L., Marland, G., Spitzer, J., 1997. Bioenergy strategies and the global carbon cycle. Sci. Geol. Bul. 50, 157– 182.
- Schlamadinger, B., Marland, G., 1996. The role of forest and bioenergy strategies in the global carbon cycle. Biomass. Bioenerg. 10, 275–300. https://doi.org/10.1016/0961-9534(95)00113-1.
- Schlamadinger, B., Spitzer, J., Kohlmaier, G.H., Lüdeke, M., 1995. Carbon balance of bioenergy from logging residues. Biomass. Bioenerg., 8, 221– 234.
- Štícha, Václav, 2019. Elektrický vyvážecí stroj usnadní soustřeďování slabšího dříví v porostech. Živá univerzita. 6–7.
- Zanchi, G., Pena, N., Bird, N., 2012. Is woody bioenergy carbon neutral? A comparative assessment of emissions from consumption of woody bioenergy and fossil fuel. GCB Bioenergy. B.m.: John Wiley & Sons, Ltd (10.1111), 4(6), 761–772. ISSN 17571693. doi:10.1111/j.1757-1707.2011.01149.xe storage of wood chips. Eur. J. Wood Prod. 69, 587.https://doi.org/10.1007/s00107-010-0512-0.

Contact information

Ondřej Nuhlíček, Email: nuhlicek@fld.czu.cz

Faculty of Forestry and Wood Sciences, Czech
University of Life Sciences Prague, Kamýcká
129, 165 00 Praha 6, Czech Republic

Identification of the successfully reproduced individuals of spruce bark beetles *Ips typographus* in the windfall area of Smrčina.

Czech University of Life Sciences Prague
Faculty of Forestry and Wood Sciences

Doctorant: Ing. Stepan Raevsky
Superviser: prof. Ing. Marek Turčáni, Ph.D.

VEDA MLADÝCH 2021

Introduction:

Figure 1. The Šumava National Park in the Czech Republic

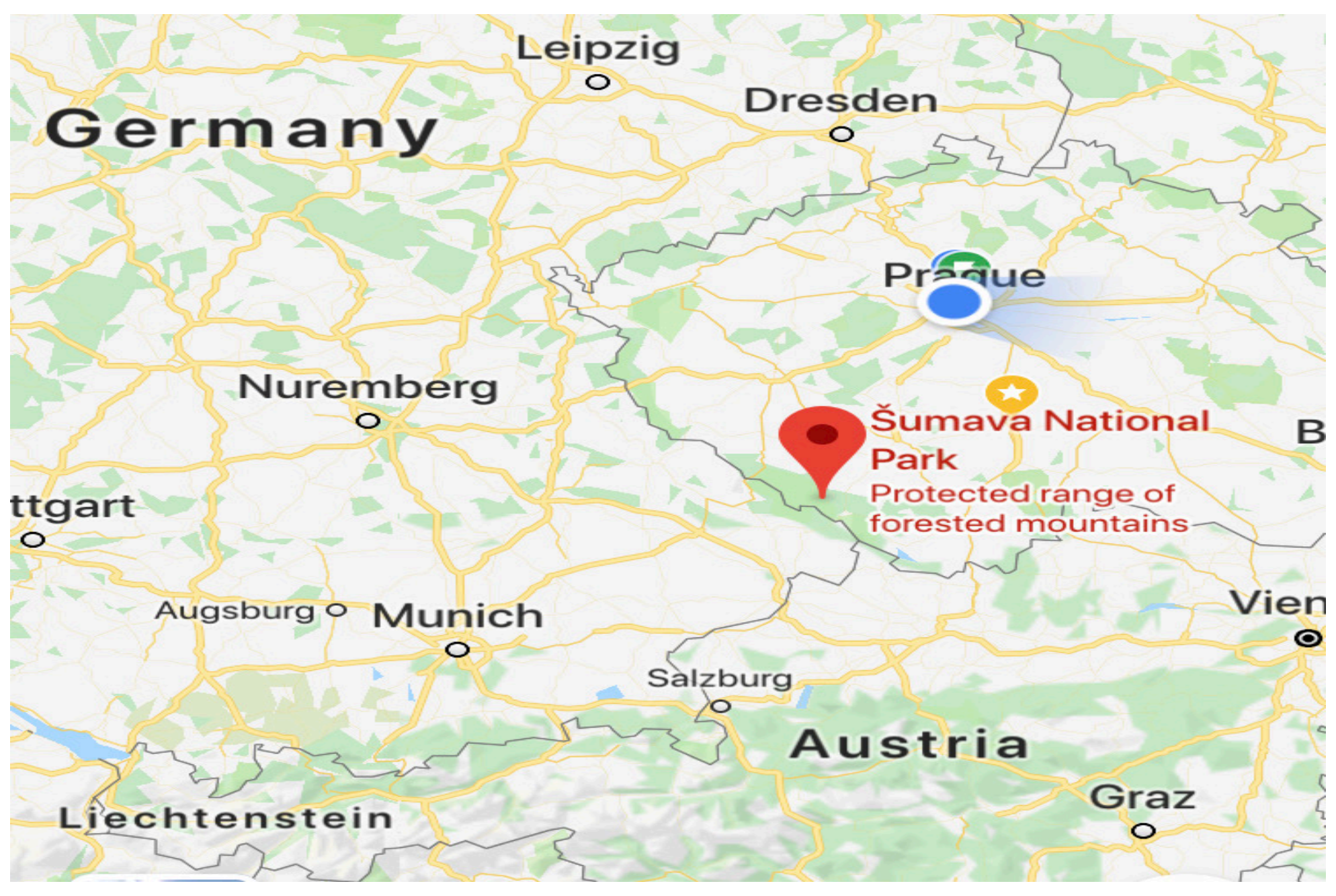

The area of Smrčina is the spruce forest on the Šumava National Park in the Czech Republic (Fig. 1).

- **Mountain spruce forests were strongly affected by natural disturbances.**
- **The fallen by wind spruce trees have a lower defense against bark beetles attack and easily accessible source to the future outbreaks of *Ips typographus* (L.).**
- **Population density of spruce bark beetles will increase above the threshold necessary for colonization of apparently healthy standing trees, accompanied by the emergence of outbreaks.**

Main Goals:

- **Determining the reproduction of spruce bark beetles in the windfall.**
- **Test the remote sensing method to assess the spread of spruce bark beetle at tree level.**
- **To monitor the development of spruce bark beetles in connection with the accumulation of windfall.**

Methodology:

- **Creation of a map, which describes the measures of the trees, height and width (Fig. 2 - 3).**
- **Scanning of the monitored area high spatial resolution data, using UAV.**
- **An ultra-high-resolution ortho-photo image will be produced which, together with a 3D point cloud, allows automatic detection of individual trees.**

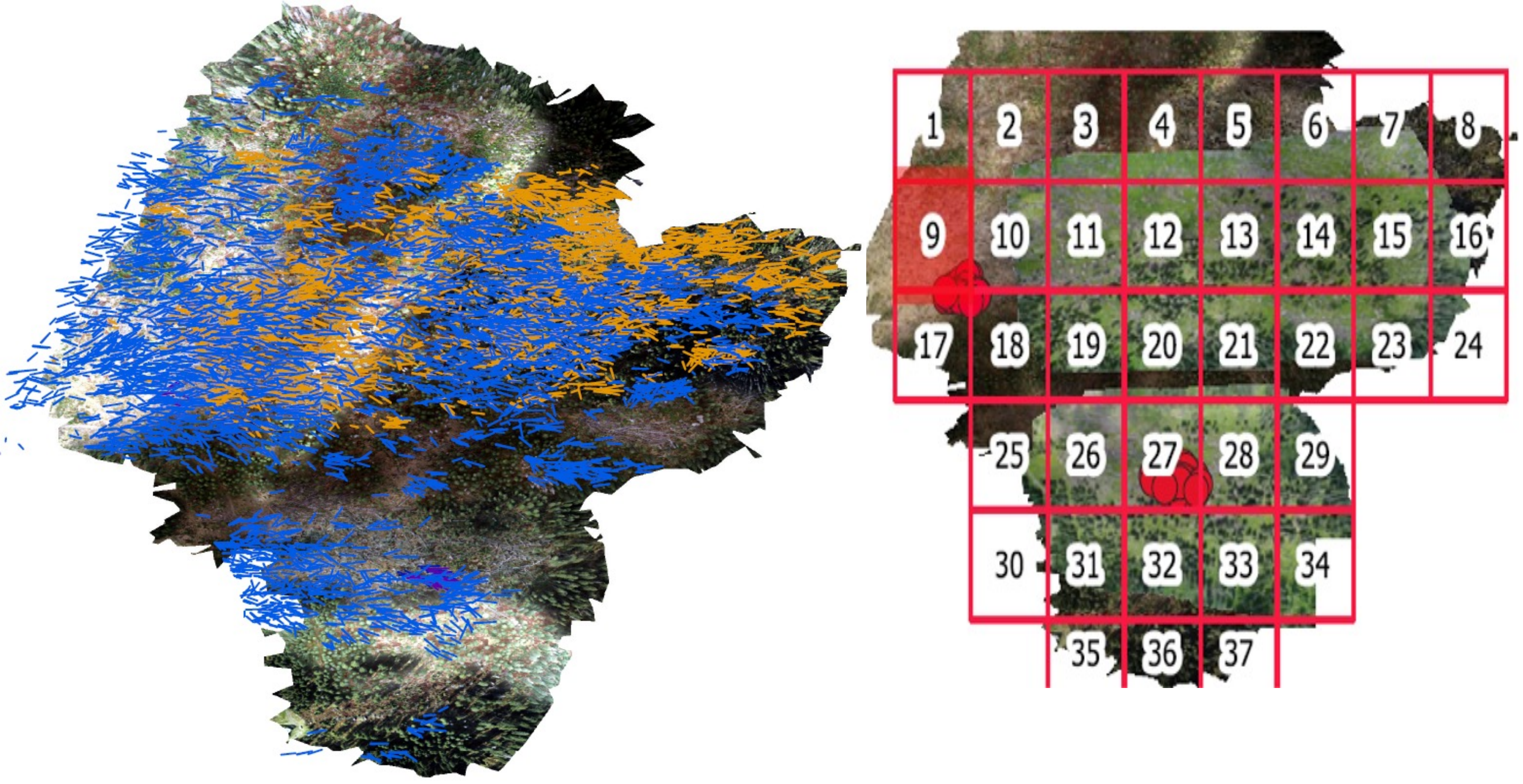

Figure 2. Map of marked windfall spruce trees in the area of Smrčina in the Šumava National Park.

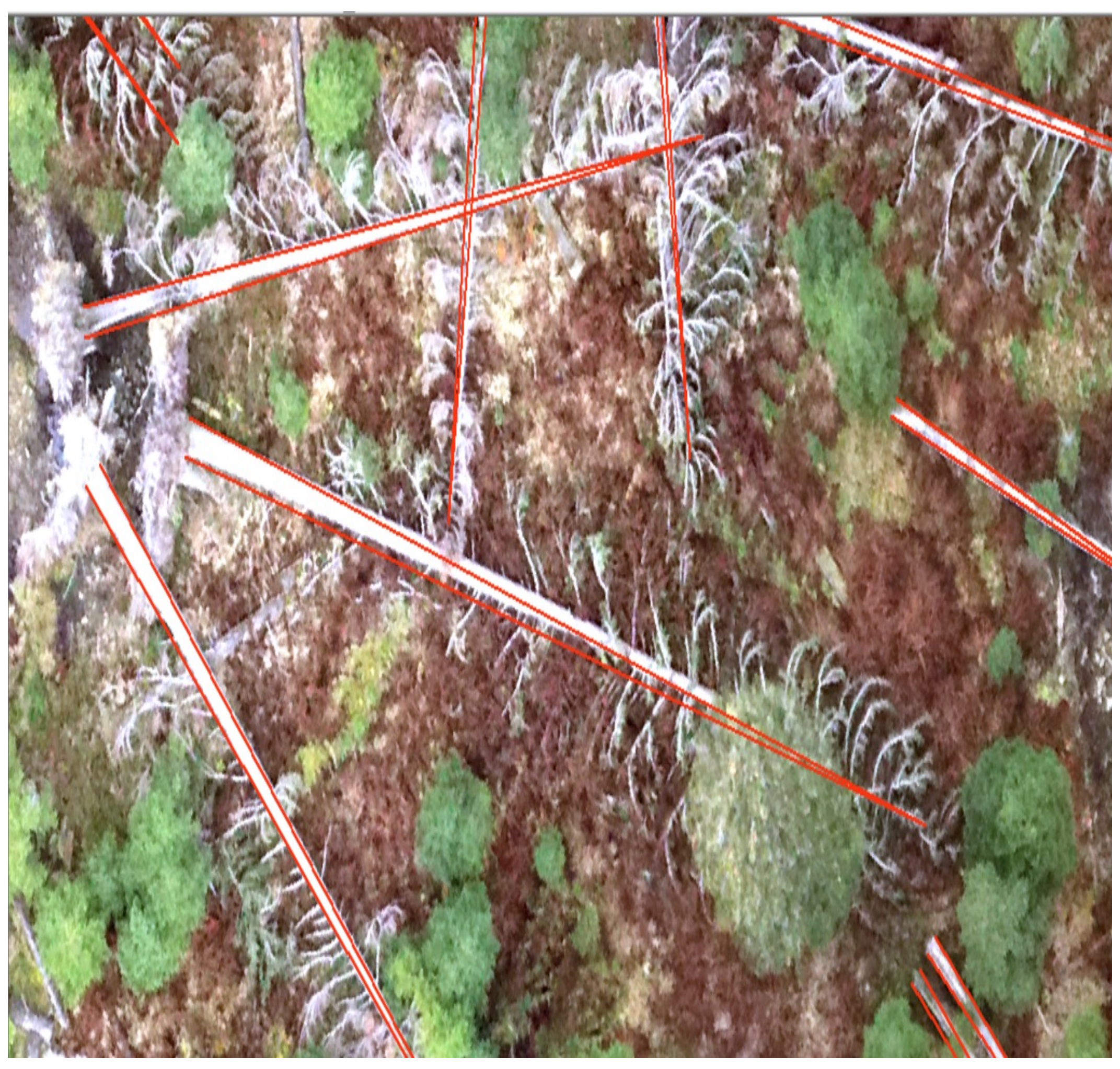

Figure 3. Marking the fallen by wind trees, give us the way to measure hight and width. zoom 1:150

Results:

As a result was build the map of the successfully reproduced individuals of spruce bark beetles, during the seasons 2018 -2020 (Fig. 4 - 5).

Figure 4. Monitoring of the new generation and produced idividuals of *Ips typographus* (L.).

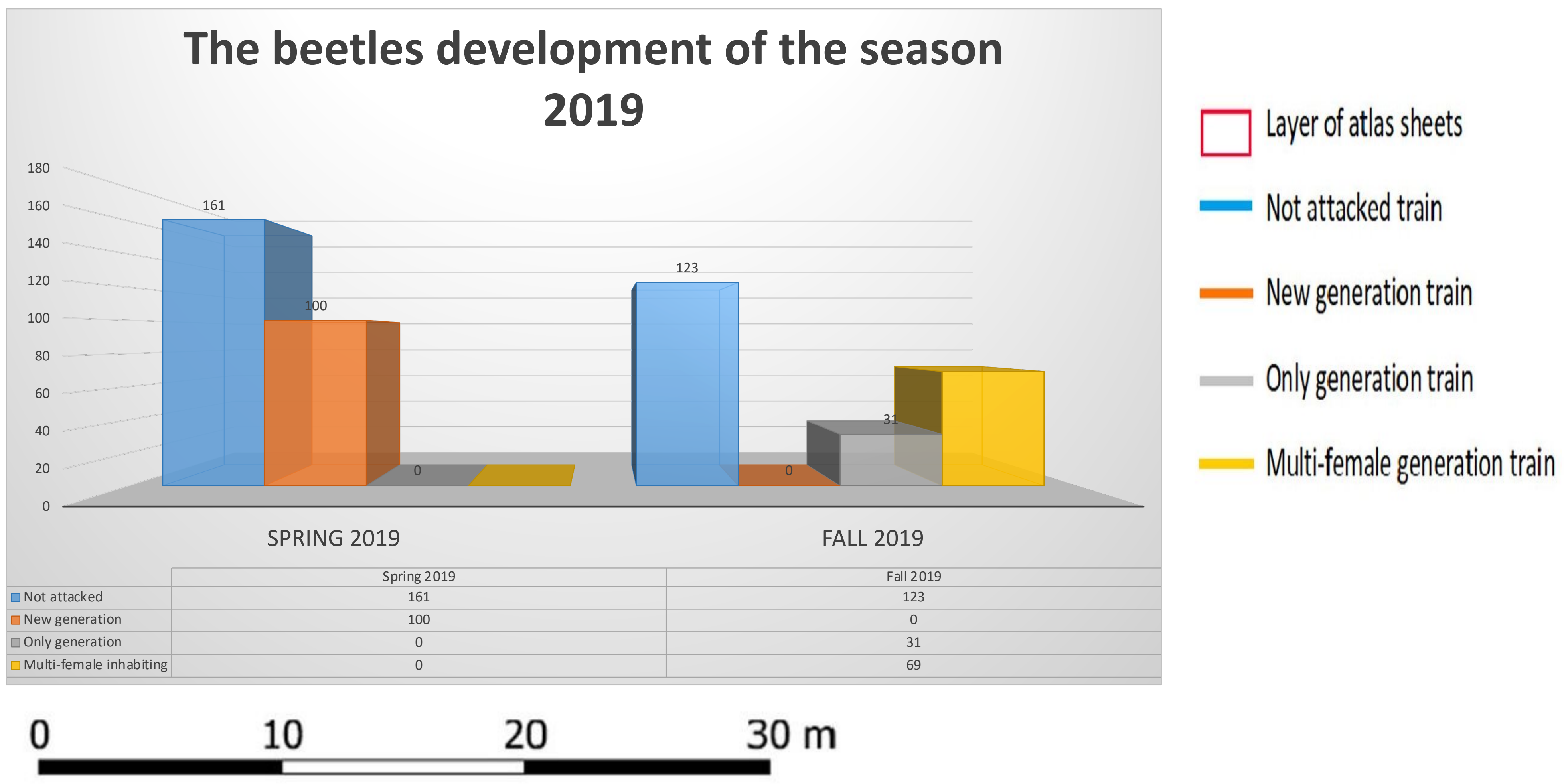

	Spring 2019	Fall 2019
Not attacked	161	123
New generation	100	0
Only generation	0	31
Multi-female inhabiting	0	69

Figure 5. The successful development produced idividuals of *Ips typographus* (L.).

ACKNOWLEDGEMENT :This research was supported by the EU project "EXTEMIT - K", No. CZ.02.1.01/0.0/0.0/15_003/0000433 financed by OP RDE.

Impact of pathogens on fitness of *Ips typographus* and *Ips amitinus* (Coleoptera: Curculionidae)

Schovánková J.

Department of Forest Protection and Game Management, Faculty of Forestry and Wood Sciences, Kamýcká 129,
CZ-16500 Praha 6-Suchdol, Czech Republic

Introduction

The aim of study is to determine how pathogens of beetles affect the establishment of reemerging, especially how *Mattesia schwenkei* attacking fat body affects the flight of beetles.

Ips typographus

X

Ips amitinus

X

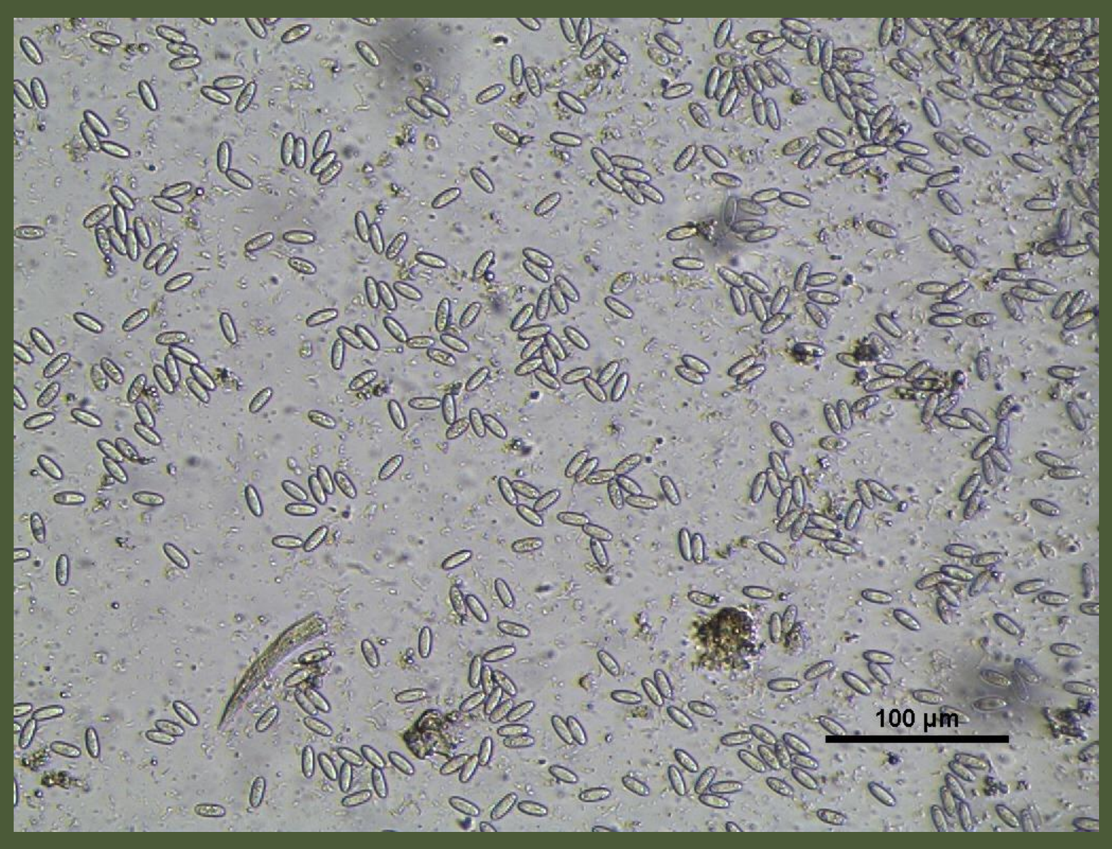

Mattesia schwenkei

- two serious pests of spruce in Europe
- they have similar bionomics
- ? what about their reemerging with pathogens ?

Material and Methods

- logs infested by beetles imported from Krkonoše mountains in Czech Republic in June 2016 - 2020
- part of the logs placed into rearing box in laboratory (constant temperature 25 °C and L/D = 16/8), another logs placed in the field
- specially modified Eppendorf tubes attached on each enter hole for capture beetles
- beetles collected every day
- part of captured beetles placed on new logs for monitor further breeding (reemerging)
- after collecting beetles were dissected for determination of pathogens

logs in laboratory

logs in field

placing beetles on new logs (reemerging)

collecting beetles and describing enter holes

determination pathogens in laboratory

Results and Conclusions:

- in total, 1650 mature *Ips typographus* beetles and 430 of *Ips amitinus* were dissected and sex determinated
- in the field 28 % beetles of *Ips typographus* and 29,7 % beetles of *Ips amitinus* established the second brood (reemerging), laboratory: 23,7 % IT and 6,2 % IA
- spectrum of pathogens in beetles: intestinal nematodes, extraintestinal nematodes, *Gregarina typograhpi*, *Chytridiopsis typographi*, Entomopoxvirus, *Mattesia schwenkei (M.s.)*
- *M.s.* detected in 38 beetles – all beetles stayed in gallery and did not reemerged, which confirm hypothesis
- it could help forestry practice – cut down smaller number of tree traps and reduce the spread of bark beetles again

Assessment of the effect of mycorrhizae on *Gemmamyces piceae* infection

Ing. Jana Vachová
Czech University of Life Sciences Prague, Faculty of Forestry and Wood Sciences - Department of Forest Protection and Entomology
Kamýcká 129, 165 00 Prague 6 - Suchdol, Czech Republic; ruckova@fld.czu.cz

Summary

- *Gemmamyces piceae* (Borthw.) Casagr. is a significant invasive fungal pathogen of several species of the genus *Picea* [2]
- Mycorrhizal fungi improve plant growth, health and resistance to pests and diseases [1]
- Non-infested trees have a higher percentage of active mycorrhizal (AM) tips than infested trees (Wilcoxon test, α = 0.05, p = 0.0455)

Introduction

- *Gemmamyces piceae* (Borthw.) Casagr is a significant pathogen of coniferous trees belonging to the *Ascomycota* [2]
- The outbreak of the disease was first recorded in the Czech Republic in 2009 at *Picea pungens* in the Ore Mountains. Since 2014, it has started to spread significantly to another species of spruce - *Picea abies* [2]
- This pathogen attacks the buds and causes characteristic and practically unmistakable symptoms (buds swell and continue to spiral and are covered with black basal stroma of the fungus from summer) [2]

Symptoms of disease caused by *Gemmamyces piceae*

- Mycorrhizae has a positive effect on the ecosystem and health of trees [1]
- Trees with well-developed mycorrhizae show a better ability to adapt to adverse environmental conditions than trees with less developed mycorrhizae[3][4]
- Plants living in mycorrhizae are characterized by increased and better resistance to low temperatures, drought, pH changes and toxins and attack by pathogens[3][4]

Methodology

- In the autumn of 2020, 49 soil probes were taken from 6 forest stands from FA Litvínov (LČR, s.p.) in the Ore Mountains (CZ)
- Soil probes were collected from 24 infested and 25 non-infested *P. abies* individuals
- Infestation of *P. abies* was assessed based on the degree of defoliation and the incidence of disease symptoms

Detail of soil probe [4]

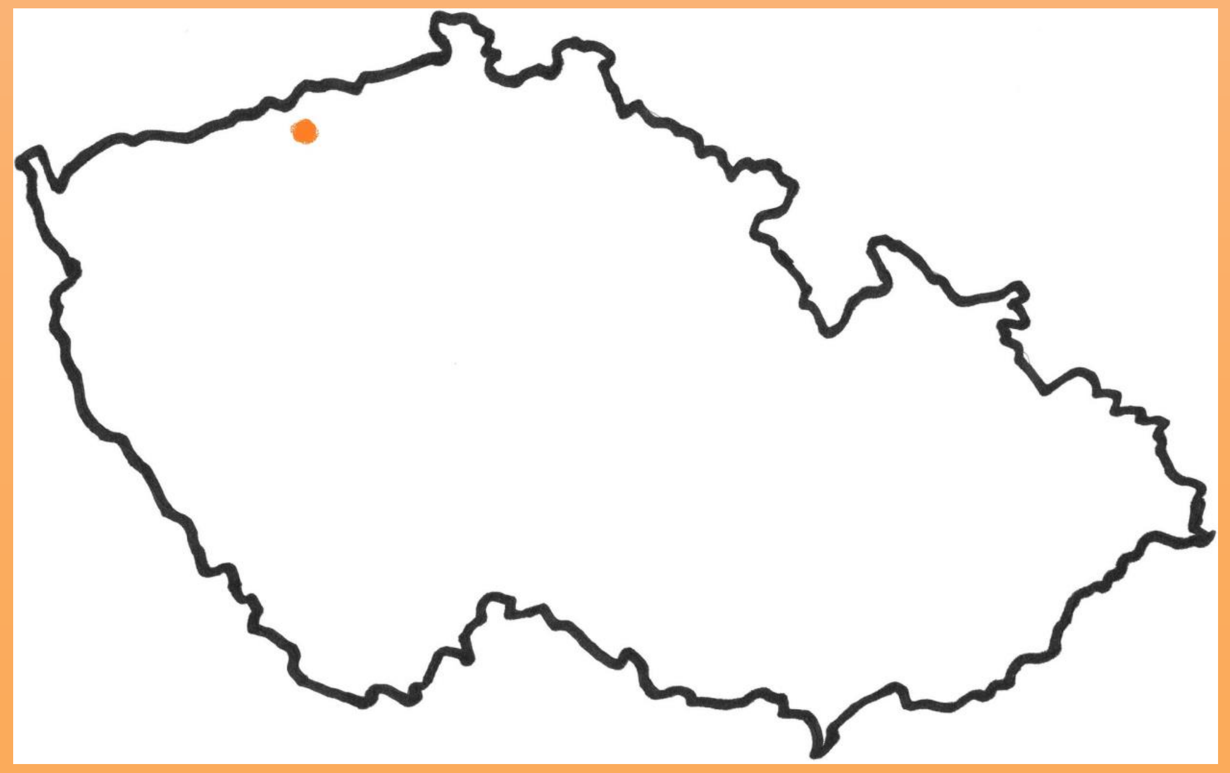

Forest Authorities Litvínov in Ore Mouintains

- Mycorrhizal conditions were evaluated on roots up to 1 mm in diameter with a basic length of 5 cm
- Active and nonactive mycorrhizal (AM and NM) tips were sorted and counted under a binocular magnifier (Olympus SZ61)

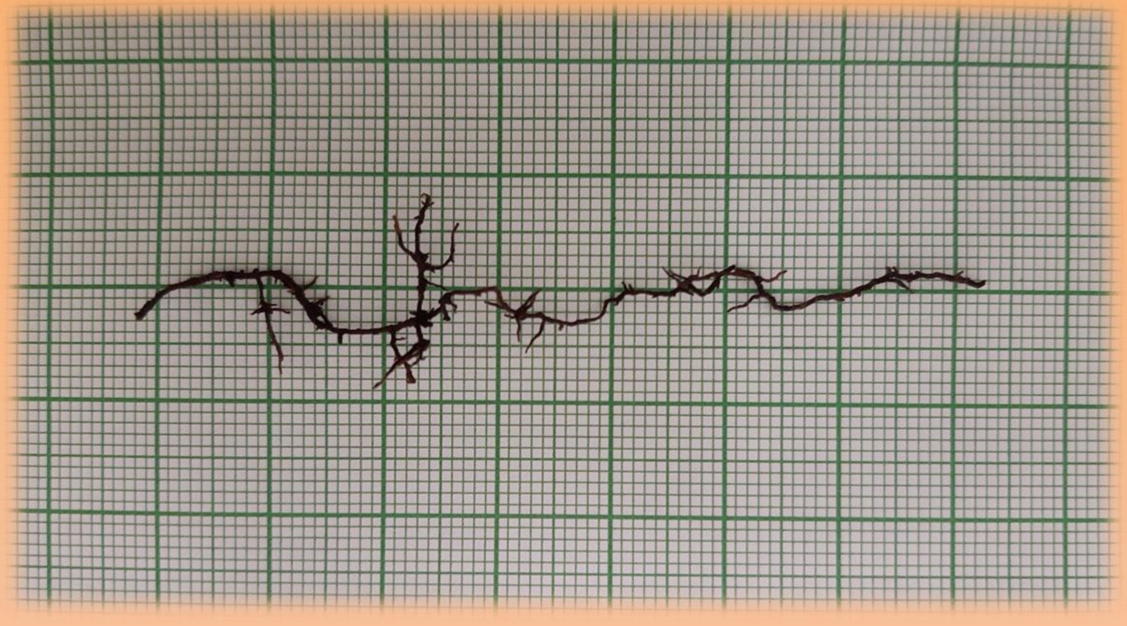

Individual root segments (up to 1 mm in diameter) from the soil probe

- According to the character of the hyphal mantle, Hartig's network and hyphae, morphotypes of AM tips were recognized, which will be analyzed by PCR - RFLP and fungi involved in mycorrhizae will be determined (during the year 2021).

Results

- The average value of the percentage of AM was 53.6 % and NM 46.4 %
- The average total density of mycorrhizal tips was 2.9, of which the density of AM was 1.6 and NM 1.4
- There was statistically significant difference between the percentage of AM in non-infested and infested trees (Wilcoxon test, α = 0.05, p = 0.0455)

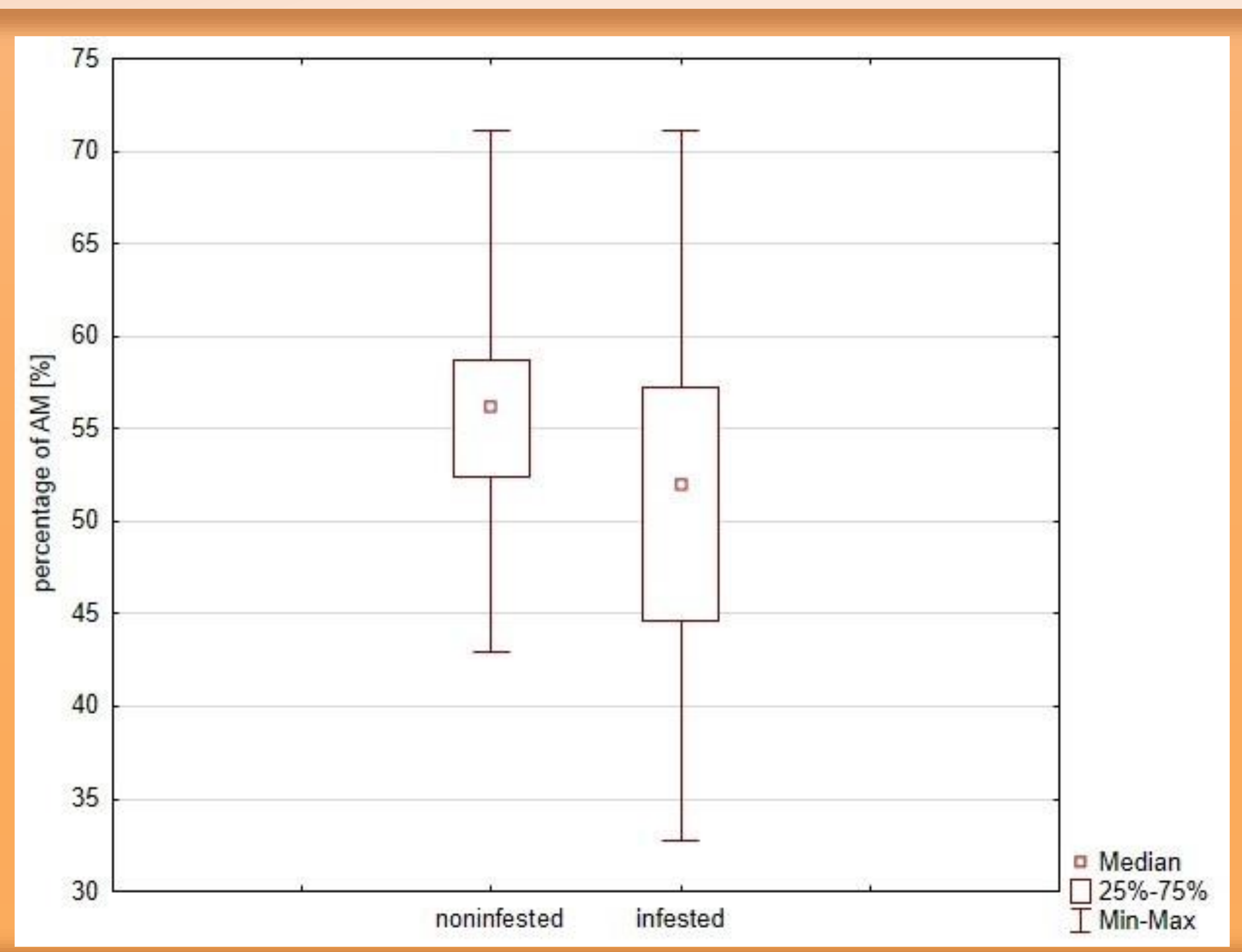

- 5 different morphotypes of active mycorrhizal tips were determined (total 154 from all samples)
- The most common were morphotype a (bulbous, thick shape and khaki green color) and morphotype b (significantly lighter yellow) tip and the rest brown)

Morphotype a

Morphotype b

Acknowledgements

IGA FFWS; doc. Ing. V. Pešková, Ph.D.; doc. Ing. I. Tomášková, Ph.D.; Ing. M. Samek and Ing. F. Pastierovič for collecting soil probes, assessing of tree infestation and expert consultations

References

[1] Gryndler, M. 2009. Mykorhizní symbióza – o soužití hub s kořeny rostlin. In: Sborník referátů – Mykorhiza v lesích a možnost její podpory. Nakladatelství Lesnická práce, s.r.o. Kostelec nad Černými lesy. Česká lesnická společnost. s. 4 – 9. ISBN: 41 9788002021216
[2] Černý, K., Pešková, V., Soukup, F. Havrdová, L., Strnadová, V., Zahradník, D., Hrabětová, M. 2016. *Gemmamyces* bud blight of *Picea pungens*: a sudden disease outbreak in Central Europe. Plant Pathology. 65:1267-1278.
[3] Peterson R. L., Massicotte H. B., Melville H., 2004: Mycorrhizas: Anatomy and Cell Biology. – Ottawa, NRC Research Press: 173 pp
[4] Pešková, V. 2008. Houby na kořenech lesních dřevin. Mykorhizy. Lesnická práce, 87 (12): 1-4 leták.

Effect of elevated CO_2 and nitrogen supply on biometry, wood density and wood structure of young sessile oak trees (*Quercus petraea* (Matt.) Liebl.)

Janko Arsić[a,b]* , Marko Stojanović[a], Lucia Petrovičová[a,b], Jan Světlík[a,b], Jan Krejza[a,b]

CzechGlobe
Global Change Research Centre AS CR, v.v.i.

[a]Global Change Research Institute of the Czech Academy of Sciences, Bělidla 4a, 603 00 Brno, Czech Republic
[b]Department of Forest Ecology, Mendel University in Brno, Zemědělská 3, 613 00 Brno, Czech Republic
*Corresponding author: arsic.j@czechglobe.cz

MENDELU
Faculty of Forestry
and Wood
Technology

INTRODUCTION

Since the Industrial revolution, atmospheric CO_2 has increased by more than 45 %, reaching slightly above 410 parts per million (ppm) in 2018. Nevertheless, growth stimulation by eCO_2 may be limited by progressive scarcity of nutrients, in particular nitrogen. To summarize, at the same time with increase in CO_2 and nitrogen deposition, forest ecosystems will face challenges in the next few decades as plants will need to cope with warmer temperature, higher evaporative demand and as well as increases in frequency and severity of extreme droughts. Adaptation to these abrupt new conditions represents the main future challenge for the forest ecosystems, however, it is very hard to predict how the forest will respond to these simultaneous changes.

METHODOLOGY

The experiment was carried out inside two glass domes in the Bílý Kříž experimental ecological station situated in the Moravian-Silesian Beskydy Mountains (49°30'77" N, 18°32'28" E, 908 m a.s.l.). A total of 144 two-years-old sessile oak trees per glass dome were planted in 2017 following specific fertilization experimental design (Fig. 1). Each glass dome was split into twelve blocks: six blocks were not fertilized (control) and six blocks were enriched with N (fertilization). At the end of vegetation season 2019, we pulled out all young sessile oak trees to compare their biometric characteristics. For determination of oven-dry wood density, 5-8 cm long of wood segments from 10 cm above the ground/base from all trees - were taken. The biomass of segments was weighted with a digital scale, while volume was measured using the water displacement method according to Archimedes' principle. Subsequently, the sample oven-dry wood density (WD, g cm^{-3}) was calculated based on the wood sample oven-dry mass divided by volume. Immediately after tree harvesting, microcores with a thickness of 1.8 mm were collected from the base of a stem using Trephor increment borer. Two to three sectors of an outermost ring formed in 2019 (third year of CO_2 enrichment experiment) from each cross-section were obtained for the width of the growth ring (RW) and vessel characteristic measurements.

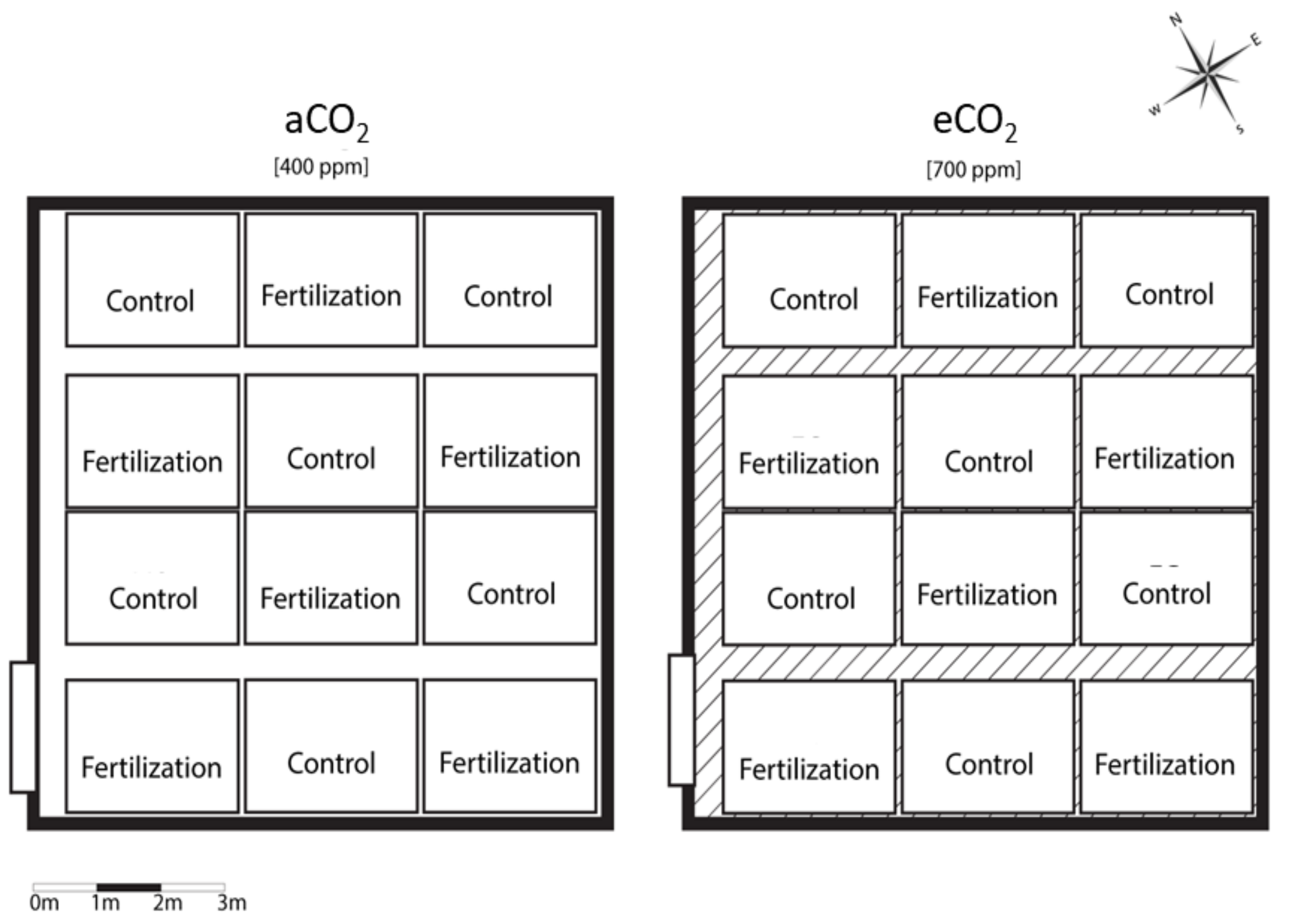

Figure 1: Experimental design scheme.
aCO_2 - ambient CO_2 concentration, eCO_2 - elevated CO_2 concentration, Control - plots without N fertilization, Fertilization - plots with N fertilization.

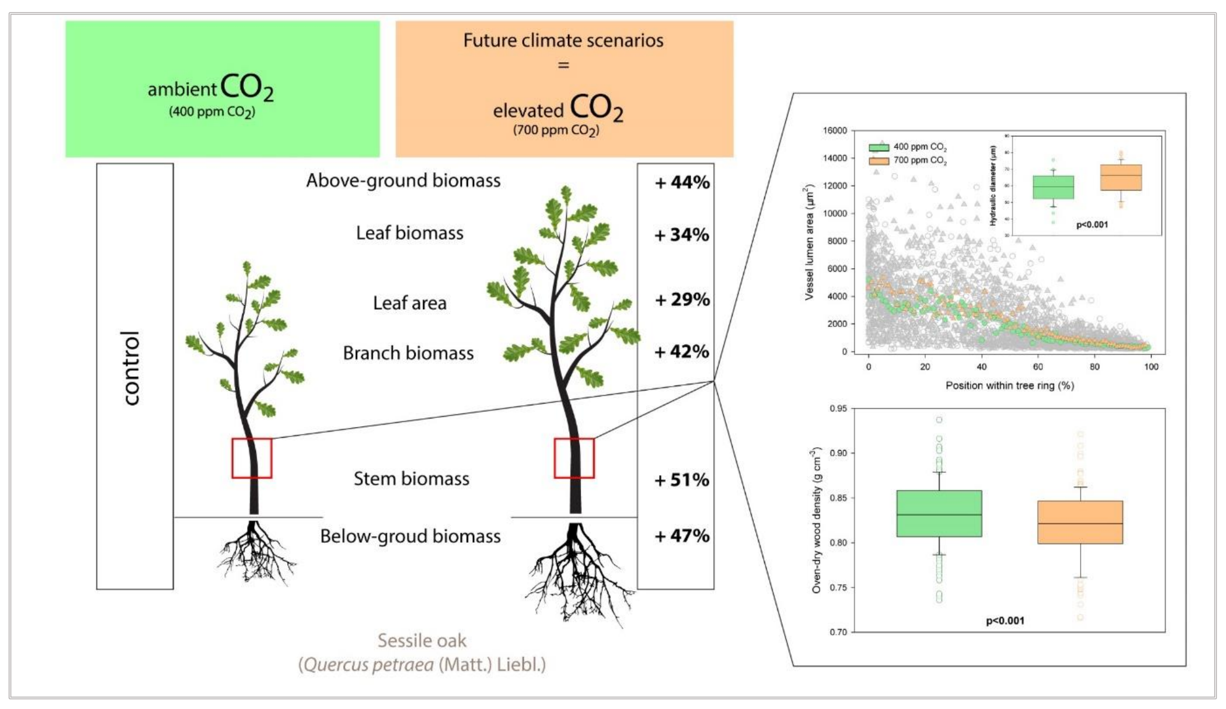

Figure 2: Graphical abstract

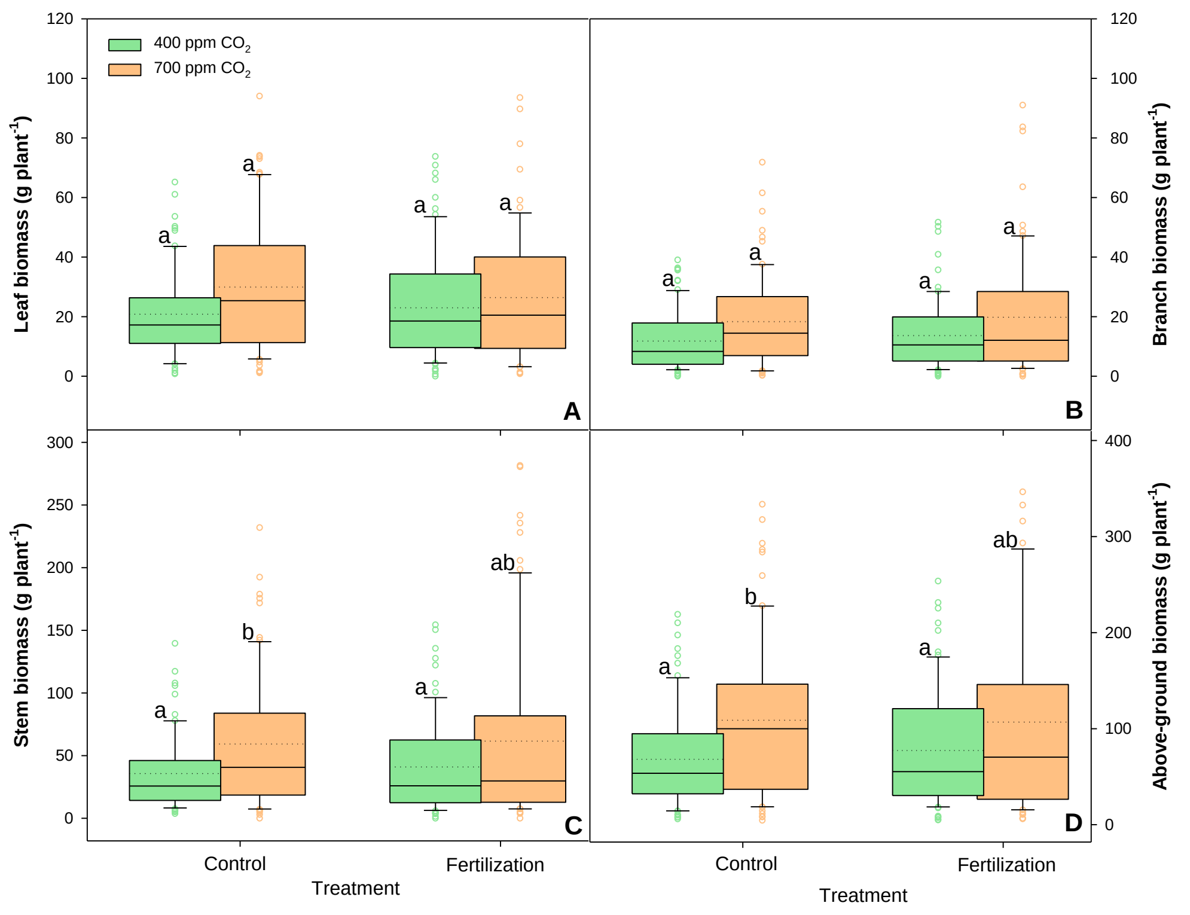

Figure 3: Changes in leaf biomass (**A**), branch biomass (**B**), stem biomass (**C**), and above-ground biomass (**D**) of (*Quercus petraea* (Matt.) Liebl.) trees treated under ambient (400 ppm CO_2) and elevated (700 ppm CO_2) and different nutrient supplies.

RESULTS

All investigated above-ground morphological parameters showed to be highly significantly ($p \leq 0.005$; Fig. 2 and 3) affected by (elevated CO_2) eCO_2 concentration, whereas nutrient supply had no statistically significant effect. The eCO_2 concentration had a highly positive effect on below-ground biomass (Fig. 2 and 4). The eCO_2 concentration had a positive effect on the total biomass of young sessile oak trees, the observed increase was, for above-ground biomass +44 % (Fig. 2 and 3), and respectively for below-ground biomass + 47 % (Fig. 2 and 4). All wood anatomical parameters except (total vessel area) TVA, (the proportion of the total vessel lumen area per analyzed sector) PTVA, and (potential specific hydraulic conductivity) K_s showed significant changes under eCO_2 while nutrient supply and combination $[CO_2] \times$ nutrient supply had no influence (Fig. 5). In young sessile oak trees, the (vessel lumen area) VLA was significantly larger under eCO_2 concentration, whereas (vessel density) VD was significantly lower (Fig. 5.) All traits related to hydraulic conductivity tended to increase under eCO_2 (Fig. 5). Overall, trees growing under eCO_2 had significantly lower densities -1.7 %, (Fig. 6), however, no effect of nutrient supply or combination of $[CO_2] \times$ fertilization was observed.

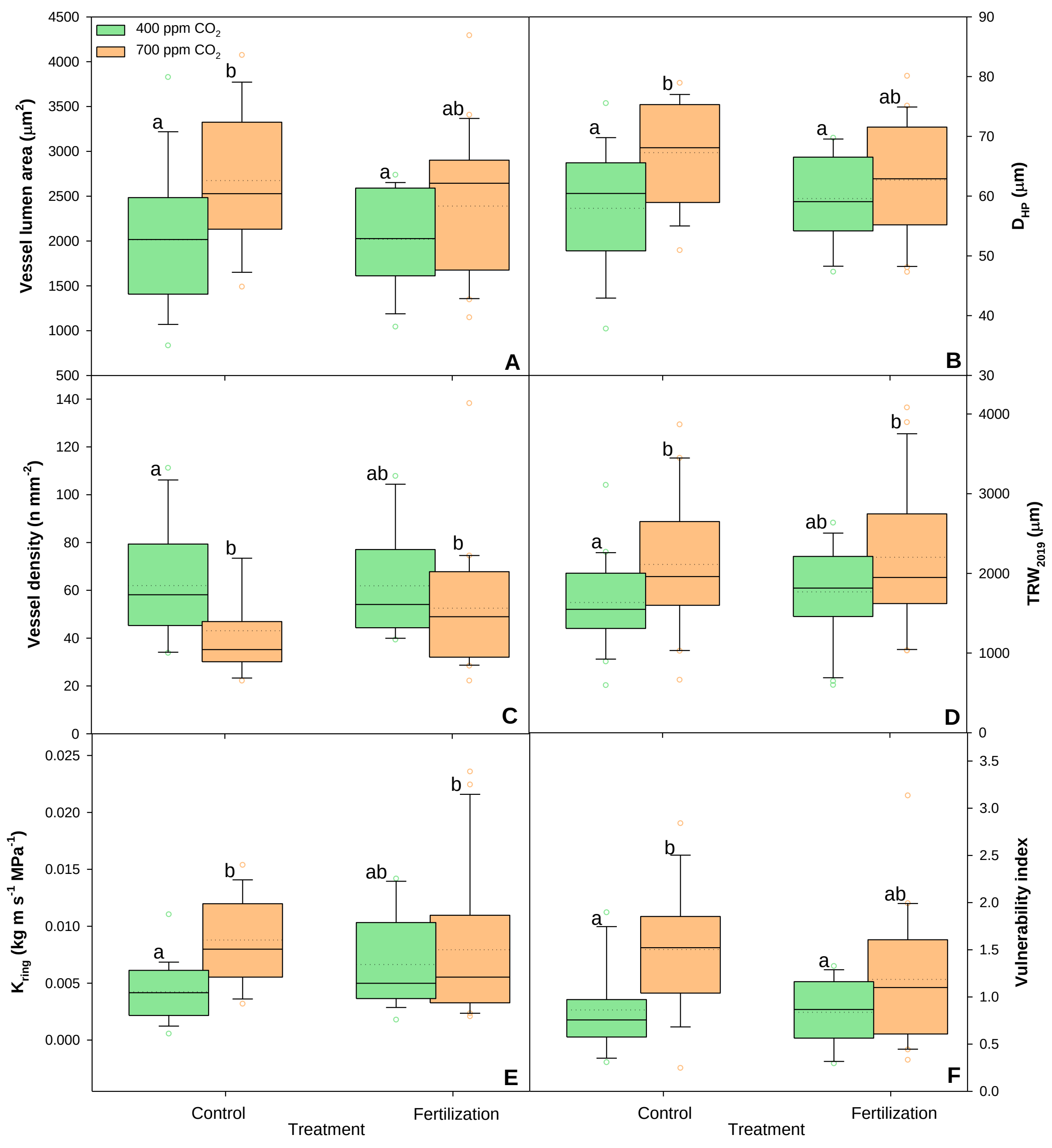

Figure 5: Changes in vessel lumen area (**A**), D_{hp} (**B**), vessel density (**C**), TRW_{2019} (**D**), K_{ring} (**E**), and Vulnerability index (**F**) of (*Quercus petraea* (Matt.) Liebl.) trees treated under ambient (400 ppm CO_2) and elevated (700 ppm CO_2) and different nutrient supplies. The data are expressed as medians (solid lines) and means (dotted lines) of measurements. The box boundaries mark the 25th and 75th percentiles and whiskers the 10th and 90th percentiles. Circles mark outliners. Different letters indicate significant differences ($p \leq 0.05$) estimated on the base of Duncan's ANOVA post-hoc test.

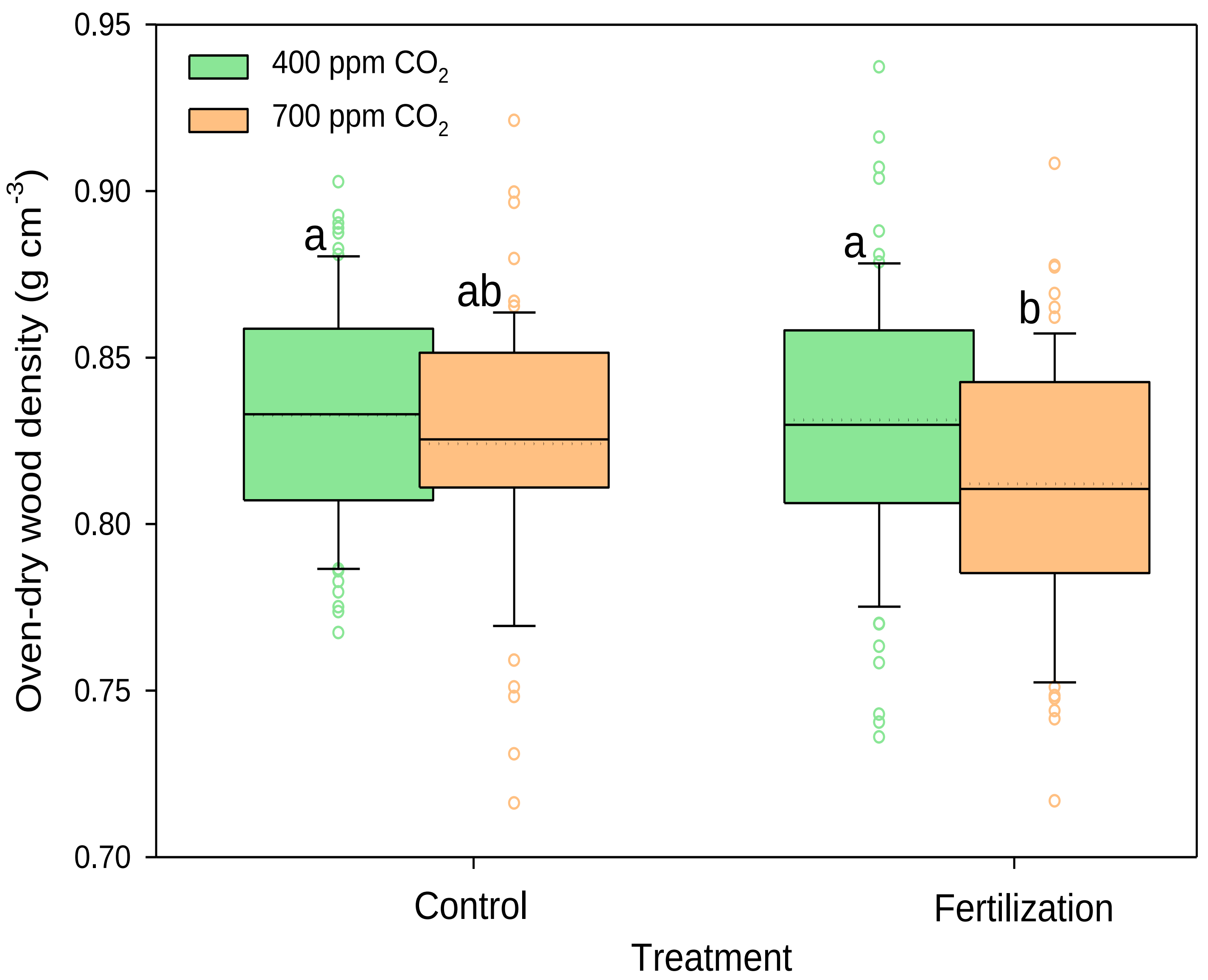

Figure 6: Changes in over-dry wood density of (*Quercus petraea* (Matt.) Liebl.) trees treated under ambient (400 ppm CO_2) and elevated (700 ppm CO_2) and different nutrient supplies. The data are expressed as medians (solid lines) and means (dotted lines) of measurements. The box boundaries mark the 25th and 75th percentiles and whiskers the 10th and 90th percentiles. Circles mark outliners. Different letters indicate significant differences ($p \leq 0.05$) estimated on the base of Duncan's ANOVA post-hoc test.

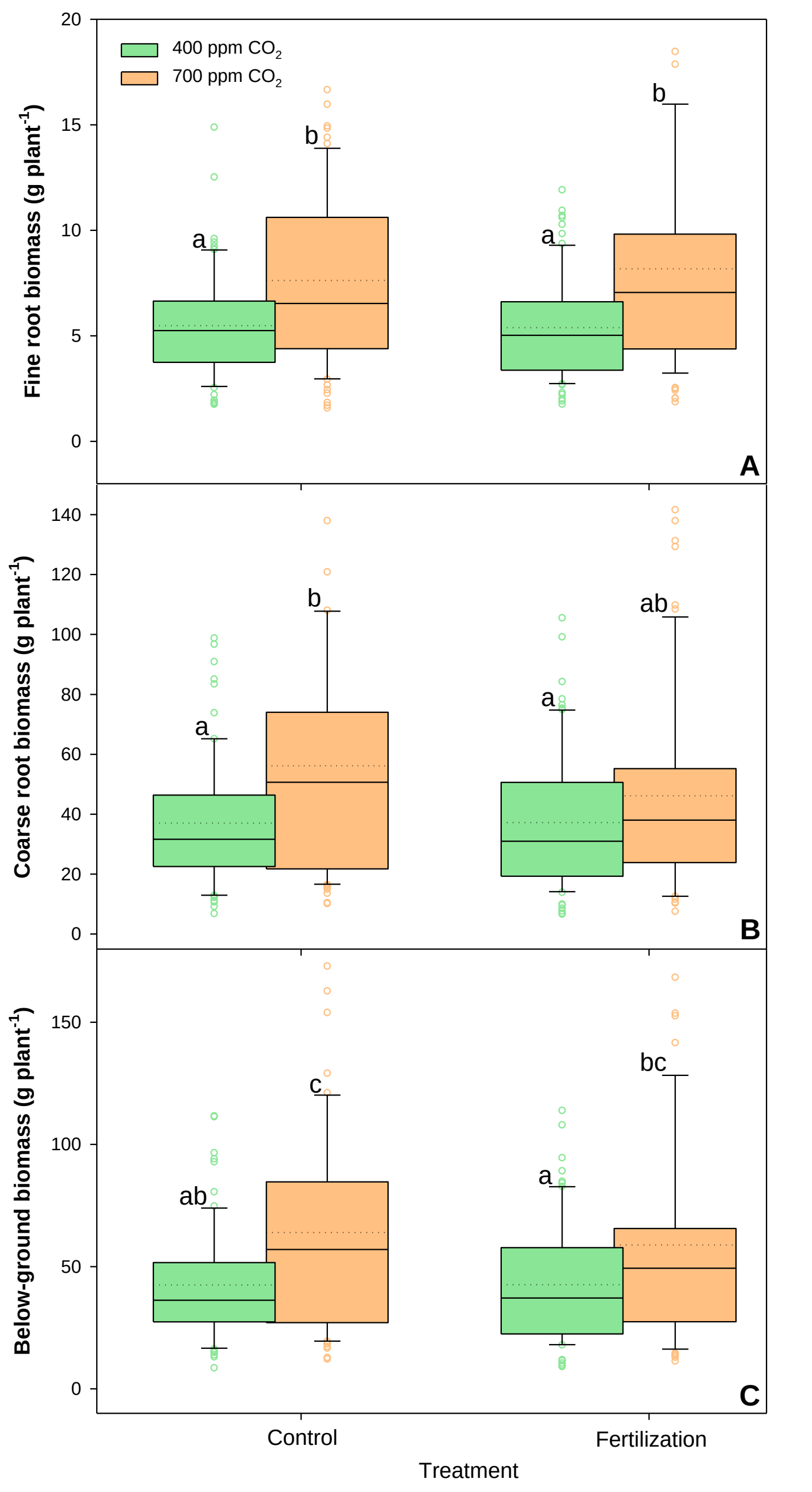

Figure 4: Changes in fine roots biomass (**A**), coarse roots biomass (**B**), and below-ground biomass (**C**) of (*Quercus petraea* (Matt.) Liebl.) trees treated under ambient (400 ppm CO_2) and elevated (700 ppm CO_2) and different nutrient supplies. The data are expressed as medians (solid lines) and means (dotted lines) of measurements.

CONCLUSIONS

Our research found that higher biomass production of young sessile oak trees under eCO_2 was supported by more efficient xylem hydraulic system. Nonetheless, the trade-off between the hydraulic efficiency and safety suggests that xylem consisted of larger vessels might be less resistant to embolism during severe droughts. However, larger absorptive area of root system indicated by higher biomass, both fine and coarse roots found in this study (Fig. 2 and 3), might be able to compensate aforesaid xylem susceptibility and increase resistance of young sessile oak trees to drought. This study also reported a significant effect of eCO_2 on (wood density) WD (Fig. 5), which is well related to many wood quality properties. Low WD generally means lower stiffens and therefore higher susceptibility of tree damage by different abiotic factors. It should be emphasised that our study focused on juvenile wood, however, reasonably good correlations between quality of juvenile and mature wood has been reported by different authors, thus the wood of young trees may indicate the wood quality in mature trees. In spite of the increase of biomass production at eCO_2 in this economically and ecologically important tree species in Europe, mechanical strength indicated by lower density and more vulnerable xylem to drought may lead to earlier mortality offsetting the positive effect of future eCO_2.

ACKNOWLEDGEMENTS

The work was supported by the Internal Grant Agency of Mendel University in Brno with grant number 030/2020 and also we would like to thank the Global Change Research Institute of the Czech Academy od Sciences for their technical and logistical help during this research.

DESIGN OF AN INFORMATION SYSTEM FOR THE AGRICULTURAL COOPERATIVE NEDOŽERY-BREZANY

PETRA PIPÍŠKOVÁ
Department of Landscape Planning and Land Consolidation
Faculty of Horticulture and Landscape Engineering
Slovak University of Agriculture in Nitra

XV. International scientific conference
Veda mladých 2021 - Science of Youth 21. 05. 2021

INTRODUCTION

For agriculture, information on soil units is an important factor influencing overall production. With a help of information systems in agricultural production, is it possible to monitor the soil, its features and obtain detailed information on agricultural land. Geographic information systems (GIS) are widely used in agricultural production. In particular, they function for the obtaining, storage and analysis of related data that are spatially bound to the earth's surface.

The goal of the thesis is design and build up of the information system for the Agricultural Cooperative Horná Nitra (PDHN) based in Nedožery-Brezany (district Prievidza). The information system is focused on the characteristics of individual soil units and the surrounding environment, which is managed by PDHN.

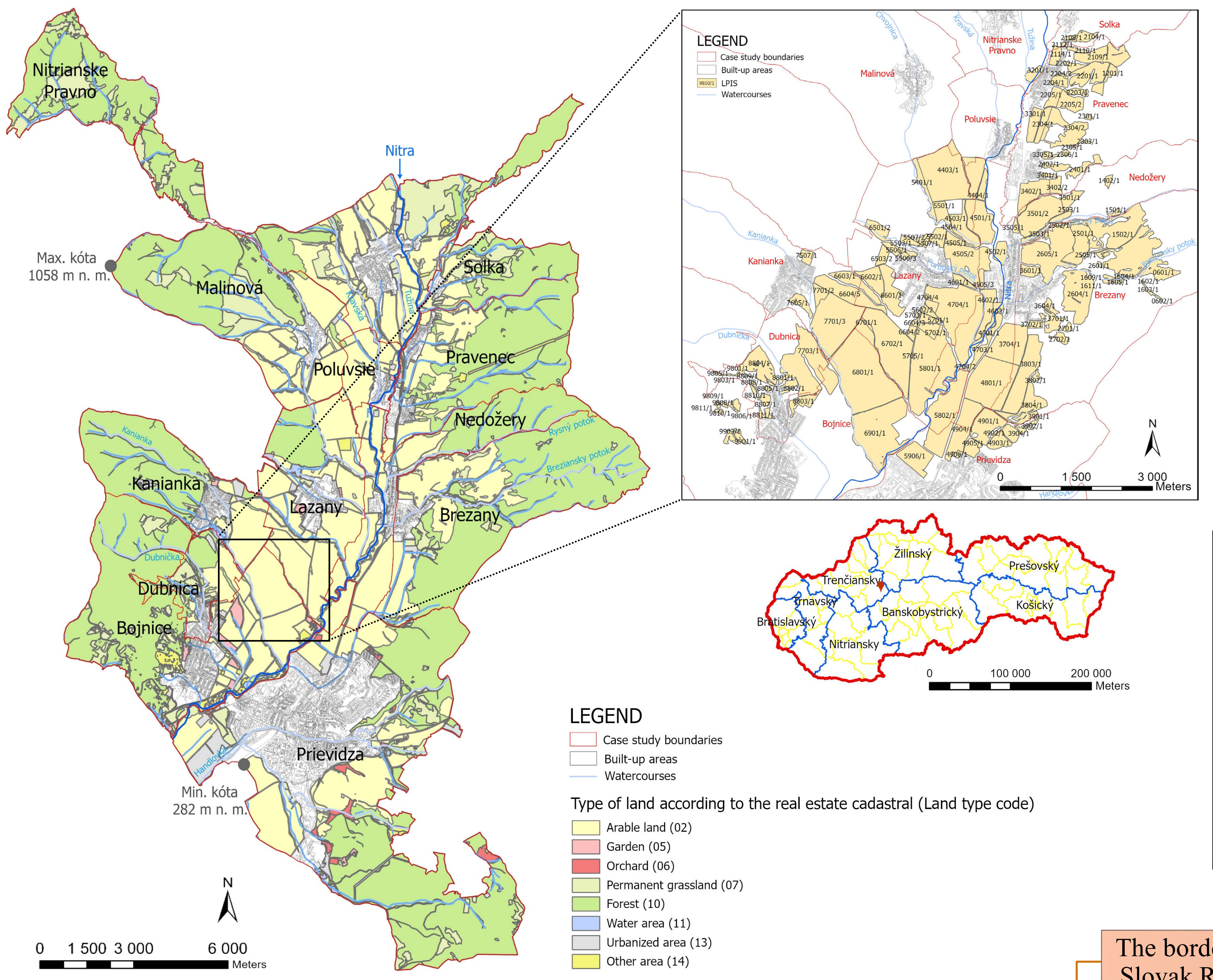

Figure 1: Map of the current land use with details of managed land units

MATERIAL AND METHODS

The thesis uses procedures related to the preparation of layers in ArcGIS Pro followed by publishing in ArcGIS online. We managed to process a detailed characteristic of 140 land units with an area of 2264,52 ha, which is farmed by PDHN. Based on the maps of the Real Estate Cadastre and the reconnaissance of the area, we prepared a graphic underlay for the current use of the land. We created a database of LPIS blocks. Individual information were obtained from PDHN internal sources. We used the universal equation - USLE, to calculate the soil loss. We determined the coefficient of ecological stability according to formula expressing the degree of anthropogenic influence in terms of ecostability. These input data were analyzed and then necessary databases were developed based on them. Through ArcGIS Pro, the pre-prepared layers with legends and data in the attribute table have been shared through our ArcGIS online account. In the Web application, we set the necessary templates, icons and completed the overall visual page of the information system. The content of the information system consists of shapefile layers based on which the user can find out essential information about LPIS blocks. After consultation with the management of the agricultural cooperative, we included 21 shapefile layers among the shared layers.

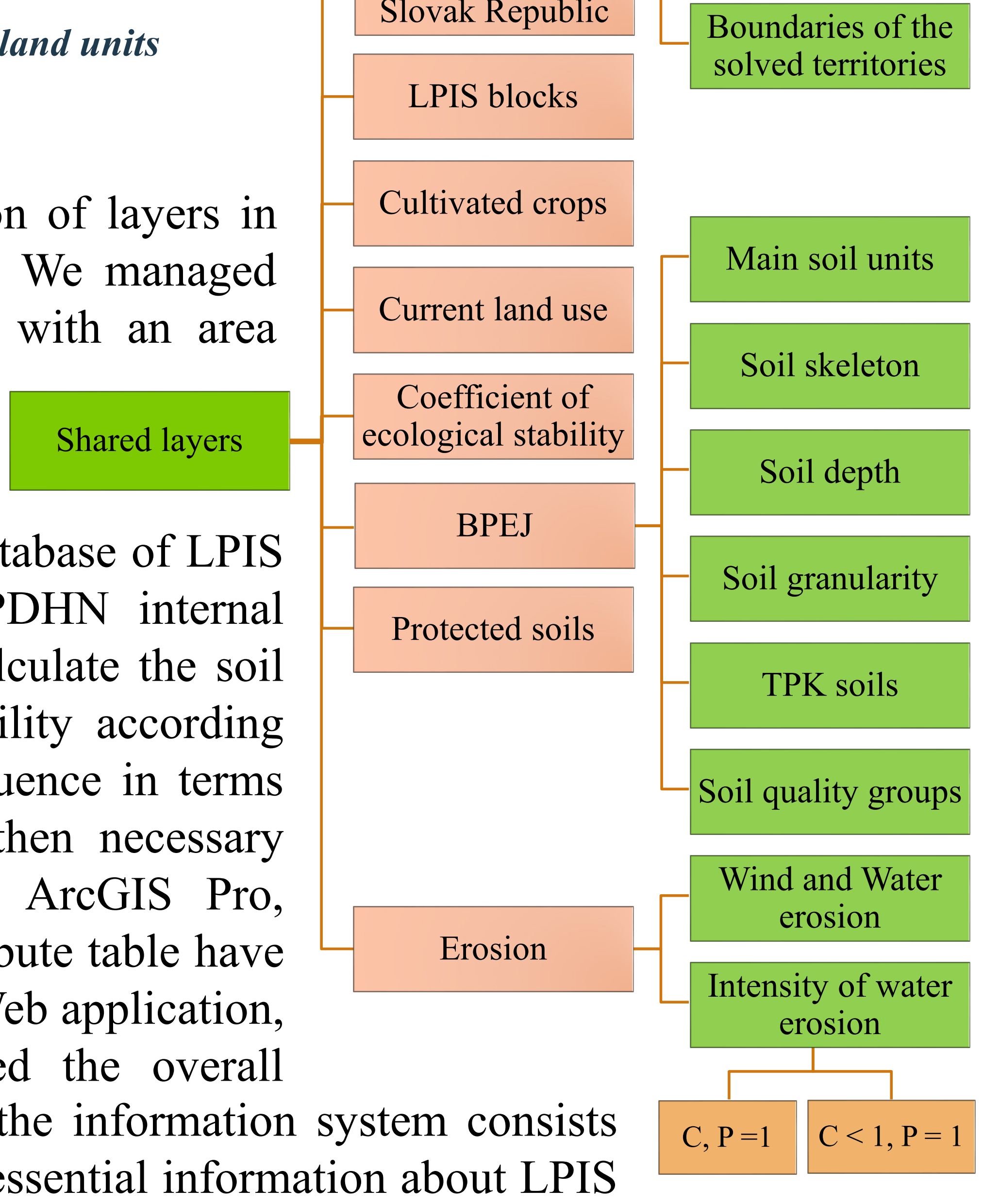

- Shared layers
  - The border of the Slovak Republic
    - Borders of regions and districts
    - Boundaries of the solved territories
  - LPIS bloky
  - Cultivated crops
  - Current land use
  - Coefficient of ecological stability
  - BPEJ
    - Main soil units
    - Soil skeleton
    - Soil depth
    - Soil granularity
    - TPK soils
    - Soil quality groups
  - Protected soils
  - Erosion
    - Wind and Water erosion
    - Intensity of water erosion
      - C, P =1
      - C < 1, P = 1

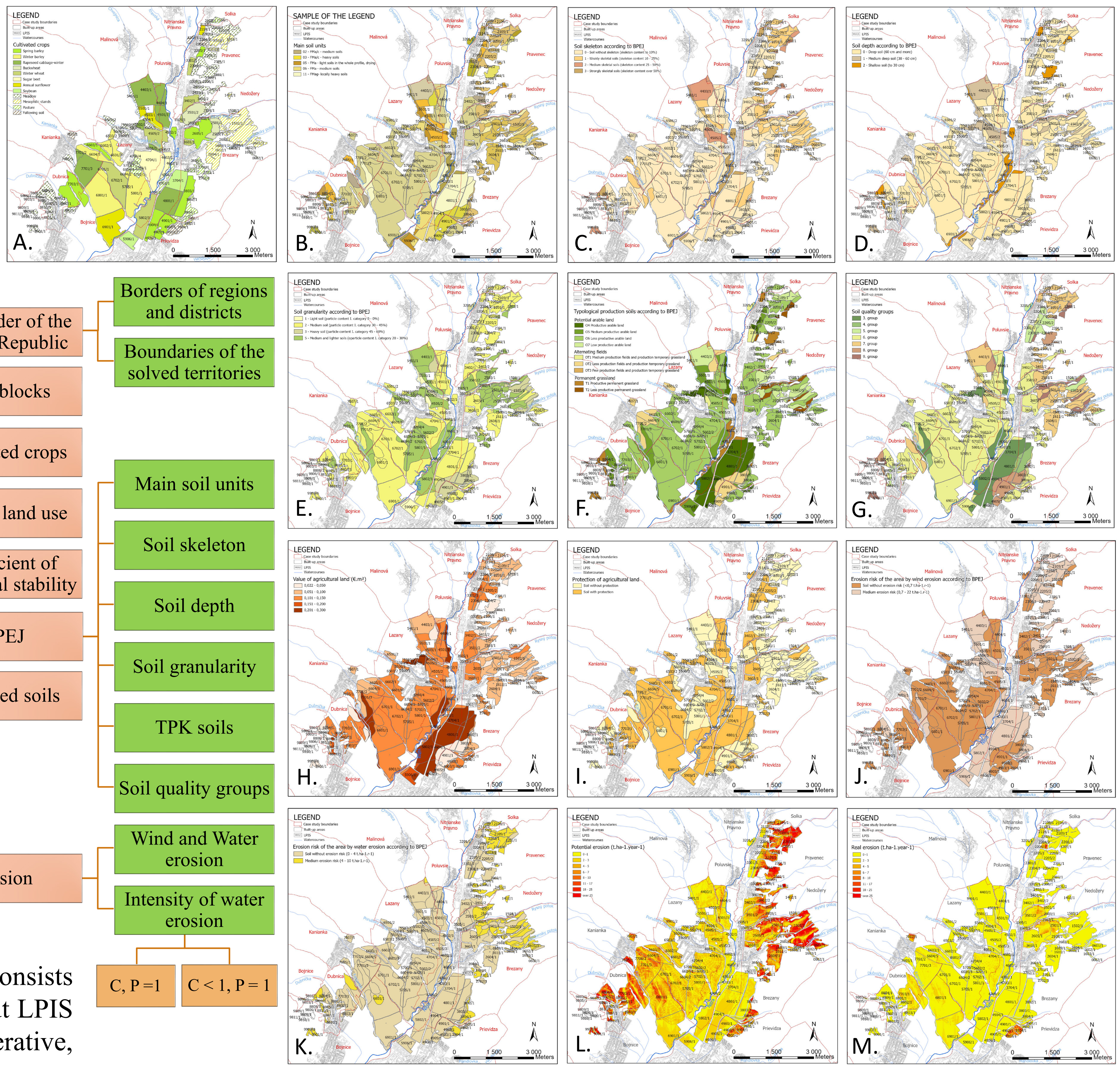

Figure 2: Schematic representation of used map layers in IS PDHN

(**A**-Cultivated crops, **B**-Main soil units according to BPEJ, **C**-Soil skeleton according to BPEJ, **D**-Soil depth according to BPEJ, **E**-Soil granularity according to BPEJ, **F**-Typological production soils according to BPEJ, **G**-Soil quality groups, **H**-Value of agricultural land, **I**-Protection of agricultural land, **J**-Wind erosion, **K**-Water erosion, **L**-Potential erosion, **M**-Real erosion)

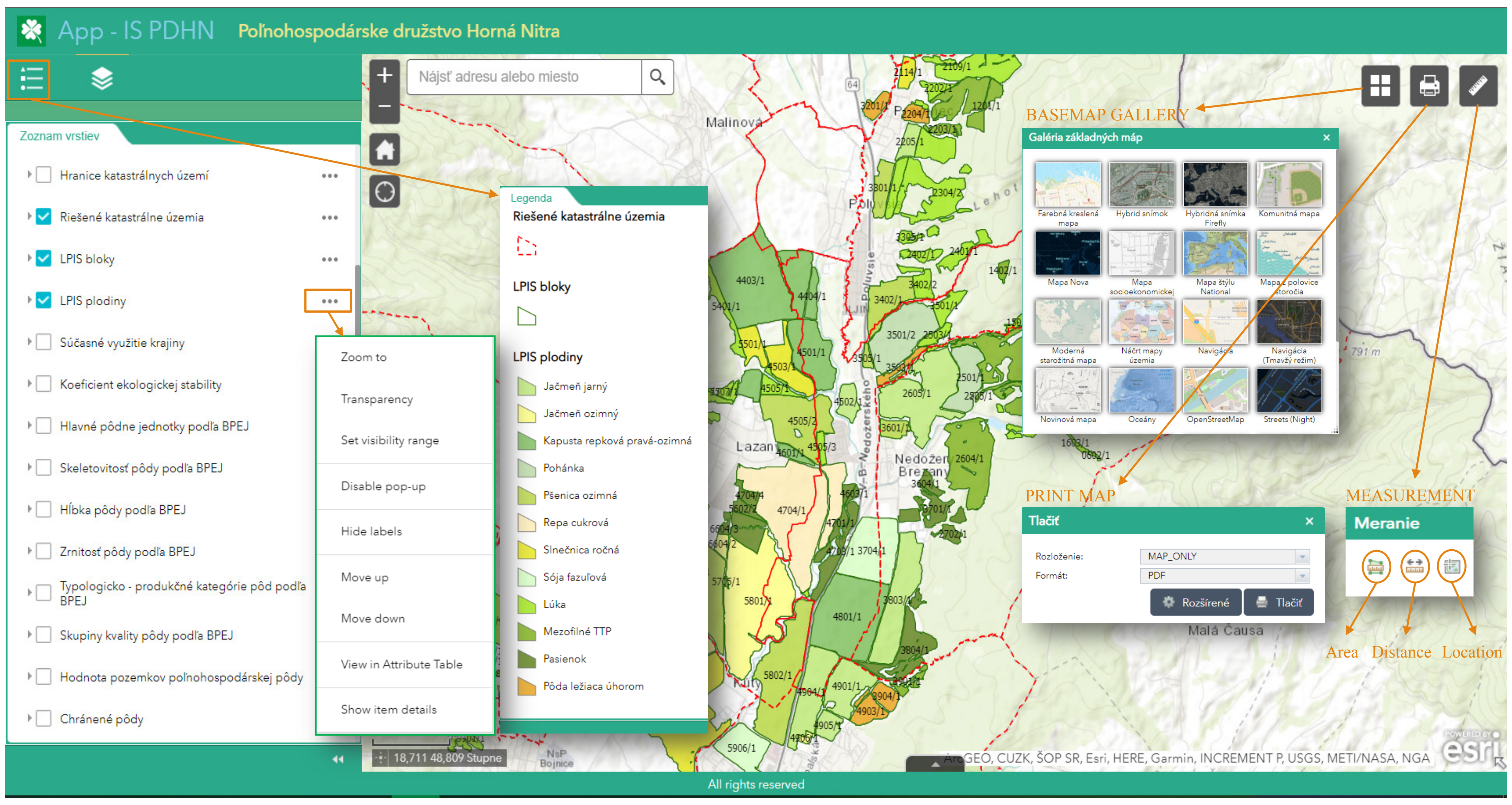

RESULTS

PDHN keeps records of soil units in a written form. These are outdated and confusingly processed in many cases. The information system is designed because of modern archiving and innovation of individual data on cultivated soil to an electronic form. On-line mediated layers provide to PDHN employees, along with public, the opportunity to get to know the features of the soil, the surrounding landscape and erosively endangered localities in the managed LPIS blocks. At the beginning, the user can expand and click on the desired shapefile layers using the Layers icons. Layers can be customized as needed: zoom in, make it more transparent, turn pop-ups on / off, change layer order, view attribute table and system details. The user can change the base map, print a map report or measure the distance between certain points. The online version of the PDHN Information System is available at https://arcg.is/1n0Cn00.

ACKNOWLEDGEMENT

Work was supported under the Integrated Infrastructure Operational Program for the project: "Data and knowledge support for decision-making and strategic planning systems for adapting agricultural land to climate change and minimizing agricultural land degradation" (code ITMS2014 + 313011W580), co-financed by the European Parliament's Regional Development Fund.

REFERENCES

PIPÍŠKOVÁ, P., 2020. *Design of an information system for the agricultural cooperative Nedožery-Brezany: Thesis. Nitra: SPU. 96 s.*

CONTACT

Ing. Petra Pipíšková, Slovak Univerzity of Agriculture in Nitra, Faculty of Horticulture and Landscape Engineering,
Department of Landscape Planning and Land Consolidation, Hospodárska 7, 949 76, Nitra, Slovakia, e-mail: pipiskova.petra@gmail.com

Veda mladých 2021 - Science of Youth 2021

XV. International scientific conference

DIGITAL RECONSTRUCTION OF A CLIMBING GUIDE USING LOWCOST AERIAL PHOTOGRAMMETRY

Dávid DEŽERICKÝ

Department of Landscape Planning and Land Consolidation, FHLE SUA in Nitra

Abstract

The aim of the work is the photogrammetric survey and digital reconstruction of a climbing area of the western part of the climbing rock below Kalvária in the city of Nitra. The accuracy of the photogrammetric model is supplemented by geodetic measurements using a total station and GNSS reference coordinates. The result of the work is the georeferenced model of the climbing area with drawn climbing routes, as well as the case study of use of aerial photogrammetry in recreational and leisure activities.

Key words:

Lowcost photogrammetry, Close-range photogrammetry, Structure from Motion

Materials and methods

Site description:

- City of Nitra, southwestern orientation under a limestone peak altitude 215 meters above sea level.
- The rock belt of the climbing area is 300m long, large part is not suitable for climbing due to unstable rock affected by limestone mining in the past.

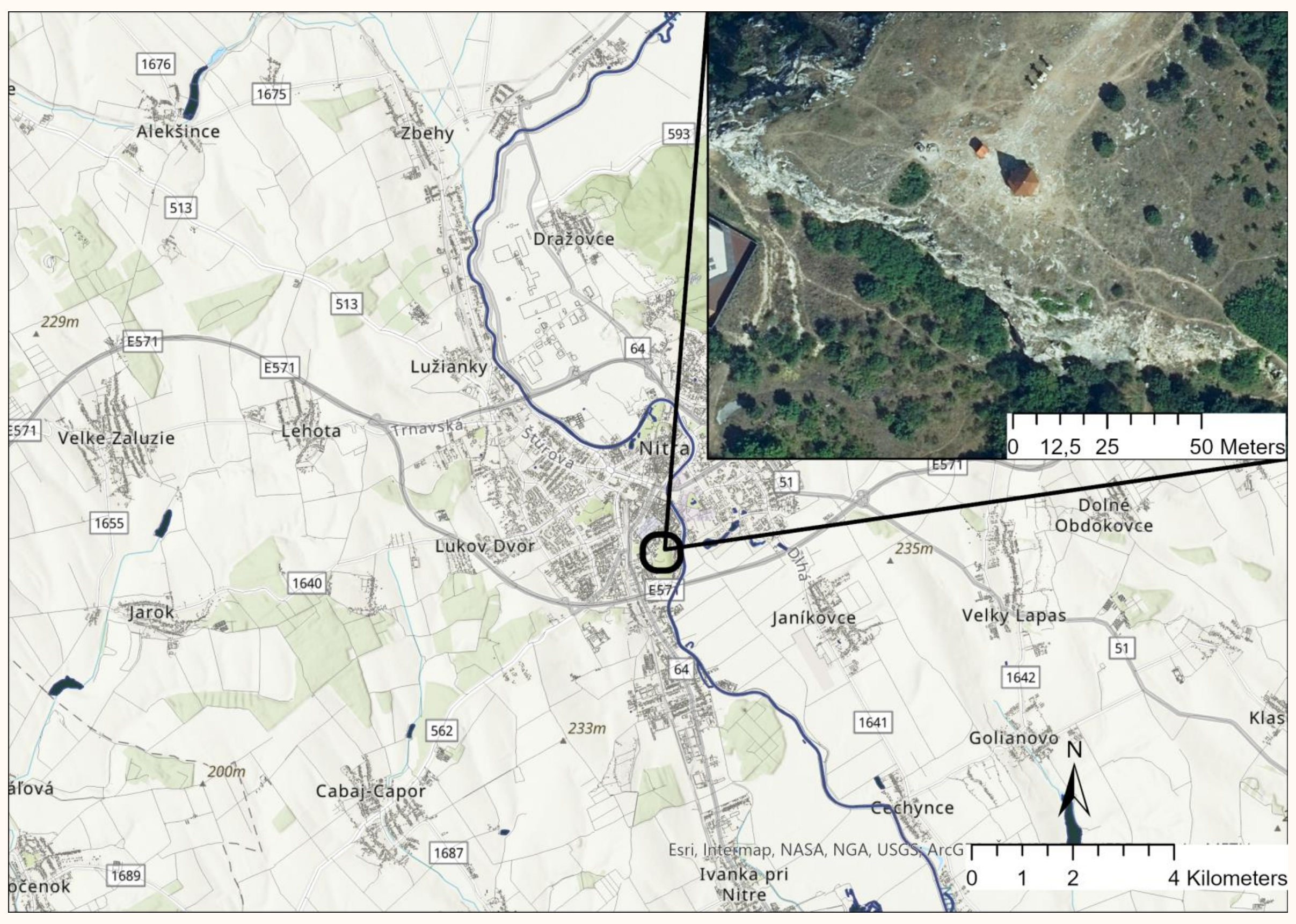

Figure 1. Location of the climbing area

Before the image capturing, a network of 11 ground control points (GCP) has been installed at different elevations for precise positional determination of the model. The GCP's surveyed with the total station Trimble M3 (DR5). Once the GCP's were surveyed, the site was aerially photographed by a DJI PHANTOM 4 PRO V2 with a 1 "CMOS chip with a resolution of 20MPx and a focal length of 8.8mm. To ensure coverage of the entire site, the photos was taken from several angles and distances, where we tried to maintain a high overlap of images to minimize blind spots in the processing of the model.

Figure 2. Installing and measuring the control points

Total of 439 images were processed using Agisoft Metashape software. During this process, program calculates the position and orientation of each photo and creates a sparse point cloud of the surveyed rock site. After images were aligned, we manually plotted control points with coordinates into the software by using reference tools. At this stage software recalculated the position of sparse point cloud and georeference points into S-JTSK Křovak East North [EPSG: 5514] coordinate system. In same way, once the images were aligned it is possible to generate dense cloud and then TIN model. The next step of processing was adding textures on 3D model based on captured images.

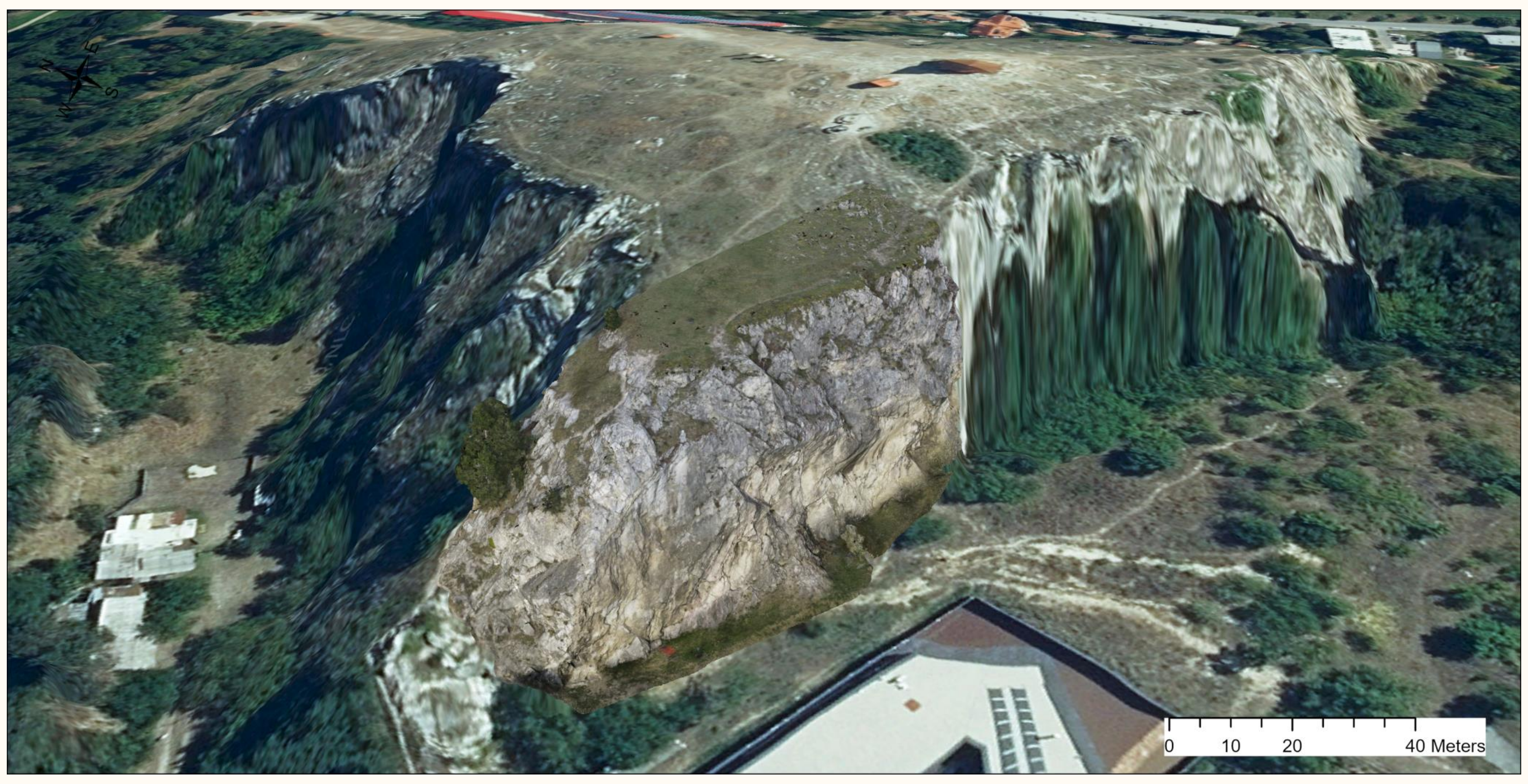

Figure 3. Georeferenced TIN model of Kalvária rock in GIS

In the last step we exported the TIN model to the software Blender 3D model suite, where we used the curves to redraw the climbing routes from the climbing guide to the 3D model by comparing routes in topo guide with topography of model.

Figure 4. Planar orthomosaic of Kalvária - projection plane XZ

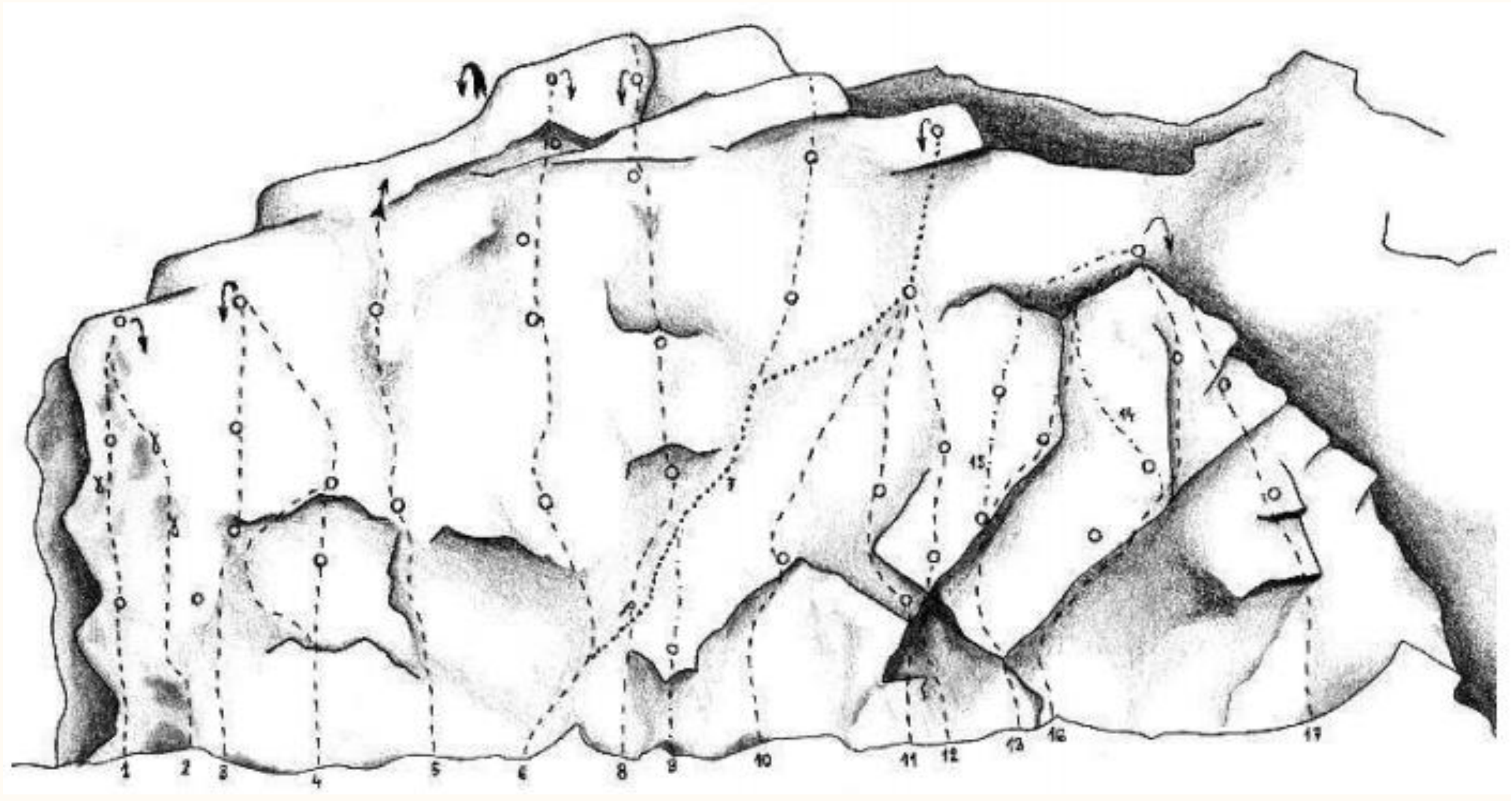

Figure 5. Hand drawn Topo sketch of Kalvária rock

Results

By photogrammetric processing we have created a highly detailed 3D model with over 10,000,000 vertices and 21,000,000 faces. The model was decimated to 1,000,000 faces due to the reduction of data volume and easier handling of the model. Using the open-source software Blender 2.91, 19 climbing routes were drawn into the model based on a topographic sketch of a rock surface. Following the drawing of climbing routes, the model was uploaded to the viewing platform Sketchfab. <https://skfb.ly/onSZQ>

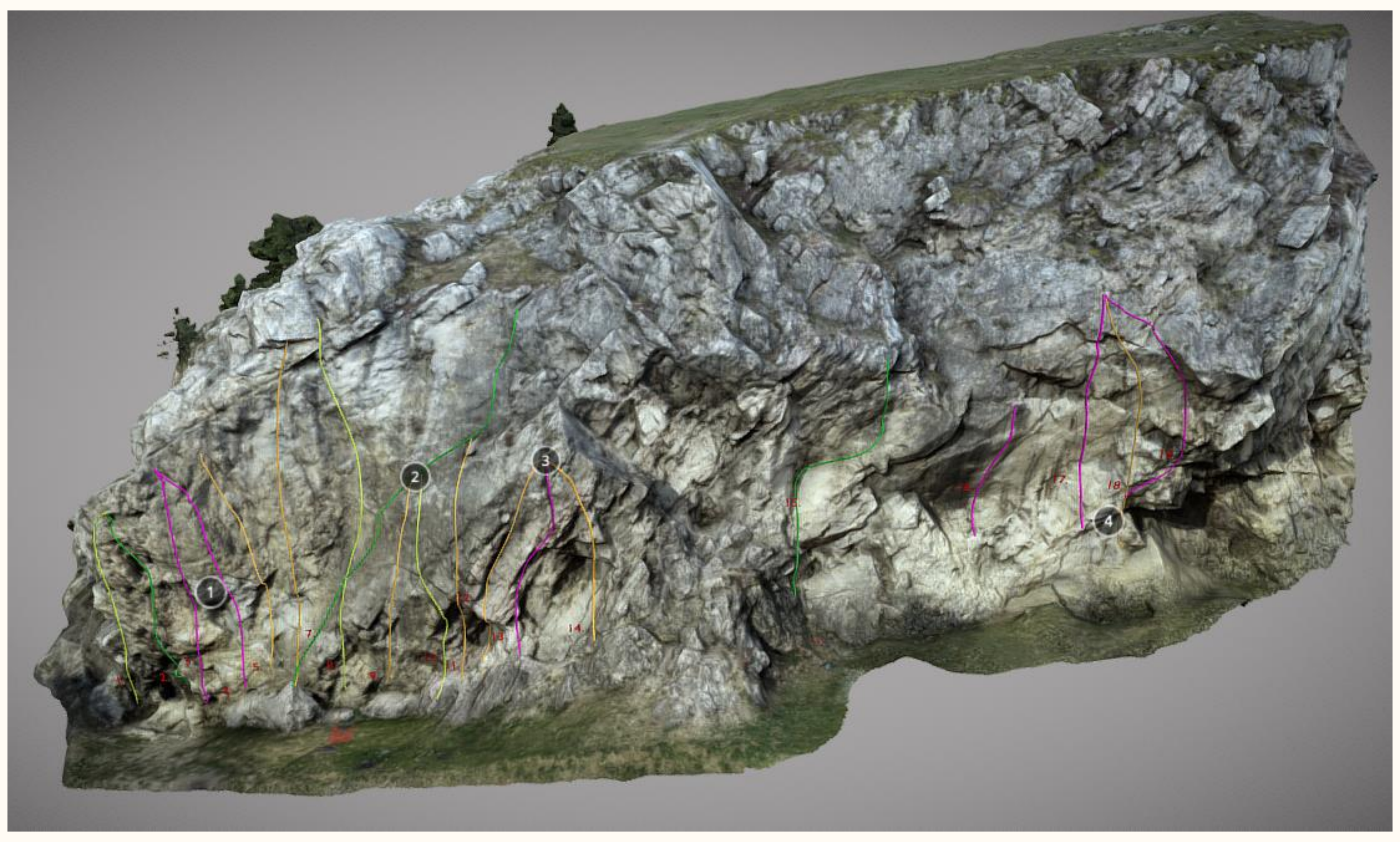

Figure 6. Pciture of 3D model with drawn climbing routes

Conclusion

Decisive aspects of mapping of the steep and hard-to-reach forms of rock walls in 2D cartography is visualization. In this case we used low-cost aerial photogrammetry to capture, visualize and reconstruct the climbing guide of Kalvária in 3D. By making a 3D model and then drawing climbing routes based on a topographic sketch we added details and information to the „topo" model of surface, which can be used by the climber to plan and facilitate climbing. Adding more details and information to topos could make the preparation make the climbing route easy to spot and compare to others in the same area. However, we want to point out that by helping the climbing community with the digitization of climbing guides, we can raise awareness and interest in photogrammetry and encourage more people to digitize not only climbing areas but also natural, cultural heritage.

Acknowledge:

"This publication is the result of the project implementation: „ Scientific support of climate change adaptation in agriculture and mitigation of soil degradation " (ITMS2014+ 313011W580) supported by the Integrated Infrastructure Operational Programme funded by the ERDF."

Contact: Ing. Dávid Dežericky, e-mail: xdezericky@uniag.sk

IMPACT OF LAND-COVER ON THE LOCAL CLIMATE: CASE OF FOUR URBAN AREAS IN THE CZECH REPUBLIC

Author: Swati Surampally I Czech University of Life Sciences Prague I ✉ swa09ti@gmail.com

Supervisor: Prof. RNDr. Dana Komínková, Ph.D. I Consultants: doc. RNDr. Jan Pokorný, CSc. & RNDr. Petra Hesslerová, Ph.D.

1 AIM & OBJECTIVES

AIM: To analyse the relationship between changes in the land-cover and changes in the climate on a local scale by a comparative analysis of four city areas in the Czech Republic.

OBJECTIVES:

1. To determine the long-term trends in changes in land-cover and climate in the four study areas.
2. To identify if there is a positive relationship between the changes in forest cover and changes in the amount of local precipitation in each study area.
3. To examine the effects of land-cover on the local climate by comparing the climate and land-cover trends across the four study areas.

2 STUDY AREAS

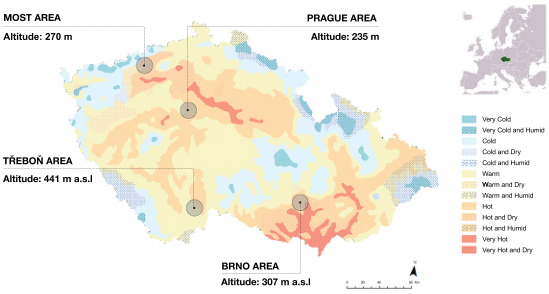

STUDY AREAS SELECTION CRITERIA:

1. Similar climate zone 2. Similar altitude 3. Availability of long term data

3 DATA & METHODOLOGY

DATA

METHODOLOGY

Climate Data
(1961 - 2016)
Source: Czech Hydrometeorological Institute

Statistical Tests (XLSTAT)
1. Mann-Kendall Test
2. Pettitt's Test
3. Kruskal-Wallis Test

Land-cover Data
(1990; 2000; 2006; 2012; 2018)
Source: Copernicus Land Monitoring System by EEA

Land-cover Maps (ArcGIS)

Land-cover Graphs (Excel)

4 RESULTS: CLIMATE TRENDS

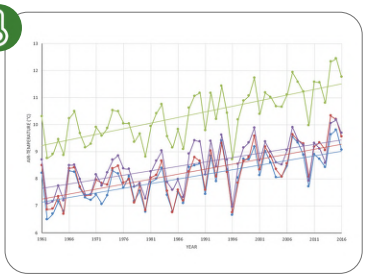

Statistically Significant 🔵 🟣 🔴 🟢

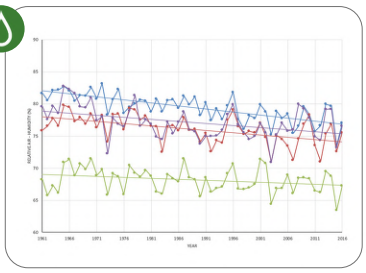

Statistically Significant 🔵 🟣 🔴 🟢

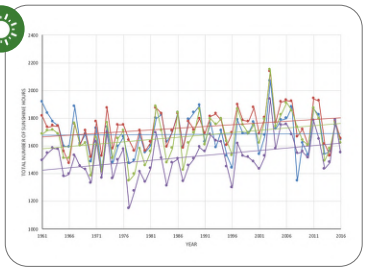

Statistically Significant ⚪ 🟣 🔴 🟢

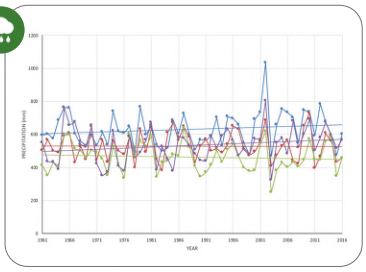

Statistically Significant ⚪ ⚪ ⚪ ⚪

Třeboň Area Brno Area
Prague Area Most Area

5 RESULTS: LAND-COVER TRENDS

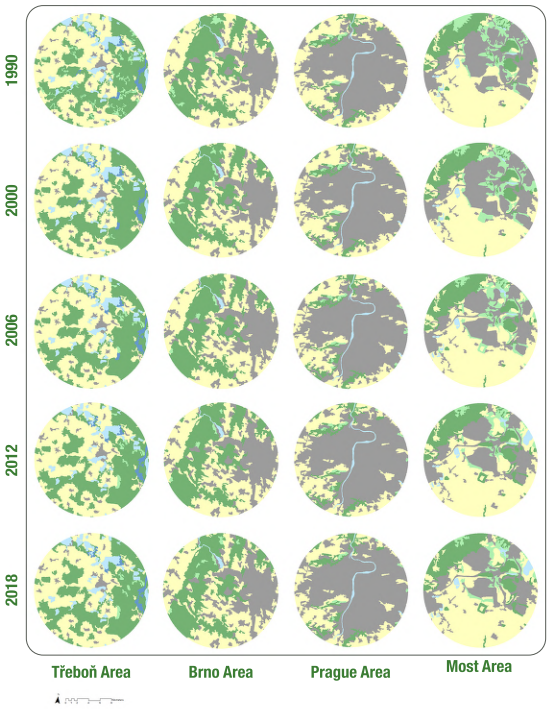

Maps of changes in land-cover in the four study areas from 1990-2018

Graphs depicting percentage of changes in land-cover in the four study areas from 1990-2018

6 FOREST-COVER & PRECIPITATION DYNAMICS

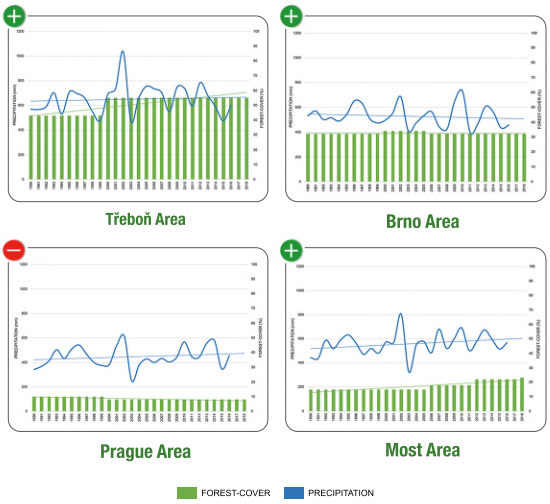

Graphs depicting relationship between trends in forest-cover and precipitation in the four study areas from 1990-2018.

7 COMPARITIVE ANALYSIS

🟢	Artificial Surfaces	10.38 °C	↑ sig.	463 mm	↓ not sig.
🔴	Agricultural Areas	08.26 °C	↑ sig.	530 mm	↓ not sig.
🟣	Agricultural Areas	08.54 °C	↑ sig.	535 mm	↑ not sig.
🔵	Forests	08.07 °C	↑ sig.	630 mm	↑ not sig.

I sig. = stsistically significant I not sig. = statistically not significant I

8 CONCLUSIONS

Climate Trends:
Changes in temperature are quite evident and predictable while precipitation trends are uncertain.

Forest-Precipitation Dynamics:
3 out of 4 study areas indicate a positive relationship.

Land-Cover & Climate Dynamics:
Study area with largest natural land-cover has highest annual mean precipitation and lowest mean temperature.

Change of soil surface roughness by the simulated rainfalls

Tatiana Kaletová[1], Branislav Pospiš[1], Jozef Halva[1]

[1]Slovak University of Agriculture in Nitra, Tr. A. Hlinku 2, 94976 Nitra, Slovakia; phone: +421 (0)37 641 5238; e-mail: tatiana.kaletova@uniag.sk

Aim of study

- a comparison of changes of soil surface roughness by simulated rainfalls

- selected 6 plots with the same slope, soil type, without vegetation cover (bare soil)
- 6 photos of each plot before and after the rainfall simulation

- rainfall simulation (2.3 l per 3 min.), rainfall simulator of Eijkelkamp company (33 x 33 cm)
- plot area 26 x 26 cm
- distances of rainfall holes 3.5 x 3.5 cm

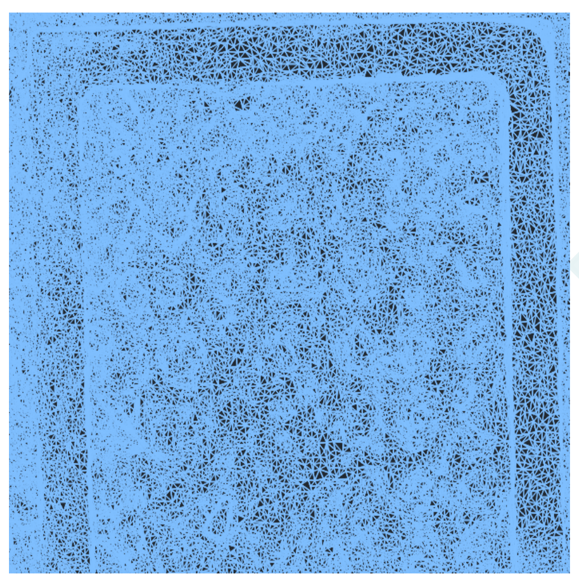

- use of Agisoft Metashape Professional v. 1.5.5
- generation 18,000 – 22,000 identical points
- creation of point cloud with xyz coordinates – about 3,000,000 points
- TIN model creation – about 300,000 points and 600,000 sites

- surface cross section creation by AutoCAD
- measurement of cross section length
- measurement of vertical elevation differences

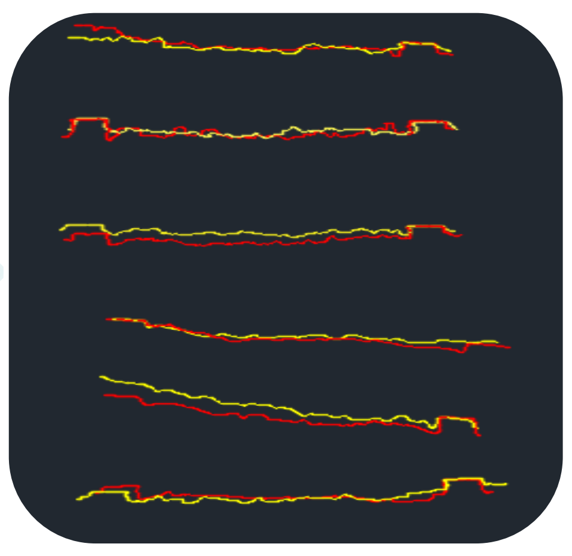

plot	L1b, m	L1a, m	L2b, m	L2a, m	SRFb, %	SRFa, %	SRF - D	SD b	SD a
1	0.3347	0.3533	0.2991	0.3001	10.64	15.06	4.42	0.000484	0.000576
2	0.429	0.3515	0.2929	0.2965	31.72	15.65	-16.07	0.000725	0.000517
3	0.3357	0.3379	0.2906	0.2969	13.43	12.13	-1.3	0.000601	0.000575
4	0.3213	0.3367	0.3114	0.2817	3.08	16.34	13.26	0.000206	0.000287
5	0.3161	0.3235	0.2909	0.2912	7.97	9.98	2.01	0.000237	0.000319
6	0.3137	0.346	0.2962	0.3076	5.58	11.1	5.52	0.000262	0.000346

L1 – full length of the chain, L2 – the horizontal distance between chain ends when placed on the soil, a – after the simulation, b – before the simulation, SD – standard deviation

- calculation of Saleh roughness factor (SRF) – chain method
- calculation of standard deviation of points elevation

Conclusions

- SRF mostly increased after the simulated rainfalls about 1.3%; highest increase 13.26 %, lowest one -16.07
- impact of rainfall drops on the soil surface is evident; even results of standard deviation of point elevations confirm it
- rainfall drops decreased the higher values of SRF which have tendency to destroy the soil particles blocks

This publication is the result of the project implementation: „Scientific support of climate change adaptation in agriculture and mitigation of soil degradation" (ITMS2014+ 313011W580) supported by the Integrated Infrastructure Operational Programme funded by the ERDF.

SCIENCE OF YOUTH 2021 - PROCEEDINGS OF SCIENTIFIC PAPERS

Nitra, Slovakia
21.05.2021

Held under the auspices
prof. Ing. Dušan Igaz, PhD., dean of FHLE SUA in Nitra

Publisher: Slovak University of Agriculture in Nitra

Edition: first

Year of Publication: 2021

Form of Publication: online

Not edited at the Publishing Center of the SUA in Nitra.

ISBN 978-80-552-2338-4